**Immune evasion strategies utilized by *Francisella tularensis***

Lydia Marie Barrigan

A dissertation submitted to the faculty of the University of North Carolina at Chapel Hill in partial fulfillment of the requirements for the degree of Doctor of Philosophy in the Department of Microbiology and Immunology.

Chapel Hill
2013

Approved by:

Thomas Kawula, Ph.D

Jeffrey Frelinger, Ph.D

Edward Collins, Ph.D

Lishan Su, Ph.D

Jenny Ting, Ph.D

## ABSTRACT

LYDIA MARIE BARRIGAN: Immune evasion strategies utilized by *Francisella tularensis* (Under the direction of Jeffrey Frelinger)

*Francisella tularensis* is a highly pathogenic, gram-negative, facultative intracellular bacterium and the causative agent of tularemia. *Francisella* has evolved numerous mechanisms to evade host immune responses. One immune evasion mechanism utilized by *Francisella* is its ability to induce prostaglandin $E_2$ ($PGE_2$) secretion from infected host cells. We identified 20 *Francisella* genes necessary for the induction of $PGE_2$ secretion in infected host cells. One of the genes necessary for $PGE_2$ induction encodes a highly conserved AAA+ ATPase chaperone protein, ClpB. *F. tularensis* live vaccine strain (LVS) *clpB* is attenuated in vivo, despite normal intracellular growth in vitro. LVS *clpB* fails to inhibit pro-inflammatory cytokine responses in the lung early after inoculation, a process normally inhibited by LVS. The adaptive immune response is also altered compared to LVS with increased IFN-γ or IL-17A production by T cells. Although LVS *clpB* is attenuated, it induces an immune response that is as protective as LVS following lethal challenge indicating *clpB* is a potential target for vaccine development. Although the primary immune response is altered during LVS *clpB* infection, there are no differences in the secondary immune response to LVS. The primary immune response to LVS requires IFN-γ and IL-17A production to control bacterial replication. Few Th17 cells were identified during the secondary response in the lung whereas there were numerous $CD4^+$ and $CD8^+$ T cells

producing IFN-γ. IFN-γ production is required for controlling bacterial replication during the secondary response, but IL-17A production is dispensable for survival during re-infection.

*Francisella* also evades host immunity by targeting innate immune cells for infection. *Francisella* infects different cell types in the lung depending on the route of inoculation; alveolar macrophages are infected following intranasal inoculation while interstitial macrophages and neutrophils are infected in the lung after intradermal inoculation. The lung's cytokine milieu is more pro-inflammatory after intradermal inoculation compared to intranasal inoculation, consistent with the development of a more robust IFN-γ mediated adaptive immune response. A better understanding of the mechanisms of *Francisella* infection will not only result in understanding important concepts in pathogenesis, but will suggest key pathways to impact for the development of drugs and vaccines.

## DEDICATION

To my parents, Bill and Natalie Roberts, and my entire family for their guidance, endless support, and unconditional love.

## ACKNOWLEDGEMENTS

I thank H-J. Wu, Kurt Griffin, Lucinda L. Hensley, Michael Kuhns, and Kenneth Peterson for helpful conversations and thoughtful review of several manuscripts. I also thank Paula Campbell and the University of Arizona Flow Cytometry Core Facility and William Day and the University of Arizona's University Spectroscopy and Imaging Facilities for their assistance and technical expertise. Select studies were performed in the Regional Biocontainment Laboratory at Duke which received partial support for construction from the National Institutes of Health, National Institute of Allergy and Infectious Diseases (UC6-AI058607). Biomarker profiling was performed in the Duke Human Vaccine Institute/Regional Biocontainment Laboratory Biomarker Analysis Shared Resource Facility (Durham, NC) by Ms. Kristina Riebe. This work was supported by the National Institutes of Health Grants R01-AI078345 and K22-AI083373 and the National Institute of Allergy and Infectious Diseases Southeast Regional Center of Excellence for Emerging and Infections and Biodefense Grant U54-AI057157.

## TABLE OF CONTENTS

## LIST OF TABLES

Table

## LIST OF FIGURES

Figure

## LIST OF ABBREVIATIONS AND SYMBOLS

| | |
|---|---|
| AM | Alveolar macrophage |
| ANOVA | Analysis of variance |
| ATCC | American Type Culture Collection |
| ATII | Alveolar type II epithelial cell |
| BALF | Bronchoalveolar lavage fluid |
| BEI | Biodefense and Emerging Infections |
| BHI | Brain heart infusion |
| BMDC | Bone marrow dendritic cell |
| BMDM | Bone marrow-derived macrophage |
| BSA | Bovine serum albumin |
| CDC | Centers for Disease Control and Prevention |
| CDM | Chamberlain's defined media |
| CFSE | Carboxyfluorescein succinimidyl ester |
| CFU | Colony forming units |
| CR3 | Complement receptor 3 |
| DC | Dendritic cell |
| DMEM | Dulbecco's Modified Eagle Medium |
| EEA-1 | Early endosome antigen-1 |
| FPI | *Francisella* pathogenicity island |
| GFP | Green fluorescent protein |
| IACUC | Institutional Animal Care and Use Committee |
| IM | Interstitial macrophage |

| | |
|---|---|
| LAMP-1/2 | Lysosome associated membrane protein 1/2 |
| LPS | Lipopolysaccharide |
| LVS | Live vaccine strain |
| MDM | Monocyte-derived macrophage |
| MDDC | Monocyte-derived dendritic cell |
| MHC | Major histocompatibility complex |
| MMP | Matrix metalloproteinase |
| MOI | Multiplicity of infection |
| OD | Optical density |
| ORF | Open reading frame |
| PBS | Phosphate buffered saline |
| $PGE_2$ | Prostaglandin $E_2$ |
| RIPA | Radioimmunoprecipitation assay buffer |
| RPMI | Roswell Park Memorial Institute |
| T6SS | Type six secretion system |
| TLR | Toll-like receptor |
| WHO | World Health Organization |
| :: | Insertion |

# CHAPTER 1

INTRODUCTION

## Discovery of *Francisella*

In 1911, George McCoy described a plague-like disease in ground squirrels in Tulare County California (1). By 1912, McCoy and Chapin had isolated a gram-negative coccobacillus as the causative agent of this plague-like disease and named it *Bacterium tularense* (2). Wherry and Lamb were the first to isolate *Bacterium tularense* in 1914 from a man's conjunctival ulcer (3). In subsequent years, Edward Francis of the Public Health Service extensively studied *Bacterium tularense* and named the disease caused by *Bacterium tularense* tularemia (4). During Francis's studies, it became clear to him that *Bacterium tularense* was also the causative agent rabbit fever, deer fly fever, tick fever and lemming fever. Francis determined *Bacterium tularense* was transmitted to humans via the bite of an infected insect or by handling infected animal carcasses after hunting (4). Indeed, many of the early cases described by Francis were farmers who had been bitten by an infected insect. Laboratory workers were also at risk for contracting tularemia; Francis is reported to have contracted tularemia on four separate occasions (4, 5). In a lecture given by Francis in 1927, he claimed tularemia was, "elucidated from beginning to end by American investigators alone" (5). While early studies of *Bacterium tularense* were conducted by researchers within the Public Health Service, it is clear now that tularemia was not a disease confined to the U.S. Francis serologically confirmed 3 cases of human tularemia in Japan in 1925 and there

are earlier reports from Japan and Europe of symptoms consistent with tularemia (6, 7). In the 1920's *Bacterium tularense* was designated *Pasteurella tularensis*, but DNA hybridization studies performed by Ritter and Gerloff in 1966 indicated the bacteria were not closely related to *Pasteurella* (8). Ritter and Gerloff's data supported earlier groups' work that certain species within the *Pasteurella* genus were more closely related to one another than to other species within the genus (9, 10). In honor of Francis's many contributions to the understanding tularemia, *Pasteurella tularensis* was renamed *Francisella tularensis*. To date, *Francisella* remains the only genus within the family *Francisellaceae* (11).

**Commonly studied *Francisella* laboratory strains**

There are three closely related strains of *Francisella* that differ in pathogenicity in both humans and mice. A summary of the properties of the three commonly used *Francisella* strains is shown in table 1. The most virulent strain is ***F. tularensis*** subspecies (subsp.) *tularensis* (SchuS4). SchuS4 has an infectious dose of 10 bacteria in humans and the $LD_{100}$ for all inoculation routes in C57Bl/6J or BALB/c mice less than 10 colony forming units (CFU) (12-14). Mice inoculated with SchuS4 succumb to infection within 5 days. ***F. tularensis*** subsp. *tularensis* is typically found in Northern America and is classified as a Type A strain (15). Type A strains can be further broken down into two clades- A1 and A2. Clade A1 is found in the eastern U.S. and California while clade A2 is predominately found in the western half of the U.S. (16). The A1 clade is further broken down into A1a and A1b based on the genotypes of human and animal isolates using pulsed field gel electrophoresis (17). Epidemiologic analysis revealed infection with clade A1b causes more severe disease (24% mortality) than A1a (4%) or A2 (0%) (17). It is important to note, however, that the data set

could be biased because isolates are more likely to be collected from severe cases of tularemia.

*F. tularensis* subsp. *holartica* is a Type B strain widely distributed in Asia, Europe, and North America and is less virulent in mice and man compared to Type A strains (16, 18). The commonly used Type B laboratory strain is *F. tularensis* subsp. *holartica* (live vaccine strain (LVS)) (15). The inoculation route dictates the $LD_{50}$ in mice for LVS. For intranasal inoculations, the $LD_{50}$ is $10^3$ CFU whereas intradermal inoculation has an $LD_{50}$ of $10^6$ CFU (19-21). The infectious dose in humans has not been explicitly tested, but 90 % of humans given a respiratory LVS vaccine with $10^4$ organisms developed detectable antibody titers and 59% required no treatment during a SchuS4 challenge (22).

The inclusion of *F. novicida* as a *F. tularensis* subspecies is controversial (23-25). *F. novicida* (U112) is considered a separate species from *Francisella tularensis* due to, "differences in phenotype including chemotaxonomic markers, distinct ecological roles, different clinical and epidemiological characteristics, and differing abilities and modes of invasion and mechanisms of tissue damage in mammals" (23). Huber, et al. argues that DNA-DNA hybridization studies and 16S rRNA and *recA* sequencing indicates *F. novicida* should be a subspecies within the *F. tularensis* species (25). Because *F. novicida* has not been officially recognized as a subspecies, it will be referred to as a separate species here. *F. novicida* is found in Australia and North America and is avirulent in immunocompetent humans (26). In mice, however, it is highly pathogenic with infectious doses (intranasal $LD_{50}$ approximately 10 CFU; intradermal $LD_{50}$ $2.4x10^3$ CFU) and a disease course similar to SchuS4 (27, 28).

### *Francisella* genome properties

Despite vast differences in virulence within mouse and man, the genomes of SchuS4, LVS, and U112 are highly similar with >97% sequence identity (SchuS4 accession number NC 006570, LVS accession number NC 007880, U112 accession number NC 008601). Despite the high degree of sequence identity between Type A strains (SchuS4) and type B strains (LVS), the chromosomes are extensively rearranged compared to one another (29). Type A strains also demonstrate gene rearrangement compared to one another while there is no observed rearrangement observed between two different Type B strains (29). The *Francisella* species' and subspecies' chromosome contains approximately 1.9 Mb, encodes about 1,700 genes, and has a low % G+C content (32%) (30, 31). Basic genome properties for all three strains are summarized in table 1. Nearly one-third of all *Francisella* open reading frames encode hypothetical proteins of unknown function (30). *F. novicida* has very few pseudogenes (14), which may not encode functional proteins, compared to both Type A and Type B strains (303 and 254, respectively) (30). The large number of pseudogenes in Type A and Type B strains suggests these genomes are deteriorating while *F. novicida*'s genome is intact (30). A highly conserved region of *Francisella*'s chromosome between species and subspecies is the *Francisella* pathogenicity island (FPI). The FPI encodes 19 genes and was originally identified because of its reduced %G+C content. Type A and Type B strains have two nearly identical copies of the FPI, while *F. novicida* only has one. Another difference between strains is that SchuS4 and U112 contain *anmK* and *pdpD*, while these genes are absent in LVS (32). While the presence of only one FPI copy in *F. novicida* may explain its decreased virulence in humans, this strain is still highly virulent in mice. Both copies of FPI genes seem to be functionally redundant because deletion or transposon

insertion does not impact virulence; attenuation only occurs when both copies are deleted (33-37). As the name suggests, the FPI is required for *Francisella* virulence. The role of the FPI during infection will be discussed in a later section.

**Tularemia**

Individuals can contact tularemia in a variety of different ways including inhalation, direct contact of infected tissue through a cut in the skin, a bite from an infected arthropod vector, or ingesting contaminated food or water. Tularemia has an incubation period of 3-6 days and is sometimes difficult to diagnose because of the non-specific symptoms, such as: malaise, fever, chills, cough, myalgias, and headache (18, 38, 39). Ulceroglandular tularemia is the most common type of tularemia (90% of cases) and presents with an ulcer, the location of which can help determine how the patients contracted the disease (39). Ulceroglandular patients have swollen lymph nodes that are painful to the touch (40). When an ulcer cannot be found, the patient has glandular tularemia (41). In rare cases, individuals can become infected through the conjunctiva and develop oculoglandular tularemia. Clinical symptoms of oculoglandular tularemia include swollen eyelids, ocular erythema, excessive lacrimation, and pain (38, 41). Another rare form of tularemia is oropharyngeal which is caused by ingesting contaminated food or water. Patients present with ulcerative-exudative stomatitis, pharyngitis, and swelling of the regional lymph nodes (38, 41). Occasionally, there are outbreaks of oropharyngeal tularemia where contaminated water is typically found to be the source of *Francisella* (42-45).

The most severe form of tularemia is the pneumonic form that occurs when *Francisella* is inhaled. Individuals can contract pneumonic tularemia when working with hay on a farm or working as a landscaper. In fact, several of the early cases of tularemia

described by Francis were men working on the farm (4). There is also the risk of aerosol exposure during a bioterrorism attack. Patients with pneumonic tularemia have symptoms generally associated with pneumonia- fever, headache, sore throat, cough, malaise, and increased respiratory rate (38, 41). Chest x-rays are typically un-informative because they are similar to x-rays from patients with tuberculosis, lymphoma, or pneumococcal pneumonia (38, 41, 46). Pneumonic tularemia can also be caused by bacterial dissemination from distal sites and lung pathology is found in approximately 30% of ulceroglandular tularemia patients (39). Before the advent of antibiotics, between 30-60% of individuals with pneumonic tularemia caused by a Type A strain would die (41). Today, the mortality rate is less than 2% (47). To treat tularemia, streptomycin is the first drug of choice, although gentamicin is an acceptable alternative treatment (47). β-lactam antibiotics are ineffective because *Francisella* encodes a β-lactamase (48).

### *Francisella* as a Bioterrorism Threat

Within a few decades of *Francisella*'s discovery in California, it became clear this bacterium could be used in a bioweapon. *Francisella* was tested on prisoners by Japanese scientists led by Ishii Shiro and Kitano Misaji in Manchuria starting in 1932 and continuing until 1945 (49). Experiments involving *Francisella* and other potential bioweapon agents were conducted at a research facility called Unit 731 that employed more than 3000 researchers (49). Also during World War II, tularemia outbreaks affected German and Soviet Union soldiers. Ken Alibeck, a bioweapons scientist from the former Soviet Union, has suggested those outbreaks were intentional (50). The United States began an offensive bioweapon program in 1942 with assistance from Shiro and Misaji who received immunity in exchange for disclosing information regarding their work in Unit 731 (51-53). In the 1950's,

volunteers were exposed to *Francisella* aerosols in Fort Detrick, Maryland to determine human susceptibility and to test potential vaccines and therapies (51). *Francisella* was one of 7 agents weaponized by the United States (51). In 1975, the United Nations held the Convention on the Prohibition of the Development, Production, and Stockpiling of Bacteriological (Biological) and Toxin Weapons and on Their Destruction (BWC) went into effect (54). This treaty prohibited signatories from developing or stockpiling pathogens or toxins, "of types and in quantities that have no justification for prophylactic, protective, or other peaceful purposes" (55). All U.S. offensive biological weapons programs were ended by President Nixon's executive orders in 1969 and 1970 and all stocks were destroyed between 1971 and 1973 (51, 56). Despite the Soviet Union acting as a signatory to the 1972 BWC treaty, Ken Alibeck claims the Soviet Union continued to stockpile *Francisella*, engineered to be antibiotic resistant, until the 1990's (50).

The use of *Francisella* as the infectious agent in a bioweapon would have devastating consequences. *F. tularensis* subsp. *tularensis* has a low infectious dose; as few as 10 organisms can cause severe disease in humans via either cutaneous or aerosol exposure (12, 13). Pneumonic tularemia is the most severe form of disease with high rates of fatality if left untreated (57). Therefore, aerosolization of *Francisella* has the potential to expose a large number of individuals via the most virulent route. A World Health Organization (WHO) committee estimated in 1969 that aerosolization of 50 kilograms of *F. tularensis* over a metropolitan area with a population of 5 million people would result in 250,000 incapacitating casualties and 19,000 deaths (58). One risk noted by the WHO as problematic with *Francisella* was the ability of tularemia outbreaks to persist for weeks, even months, after the initial attack (58). Using the model devised by the WHO, the Centers for Disease

Control and Prevention (CDC) estimated that such an attack would cost society $5.4 billion per 100,000 people exposed (59). Because of its low infectious dose, ease of aerosolization, ability to persist in the environment, and high rates of morbidity and mortality, *F. tularensis* subsp. *tularensis* is classified as a Tier 1 Select Agent by the U.S. government. Because *F. tularensis* subsp. *holartica* LVS and *F. novicida* have been shown to not cause severe disease in man, the CDC has exempted these strains from the regulations governing select agent use.

**Intracellular lifestyle of *Francisella***

*Francisella* is a facultative intracellular pathogen that can infect a wide variety of hosts including amoeba, arthropod vectors, and mammals. One inside the host, *Francisella* targets a variety of cell types for infection. Experiments with human cell lines found *Francisella* is taken into host cells by looping phagocytosis (60). Serum opsonization enhances phagocytosis of *Francisella* and in the absence of opsonization, the mannose receptor can mediate uptake of bacteria (60-64). Complement receptor 3 (CR3), Fcγ receptors, scavenger receptor class A, nucleolin, and lung surfactant protein A also mediate uptake of *Francisella* in mouse and human macrophages, dendritic cells, and neutrophils (62-70). Opsonization of SchuS4 by human C3 increases bacterial uptake into human monocyte-derived macrophages (hMDMs) via CR3 (64). Importantly, C3-mediated SchuS4 uptake does not lead to efficient NF-κB activation or elicit a pro-inflammatory response by hMDMs like C3-independent uptake does (64). C3-mediated uptake of U112 into hMDMs does elicit a pro-inflammatory cytokine response which could partially explain why U112 is non-pathogenic in immunocompetent humans (64). The lack of pro-inflammatory cytokines after C3-mediated SchuS4 uptake is not due to bacterial factors because C3-dependent uptake of paraformaldehyde-fixed SchuS4 does not lead to phosphorylation of ERK whereas C3-

independent uptake of fixed SchuS4 does (64). Dai, et al. proposes that C3-mediated uptake results in a signaling cascade that negatively regulates TLR2 activation (64). C3-mediated uptake is advantageous for SchuS4 because it gains entry to the host cell, but does so in a "silent" fashion.

Once inside the host cell, *Francisella* escapes the phagosome to avoid degradation. The *Francisella*-containing phagosome does undergo portions of the normal phagosome maturation process (reviewed in (71)). Several groups have characterized *Francisella*'s fate upon phagocytosis. Because the groups used different *Francisella* strains, cell lines, and microscopy techniques, the timing of events vary; however, broad and consistent themes emerged. *Francisella* resides in a phagosome for up to 4 hours post-infection. During this time, the phagosome fuses with early endosomes (marked by EEA1) and then late endosomes (marked by CD63, LAMP1/2, and Rab7 GTPase) (61, 72-77). *Francisella*-containing phagosomes do not fully mature into phagolysosomes because they never acquire cathepsin D (61, 72, 75, 78). Whether or not the *Francisella*-containing phagosome becomes acidified is not clear. Two groups have shown limited vacuolar ATPase accumulation on LVS- or Schus4-containing vacuoles in J774.1 and human macrophages (61, 72, 79). Two other groups have found U112- or SchuS4-containing vacuoles to contain vacuolar ATPases and blocking acidification delayed disruption of the phagosomal membrane and consequently bacterial escape (73, 76). The disparate results by these two groups may be a consequence of the mechanism of bacterial uptake. Acidification did not occur when cells were infected with serum opsonized bacteria but did occur when non-opsonized bacteria were used. Further experiments are necessary to clarify whether acidification occurs prior to *Francisella*'s escape from the phagosome.

*Francisella* has completely escaped the phagosome within 4-8 hours post-infection and grows in the cytosol. In vitro and in vivo screens have identified *Francisella* genes necessary for growth and virulence (80-92). However, it is difficult to separate a failure to escape the phagosome from a failure to grow intracellularly because growth requires the bacteria to escape the phagosome. Therefore, additional experiments examining intracellular trafficking of mutants can determine whether a gene is critical for escaping the phagosome or for intracellular growth. The ability of several *Francisella* mutants to escape the phagosome has been determined by microscopy. The best characterized mutant is *iglC*. Several groups, including our own, have found that *iglC* is required for *Francisella* to escape the phagosome (36, 73, 93-95). DotU, IglG, IglI, PdpA, PdpC, and VgrG are other FPI proteins necessary for phagosomal escape (95-101). IglD is required for LVS to escape the phagosome but not U112 (36, 102). MglA, FevR, and MigR are also required for phagosomal escape (36, 94, 103, 104). Because these proteins all regulate FPI expression, it is unlikely they directly disrupt the phagosomal membrane but instead drive expression of proteins that do. Outside of the FPI or regulators thereof, FTT0383, FTT1103, FTT1676, and *carA* are required for phagosomal escape (86, 91, 105). U112 *acpABC* and *hap* have been shown to be required for phagosomal escape; however, other groups have found them dispensable in both SchuS4 and U112 (104, 106-108). Additional experiments are required to resolve these differing results.

As stated before, many screens have identified genes necessary for *Francisella* to grow intracellularly. Several mutations have been well characterized and have shown a dissociation between intracellular growth and escape from the phagosome, i.e. *Francisella* mutants can escape the phagosome but cannot replicate in the cytosol. One such example is

*ripA* (109). LVS *ripA* escaped the phagosome at the same frequency as wild-type but once in the cytosol, did not replicate (109). Other well characterized examples are: FTT0369c, *gtt*, and *purMCD* (90, 91, 110). Two things are necessary to further characterize the genes necessary for phagosomal escape or intracellular growth. First, in-frame deletion strains must be made to confirm the requirement of genes identified from transposon mutant screens. It is possible that polar effects could alter downstream gene transcription and the construction of in-frame deletion strains will avoid that potential issue. Second, phagosomal trafficking needs to be determined for each clean deletion strain to determine whether a gene is required for escape or for growth. These studies are important for our understanding of *Francisella* pathogenesis since escape and intracellular growth are required for virulence.

*Francisella* replicates in the cytosol of host cells until approximately 24 hours post-inoculation until the host cell lyses and bacteria are released or the bacteria are surrounded by a double-membrane structure termed the *Francisella*-containing vacuole (FCV). The FCV is marked by LAMP-1 and cathepsin D indicating fusion with endosomal and lysosomal vacuoles and by autophagosome markers dansylcadaverin and LC3 (77). Despite the presence of lysosomal components, bacteria within the FCV remain intact and do not appear to become damaged (77, 111). Strains that fail to replicate intracellularly (*dipA*, *purMCD*) are found in autophagic-vacuoles, but these strains are destroyed indicating wild-type bacteria prevent destruction by an undefined mechanism (111). Clemens and Horwitz did not observe autophagic vacuoles in human monocyte-derived macrophages or THP-1 cells following SchuS4 inoculation (112). They attributed the difference in the formation of autophagic vacuoles to the use of human versus mouse macrophages. More recently, however, Chong, et al. found autophagic vacuoles did form in human macrophages (111). It

is possible that the formation of autophagic vacuoles is dependent on the culture conditions. Autophagy is used by the host to control other intracellular infections such as *Salmonella*, *Listeria*, or *Streptococcus* (113-115). In the case of these intracellular pathogens the autophagic vacuole forms early after infection; however, *Francisella* isn't found in the FCV until 20 hours post-inoculation (77). Because the FCV forms late in infection and doesn't result in bacterial destruction, its formation could be utilized by *Francisella* to leave the host cell if the host cell does lyse.

### *Francisella* pathogenicity island

Pathogenicity islands are regions of bacterial chromosomes that encode proteins necessary for virulence (reviewed in (116)). The FPI is a 33 kb region that encodes 16-19 open reading frames that are highly conserved between *Francisella* species and subspecies. Nano, et al. first identified the FPI in 2004 by examining partially sequenced *Francisella* genomes (32). Even before the identification of the FPI in 2004, genes within the FPI had already been identified as necessary for *Francisella* virulence (117). Since the initial characterization of the FPI, numerous studies have been conducted examining the requirement of genes within the pathogenicity for intracellular growth, phagosomoal escape, cytopathogenicity, and virulence in mice and Drosophila (see Table 2 in (118)). All FPI genes have been tested for their requirement for intracellular growth and only *pdpC*, *pdpD*, *pdpE*, and *amnK* are dispensable for intracellular growth (118). These four genes are also dispensable for virulence in Drosophila (118). The only FPI gene not required for virulence in mice is *pdpE* (118). Not all FPI genes have been tested for their requirement for phagosomal escape or cytopathogenicity but of the genes tested, *pdpE* is dispensable for both properties, while *iglG* is not required for phagosomal escape and *iglA* is not required

cytopathogenicity (118). Of all genes within the FPI, only *pdpE* is dispensable for all aspects of Francisella virulence. Further studies are necessary to define the requirement of remaining FPI genes for phagosomal escape and cytopathogenicity. It is clear, however, that the FPI is required for *Francisella* to grow in its intracellular niche and to cause disease in mice.

**Type six secretion system encoded by the *Francisella* pathogenicity island**

Genes within the FPI share limited homology with genes encoding type six secretion systems (T6SS) first discovered in *Vibrio cholerae* (97, 100, 119-122). The FPI is a distant relative of all other identified T6SS (123). The core components of T6SS are (*V. cholerae* annotation): ClpV, DotU, Hcp, IcmF, VipA, VipB, and VgrG (118). The most conserved components of the FPI are IglA, IglB, DotU, and VgrG which are homologous to *V. cholerae* VipA, VipB, DotU, and VgrG, respectively (120, 124). Interaction between IglA and IglB depends on a highly conserved IglA α-helix (124). Based on homology with other T6SS, IglA and IglB are hypothesized to form a transmembrane structure capable of mediating the transport of effector proteins into the host cell; this hypothesis still needs to be directly tested in *Francisella* (125, 126). DotU is required for functional T6S and is thought to stabilize the secretion apparatus (100). While VgrG is also highly conserved, it lacks the C-terminal active domain found in other homologs (100). *Francisella* VgrG is predicted to contain multiple β-strands and structural algorithms found it to show structural similarity to bacteriophage tail spike proteins suggesting VgrG could be involved in forming a bridge between *Francisella* and the host cell membrane (100). Like other VgrG homologs, *Francisella* VgrG is secreted into the cytosol of infected macrophages and broth culture supernatants but in a FPI-independent manner (97, 119, 127). U112 IglI was shown by Barker, et al. to be secreted in an FPI- and VgrG-dependent manner but Broms, et al. only

found FPI-independent secretion of LVS IglI (97, 99). It is possible the difference in secretion profiles could have been strain specific, however, more recent work from Broms, et al. demonstrated LVS IglI secretion did require the FPI (128). Broms, et al. used two different approaches (CyaA or TEM beta-lactamase fusion) to determine whether LVS IglI was secreted so it is possible the reporter tag affected secretion and lead to differing results. Using TEM beta-lactamase tags, Broms, et al. determined whether all FPI proteins were secreted into the host cell based on cleavage of the substrate CCF2-AM (128). They found secretion of IglC, IglE, IglF, IglI, IglJ, PdpA, PdpE, and VgrG was dependent on DotU, IglC, IglG, and VgrG (128). All but two of the proteins identified are novel T6SS effector proteins.

Whether *Francisella* encodes a true T6SS is still unclear because three core T6SS components (ClpV, IcmF, and Hcp) have only limited homology with *Francisella* proteins. *Francisella* IglF shares some homology with ClpV, however IglF lacks the conserved AAA+ ATPase domain that supplies energy to drive T6S. PdpB contains some IcmF homology but lacks the Walker A boxes found in conserved IcmF homologs. Finally, IglC has structural, but not sequence, homology to *Pseudomonas aeruginosa* Hcp and is proposed to form a hexameric ring structure due this homology (122). Additional support that *Francisella* uses a T6S-like system is that all of the secreted effectors identified by Broms, et al. are unique to *Francisella* and do not share homology with other T6SS effectors (128). More studies are required to determine whether the function of the proteins encoded by the FPI and whether *Francisella* effectors are secreted by a T6SS or T6S-like system.

**Regulation of the *Francisella* pathogenicity island**

FPI expression is required for intracellular growth so it is not surprising that these genes are up-regulated once the bacteria are inside of host cells (73, 91, 120, 129-131). Expression of FPI genes is regulated by at least six proteins: MglA, SspA, FevR (also referred to as PigR), MigR, PrmA, and Hfq (27, 103, 130, 132-136). MglA and SspA form a heterodimer and interact with RNA polymerase to drive gene expression (133). FevR interacts with the MglA/SspA heterodimer and this interaction is mediated by ppGpp; *fevR* expression is also enhanced by increased ppGpp (137). The FevR regulon is identical to the MglA/SspA regulon except that MglA/SspA regulate *fevR* expression further supporting the importance of the interaction between FevR and MglA/SspA to drive gene expression (132, 137). FevR contains a helix-turn-helix motif that shares homology with MerR transcriptional activators suggesting FevR could target MglA/SspA/RNA polymerase to the FPI (132). MigR also regulates expression of the FPI but since it is required for *fevR* expression, it may be acting indirectly through FevR (103). PrmA regulates expression of the FPI and binds its own promoter and *pdpD*'s promoter following phosphorylation by KdpD (136). Phosphorylated PrmA co-immunoprecipitates with MglA and SspA suggesting these proteins form a complex and regulate gene expression (136). Unlike all other discussed regulators of the FPI which positively regulate gene expression, Hfq represses expression of *Francisella* genes within and outside of the FPI (135). Specifically within the FPI, Hfq represses expression of genes from *pdpA* to *iglJ*, but not all FPI genes leading to speculation that the two operons within the FPI may be regulated differentially (135).

## Innate immune response to *Francisella*

### Macrophages

Macrophages are targeted by *Francisella* for infection in vivo and in vitro experiments often use human or mouse primary macrophages or macrophage-like cell lines to examine various aspects of *Francisella* pathogenicity. In vivo, *Francisella* infects peritoneal, airway, lung interstitial, and alveolar macrophages (Chapter 4, (138-141)). Mouse macrophages infected with LVS are unable to produce pro-inflammatory cytokines, even when stimulated with *E. coli* LPS (140, 142, 143). Macrophages infected with LVS are also subject to MHCII down-regulation (144). These results will be discussed further in the immune evasion section. Macrophage activation by IFN-γ prevents intracellular growth of U112, LVS, and SchuS4 (36, 75, 145). U112 does not escape the phagosome of human monocyte-derived macrophages activated with IFN-γ (75). IFN-γ activation of J774.1 mouse macrophages decreases, but does not abolish, LVS's ability to escape the phagosome (93). SchuS4 escapes the phagosome of IFN-γ activated bone marrow-derived macrophages and human monocyte-derived macrophages but replication in the cytosol is abrogated (145). Differences in experimental design could impact when replication is affected from strain to strain; however, it is clear that macrophage activation by IFN-γ prevents *Francisella* replication and is a mechanism by which the immune system controls the infection.

### Dendritic Cells

*Francisella* also infects dendritic cells (DC) in vivo (Chapter 4, (140, 141)). SchuS4 also replicates in human monocyte-derived DCs (146). DCs are professional antigen presenting cells and are therefore a key bridge between innate and adaptive immunity (reviewed in (147)). During antigen presentation, DCs secrete cytokines that influence how

naïve T cells differentiate into effector T cells (147). Because DCs are a crucial component of the immune response, they serve as an excellent target for immune suppression by *Francisella*. SchuS4 actively suppresses cytokine responses and up-regulation of MHCII and CD86 in human and mouse DCs whereas LVS does not (66, 140, 141, 146, 148-150). Immune suppression in DCs will be discussed in more detail below in the immune evasion section.

**Natural Killer Cells**

Natural killer (NK) cells are an important component of innate immunity and have cytolytic activity in the absence of antigen specificity (reviewed in (151)). NK cells produce perforin and IFN-γ. Production of perforin is dispensable during a LVS infection because perforin-deficient mice are not more susceptible than wild-type (152). IFN-γ is critical for controlling *Francisella* infection and is produced by NK cells following LVS infection (153-157). Depletion of NK cells renders mice more susceptible to intranasal LVS infection; however, has no effect on disease course (bacterial burdens and weight loss) during primary intranasal SchuS4 infection (153, 158). It is important to note, however, that mice succumb so rapidly to SchuS4 infection that it may be difficult determine whether a treatment worsens disease course. Crane, et al. found very few IFN-$\gamma^+$ NK cells in the spleen or lung of mice intranasally inoculated with SchuS4 further supporting data that NK cell depletion does not impact survival (159). While NK cells do not play a protective role during SchuS4 infection, treatment of mice with Acai polysaccharide potentiates IFN-γ production by NK cells and increases percent survival after SchuS4 aerosol challenge (160). Administration of CpG primes NK cells in a TLR9-dependent manner and enhances their ability to control an

infection of BMDMs (161). These data suggest that immunomodulating therapy targeting IFN-γ production by NK cells could be used to treat tularemia.

**Neutrophils**

Neutrophils are critical during infection and assist in bacterial clearance by phagocytosis and the production of reactive oxygen species (reviewed in (162)). Neutrophils also produce chemotactic factors that recruit other innate immune cells to the site of infection (162). In a *Francisella* infection, neutrophils are present at the site of infection in a variety of inoculation routes (163-165). Depletion of neutrophils using monoclonal antibody had only moderate effects of bacterial burdens in an aerosolized LVS model, despite the presence of neutrophils present in the lungs early after infection (165). Neutrophil depletion during intravenous or intradermal infection with LVS caused mice to succumb to otherwise sub-lethal doses (166). The differences observed in mice infected with LVS could be attributable to the different routes of infection. Depletion of neutrophils had no effect on mean time to death compared to control mice in an aerosolized SchuS4 model, however, death occurs so rapidly following SchuS4 infection (5 days) that it might be difficult to shorten time to death (167). Similar results were found when neutrophils were depleted during an intranasal infection with SchuS4 (168). It is important to note, however, that the studies examining the importance of neutrophils used the monoclonal antibody RB6-8C5, which recognizes Ly6G and Ly6C (169). Ly6C is also present on dendritic cells, some lymphocytes, and monocytes (169). Therefore, the results are confounded by the possibility that other cell types important during a *Francisella* infection were also depleted. To avoid depleting other cell types, studies should use clone 1A8 which is specific for Ly6G and will only deplete neutrophils (169). The presence of neutrophils could be detrimental during infection if the neutrophils

severe host tissue damage. Matrix metalloproteinase 9 (MMP9) is an enzyme that degrades the extracellular matrix and recruits neutrophils and macrophages by creating a gradient of KC. Recruitment of neutrophils in turn leads to additional MMP9 release and amplification of the recruitment signal. Mice deficient in MMP9 have increased bacterial burdens and are more susceptible to infection with LVS or SchuS4 (170). Altogether, these results suggest that neutrophils can play a beneficial role in the immune response to *Francisella*, however, too much of a neutrophil response is detrimental to the host.

The importance of neutrophil effector function (i.e. reactive oxygen species (ROS) production) has also been investigated. LVS infection of mice deficient in phagocyte oxidase ($p47^{phox-/-}$) have a decreased $LD_{50}$ compared to wild-type mice (171). $gp91^{phox-/-}$ mice exhibit similar survival curves as wild-type mice but do have significantly increased bacterial burdens (168). It is important to note that neutrophils are not the only source of ROS; macrophages also produce ROS (172). Therefore mice deficient in enzymes required to produce ROS affect multiple cell types and this must be taken into account when considering the previous data. In human neutrophils, opsonized LVS is capable of infecting cells but inhibits respiratory burst and replicates in the cytoplasm (173). *katG* encodes a catalase capable of neutralizing ROS (174). LVS *katG* and SchuS4 *katG* are more susceptible to $H_2O_2$ but only LVS *katG* is highly attenuated in vivo (174). The difference between *katG* strains could be caused by the difference in pathogenicity of the parental strains; LVS is highly attenuated compared to SchuS4 in mice. These data indicate that *Francisella* has evolved mechanisms to include inhospitable neutrophils in its replicative niche and expressed proteins to combat ROS. *Francisella* certainly targets neutrophils for infection; neutrophils comprise the dominant population infected with U112, LVS, and SchuS4 on day 3 post-

infection in the lung (139). We also found neutrophils to be the dominant infected cell type in the epidermis and dermis following intradermal inoculation (Chapter 5). Because neutrophils do not reside in normal, naïve skin, we hypothesize neutrophils are recruited to the site of infection where they ingest invading *Francisella*.

**Innate immune detection of *Francisella***

**Toll-like receptors**

Toll-like receptors (TLRs) are a class of pattern recognition receptors (PRRs) that recognize conserved microbial products (reviewed in (175)). TLRs are expressed on the surface of host cells or in the endosome (176). Signaling through TLRs requires adaptor proteins such as MyD88, TRIF, and TIRAP and leads to the production of type I interferon and pro-inflammatory cytokines (176). TLR2 recognizes lipoproteins and is the most important TLR during infection with *Francisella* (177). *Francisella* has three identified TLR2 ligands- LpnA (also known as Tul4), FTT_1103, and FTL_0645 (178-180). $TLR2^{-/-}$ mice are more susceptible to LVS intranasal and intradermal infection and have increased bacterial burdens in the spleen, liver, and lung (177). TLR2 signaling is required for the induction of pro-inflammatory cytokines in LVS infected peritoneal macrophages and BMDCs (181, 182). Since TLR2 signals through the adaptor, MyD88, it is not unexpected that $MyD88^{-/-}$ mice are also more susceptible to LVS infection than wild-type mice (155, 177). The phenotype of $MyD88^{-/-}$ mice is more severe than $TLR2^{-/-}$ mice suggesting there are other PRRs that signal through MyD88. TLR4 also signals through MyD88, however, $TLR4^{-/-}$ mice are not more susceptible to intranasal infection with U112 or LVS or aerosolized SchuS4 (177, 183, 184). TLR4 recognizes lipopolysaccharide (LPS), but *Francisella* expresses an altered form of LPS that does not initiate signaling through TLR4

(185). This immune evasion mechanism is discussed in more detail below. Two TLRs have been shown to have no role in *Francisella* infection. TLR5 recognizes flagellin, but *Francisella* does not express flagellin. Therefore, a NF-κB luciferase reporter is not activated when TLR5-expressing cells are stimulated with LVS (150). TLR9 senses CpG DNA in the endosome/phagosome. $TLR9^{-/-}$ mice have similar bacterial burdens and survival curves as wild-type mice when inoculated intradermally with LVS indicating this PRR is not required to sense infection with *Francisella* (155).

**Inflammasome**

As discussed above, *Francisella* escapes the phagosome and replicates in the cytosol. *Francisella* evolved the ability to live intracellularly as a way to "hide" from the immune response, yet in the constant dance between host and pathogens, the host has evolved cytosolic sensors to detect pathogens, like *Francisella*, that violate the sanctity of the cytosol. A major class of cytosolic PRRs are the NOD-like receptors (NLRs) (reviewed in (186)). NLRs form the inflammasome by interacting with the adapter protein, ASC, which recruits and then cleaves pro-caspase-1 into its active form (reviewed in (187)). Caspase-1 can then process pro-IL-1β and pro-IL-18 into their active forms. There are numerous NLRs family members (22 in humans; 34 in mice) that respond to a variety of signals from molecules associated with pathogens to self-derived molecules like cholesterol crystals (187).

In the context of LVS or U112 infection, production of IL-1β and IL-18 requires ASC, caspase-1, and AIM2 but not the alternative adaptor Ipaf (101, 188-190). Additionally, phagosomal escape is required for caspase-1 activation because U112 *mlgA* or *pdpA* mutants that do not escape are unable to cause pro-caspase-1 cleavage (101). AIM2 co-localizes with bacterial DNA suggesting that lysed *Francisella* in the cytosol activates the AIM2

inflammasome (188, 189). Mice deficient in caspase-1, ASC, or AIM2 are more susceptible to U112 infection compared to wild-type mice as measured by bacterial burdens and/or survival (101, 188, 189). Type I interferons are also required for inflammasome activation because IFNAR$^{-/-}$ macrophages do not cleave caspase-1 or produce mature IL-1β or IL-18 (191). Type I interferon increases AIM2 expression supporting a mechanism by which the cells are sensitized to DNA recognition by type I interferon signaling. Yet, despite the importance of type I inteferons for inflammasome activation in vitro and the increased susceptibility of mice deficient in required inflammasome components, IFNAR$^{-/-}$ mice are more resistant to U112 and LVS infection (our unpublished data and (192)). The discordance in results could be explained by the finding that IFNAR$^{-/-}$ mice have increased IL-17A production and increased neutrophil numbers which could increase bacterial clearance, thereby promoting host survival (192).

**Immune evasion by *Francisella***

**Targets innate immune cells**

One immune evasion strategy utilized by pathogenic bacteria is to target innate immune cells for infection and subsequent killing (193). *Francisella* has been shown to target a variety of cell types following infection including dendritic cells, macrophages, monocytes, neutrophils, and alveolar type II (ATII) epithelial cells (139-141, 194). Hall, et al. performed a comprehensive study to identify the infected cell repertoire in the lungs of mice inoculated with GFP-expressing U112, LVS, or SchuS4 using flow cytometry (139). Alveolar macrophages compose 50-80% of all infected cells for all three *Francisella* strains one day post-infection (139). By day 3 post-inoculation, the infected cell repertoire is very different with neutrophils comprising 45-80% of infected cells (139). The experiments by

Hall, et al. provided insight into *Francisella*-host interactions later in infection, but did not identify the cell types that *Francisella* initially targeted for infection. Bosio, et al. identified *Francisella* infected airway macrophages and lung dendritic cells one hour post-inoculation (140, 141). Our laboratory has also worked to identify the infected cell repertoire in the lung and skin after intranasal or intradermal inoculation. These data are presented in Chapter 4.

### *Francisella* modulates macrophage function

As indicated in the preceding section, *Francisella* targets a variety of immune cells for infection. Once inside of these cells, *Francisella* is capable of modulating their cytokine response. J774.1 cells infected with LVS do not secrete TNF-α or IL-1β, even when stimulated with *E. coli* LPS (142). Bone marrow-derived macrophages (BMDM) do not significantly up-regulate MHCII or CD86 (co-stimulatory molecule) upon inoculation with LVS (140). Additionally, infected BMDMs do not produce detectable CCL2, IL-1β, IL-6, IL-10, MIP-2, or TNF-α when infected with LVS (140, 143). Human monocyte-derived macrophages are able to produce pro-inflammatory cytokines after infection with LVS (143). Alveolar macrophages purified from the lung after intratracheal inoculation with LVS behaved like BMDMs with no up-regulation of MHCII or CD86 and no cytokine production (140). Together, these data indicate that infection with LVS does not induce phenotypic (antigen presentation) or functional (cytokine production) maturation of macrophages. These data are summarized in table 2.

### *Francisella* modulates DC function

DCs infected with *Francisella* also have their responses modulated. LVS infection of bone marrow-derived DCs (BMDC) leads to up-regulation of MHCII and CD86 but not production of IL-6, IL-10, or TNF-α (140). Therefore, unlike BMDMs, BMDCs can undergo

phenotypic maturation without undergoing functional maturation. Airway DCs are infected with LVS following intratracheal inoculation and these cells support bacterial replication (140). Like BMDCs, mouse airway and lung DCs up-regulate MHCII and CD86 upon LVS infection and these cells do not produce TNF-α as determined by flow cytometry (140). SchuS4 infection, on the other hand, does not cause MHCII or CD86 up-regulation of airway, lung, or lymph node DCs (141). Furthermore, cultured lung and airway cells from SchuS4 infected mice do not produce levels of TNF-α or IL-12p40 that is increased compared to uninfected mice (141). LVS infection of DCs also inhibits cytokine production when infected cells are stimulated with LPS (TLR4 agonist) or zymosan (TLR2 agonist) (140). Likewise, SchuS4 infection prevents CD86 up-regulation on DCs or monocyte recruitment when mice are treated with intranasal LPS (141). Both LVS and SchuS4 infection lead to the production of the anti-inflammatory cytokine, TGF-β (140, 141). Together, these data indicate that infection with LVS and SchuS4 suppress host immunity by decreasing antigen presentation by preventing functional maturation of DCs and by inducing TGF-β to form an immunosuppressive environment. As a consequence, *Francisella* can persist in the host.

Human monocyte-derived DCs infected with SchuS4 up-regulate MHCII and CD86 but do not produce any pro- or anti-inflammatory cytokines (146). SchuS4 infected cells also fail to respond to secondary stimulation with *E. coli* LPS (146). The inhibition of cytokine production is an active process by SchuS4 because cells inoculated with killed SchuS4 can produce cytokine in response to *E. coli* LPS (146). Monocyte-derived DCs express little surface CD14, a co-receptor for TLR2 and TLR4 (149). Addition of soluble CD14 allows monocyte-derived DCs to produce cytokine after SchuS4 inoculation (149). SchuS4

inoculation of monocyte-derived DCs leads to the production of IFN-β and the selective inhibition of IL-12p40, but not TNF-α, production (148). Incubation of human DCs with SchuS4 conditioned media also resulted in a failure of those to produce cytokine after *E. coli* LPS stimulation suggesting that SchuS4 secretes molecule(s) that can inhibit cytokine production (146). LVS does not have the same inhibitory effect on human monocyte-derived DCs. DCs up-regulate CD40, CD86, and MHCII and produce a variety of cytokines after LVS inoculation (66, 150). The ability of LVS to induce a pro-inflammatory response in human DCs and macrophages could indicate why LVS is not pathogenic in humans, while the inability of human DCs to respond to a SchuS4 infection is likely one reason SchuS4 is highly pathogenic in people. These data are summarized in table 2.

**Altered LPS structure**

LPS is a pathogen associated molecular pattern (PAMP) abundantly present on the surface of gram negative bacteria (195). LPS consists of 3 distinct structural regions: O-antigen, core, and lipid A (196). LPS lipid A signals through TLR4 to activate pro-inflammatory immune responses (197). MALDI-TOF mass spectrometry showed that many different *Francisella* isolates (including subsp. *tularensis*, *holartica*, and *mediasiatica*, and *F. novicida*) have conserved tetra-acetylated lipid A with longer carbon chains (185, 198-200). Purified *F. novicida* LPS fails to stimulate human or mouse cell lines to produce cytokines like IL-8, TNF-α, or IL-1β (185). Additionally, *F. novicida* LPS does not act as a TLR4 antagonist, as cells can respond to *Salmonella* LPS even in the presence of 100 ng/mL *F. novicida* LPS (185). Finally, aerosol delivery of *F. novicida* LPS does not result in neutrophil recruitment to the lung like *E. coli* LPS does (185). Together, these data indicate

that *Francisella* LPS does not stimulate a pro-inflammatory immune response, allowing the bacteria to evade TLR4 mediated detection.

**Induction of $PGE_2$**

SchuS4, LVS and U112 induce infected bone marrow derived macrophages to synthesize and secrete the lipid mediator, prostaglandin $E_2$ ($PGE_2$) (95, 201). Induction of $PGE_2$ synthesis and secretion alters the immune response so that *Francisella* can persist in the host. $PGE_2$ is a pleotropic molecule that has a variety of effects on the immune response depending on its local concentration and the E-prostanoid receptor (EP) that binds $PGE_2$ (reviewed (202)). $PGE_2$ is required for dendritic cell migration from the infected tissue to the draining lymph node (203-205). $PGE_2$ also effects cytokine production, and therefore naïve T cell differentiation, by antigen presenting cells via inhibition of IL-12 production (decreases Th1) and enhancement of IL-23 production (increases Th17) (206-209). Finally, $PGE_2$ signaling through E-prostainoid receptor 4 (EP4) decreases calcium flux and therefore early T cell activation (210). $PGE_2$ engagement of EP4 causes T cells produce less IL-2 thereby decreasing T cell proliferation (210, 211). $PGE_2$ signaling through EP4 also causes T cells to produce less IFN-γ, but more IL-4 and IL-5 thus skewing the T cell response from a Th1 response that mediates clearance of intracellular pathogens like *Francisella* towards a Th2 response that is suited for clearing extracellular pathogens (211, 212). Overall, $PGE_2$ induced by *Francisella* decreases the number of responding T cells and skews the T cells that do respond towards effector functions that are ineffective at bacterial clearance. Intranasal inoculation of B6 mice with LVS increases $PGE_2$ concentration in the lung (213). Inhibition of $PGE_2$ synthesis with indomethacin, a COX1/2 inhibitor, decreases $PGE_2$ concentration, increases the number of IFN-γ producing T cells, and results in faster bacterial clearance

(213). Therefore, induction of $PGE_2$ is an effective immune evasion strategy utilized by *Francisella* to persist in the host.

We have identified the *Francisella* genes necessary for induction of $PGE_2$ synthesis and secretion (95). These data are presented and discussed in Chapter 5.

**Down-regulation of MHC**

*Francisella* further modulates the adaptive immune response by causing down-regulation of MHCII expression on IFN-γ activated bone marrow derived macrophages (144). The ability of *Francisella* to decrease surface expression of MHCII is dependent on $PGE_2$ synthesis by infected host cells (144). Autocrine and/or paracrine $PGE_2$ signaling through a yet unidentified EP leads to the production of a >10 kDa soluble factor, termed FTMØSN, that induces IL-10 production (214). IL-10 signaling leads to increased expression of the ubiquitin ligase MARCH1 (214). Ubiquitination of MHCII leads to its degradation and therefore decreased antigen presentation to $CD4^+$ T cells. The identity of FTMØSN remains unknown, but Hunt, et al. report it is not IL-10, TGF-β, IL-6, VEGF, MIP-1α, or leukemia inhibitory factor (214). Additionally, production of FTMØSN does not require TLR2 signaling or caspase-1 processing (214). Although the signaling cascade that leads to MHCII down-regulation is complex, it does require $PGE_2$. Therefore, inhibition of $PGE_2$ synthesis would not only increase antigen presentation to $CD4^+$ T cells but those T cells would make a more effective response, as described in a subsequent section.

**Adaptive immune response to *Francisella***

**Primary response by γδ T cells**

While $\alpha\beta^+$ TCR T cells are critical during primary and secondary infection with *Francisella*, $\gamma\delta^+$ TCR T cells are dispensable. γδ $TCR^{-/-}$ mice are not more susceptible to

primary intranasal or intradermal infection with LVS (215, 216). During primary infection with SchuS4 in a convalescent model, γδ TCR$^{-/-}$ mice are not more susceptible than wild-type mice (159). Additionally, γδ TCR$^{-/-}$ survivors of the primary infection were also not more susceptible than wild-type survivors during a secondary infection (159). γδ T cells produce IL-17 upon intranasal infection with LVS, but since γδ TCR$^{-/-}$ mice are not anymore susceptible to infection than wild-type mice, γδ T cells and their effector functions are not essential in mouse models of tularemia (215, 217).

Although γδ T cells appear to be dispensable in mice, γδ T cells respond to *Francisella* infection in humans. In particular, Vγ9/Vδ2 γδ T cells comprise almost all peripheral blood γδ T cells and 30-40% of all CD3$^{+}$ T cells even one month after infection (218, 219). Vγ9/Vδ2 γδ T cells respond to phosphoantigens and are capable of controlling LVS-infected THP-1 cells (human monocyte cell line) (220). Some, but not all patient Vγ9/Vδ2 γδ T cells were also capable of controlling growth of SchuS4 in THP-1 cells (220). Depletion of IFN-γ increased the number of intracellular LVS suggesting IFN-γ is produced by Vγ9/Vδ2 γδ T cells and helps control the infection (220). Whereas Vγ9/Vδ2 γδ T cells tremendously expand after a naturally acquired *Francisella* infection, LVS vaccination by scarification does not cause this same expansion (218). Unfortunately, mice lack γδ T cells analogous to Vγ9/Vδ2 in humans so this result cannot be studied further.

**Primary response by B cells**

*Francisella* has long been thought of as an intracellular pathogen that spends little time outside of host cells during infection. Furthermore, when bacteria were detected in the blood, they were thought to reside within migrating leukocytes (221). Forestal, et al. was the first to counter the long-held paradigm by showing that non-cell associated *Francisella* are

found in the plasma of infected mice (222). Both LVS and SchuS4 were found free in the plasma following intranasal or intradermal inoculation indicating the phenomena was not specific to a specific *Francisella* strain or route of infection (222). Yu, et al. also found U112 free in the plasma of intranasally infected mice (223). Moreover, LVS and SchuS4 were capable of growing in whole mouse blood indicating the blood represents another replicative niche for *Francisella* (222). Data revealing an extracellular lifecycle stage of *Francisella* within a host highlighted the potential importance of B cells in clearance of the primary infection.

Despite an extracellular phase of infection, mice deficient in B cells are only moderately more susceptible to intradermal or aerosol LVS infection than wild-type mice suggesting B cells aren't mediating bacterial clearance (167, 224). In a convalescent model of SchuS4 infection, B cell deficient mice succumb to infection 10 days after stopping levofloxacin treatment (159). *Francisella* can adhere to and infect B cell lines or splenocytes and induce apoptosis (225). Because *Francisella* can infect a variety of cell types, it isn't surprising that B cells can be infected as well (139). Infection of B cells also allows them to serve as antigen presenting cells and have another role in the infection besides antibody production. In fact, during secondary infection B cells likely play a role in antigen presentation and/or cytokine production (discussed below) (224).

B-1a cells, or innate immune B cells, are sources of natural antibody and respond to T-independent antigens. Because they are T-independent, B-1a cells respond rapidly to antigen and produce antibodies within 2-3 days of vaccination. B-1a cells can be stimulated with LVS LPS to produce anti-LPS antibodies (226, 227). LVS LPS vaccination causes an increase in splenic and peritoneal cavity B-1a cells which peak at day 5 post-vaccination

(226). Splenic B-1a cells rapidly decline after day 5 but peritoneal B-1a cells are detectable for up to 2 months post-vaccination (226). In the case of a convalescent SchuS4 infection, B-1a cells exacerbate the infection by producing IL-10 which decreases IFN-γ production by NK cells (228). These data highlight another difference between LVS and SchuS4 infection where B-1a cells help resolve LVS infection via antibody production and B-1a cells are detrimental during SchuS4 infection.

In humans, the presence of serum anti-*Francisella* antibodies is often used to diagnose tularemia. Natural infection with *Francisella* induces IgM, IgG, and IgA antibodies that peak between 4 and 7 weeks after infection and are present in the serum for up to11 years after infection (229-231). When anti-*Francisella* titers were determined in a cohort of individuals in Sweden infected 25 years prior, titers were below detection limit (232). Intradermal vaccination with LVS also leads to peak agglutination titers between 2 and 4 weeks post-vaccination (233, 234). Anti-*Francisella* antibodies were also present when serum was tested 1.5 years after vaccination (233).

**Secondary response by B cells**

Early studies examining the ability of immune sera to transfer protection to naïve mice indicated antibodies did not confer protection upon SchuS4 challenge (235). On the other hand, mice could be protected during LVS challenge by transfer of LVS immune sera or anti-*Francisella* LPS antibodies (19, 236-239). Passive transfer of antibody from SchuS4 infected mice treated with levofloxacin (to help resolve the primary infection) was able to mediate protection during lethal SchuS4 challenge (240). Immunization with *Francisella* LPS or conjugates thereof were also protective during LVS but not SchuS4 challenge (28,

226, 227, 241-243). B-1a cells produce antibodies directed against LVS O-antigen that are protective during LVS challenge (226, 227).

More recent studies have vaccinated mice with inactivated LVS in the presence of immunostimulatory compounds like IL-12, immunostimulatory complexes (ISCOMs), or cholera toxin and found some protection during SchuS4 challenge (239, 244-247). Vaccination with heat killed LVS plus IL-12 provided 100% protection during intranasal LVS challenge and was dependent on IgA (244). When mice were vaccinated with heat killed LVS and an IL-12-expressing viral vector, mice were protected during lethal intraperitoneal challenge (239). The authors did not directly show the requirement of B cells but did show high IgG titers and the absence of a T cell response after vaccination, leading them to conclude protection was B cell-mediated (239). While several groups have shown partial protection during SchuS4 challenge in mice vaccinated with inactivated LVS in the presence of immunostimulatory compounds, they have not shown any evidence that protection was antibody-dependent (245-247). In fact, Bitsaktis, et al. found their vaccination regimen was protective in IgA-deficient mice indicating the B cell response was not required to mediate protection in their model (245). Oral vaccination with LVS did confer protection during SchuS4 challenge that was mediated by $CD4^+$ T cells and B cells (248). Additional studies are necessary to identify whether B and/or T cells are mediating protection in vaccination studies. A better understanding of the mechanisms underlying protection will assist in the rationale design of vaccines.

During a secondary infection, B cell deficient mice are much more susceptible than their wild-type counterparts (224). Susceptibility is not caused by a lack of antibody production because passive transfer of sera does not confer protection (224). Instead,

transfer of B cells from immune mice leads to protection suggesting another role for the B cells besides antibody production (224). B cells could be an important source of antigen presentation during the secondary infection or could produce cytokines and/or chemokines that influence both innate and adaptive responses. The mechanisms that cause B cells to confer protection need to be further elucidated.

**Primary response by αβ T cells**

Years of *Francisella* research have conclusively shown the requirement of T cells for the clearance of a primary infection and the development of protective immunity. Mice lacking all T cells such as αβ $TCR^{-/-}$ or *nu*/*nu* mice develop a chronic infection that they eventually succumb to (216, 249, 250). When either $CD4^+$ or $CD8^+$ T cells are singly depleted, mice can resolve the primary LVS intradermal infection and can survive a lethal LVS secondary intraperitoneal infection (216). Mice depleted of both $CD4^+$ and $CD8^+$ T cells develop a chronic LVS infection with steady bacterial burdens for months after infection (216). The cells that control, but not are incapable of clearing, the infection are $CD4^-CD8^-NK1.1^-TCR\alpha\beta^+Thy1.2^+$ double negative (DN) T cells (251, 252). These cells are prevalent in the lungs of intranasally inoculated mice, but are less abundant in the spleen and lung after intradermal inoculation (252). The $LD_{50}$ of SchuS4 in mice is <10 CFU and immunocompetent mice succumb rapidly to infection (5 days) (14). Therefore, it is not surprising that mice lacking T cells also succumb rapidly to SchuS4 infection (21, 159, 167). Chen, et al. has shown that SchuS4 infection causes thymic atrophy and decreased numbers of $CD4^+CD8^+$ (double positive) thymocytes (253). T cell responses during LVS infection peak on day 10 post-inoculation (213). During a convalescent SchuS4 infection, T cell

responses were maximal on day 7 post-inoculation (159). The authors only examined days 7, 14, and 21 so the peak could be a consequence of the time points analyzed (159).

There are three key effector cytokines produce by $CD4^+$, $CD8^+$, and/or DN T cells during *Francisella* infection. IFN-γ is critical for survival during primary LVS infection. Depletion using anti-IFN-γ antibody significantly increases bacterial burdens (156, 254). Additionally, IFN-γ-deficient mice succumb to sub-lethal LVS infectious doses (155). IFN-$\gamma R^{-/-}$ mice even succumb to SchuS4 during treatment with levofloxacin, highlighting the importance of IFN-γ during infection (159). To complete molecular Koch's postulates, treatment with recombinant IFN-γ decreases bacterial burdens, confirming the requirement of IFN-γ during LVS infection (255). While a variety of cell types produce IFN-γ during *Francisella* infection, IFN-γ production by T cells is necessary to control bacterial growth in infected BMDMs (157, 256). $CD8^+$ and DN T cells also produce IFN-γ that is capable of controlling bacterial growth in BMDMs but these T cell subsets don't rely on IFN-γ as much as $CD4^+$ T cells do to control infection (256). $CD8^+$ T cells required TNF-α to control LVS growth in BMDMs (256, 257). Depletion of TNF-α significantly increases bacterial burdens following LVS infection (254). In vivo, $CD4^+$, $CD8^+$, and DN T cells produce IFN-γ after intradermal and intranasal inoculation with LVS (213, 252, 258). Another critical cytokine during *Francisella* infection is IL-17. Intranasal inoculation with LVS leads to the expansion of IL-$17A^+$ $CD4^+$ (Th17) cells and IL-$17A^+$ DN T cells (213, 252, 258). Production of IL-17A is critical for controlling infection because IL-17A- or IL-17 receptor-deficient mice have increased bacterial burdens during respiratory infection (217, 252). IL-17A depletion also results in increased bacterial burdens and quicker mean time to death during respiratory infection (215, 217). Th17 cells are only detected in the lung following intranasal infection

and not intradermal infection, despite similar bacterial burdens early after infection (213). Similar results are seen during *Listeria monocytogenes* infection where Th17 cells are only found after intranasal infection and not intravenous infection (259). To further support the role of Th17 cells during intranasal but not intradermal infection, IL-17A deficient mice do not have higher lung or liver burdens compared to wild-type mice (252). There is a slight, but statistically significant increase in spleen bacterial burdens in IL-17A$^{-/-}$ mice compared to wild-type controls (252).

Without MHCI or MHCII tetramers, it has been difficult to study the responses of antigen-specific T cells (tetramers reviewed in (260)). An immunodominant CD4$^{+}$ epitope (LpnA$_{86-99}$) comprises up to 20% of CD4$^{+}$ T cells in B6 mice and is therefore an excellent candidate for the use in MHCII tetramer development (261). T cells from mice vaccinated intradermally responded to purified bacterioferritin, GroEL, and KatG suggesting these proteins also contain CD4$^{+}$ and/or CD8$^{+}$ epitopes (262). Humanized HLA-DR4 transgenic mice have been used to identify human MHCII epitopes (263). FopB was identified in a screen and contains an epitope that human CD4$^{+}$ T cells respond to; immunization with FopB also protected HLA-DR4 transgenic mice during lethal LVS challenge (263). McMurry, et al. predicted human MHCI and MHCII epitopes using bioinformatics and then tested these epitopes on peripheral blood mononuclear cells (PBMCs) from individuals that had previously contracted tularemia (264). Using this approach, they identified candidate peptides that 95% of patients responded to (264). The authors then tested whether these peptides could be used in a vaccination regimen in HLA-DR4 transgenic mice and found some protection during lethal LVS infection (265). Because the authors used HLA-DR4 transgenic mice, they were only able to examine "human" CD4$^{+}$ T cell responses and not

$CD8^+$ T cell responses, even though the identified peptides could be stimulating both T cell subsets. Further identification of $CD4^+$ and $CD8^+$ epitopes is important for two reasons. First, the ability to use tetramer will allow researchers to track *Franicsella*-specific T cells throughout the primary infection, the development of memory, and a secondary response. MHCII tetramer with $IA^b$ presenting $LpnA_{86\text{-}99}$ is currently being developed. Although $CD8^+$ T cells clearly respond to *Francisella* antigen, an epitope has not yet been identified. Epitope identification is also important for vaccine development so that humans could be immunized with peptides that induce a robust, protective immune response. The use of humanized HLA-A2/DR4 mice could assist in these efforts.

Because T cells are required for the clearance of a primary infection and the development of protective immunity, it is not surprising that *Francisella* has evolved mechanisms to interfere with T cell responses. *Francisella* infection causes host cells to synthesize and secrete prostaglandin $E_2$ ($PGE_2$) which shifts the immune away from a Th1 response and towards a less effective Th2 response (201, 266). MHCII is also down-regulated in a $PGE_2$-dependent process (144, 214). Both of these immune evasion mechanisms are discussed in more detail above.

**Secondary response by αβ T cells**

Survival of a secondary LVS infection requires $CD4^+$ or $CD8^+$ T cells; either subset is sufficient to mediate bacterial clearance (216). Both IFN-γ and TNF-α are necessary for survival during secondary infection with LVS (Chapter 4, (254, 267)). During SchuS4 secondary infection, both $CD4^+$ and $CD8^+$ T cells are required for protection (21, 268, 269). IL-17 production in the lung correlated with protection in mice challenged with aerosolized SchuS4 (270). Despite correlating with protection, depletion of IL-17 with antibody did not

significantly increase bacterial burdens (270). Similarly, we found IL-17A depletion had no effect on weight loss or bacterial burdens in mice challenged intranasally with LVS (Chapter 4).

Memory T cells persist in patients that were vaccinated or naturally acquired tularemia. Upon re-stimulation, T cells produced IFN-γ, IL-2, and TNF-α (271-273). When the ability of T cells to produce IL-17 and IL-22 was evaluated in PBMCs from LVS vaccinated individuals, both IL-17 and IL-22 were detected in $CD4^+$ T cells (274). These data indicate that human infection also induces Th17 cells. Despite the absence of detectable anti-*Francisella* antibodies in people 25 years after infection, peripheral blood did contain T cells that produced IFN-γ following stimulation with *Francisella* antigen (232). After a specific outbreak of tularemia, there were very few cases for the next 25 years in the region these individuals lived, therefore it was unlikely they were exposed to *Francisella* again (232). In a more recent study, T cells from peripheral blood of donors vaccinated with LVS by scarification up to 34 years prior were able to produce IFN-γ in response to re-stimulation (275). These data indicate that T cell mediated immunity is long-lasting in humans in the absence of a recurring infection of vaccination booster.

**Objectives**

*Francisella* has evolved several mechanisms to evade and/or suppress host immunity. We will focus on three immune evasion mechanisms in this dissertation: the ability to induce infected cells to synthesis and secrete $PGE_2$ which suppresses the T cell response (Chapters 2 and 5), the failure to induce pro-inflammatory cytokine production (Chapter 2), and targeting innate immune cells for infection (Chapter 4). We will also examine what cytokines are necessary for survival during a lethal secondary infection (Chapter 3). Overall, the work presented here increases our understanding of the underlying mechanisms by which

*Francisella* subverts host immunity. This knowledge not only increases our understanding of *Francisella* pathogenesis but also identifies pathways that could be targeted during future vaccine or drug development.

**Table 1**

**Table 1. Properties of *Francisella* strains**

| | *Francisella* strain | | |
|---|---|---|---|
| | *Francisella novicida* | *Francisella tularensis* subsp. *holartica* | *Francisella tularensis* subsp. *tularensis* |
| Laboratory strain name | U112 | LVS | SchuS4 |
| Virulence in humans | - | + | +++ |
| Human intranasal infectious dose (12, 13, 22, 26) | Not infectious[a] | $10^4$ CFU | 10 CFU |
| Virulence in mice | +++ | ++ | +++ |
| $LD_{50}$ | | | |
| Intranasal (14, 19, 20, 21, 27) | 10 CFU | $10^3$ CFU | < 10 CFU |
| Intradermal (14, 19, 28) | $2.4x10^3$ CFU | $10^6$ CFU | < 10 CFU |
| Genome properties (30, 31) | | | |
| Genome size (bp) | 1,910,031 | 1,895,998 | 1,892,819 |
| Number of open reading frames (predicted) | 1731 | 1380 | 1445 |
| Number of pseudogenes | 14 | 303 | 254 |
| % G+C content | 32.47 | 32.15 | 32.26 |

[a] immunocompetent individuals

**Table 2**

**Table 2: Immune evasion of phenotypic and functional maturation of antigen presenting cells**

| | *Francisella* strain | |
|---|---|---|
| | LVS | SchuS4 |
| Mouse BMDM | | |
| Up-regulate MHCII/CD86 (140) | No | ND |
| Produce pro-inflammatory cytokines (140, 143) | No | ND |
| Alveolar macrophages | | |
| Up-regulate MHCII/CD86 (140) | No | ND |
| Produce pro-inflammatory cytokines (140) | No | ND |
| Human MDM | | |
| Up-regulate MHCII/CD86 | ND | ND |
| Produce pro-inflammatory cytokines (143) | Yes | ND |
| Mouse BMDC | | |
| Up-regulate MHCII/CD86 (140) | Yes | ND |
| Produce pro-inflammatory cytokines (140) | No | ND |
| Mouse lung or lymph node dendritic cells | | |
| Up-regulate MHCII/CD86 (140, 141) | Yes | No |
| Produce pro-inflammatory cytokines (140, 141) | No | No |
| Human MDDC | | |
| Up-regulate MHCII/CD86 (66, 149, 150) | Yes | Yes |
| Produce pro-inflammatory cytokines (66, 148, 149, 150) | Yes | No |

ND: not determined

## REFERENCES


1. McCoy G. A plague-like disease of rodents. Public Health Bull. 1911;43:53-71.

2. McCoy G, Chapin C. Bacterium tularense, the cause of a plaguelike disease in rodents. Public Health Bull. 1912;53:17-23.

3. Wherry W, Lamb B. Infection of man with *Bacterium tularense*. The Journal of infectious diseases. 1914;15:331-40.

4. Francis E. Tularemia. Public Health Reports. 1921;36(30):1731-53.

5. Francis E. A summary of the present knowledge of tularemia. Medicine (Baltimore). 1928;7:411-32.

6. Ohara S. Studies on yato-byo (Ohara's disease, tularemia in Japan). I. The Japanese journal of experimental medicine. 1954;24(2):69-79. Epub 1954/04/01. PubMed PMID: 13221352.

7. Olsen P. Tularemia. 6th ed. Hubbert W, McCulloch W, Schnurrenbeger P, editors. Springfield, IL: Charles C. Thomas Publishers; 1970.

8. Ritter DB, Gerloff RK. Deoxyribonucleic acid hybridization among some species of the genus Pasteurella. J Bacteriol. 1966;92(6):1838-9. PubMed PMID: 5958114; PubMed Central PMCID: PMC316270.

9. Dorofer K. Symp Res Work Inst Epidemiol Microbiol Chita. 1947;1:177.

10. Philip C, Owen C. Intern Bull Bacteriol Nomencl Taxon. 1961;11:67.

11. Sjostedt A. Francisella. 2nd ed. Brenner D, Staley J, Garrity G, editors. New York, NY: Springer; 2005.

12. Saslaw S, Eigelsbach HT, Prior JA, Wilson HE, Carhart S. Tularemia vaccine study. II. Respiratory challenge. Arch Intern Med. 1961;107:702-14. Epub 1961/05/01. PubMed PMID: 13746667.

13. Saslaw S, Eigelsbach HT, Wilson HE, Prior JA, Carhart S. Tularemia vaccine study. I. Intracutaneous challenge. Arch Intern Med. 1961;107:689-701. Epub 1961/05/01. PubMed PMID: 13746668.

14. Conlan JW, Chen W, Shen H, Webb A, KuoLee R. Experimental tularemia in mice challenged by aerosol or intradermally with virulent strains of Francisella tularensis: bacteriologic and histopathologic studies. Microb Pathog. 2003;34(5):239-48. PubMed PMID: 12732472.

15. Jellison W. Tularemia in North America. 1930-1974. Missoula, MT: University of Montana; 1974.

16. Nakazawa Y, Williams RA, Peterson AT, Mead PS, Kugeler KJ, Petersen JM. Ecological niche modeling of Francisella tularensis subspecies and clades in the United States. The American journal of tropical medicine and hygiene. 2010;82(5):912-8. doi: 10.4269/ajtmh.2010.09-0354. PubMed PMID: 20439975; PubMed Central PMCID: PMC2861374.

17. Kugeler KJ, Mead PS, Janusz AM, Staples JE, Kubota KA, Chalcraft LG, et al. Molecular Epidemiology of Francisella tularensis in the United States. Clin Infect Dis. 2009;48(7):863-70. doi: 10.1086/597261. PubMed PMID: 19245342.

18. Sjostedt A. Tularemia: history, epidemiology, pathogen physiology, and clinical manifestations. Ann N Y Acad Sci. 2007;1105:1-29. doi: 10.1196/annals.1409.009. PubMed PMID: 17395726.

19. Fortier AH, Slayter MV, Ziemba R, Meltzer MS, Nacy CA. Live vaccine strain of Francisella tularensis: infection and immunity in mice. Infect Immun. 1991;59(9):2922-8. PubMed PMID: 1879918; PubMed Central PMCID: PMC258114.

20. Duckett NS, Olmos S, Durrant DM, Metzger DW. Intranasal interleukin-12 treatment for protection against respiratory infection with the Francisella tularensis live vaccine strain. Infect Immun. 2005;73(4):2306-11. Epub 2005/03/24. doi: 73/4/2306 [pii] 10.1128/IAI.73.4.2306-2311.2005. PubMed PMID: 15784575; PubMed Central PMCID: PMC1087453.

21. Wu TH, Hutt JA, Garrison KA, Berliba LS, Zhou Y, Lyons CR. Intranasal vaccination induces protective immunity against intranasal infection with virulent Francisella tularensis biovar A. Infect Immun. 2005;73(5):2644-54. Epub 2005/04/23. doi: 73/5/2644 [pii] 10.1128/IAI.73.5.2644-2654.2005. PubMed PMID: 15845466; PubMed Central PMCID: PMC1087315.

22. Hornick RB, Eigelsbach HT. Aerogenic immunization of man with live Tularemia vaccine. Bacteriol Rev. 1966;30(3):532-8. PubMed PMID: 5917334; PubMed Central PMCID: PMC378235.

23. Johansson A, Celli J, Conlan W, Elkins KL, Forsman M, Keim PS, et al. Objections to the transfer of Francisella novicida to the subspecies rank of Francisella tularensis. Int J Syst Evol Microbiol. 2010;60(Pt 8):1717-8; author reply 8-20. doi: 10.1099/ijs.0.022830-0. PubMed PMID: 20688748.

24. Busse HJ, Huber B, Anda P, Escudero R, Scholz HC, Seibold E, et al. Objections to the transfer of Francisella novicida to the subspecies rank of Francisella tularensis - response to Johansson et al. Int J Syst Evol Microbiol. England2010. p. 1718-20.

25. Huber B, Escudero R, Busse HJ, Seibold E, Scholz HC, Anda P, et al. Description of Francisella hispaniensis sp. nov., isolated from human blood, reclassification of Francisella novicida (Larson et al. 1955) Olsufiev et al. 1959 as Francisella tularensis subsp. novicida comb. nov. and emended description of the genus Francisella. Int J Syst Evol Microbiol. England2010. p. 1887-96.

26. Oyston PC, Sjostedt A, Titball RW. Tularaemia: bioterrorism defence renews interest in Francisella tularensis. Nat Rev Microbiol. 2004;2(12):967-78. Epub 2004/11/20. doi: nrmicro1045 [pii] 10.1038/nrmicro1045. PubMed PMID: 15550942.

27. Lauriano CM, Barker JR, Yoon SS, Nano FE, Arulanandam BP, Hassett DJ, et al. MglA regulates transcription of virulence factors necessary for Francisella tularensis intraamoebae and intramacrophage survival. Proc Natl Acad Sci U S A. 2004;101(12):4246-9. Epub 2004/03/11. doi: 10.1073/pnas.0307690101 [doi] 0307690101 [pii]. PubMed PMID: 15010524; PubMed Central PMCID: PMC384726.

28. Kieffer TL, Cowley S, Nano FE, Elkins KL. Francisella novicida LPS has greater immunobiological activity in mice than F. tularensis LPS, and contributes to F. novicida murine pathogenesis. Microbes Infect. 2003;5(5):397-403. PubMed PMID: 12737995.

29. Petrosino JF, Xiang Q, Karpathy SE, Jiang H, Yerrapragada S, Liu Y, et al. Chromosome rearrangement and diversification of Francisella tularensis revealed by the type B (OSU18) genome sequence. J Bacteriol. 2006;188(19):6977-85. doi: 10.1128/JB.00506-06. PubMed PMID: 16980500; PubMed Central PMCID: PMC1595524.

30. Titball RW, Petrosino JF. Francisella tularensis genomics and proteomics. Ann N Y Acad Sci. 2007;1105:98-121. doi: 10.1196/annals.1409.015. PubMed PMID: 17435122.

31. Rohmer L, Fong C, Abmayr S, Wasnick M, Larson Freeman TJ, Radey M, et al. Comparison of Francisella tularensis genomes reveals evolutionary events associated with the emergence of human pathogenic strains. Genome Biol. 2007;8(6):R102. doi: 10.1186/gb-2007-8-6-r102. PubMed PMID: 17550600; PubMed Central PMCID: PMC2394750.

32. Nano FE, Zhang N, Cowley SC, Klose KE, Cheung KK, Roberts MJ, et al. A Francisella tularensis pathogenicity island required for intramacrophage growth. J Bacteriol. 2004;186(19):6430-6. Epub 2004/09/18. doi: 10.1128/JB.186.19.6430-6436.2004 186/19/6430 [pii]. PubMed PMID: 15375123; PubMed Central PMCID: PMC516616.

33. Kawula TH, Hall JD, Fuller JR, Craven RR. Use of transposon-transposase complexes to create stable insertion mutant strains of Francisella tularensis LVS. Appl Environ Microbiol. 2004;70(11):6901-4. doi: 70/11/6901 [pii] 10.1128/AEM.70.11.6901-6904.2004. PubMed PMID: 15528561.

34. Golovliov I, Sjostedt A, Mokrievich A, Pavlov V. A method for allelic replacement in Francisella tularensis. FEMS Microbiol Lett. 2003. p. 273-80.

35. Qin A, Mann BJ. Identification of transposon insertion mutants of Francisella tularensis tularensis strain Schu S4 deficient in intracellular replication in the hepatic cell line HepG2. BMC microbiology. 2006. p. 69.

36. Bonquist L, Lindgren H, Golovliov I, Guina T, Sjostedt A. MglA and Igl proteins contribute to the modulation of Francisella tularensis live vaccine strain-containing phagosomes in murine macrophages. Infect Immun. 2008. p. 3502-10.

37. Broms JE, Lavander M, Sjostedt A. A conserved alpha-helix essential for a type VI secretion-like system of Francisella tularensis. J Bacteriol. 2009. p. 2431-46.

38. Hepburn MJ, Simpson AJ. Tularemia: current diagnosis and treatment options. Expert review of anti-infective therapy. 2008;6(2):231-40. doi: 10.1586/14787210.6.2.231. PubMed PMID: 18380605.

39. Evans ME, Gregory DW, Schaffner W, McGee ZA. Tularemia: a 30-year experience with 88 cases. Medicine (Baltimore). 1985;64(4):251-69. PubMed PMID: 3892222.

40. Cross J, Penn R. Francisella tularensis (tularemia). 5th ed. Mandell G, Bennett J, R D, editors. Philadelphia, PA: Churchill Livingstone; 2000.

41. Tarnvik A, Chu MC. New approaches to diagnosis and therapy of tularemia. Ann N Y Acad Sci. 2007;1105:378-404. doi: 10.1196/annals.1409.017. PubMed PMID: 17468229.

42. Helvaci S, Gedikoglu S, Akalin H, Oral HB. Tularemia in Bursa, Turkey: 205 cases in ten years. Eur J Epidemiol. 2000;16(3):271-6. PubMed PMID: 10870943.

43. Larssen KW, Afset JE, Heier BT, Krogh T, Handeland K, Vikoren T, et al. Outbreak of tularaemia in central Norway, January to March 2011. Euro surveillance : bulletin europeen sur les maladies transmissibles = European communicable disease bulletin. 2011;16(13). PubMed PMID: 21489376.

44. Chitadze N, Kuchuloria T, Clark DV, Tsertsvadze E, Chokheli M, Tsertsvadze N, et al. Water-borne outbreak of oropharyngeal and glandular tularemia in Georgia: investigation and follow-up. Infection. 2009;37(6):514-21. doi: 10.1007/s15010-009-8193-5. PubMed PMID: 19826763.

45. Willke A, Meric M, Grunow R, Sayan M, Finke EJ, Splettstosser W, et al. An outbreak of oropharyngeal tularaemia linked to natural spring water. Journal of medical microbiology. 2009;58(Pt 1):112-6. doi: 10.1099/jmm.0.002279-0. PubMed PMID: 19074661.

46. Rubin SA. Radiographic spectrum of pleuropulmonary tularemia. AJR American journal of roentgenology. 1978;131(2):277-81. doi: 10.2214/ajr.131.2.277. PubMed PMID: 98007.

47. Dennis DT, Inglesby TV, Henderson DA, Bartlett JG, Ascher MS, Eitzen E, et al. Tularemia as a biological weapon: medical and public health management. JAMA. 2001;285(21):2763-73. Epub 2001/06/21. doi: jst10001 [pii]. PubMed PMID: 11386933.

48. LoVullo ED, Molins-Schneekloth CR, Schweizer HP, Pavelka MS, Jr. Single-copy chromosomal integration systems for Francisella tularensis. Microbiology. 2009;155(Pt 4):1152-63. Epub 2009/04/01. doi: 155/4/1152 [pii] 10.1099/mic.0.022491-0. PubMed PMID: 19332817.

49. Harris S. Japanese biological warfare research on humans: a case study of microbiology and ethics. Ann N Y Acad Sci. 1992;666:21-52. PubMed PMID: 1297279.

50. Alibek K, Handelman S. Biohazard : the chilling true story of the largest covert biological weapons program in the world, told from the inside by the man who ran it. 1st ed. New York: Random House; 1999. xi, 319 p., 8 p. of plates p.

51. Christopher GW, Cieslak TJ, Pavlin JA, Eitzen EM, Jr. Biological warfare. A historical perspective. JAMA. 1997;278(5):412-7. Epub 1997/08/06. PubMed PMID: 9244333.

52. Harris S. Factories of Death. New York, NY: Routledge; 1994.

53. Williams P, Wallace D. Unit 731: Japan's Secret Biological Warfare in World War II. New York, NY: Free Press; 1989.

54. Sims N. The Diplomacy of Biological Disarmament. New York, NY: Plenum Press; 1983.

55. United Nations General Assembly. The Convention on the Prohibition of the Development, Production and Stockpiling of Bacteriological (Biological) and Toxin Weapons and on their Destruction. 1972.

56. US Dept of the Army. US Army Activity in the US Biological Warfare Programs. US Dept of the Army; 1977.

57. American Public Health Association. Tularemia. Chin J, editor. Washington, DC: American Public Health Association; 2000.

58. Health Aspects of Chemical and Biological Weapons. Geneva, Switzerland: World Health Organization; 1970. p. 105-7.

59. Kaufmann AF, Meltzer MI, Schmid GP. The economic impact of a bioterrorist attack: are prevention and postattack intervention programs justifiable? Emerg Infect Dis. 1997;3(2):83-94. doi: 10.3201/eid0302.970201. PubMed PMID: 9204289; PubMed Central PMCID: PMC2627615.

60. Clemens DL, Lee BY, Horwitz MA. Francisella tularensis enters macrophages via a novel process involving pseudopod loops. Infect Immun. 2005;73(9):5892-902. doi: 10.1128/IAI.73.9.5892-5902.2005. PubMed PMID: 16113308; PubMed Central PMCID: PMC1231130.

61. Clemens DL, Lee BY, Horwitz MA. Virulent and avirulent strains of Francisella tularensis prevent acidification and maturation of their phagosomes and escape into the cytoplasm in human macrophages. Infect Immun. 2004;72(6):3204-17. doi: 10.1128/IAI.72.6.3204-3217.2004. PubMed PMID: 15155622; PubMed Central PMCID: PMC415696.

62. Balagopal A, MacFarlane AS, Mohapatra N, Soni S, Gunn JS, Schlesinger LS. Characterization of the receptor-ligand pathways important for entry and survival of Francisella tularensis in human macrophages. Infect Immun. 2006;74(9):5114-25. doi: 10.1128/IAI.00795-06. PubMed PMID: 16926403; PubMed Central PMCID: PMC1594866.

63. Schulert GS, Allen LA. Differential infection of mononuclear phagocytes by Francisella tularensis: role of the macrophage mannose receptor. J Leukoc Biol. 2006;80(3):563-71. doi: 10.1189/jlb.0306219. PubMed PMID: 16816147; PubMed Central PMCID: PMC1865506.

64. Dai S, Rajaram MV, Curry HM, Leander R, Schlesinger LS. Fine tuning inflammation at the front door: macrophage complement receptor 3-mediates phagocytosis and immune suppression for Francisella tularensis. PLoS Pathog. 2013;9(1):e1003114. doi: 10.1371/journal.ppat.1003114. PubMed PMID: 23359218; PubMed Central PMCID: PMC3554622.

65. Barker JH, McCaffrey RL, Baman NK, Allen LA, Weiss JP, Nauseef WM. The role of complement opsonization in interactions between F. tularensis subsp. novicida and human neutrophils. Microbes Infect. 2009;11(8-9):762-9. doi: 10.1016/j.micinf.2009.04.016. PubMed PMID: 19409509; PubMed Central PMCID: PMC2715441.

66. Ben Nasr A, Haithcoat J, Masterson JE, Gunn JS, Eaves-Pyles T, Klimpel GR. Critical role for serum opsonins and complement receptors CR3 (CD11b/CD18) and CR4 (CD11c/CD18) in phagocytosis of Francisella tularensis by human dendritic cells (DC): uptake of Francisella leads to activation of immature DC and intracellular survival of the bacteria. J Leukoc Biol. 2006;80(4):774-86. doi: 10.1189/jlb.1205755. PubMed PMID: 16857732.

67. Pierini LM. Uptake of serum-opsonized Francisella tularensis by macrophages can be mediated by class A scavenger receptors. Cell Microbiol. 2006;8(8):1361-70. doi: 10.1111/j.1462-5822.2006.00719.x. PubMed PMID: 16882038.

68. Barel M, Hovanessian AG, Meibom K, Briand JP, Dupuis M, Charbit A. A novel receptor - ligand pathway for entry of Francisella tularensis in monocyte-like THP-1 cells: interaction between surface nucleolin and bacterial elongation factor Tu. BMC microbiology.

2008;8:145. doi: 10.1186/1471-2180-8-145. PubMed PMID: 18789156; PubMed Central PMCID: PMC2551611.

69. Barel M, Meibom K, Charbit A. Nucleolin, a shuttle protein promoting infection of human monocytes by Francisella tularensis. PLoS One. 2010;5(12):e14193. Epub 2010/12/15. doi: 10.1371/journal.pone.0014193. PubMed PMID: 21152024; PubMed Central PMCID: PMCPMC2995743.

70. Dai S, Rajaram MV, Curry HM, Leander R, Schlesinger LS. Fine tuning inflammation at the front door: macrophage complement receptor 3-mediates phagocytosis and immune suppression for Francisella tularensis. PLoS Pathog. United States2013. p. e1003114.

71. Haas A. The phagosome: compartment with a license to kill. Traffic. 2007;8(4):311-30. doi: 10.1111/j.1600-0854.2006.00531.x. PubMed PMID: 17274798.

72. Bonquist L, Lindgren H, Golovliov I, Guina T, Sjostedt A. MglA and Igl proteins contribute to the modulation of Francisella tularensis live vaccine strain-containing phagosomes in murine macrophages. Infect Immun. 2008;76(8):3502-10. doi: 10.1128/IAI.00226-08. PubMed PMID: 18474647; PubMed Central PMCID: PMC2493230.

73. Chong A, Wehrly TD, Nair V, Fischer ER, Barker JR, Klose KE, et al. The early phagosomal stage of Francisella tularensis determines optimal phagosomal escape and Francisella pathogenicity island protein expression. Infect Immun. 2008;76(12):5488-99. doi: 10.1128/IAI.00682-08. PubMed PMID: 18852245; PubMed Central PMCID: PMC2583578.

74. Golovliov I, Baranov V, Krocova Z, Kovarova H, Sjostedt A. An attenuated strain of the facultative intracellular bacterium Francisella tularensis can escape the phagosome of monocytic cells. Infect Immun. 2003;71(10):5940-50. PubMed PMID: 14500514; PubMed Central PMCID: PMC201066.

75. Santic M, Molmeret M, Abu Kwaik Y. Modulation of biogenesis of the Francisella tularensis subsp. novicida-containing phagosome in quiescent human macrophages and its maturation into a phagolysosome upon activation by IFN-gamma. Cell Microbiol. 2005;7(7):957-67. doi: 10.1111/j.1462-5822.2005.00529.x. PubMed PMID: 15953028.

76. Santic M, Asare R, Skrobonja I, Jones S, Abu Kwaik Y. Acquisition of the vacuolar ATPase proton pump and phagosome acidification are essential for escape of Francisella tularensis into the macrophage cytosol. Infect Immun. 2008;76(6):2671-7. doi: 10.1128/IAI.00185-08. PubMed PMID: 18390995; PubMed Central PMCID: PMC2423071.

77. Checroun C, Wehrly TD, Fischer ER, Hayes SF, Celli J. Autophagy-mediated reentry of Francisella tularensis into the endocytic compartment after cytoplasmic replication. Proc Natl Acad Sci U S A. 2006;103(39):14578-83. doi: 10.1073/pnas.0601838103. PubMed PMID: 16983090; PubMed Central PMCID: PMC1600002.

78. Anthony LD, Burke RD, Nano FE. Growth of Francisella spp. in rodent macrophages. Infect Immun. 1991;59(9):3291-6. PubMed PMID: 1879943; PubMed Central PMCID: PMC258167.

79. Clemens DL, Lee BY, Horwitz MA. Francisella tularensis phagosomal escape does not require acidification of the phagosome. Infect Immun. 2009;77(5):1757-73. Epub 2009/02/25. doi: IAI.01485-08 [pii] 10.1128/IAI.01485-08. PubMed PMID: 19237528; PubMed Central PMCID: PMC2681761.

80. Kadzhaev K, Zingmark C, Golovliov I, Bolanowski M, Shen H, Conlan W, et al. Identification of genes contributing to the virulence of Francisella tularensis SCHU S4 in a mouse intradermal infection model. PLoS One. 2009;4(5):e5463. Epub 2009/05/09. doi: 10.1371/journal.pone.0005463. PubMed PMID: 19424499; PubMed Central PMCID: PMC2675058.

81. Su J, Yang J, Zhao D, Kawula TH, Banas JA, Zhang JR. Genome-wide identification of Francisella tularensis virulence determinants. Infect Immun. 2007;75(6):3089-101. Epub 2007/04/11. doi: IAI.01865-06 [pii] 10.1128/IAI.01865-06. PubMed PMID: 17420240; PubMed Central PMCID: PMC1932872.

82. Weiss DS, Brotcke A, Henry T, Margolis JJ, Chan K, Monack DM. In vivo negative selection screen identifies genes required for Francisella virulence. Proc Natl Acad Sci U S A. 2007;104(14):6037-42. Epub 2007/03/29. doi: 0609675104 [pii] 10.1073/pnas.0609675104. PubMed PMID: 17389372; PubMed Central PMCID: PMC1832217.

83. Llewellyn AC, Jones CL, Napier BA, Bina JE, Weiss DS. Macrophage replication screen identifies a novel Francisella hydroperoxide resistance protein involved in virulence. PLoS One. 2011;6(9):e24201. Epub 2011/09/15. doi: 10.1371/journal.pone.0024201 PONE-D-11-05529 [pii]. PubMed PMID: 21915295; PubMed Central PMCID: PMC3167825.

84. Ahlund MK, Ryden P, Sjostedt A, Stoven S. Directed screen of Francisella novicida virulence determinants using Drosophila melanogaster. Infect Immun. 2010;78(7):3118-28. doi: 10.1128/IAI.00146-10. PubMed PMID: 20479082; PubMed Central PMCID: PMC2897386.

85. Kraemer PS, Mitchell A, Pelletier MR, Gallagher LA, Wasnick M, Rohmer L, et al. Genome-wide screen in Francisella novicida for genes required for pulmonary and systemic infection in mice. Infect Immun. 2009;77(1):232-44. doi: 10.1128/IAI.00978-08. PubMed PMID: 18955478; PubMed Central PMCID: PMC2612238.

86. Schulert GS, McCaffrey RL, Buchan BW, Lindemann SR, Hollenback C, Jones BD, et al. Francisella tularensis genes required for inhibition of the neutrophil respiratory burst and intramacrophage growth identified by random transposon mutagenesis of strain LVS.

Infect Immun. 2009;77(4):1324-36. doi: 10.1128/IAI.01318-08. PubMed PMID: 19204089; PubMed Central PMCID: PMC2663180.

87. Brotcke A, Weiss DS, Kim CC, Chain P, Malfatti S, Garcia E, et al. Identification of MglA-regulated genes reveals novel virulence factors in Francisella tularensis. Infect Immun. 2006;74(12):6642-55. Epub 2006/09/27. doi: IAI.01250-06 [pii] 10.1128/IAI.01250-06. PubMed PMID: 17000729; PubMed Central PMCID: PMC1698089.

88. Qin A, Mann BJ. Identification of transposon insertion mutants of Francisella tularensis tularensis strain Schu S4 deficient in intracellular replication in the hepatic cell line HepG2. BMC microbiology. 2006;6:69. doi: 10.1186/1471-2180-6-69. PubMed PMID: 16879747; PubMed Central PMCID: PMC1557513.

89. Tempel R, Lai XH, Crosa L, Kozlowicz B, Heffron F. Attenuated Francisella novicida transposon mutants protect mice against wild-type challenge. Infect Immun. 2006;74(9):5095-105. Epub 2006/08/24. doi: 74/9/5095 [pii] 10.1128/IAI.00598-06. PubMed PMID: 16926401; PubMed Central PMCID: PMC1594869.

90. Alkhuder K, Meibom KL, Dubail I, Dupuis M, Charbit A. Glutathione provides a source of cysteine essential for intracellular multiplication of Francisella tularensis. PLoS Pathog. 2009;5(1):e1000284. doi: 10.1371/journal.ppat.1000284. PubMed PMID: 19158962; PubMed Central PMCID: PMC2629122.

91. Wehrly TD, Chong A, Virtaneva K, Sturdevant DE, Child R, Edwards JA, et al. Intracellular biology and virulence determinants of Francisella tularensis revealed by transcriptional profiling inside macrophages. Cell Microbiol. 2009;11(7):1128-50. doi: 10.1111/j.1462-5822.2009.01316.x. PubMed PMID: 19388904; PubMed Central PMCID: PMC2746821.

92. Asare R, Akimana C, Jones S, Abu Kwaik Y. Molecular bases of proliferation of Francisella tularensis in arthropod vectors. Environmental microbiology. 2010;12(9):2587-612. doi: 10.1111/j.1462-2920.2010.02230.x. PubMed PMID: 20482589; PubMed Central PMCID: PMC2957557.

93. Lindgren H, Golovliov I, Baranov V, Ernst RK, Telepnev M, Sjostedt A. Factors affecting the escape of Francisella tularensis from the phagolysosome. Journal of medical microbiology. 2004;53(Pt 10):953-8. Epub 2004/09/11. PubMed PMID: 15358816.

94. Santic M, Molmeret M, Klose KE, Jones S, Kwaik YA. The Francisella tularensis pathogenicity island protein IglC and its regulator MglA are essential for modulating phagosome biogenesis and subsequent bacterial escape into the cytoplasm. Cell Microbiol. 2005;7(7):969-79. Epub 2005/06/15. doi: CMI526 [pii] 10.1111/j.1462-5822.2005.00526.x [doi]. PubMed PMID: 15953029.

95. Woolard MD, Barrigan LM, Fuller JR, Buntzman AS, Bryan J, Manoil C, et al. Identification of Francisella novicida mutants that fail to induce prostaglandin E(2) synthesis

by infected macrophages. Front Microbiol. 2013;4:16. doi: 10.3389/fmicb.2013.00016. PubMed PMID: 23403609.

96. Schmerk CL, Duplantis BN, Howard PL, Nano FE. A Francisella novicida pdpA mutant exhibits limited intracellular replication and remains associated with the lysosomal marker LAMP-1. Microbiology. 2009;155(Pt 5):1498-504. Epub 2009/04/18. doi: mic.0.025445-0 [pii] 10.1099/mic.0.025445-0. PubMed PMID: 19372155.

97. Barker JR, Chong A, Wehrly TD, Yu JJ, Rodriguez SA, Liu J, et al. The Francisella tularensis pathogenicity island encodes a secretion system that is required for phagosome escape and virulence. Mol Microbiol. 2009;74(6):1459-70. PubMed PMID: 20054881; PubMed Central PMCID: PMC2814410.

98. Lindgren M, Broms JE, Meyer L, Golovliov I, Sjostedt A. The Francisella tularensis LVS DeltapdpC mutant exhibits a unique phenotype during intracellular infection. BMC microbiology. England2013. p. 20.

99. Broms JE, Lavander M, Meyer L, Sjostedt A. IglG and IglI of the Francisella pathogenicity island are important virulence determinants of Francisella tularensis LVS. Infect Immun. 2011;79(9):3683-96. doi: 10.1128/IAI.01344-10. PubMed PMID: 21690239; PubMed Central PMCID: PMC3165494.

100. Broms JE, Meyer L, Lavander M, Larsson P, Sjostedt A. DotU and VgrG, Core Components of Type VI Secretion Systems, Are Essential for Francisella LVS Pathogenicity. PLoS One. 2012;7(4):e34639. Epub 2012/04/20. doi: 10.1371/journal.pone.0034639 PONE-D-12-02842 [pii]. PubMed PMID: 22514651; PubMed Central PMCID: PMC3326028.

101. Mariathasan S, Weiss DS, Dixit VM, Monack DM. Innate immunity against Francisella tularensis is dependent on the ASC/caspase-1 axis. J Exp Med. 2005. p. 1043-9.

102. Santic M, Molmeret M, Barker JR, Klose KE, Dekanic A, Doric M, et al. A Francisella tularensis pathogenicity island protein essential for bacterial proliferation within the host cell cytosol. Cell Microbiol. 2007. p. 2391-403.

103. Buchan BW, McCaffrey RL, Lindemann SR, Allen LA, Jones BD. Identification of migR, a regulatory element of the Francisella tularensis live vaccine strain iglABCD virulence operon required for normal replication and trafficking in macrophages. Infect Immun. 2009;77(6):2517-29. Epub 2009/04/08. doi: IAI.00229-09 [pii] 10.1128/IAI.00229-09. PubMed PMID: 19349423; PubMed Central PMCID: PMC2687360.

104. Child R, Wehrly TD, Rockx-Brouwer D, Dorward DW, Celli J. Acid phosphatases do not contribute to the pathogenesis of type A Francisella tularensis. Infect Immun. 2010;78(1):59-67. doi: 10.1128/IAI.00965-09. PubMed PMID: 19858304; PubMed Central PMCID: PMC2798210.

105. Qin A, Scott DW, Thompson JA, Mann BJ. Identification of an essential Francisella tularensis subsp. tularensis virulence factor. Infect Immun. 2009. p. 152-61.

106. Baron GS, Reilly TJ, Nano FE. The respiratory burst-inhibiting acid phosphatase AcpA is not essential for the intramacrophage growth or virulence of Francisella novicida. FEMS Microbiol Lett. 1999. p. 85-90.

107. Mohapatra NP, Balagopal A, Soni S, Schlesinger LS, Gunn JS. AcpA is a Francisella acid phosphatase that affects intramacrophage survival and virulence. Infect Immun. 2007. p. 390-6.

108. Mohapatra NP, Soni S, Reilly TJ, Liu J, Klose KE, Gunn JS. Combined deletion of four Francisella novicida acid phosphatases attenuates virulence and macrophage vacuolar escape. Infect Immun. 2008. p. 3690-9.

109. Fuller JR, Craven RR, Hall JD, Kijek TM, Taft-Benz S, Kawula TH. RipA, a cytoplasmic membrane protein conserved among Francisella species, is required for intracellular survival. Infect Immun. 2008;76(11):4934-43. Epub 2008/09/04. doi: IAI.00475-08 [pii] 10.1128/IAI.00475-08. PubMed PMID: 18765722; PubMed Central PMCID: PMC2573376.

110. Pechous R, Celli J, Penoske R, Hayes SF, Frank DW, Zahrt TC. Construction and characterization of an attenuated purine auxotroph in a Francisella tularensis live vaccine strain. Infect Immun. 2006. p. 4452-61.

111. Chong A, Wehrly TD, Child R, Hansen B, Hwang S, Virgin HW, et al. Cytosolic clearance of replication-deficient mutants reveals Francisella tularensis interactions with the autophagic pathway. Autophagy. 2012. p. 1342-56.

112. Clemens DL, Horwitz MA. Uptake and intracellular fate of Francisella tularensis in human macrophages. Ann N Y Acad Sci. 2007. p. 160-86.

113. Birmingham CL, Smith AC, Bakowski MA, Yoshimori T, Brumell JH. Autophagy controls Salmonella infection in response to damage to the Salmonella-containing vacuole. J Biol Chem. 2006. p. 11374-83.

114. Nakagawa I, Amano A, Mizushima N, Yamamoto A, Yamaguchi H, Kamimoto T, et al. Autophagy defends cells against invading group A Streptococcus. Science. 2004. p. 1037-40.

115. Rich KA, Burkett C, Webster P. Cytoplasmic bacteria can be targets for autophagy. Cell Microbiol. 2003. p. 455-68.

116. Hacker J, Kaper JB. Pathogenicity islands and the evolution of microbes. Annu Rev Microbiol. 2000. p. 641-79.

117. Gray CG, Cowley SC, Cheung KK, Nano FE. The identification of five genetic loci of Francisella novicida associated with intracellular growth. FEMS Microbiol Lett. 2002;215(1):53-6. Epub 2002/10/24. doi: S0378109702009114 [pii]. PubMed PMID: 12393200.

118. Broms JE, Sjostedt A, Lavander M. The Role of the Francisella Tularensis Pathogenicity Island in Type VI Secretion, Intracellular Survival, and Modulation of Host Cell Signaling. Front Microbiol. 2010;1:136. doi: 10.3389/fmicb.2010.00136. PubMed PMID: 21687753; PubMed Central PMCID: PMC3109350.

119. Pukatzki S, Ma AT, Sturtevant D, Krastins B, Sarracino D, Nelson WC, et al. Identification of a conserved bacterial protein secretion system in Vibrio cholerae using the Dictyostelium host model system. Proc Natl Acad Sci U S A. 2006;103(5):1528-33. doi: 10.1073/pnas.0510322103. PubMed PMID: 16432199; PubMed Central PMCID: PMC1345711.

120. de Bruin OM, Ludu JS, Nano FE. The Francisella pathogenicity island protein IglA localizes to the bacterial cytoplasm and is needed for intracellular growth. BMC microbiology. 2007;7:1. doi: 10.1186/1471-2180-7-1. PubMed PMID: 17233889; PubMed Central PMCID: PMC1794414.

121. Ludu JS, de Bruin OM, Duplantis BN, Schmerk CL, Chou AY, Elkins KL, et al. The Francisella pathogenicity island protein PdpD is required for full virulence and associates with homologues of the type VI secretion system. J Bacteriol. 2008;190(13):4584-95. doi: 10.1128/JB.00198-08. PubMed PMID: 18469101; PubMed Central PMCID: PMC2446798.

122. de Bruin OM, Duplantis BN, Ludu JS, Hare RF, Nix EB, Schmerk CL, et al. The biochemical properties of the Francisella pathogenicity island (FPI)-encoded proteins IglA, IglB, IglC, PdpB and DotU suggest roles in type VI secretion. Microbiology. 2011;157(Pt 12):3483-91. Epub 2011/10/08. doi: mic.0.052308-0 [pii] 10.1099/mic.0.052308-0. PubMed PMID: 21980115.

123. Bingle LE, Bailey CM, Pallen MJ. Type VI secretion: a beginner's guide. Current opinion in microbiology. 2008;11(1):3-8. doi: 10.1016/j.mib.2008.01.006. PubMed PMID: 18289922.

124. Broms JE, Lavander M, Sjostedt A. A conserved alpha-helix essential for a type VI secretion-like system of Francisella tularensis. J Bacteriol. 2009;191(8):2431-46. doi: 10.1128/JB.01759-08. PubMed PMID: 19201795; PubMed Central PMCID: PMC2668417.

125. Aubert D, MacDonald DK, Valvano MA. BcsKC is an essential protein for the type VI secretion system activity in Burkholderia cenocepacia that forms an outer membrane complex with BcsLB. J Biol Chem. 2010;285(46):35988-98. doi: 10.1074/jbc.M110.120402. PubMed PMID: 20729192; PubMed Central PMCID: PMC2975221.

126. Bonemann G, Pietrosiuk A, Diemand A, Zentgraf H, Mogk A. Remodelling of VipA/VipB tubules by ClpV-mediated threading is crucial for type VI protein secretion. The EMBO journal. 2009;28(4):315-25. doi: 10.1038/emboj.2008.269. PubMed PMID: 19131969; PubMed Central PMCID: PMC2646146.

127. Mougous JD, Cuff ME, Raunser S, Shen A, Zhou M, Gifford CA, et al. A virulence locus of Pseudomonas aeruginosa encodes a protein secretion apparatus. Science. 2006;312(5779):1526-30. doi: 10.1126/science.1128393. PubMed PMID: 16763151; PubMed Central PMCID: PMC2800167.

128. Broms JE, Meyer L, Sun K, Lavander M, Sjostedt A. Unique substrates secreted by the type VI secretion system of Francisella tularensis during intramacrophage infection. PLoS One. 2012;7(11):e50473. doi: 10.1371/journal.pone.0050473. PubMed PMID: 23185631; PubMed Central PMCID: PMC3502320.

129. Golovliov I, Ericsson M, Sandstrom G, Tarnvik A, Sjostedt A. Identification of proteins of Francisella tularensis induced during growth in macrophages and cloning of the gene encoding a prominently induced 23-kilodalton protein. Infect Immun. 1997;65(6):2183-9. PubMed PMID: 9169749; PubMed Central PMCID: PMC175301.

130. Baron GS, Nano FE. MglA and MglB are required for the intramacrophage growth of Francisella novicida. Mol Microbiol. 1998;29(1):247-59. Epub 1998/08/14. PubMed PMID: 9701818.

131. Twine SM, Mykytczuk NC, Petit MD, Shen H, Sjostedt A, Wayne Conlan J, et al. In vivo proteomic analysis of the intracellular bacterial pathogen, Francisella tularensis, isolated from mouse spleen. Biochem Biophys Res Commun. 2006;345(4):1621-33. doi: 10.1016/j.bbrc.2006.05.070. PubMed PMID: 16730660.

132. Brotcke A, Monack DM. Identification of fevR, a novel regulator of virulence gene expression in Francisella novicida. Infect Immun. 2008;76(8):3473-80. Epub 2008/06/19. doi: IAI.00430-08 [pii] 10.1128/IAI.00430-08. PubMed PMID: 18559431; PubMed Central PMCID: PMC2493208.

133. Charity JC, Costante-Hamm MM, Balon EL, Boyd DH, Rubin EJ, Dove SL. Twin RNA polymerase-associated proteins control virulence gene expression in Francisella tularensis. PLoS Pathog. 2007;3(6):e84. Epub 2007/06/19. doi: 06-PLPA-RA-0512 [pii] 10.1371/journal.ppat.0030084. PubMed PMID: 17571921; PubMed Central PMCID: PMC1891329.

134. Mohapatra NP, Soni S, Bell BL, Warren R, Ernst RK, Muszynski A, et al. Identification of an orphan response regulator required for the virulence of Francisella spp. and transcription of pathogenicity island genes. Infect Immun. 2007;75(7):3305-14. Epub 2007/04/25. doi: IAI.00351-07 [pii] 10.1128/IAI.00351-07. PubMed PMID: 17452468; PubMed Central PMCID: PMC1932945.

135. Meibom KL, Forslund AL, Kuoppa K, Alkhuder K, Dubail I, Dupuis M, et al. Hfq, a novel pleiotropic regulator of virulence-associated genes in Francisella tularensis. Infect Immun. 2009;77(5):1866-80. doi: 10.1128/IAI.01496-08. PubMed PMID: 19223477; PubMed Central PMCID: PMC2681744.

136. Bell BL, Mohapatra NP, Gunn JS. Regulation of virulence gene transcripts by the Francisella novicida orphan response regulator PmrA: role of phosphorylation and evidence of MglA/SspA interaction. Infect Immun. 2010;78(5):2189-98. doi: 10.1128/IAI.00021-10. PubMed PMID: 20231408; PubMed Central PMCID: PMC2863534.

137. Charity JC, Blalock LT, Costante-Hamm MM, Kasper DL, Dove SL. Small molecule control of virulence gene expression in Francisella tularensis. PLoS Pathog. 2009;5(10):e1000641. Epub 2009/10/31. doi: 10.1371/journal.ppat.1000641. PubMed PMID: 19876386; PubMed Central PMCID: PMC2763202.

138. Fortier AH, Green SJ, Polsinelli T, Jones TR, Crawford RM, Leiby DA, et al. Life and death of an intracellular pathogen: Francisella tularensis and the macrophage. Immunology series. 1994;60:349-61. Epub 1994/01/01. PubMed PMID: 8251580.

139. Hall JD, Woolard MD, Gunn BM, Craven RR, Taft-Benz S, Frelinger JA, et al. Infected-host-cell repertoire and cellular response in the lung following inhalation of Francisella tularensis Schu S4, LVS, or U112. Infect Immun. 2008;76(12):5843-52. Epub 2008/10/15. doi: IAI.01176-08 [pii] 10.1128/IAI.01176-08. PubMed PMID: 18852251; PubMed Central PMCID: PMC2583552.

140. Bosio CM, Dow SW. Francisella tularensis induces aberrant activation of pulmonary dendritic cells. J Immunol. 2005;175(10):6792-801. Epub 2005/11/08. doi: 175/10/6792 [pii]. PubMed PMID: 16272336.

141. Bosio CM, Bielefeldt-Ohmann H, Belisle JT. Active suppression of the pulmonary immune response by Francisella tularensis Schu4. J Immunol. 2007;178(7):4538-47. Epub 2007/03/21. doi: 178/7/4538 [pii]. PubMed PMID: 17372012.

142. Telepnev M, Golovliov I, Grundstrom T, Tarnvik A, Sjostedt A. Francisella tularensis inhibits Toll-like receptor-mediated activation of intracellular signalling and secretion of TNF-alpha and IL-1 from murine macrophages. Cell Microbiol. 2003;5(1):41-51. PubMed PMID: 12542469.

143. Bolger CE, Forestal CA, Italo JK, Benach JL, Furie MB. The live vaccine strain of Francisella tularensis replicates in human and murine macrophages but induces only the human cells to secrete proinflammatory cytokines. J Leukoc Biol. 2005;77(6):893-7. doi: 10.1189/jlb.1104637. PubMed PMID: 15758077.

144. Wilson JE, Katkere B, Drake JR. Francisella tularensis induces ubiquitin-dependent major histocompatibility complex class II degradation in activated macrophages. Infect Immun. 2009;77(11):4953-65. Epub 2009/08/26. doi: IAI.00844-09 [pii]

10.1128/IAI.00844-09. PubMed PMID: 19703975; PubMed Central PMCID: PMC2772548.

145. Edwards JA, Rockx-Brouwer D, Nair V, Celli J. Restricted cytosolic growth of Francisella tularensis subsp. tularensis by IFN-gamma activation of macrophages. Microbiology. 2010;156(Pt 2):327-39. doi: mic.0.031716-0 [pii] 10.1099/mic.0.031716-0. PubMed PMID: 19926654.

146. Chase JC, Celli J, Bosio CM. Direct and indirect impairment of human dendritic cell function by virulent Francisella tularensis Schu S4. Infect Immun. 2009;77(1):180-95. doi: IAI.00879-08 [pii] 10.1128/IAI.00879-08. PubMed PMID: 18981246.

147. Liu YJ. Dendritic cell subsets and lineages, and their functions in innate and adaptive immunity. Cell. 2001. p. 259-62.

148. Bauler TJ, Chase JC, Bosio CM. IFN-beta mediates suppression of IL-12p40 in human dendritic cells following infection with virulent Francisella tularensis. J Immunol. 2011;187(4):1845-55. doi: jimmunol.1100377 [pii] 10.4049/jimmunol.1100377. PubMed PMID: 21753150.

149. Chase JC, Bosio CM. The presence of CD14 overcomes evasion of innate immune responses by virulent Francisella tularensis in human dendritic cells in vitro and pulmonary cells in vivo. Infect Immun. 2010;78(1):154-67. doi: IAI.00750-09 [pii] 10.1128/IAI.00750-09. PubMed PMID: 19841074.

150. Li H, Nookala S, Bina XR, Bina JE, Re F. Innate immune response to Francisella tularensis is mediated by TLR2 and caspase-1 activation. J Leukoc Biol. 2006;80(4):766-73. Epub 2006/08/10. doi: jlb.0406294 [pii] 10.1189/jlb.0406294. PubMed PMID: 16895974.

151. Vivier E, Raulet DH, Moretta A, Caligiuri MA, Zitvogel L, Lanier LL, et al. Innate or adaptive immunity? The example of natural killer cells. Science. 2011. p. 44-9.

152. Sanapala S, Yu JJ, Murthy AK, Li W, Guentzel MN, Chambers JP, et al. Perforin- and granzyme-mediated cytotoxic effector functions are essential for protection against Francisella tularensis following vaccination by the defined F. tularensis subsp. novicida DeltafopC vaccine strain. Infect Immun. 2012. p. 2177-85.

153. Lopez MC, Duckett NS, Baron SD, Metzger DW. Early activation of NK cells after lung infection with the intracellular bacterium, Francisella tularensis LVS. Cell Immunol. 2004. p. 75-85.

154. Bokhari SM, Kim KJ, Pinson DM, Slusser J, Yeh HW, Parmely MJ. NK cells and gamma interferon coordinate the formation and function of hepatic granulomas in mice infected with the Francisella tularensis live vaccine strain. Infect Immun. 2008. p. 1379-89.

155. Collazo CM, Sher A, Meierovics AI, Elkins KL. Myeloid differentiation factor-88 (MyD88) is essential for control of primary in vivo Francisella tularensis LVS infection, but

not for control of intra-macrophage bacterial replication. Microbes Infect. 2006;8(3):779-90. Epub 2006/03/04. doi: S1286-4579(05)00364-3 [pii] 10.1016/j.micinf.2005.09.014. PubMed PMID: 16513388.

156. Leiby DA, Fortier AH, Crawford RM, Schreiber RD, Nacy CA. In vivo modulation of the murine immune response to Francisella tularensis LVS by administration of anticytokine antibodies. Infect Immun. 1992;60(1):84-9. Epub 1992/01/01. PubMed PMID: 1729199; PubMed Central PMCID: PMC257506.

157. De Pascalis R, Taylor BC, Elkins KL. Diverse myeloid and lymphoid cell subpopulations produce gamma interferon during early innate immune responses to Francisella tularensis live vaccine strain. Infect Immun. 2008. p. 4311-21.

158. Schmitt DM, O'Dee DM, Brown MJ, Horzempa J, Russo BC, Morel PA, et al. Role of NK cells in host defense against pulmonary type A Francisella tularensis infection. Microbes Infect. 2013;15(3):201-11. Epub 2012/12/06. doi: 10.1016/j.micinf.2012.11.008. PubMed PMID: 23211929.

159. Crane DD, Scott DP, Bosio CM. Generation of a convalescent model of virulent Francisella tularensis infection for assessment of host requirements for survival of tularemia. PLoS One. 2012;7(3):e33349. doi: 10.1371/journal.pone.0033349. PubMed PMID: 22428026; PubMed Central PMCID: PMC3299770.

160. Skyberg JA, Rollins MF, Holderness JS, Marlenee NL, Schepetkin IA, Goodyear A, et al. Nasal Acai polysaccharides potentiate innate immunity to protect against pulmonary Francisella tularensis and Burkholderia pseudomallei Infections. PLoS Pathog. 2012. p. e1002587.

161. Elkins KL, Colombini SM, Krieg AM, De Pascalis R. NK cells activated in vivo by bacterial DNA control the intracellular growth of Francisella tularensis LVS. Microbes Infect. 2009. p. 49-56.

162. Nathan C. Neutrophils and immunity: challenges and opportunities. Nat Rev Immunol. 2006. p. 173-82.

163. Schricker RL, Eigelsbach HT, Mitten JQ, Hall WC. Pathogenesis of tularemia in monkeys aerogenically exposed to Francisella tularensis 425. Infect Immun. 1972;5(5):734-44. Epub 1972/05/01. PubMed PMID: 4629251; PubMed Central PMCID: PMCPMC422433.

164. Dunaeva TN, Shlygina KN. [Phagocytic activity of the neutrophils in tularemia in animals with varying infective sensitivity]. Zh Mikrobiol Epidemiol Immunobiol. 1975(10):22-6. Epub 1975/10/01. PubMed PMID: 1108522.

165. Conlan JW, KuoLee R, Shen H, Webb A. Different host defences are required to protect mice from primary systemic vs pulmonary infection with the facultative intracellular bacterial pathogen, Francisella tularensis LVS. Microb Pathog. 2002. p. 127-34.

166. Sjostedt A, Conlan JW, North RJ. Neutrophils are critical for host defense against primary infection with the facultative intracellular bacterium Francisella tularensis in mice and participate in defense against reinfection. Infect Immun. 1994;62(7):2779-83. Epub 1994/07/01. PubMed PMID: 8005668; PubMed Central PMCID: PMCPMC302881.

167. Chen W, KuoLee R, Shen H, Conlan JW. Susceptibility of immunodeficient mice to aerosol and systemic infection with virulent strains of Francisella tularensis. Microb Pathog. 2004. p. 311-8.

168. KuoLee R, Harris G, Conlan JW, Chen W. Role of neutrophils and NADPH phagocyte oxidase in host defense against respiratory infection with virulent Francisella tularensis in mice. Microbes Infect. 2011. p. 447-56.

169. Daley JM, Thomay AA, Connolly MD, Reichner JS, Albina JE. Use of Ly6G-specific monoclonal antibody to deplete neutrophils in mice. J Leukoc Biol. 2008. p. 64-70.

170. Malik M, Bakshi CS, McCabe K, Catlett SV, Shah A, Singh R, et al. Matrix metalloproteinase 9 activity enhances host susceptibility to pulmonary infection with type A and B strains of Francisella tularensis. J Immunol. 2007;178(2):1013-20. doi: 178/2/1013 [pii]. PubMed PMID: 17202364.

171. Lindgren H, Stenmark S, Chen W, Tarnvik A, Sjostedt A. Distinct roles of reactive nitrogen and oxygen species to control infection with the facultative intracellular bacterium Francisella tularensis. Infect Immun. 2004. p. 7172-82.

172. van der Vliet A. NADPH oxidases in lung biology and pathology: host defense enzymes, and more. Free Radic Biol Med. 2008. p. 938-55.

173. McCaffrey RL, Allen LA. Francisella tularensis LVS evades killing by human neutrophils via inhibition of the respiratory burst and phagosome escape. J Leukoc Biol. 2006. p. 1224-30.

174. Lindgren H, Shen H, Zingmark C, Golovliov I, Conlan W, Sjostedt A. Resistance of Francisella tularensis strains against reactive nitrogen and oxygen species with special reference to the role of KatG. Infect Immun. 2007. p. 1303-9.

175. Takeda K, Kaisho T, Akira S. Toll-like receptors. Annu Rev Immunol. 2003;21:335-76. Epub 2003/01/14. doi: 10.1146/annurev.immunol.21.120601.141126 120601.141126 [pii]. PubMed PMID: 12524386.

176. Kawai T, Akira S. The role of pattern-recognition receptors in innate immunity: update on Toll-like receptors. Nat Immunol. 2010. p. 373-84.

177. Abplanalp AL, Morris IR, Parida BK, Teale JM, Berton MT. TLR-dependent control of Francisella tularensis infection and host inflammatory responses. PLoS One. 2009;4(11):e7920. Epub 2009/11/26. doi: 10.1371/journal.pone.0007920. PubMed PMID: 19936231; PubMed Central PMCID: PMC2775407.

178. Forestal CA, Gil H, Monfett M, Noah CE, Platz GJ, Thanassi DG, et al. A conserved and immunodominant lipoprotein of Francisella tularensis is proinflammatory but not essential for virulence. Microb Pathog. 2008;44(6):512-23. Epub 2008/02/29. doi: S0882-4010(08)00003-X [pii] 10.1016/j.micpath.2008.01.003. PubMed PMID: 18304778; PubMed Central PMCID: PMC2483246.

179. Thakran S, Li H, Lavine CL, Miller MA, Bina JE, Bina XR, et al. Identification of Francisella tularensis lipoproteins that stimulate the toll-like receptor (TLR) 2/TLR1 heterodimer. J Biol Chem. 2008;283(7):3751-60. doi: M706854200 [pii] 10.1074/jbc.M706854200. PubMed PMID: 18079113.

180. Parra MC, Shaffer SA, Hajjar AM, Gallis BM, Hager A, Goodlett DR, et al. Identification, cloning, expression, and purification of Francisella lpp3: an immunogenic lipoprotein. Microbiol Res. Germany: 2009 Elsevier GmbH; 2010. p. 531-45.

181. Cole LE, Shirey KA, Barry E, Santiago A, Rallabhandi P, Elkins KL, et al. Toll-like receptor 2-mediated signaling requirements for Francisella tularensis live vaccine strain infection of murine macrophages. Infect Immun. 2007;75(8):4127-37. Epub 2007/05/23. doi: IAI.01868-06 [pii] 10.1128/IAI.01868-06. PubMed PMID: 17517865; PubMed Central PMCID: PMC1951974.

182. Katz J, Zhang P, Martin M, Vogel SN, Michalek SM. Toll-like receptor 2 is required for inflammatory responses to Francisella tularensis LVS. Infect Immun. 2006;74(5):2809-16. Epub 2006/04/20. doi: 74/5/2809 [pii] 10.1128/IAI.74.5.2809-2816.2006. PubMed PMID: 16622218; PubMed Central PMCID: PMC1459727.

183. Chen W, KuoLee R, Shen H, Busa M, Conlan JW. Toll-like receptor 4 (TLR4) does not confer a resistance advantage on mice against low-dose aerosol infection with virulent type A Francisella tularensis. Microb Pathog. 2004. p. 185-91.

184. Chen W, Kuolee R, Shen H, Busa M, Conlan JW. Toll-like receptor 4 (TLR4) plays a relatively minor role in murine defense against primary intradermal infection with Francisella tularensis LVS. Immunol Lett. 2005. p. 151-4.

185. Hajjar AM, Harvey MD, Shaffer SA, Goodlett DR, Sjostedt A, Edebro H, et al. Lack of in vitro and in vivo recognition of Francisella tularensis subspecies lipopolysaccharide by Toll-like receptors. Infect Immun. 2006;74(12):6730-8. Epub 2006/09/20. doi: IAI.00934-06 [pii] 10.1128/IAI.00934-06. PubMed PMID: 16982824; PubMed Central PMCID: PMC1698081.

186. Franchi L, Munoz-Planillo R, Nunez G. Sensing and reacting to microbes through the inflammasomes. Nat Immunol. 2012. p. 325-32.

187. Davis BK, Wen H, Ting JP. The inflammasome NLRs in immunity, inflammation, and associated diseases. Annu Rev Immunol. 2011;29:707-35. doi: 10.1146/annurev-immunol-031210-101405. PubMed PMID: 21219188.

188. Fernandes-Alnemri T, Yu JW, Juliana C, Solorzano L, Kang S, Wu J, et al. The AIM2 inflammasome is critical for innate immunity to Francisella tularensis. Nature immunology. 2010;11(5):385-93. doi: 10.1038/ni.1859. PubMed PMID: 20351693; PubMed Central PMCID: PMC3111085.

189. Jones JW, Kayagaki N, Broz P, Henry T, Newton K, O'Rourke K, et al. Absent in melanoma 2 is required for innate immune recognition of Francisella tularensis. Proc Natl Acad Sci U S A. 2010;107(21):9771-6. doi: 10.1073/pnas.1003738107. PubMed PMID: 20457908; PubMed Central PMCID: PMC2906881.

190. Rathinam VA, Jiang Z, Waggoner SN, Sharma S, Cole LE, Waggoner L, et al. The AIM2 inflammasome is essential for host defense against cytosolic bacteria and DNA viruses. Nature immunology. 2010;11(5):395-402. doi: 10.1038/ni.1864. PubMed PMID: 20351692; PubMed Central PMCID: PMC2887480.

191. Henry T, Brotcke A, Weiss DS, Thompson LJ, Monack DM. Type I interferon signaling is required for activation of the inflammasome during Francisella infection. J Exp Med. 2007;204(5):987-94. doi: 10.1084/jem.20062665. PubMed PMID: 17452523; PubMed Central PMCID: PMC2118578.

192. Henry T, Kirimanjeswara GS, Ruby T, Jones JW, Peng K, Perret M, et al. Type I IFN signaling constrains IL-17A/F secretion by gammadelta T cells during bacterial infections. J Immunol. 2010;184(7):3755-67. doi: 10.4049/jimmunol.0902065. PubMed PMID: 20176744; PubMed Central PMCID: PMC2879132.

193. Finlay BB, McFadden G. Anti-immunology: evasion of the host immune system by bacterial and viral pathogens. Cell. 2006. p. 767-82.

194. Hall JD, Craven RR, Fuller JR, Pickles RJ, Kawula TH. Francisella tularensis replicates within alveolar type II epithelial cells in vitro and in vivo following inhalation. Infect Immun. 2007;75(2):1034-9. Epub 2006/11/08. doi: IAI.01254-06 [pii] 10.1128/IAI.01254-06. PubMed PMID: 17088343; PubMed Central PMCID: PMC1828526.

195. Vaara M. Endotoxin in Health and Disease. Brade H, Opal S, Vogel SN, Morrison D, editors. New York: Marcel Dekker, Inc. ; 1999.

196. Holst O. Endotoxin in Health and Disease. Brade H, Opal S, Vogel SN, Morrison D, editors. New York: Marcel Dekker, Inc.; 1999.

197. Poltorak A, He X, Smirnova I, Liu MY, Van Huffel C, Du X, et al. Defective LPS signaling in C3H/HeJ and C57BL/10ScCr mice: mutations in Tlr4 gene. Science. 1998;282(5396):2085-8. Epub 1998/12/16. PubMed PMID: 9851930.

198. Beasley AS, Cotter RJ, Vogel SN, Inzana TJ, Qureshi AA, Qureshi N. A variety of novel lipid A structures obtained from Francisella tularensis live vaccine strain. Innate immunity. 2012;18(2):268-78. Epub 2011/06/29. doi: 10.1177/1753425911401054. PubMed PMID: 21709054.

199. Phillips NJ, Schilling B, McLendon MK, Apicella MA, Gibson BW. Novel modification of lipid A of Francisella tularensis. Infect Immun. 2004;72(9):5340-8. Epub 2004/08/24. doi: 10.1128/iai.72.9.5340-5348.2004. PubMed PMID: 15322031; PubMed Central PMCID: PMCPMC517411.

200. Vinogradov E, Perry MB, Conlan JW. Structural analysis of Francisella tularensis lipopolysaccharide. European journal of biochemistry / FEBS. 2002;269(24):6112-8. Epub 2002/12/11. PubMed PMID: 12473106.

201. Woolard MD, Wilson JE, Hensley LL, Jania LA, Kawula TH, Drake JR, et al. Francisella tularensis-infected macrophages release prostaglandin E2 that blocks T cell proliferation and promotes a Th2-like response. J Immunol. 2007;178(4):2065-74. Epub 2007/02/06. doi: 178/4/2065 [pii]. PubMed PMID: 17277110.

202. Kalinski P. Regulation of immune responses by prostaglandin E2. J Immunol. 2012;188(1):21-8. doi: 10.4049/jimmunol.1101029. PubMed PMID: 22187483; PubMed Central PMCID: PMC3249979.

203. Luft T, Jefford M, Luetjens P, Toy T, Hochrein H, Masterman KA, et al. Functionally distinct dendritic cell (DC) populations induced by physiologic stimuli: prostaglandin E(2) regulates the migratory capacity of specific DC subsets. Blood. 2002;100(4):1362-72. Epub 2002/08/01. doi: 10.1182/blood-2001-12-0360. PubMed PMID: 12149219.

204. Scandella E, Men Y, Gillessen S, Forster R, Groettrup M. Prostaglandin E2 is a key factor for CCR7 surface expression and migration of monocyte-derived dendritic cells. Blood. 2002;100(4):1354-61. Epub 2002/08/01. doi: 10.1182/blood-2001-11-0017. PubMed PMID: 12149218.

205. Yang L, Yamagata N, Yadav R, Brandon S, Courtney RL, Morrow JD, et al. Cancer-associated immunodeficiency and dendritic cell abnormalities mediated by the prostaglandin EP2 receptor. The Journal of clinical investigation. 2003;111(5):727-35. Epub 2003/03/06. doi: 10.1172/jci16492. PubMed PMID: 12618527; PubMed Central PMCID: PMCPMC151895.

206. Kalinski P, Hilkens CM, Snijders A, Snijdewint FG, Kapsenberg ML. Dendritic cells, obtained from peripheral blood precursors in the presence of PGE2, promote Th2 responses. Adv Exp Med Biol. 1997;417:363-7. Epub 1997/01/01. PubMed PMID: 9286387.

207. Kalinski P, Vieira PL, Schuitemaker JH, de Jong EC, Kapsenberg ML. Prostaglandin E(2) is a selective inducer of interleukin-12 p40 (IL-12p40) production and an inhibitor of bioactive IL-12p70 heterodimer. Blood. 2001;97(11):3466-9. Epub 2001/05/23. PubMed PMID: 11369638.

208. Schnurr M, Toy T, Shin A, Wagner M, Cebon J, Maraskovsky E. Extracellular nucleotide signaling by P2 receptors inhibits IL-12 and enhances IL-23 expression in human dendritic cells: a novel role for the cAMP pathway. Blood. 2005;105(4):1582-9. Epub 2004/10/16. doi: 2004-05-1718 [pii] 10.1182/blood-2004-05-1718. PubMed PMID: 15486065.

209. Sheibanie AF, Tadmori I, Jing H, Vassiliou E, Ganea D. Prostaglandin E2 induces IL-23 production in bone marrow-derived dendritic cells. FASEB J. 2004;18(11):1318-20. Epub 2004/06/08. doi: 10.1096/fj.03-1367fje [pii]. PubMed PMID: 15180965.

210. Kvirkvelia N, Vojnovic I, Warner TD, Athie-Morales V, Free P, Rayment N, et al. Placentally derived prostaglandin E2 acts via the EP4 receptor to inhibit IL-2-dependent proliferation of CTLL-2 T cells. Clin Exp Immunol. 2002;127(2):263-9. Epub 2002/03/06. doi: 1718 [pii]. PubMed PMID: 11876748; PubMed Central PMCID: PMC1906325.

211. Harris SG, Padilla J, Koumas L, Ray D, Phipps RP. Prostaglandins as modulators of immunity. Trends Immunol. 2002;23(3):144-50. Epub 2002/02/28. doi: S1471490601021548 [pii]. PubMed PMID: 11864843.

212. Betz M, Fox BS. Prostaglandin E2 inhibits production of Th1 lymphokines but not of Th2 lymphokines. J Immunol. 1991;146(1):108-13. Epub 1991/01/01. PubMed PMID: 1845802.

213. Woolard MD, Hensley LL, Kawula TH, Frelinger JA. Respiratory Francisella tularensis live vaccine strain infection induces Th17 cells and prostaglandin E2, which inhibits generation of gamma interferon-positive T cells. Infect Immun. 2008;76(6):2651-9. Epub 2008/04/09. doi: IAI.01412-07 [pii] 10.1128/IAI.01412-07. PubMed PMID: 18391003; PubMed Central PMCID: PMC2423094.

214. Hunt D, Wilson JE, Weih KA, Ishido S, Harton JA, Roche PA, et al. Francisella tularensis elicits IL-10 via a PGE(2)-inducible factor, to drive macrophage MARCH1 expression and class II down-regulation. PLoS One. 2012;7(5):e37330. doi: 10.1371/journal.pone.0037330. PubMed PMID: 22615981; PubMed Central PMCID: PMC3355121.

215. Markel G, Bar-Haim E, Zahavy E, Cohen H, Cohen O, Shafferman A, et al. The involvement of IL-17A in the murine response to sub-lethal inhalational infection with Francisella tularensis. PLoS One. 2010;5(6):e11176. doi: 10.1371/journal.pone.0011176. PubMed PMID: 20585449; PubMed Central PMCID: PMC2887844.

216. Yee D, Rhinehart-Jones TR, Elkins KL. Loss of either CD4+ or CD8+ T cells does not affect the magnitude of protective immunity to an intracellular pathogen, Francisella tularensis strain LVS. J Immunol. 1996;157(11):5042-8. Epub 1996/12/01. PubMed PMID: 8943413.

217. Lin Y, Ritchea S, Logar A, Slight S, Messmer M, Rangel-Moreno J, et al. Interleukin-17 Is Required for T Helper 1 Cell Immunity and Host Resistance to the Intracellular Pathogen Francisella tularensis. Immunity. 2009. Epub 2009/10/27. doi: S1074-7613(09)00448-8 [pii] 10.1016/j.immuni.2009.08.025. PubMed PMID: 19853481.

218. Poquet Y, Kroca M, Halary F, Stenmark S, Peyrat MA, Bonneville M, et al. Expansion of Vgamma9 Vdelta2 T cells is triggered by Francisella tularensis-derived phosphoantigens in tularemia but not after tularemia vaccination. Infect Immun. 1998;66(5):2107-14. PubMed PMID: 9573096; PubMed Central PMCID: PMC108170.

219. Sumida T, Maeda T, Takahashi H, Yoshida S, Yonaha F, Sakamoto A, et al. Predominant expansion of V gamma 9/V delta 2 T cells in a tularemia patient. Infect Immun. 1992;60(6):2554-8. PubMed PMID: 1534075; PubMed Central PMCID: PMC257198.

220. Rowland CA, Hartley MG, Flick-Smith H, Laws TR, Eyles JE, Oyston PC. Peripheral human gammadelta T cells control growth of both avirulent and highly virulent strains of Francisella tularensis in vitro. Microbes Infect. 2012;14(7-8):584-9. doi: 10.1016/j.micinf.2012.02.001. PubMed PMID: 22370220.

221. Long GW, Oprandy JJ, Narayanan RB, Fortier AH, Porter KR, Nacy CA. Detection of Francisella tularensis in blood by polymerase chain reaction. J Clin Microbiol. 1993;31(1):152-4. PubMed PMID: 8417022; PubMed Central PMCID: PMC262641.

222. Forestal CA, Malik M, Catlett SV, Savitt AG, Benach JL, Sellati TJ, et al. Francisella tularensis has a significant extracellular phase in infected mice. The Journal of infectious diseases. 2007;196(1):134-7. doi: 10.1086/518611. PubMed PMID: 17538893.

223. Yu JJ, Raulie EK, Murthy AK, Guentzel MN, Klose KE, Arulanandam BP. The presence of infectious extracellular Francisella tularensis subsp. novicida in murine plasma after pulmonary challenge. European journal of clinical microbiology & infectious diseases : official publication of the European Society of Clinical Microbiology. 2008;27(4):323-5. doi: 10.1007/s10096-007-0434-x. PubMed PMID: 18087734.

224. Elkins KL, Bosio CM, Rhinehart-Jones TR. Importance of B cells, but not specific antibodies, in primary and secondary protective immunity to the intracellular bacterium Francisella tularensis live vaccine strain. Infect Immun. 1999;67(11):6002-7. PubMed PMID: 10531260; PubMed Central PMCID: PMC96986.

225. Krocova Z, Hartlova A, Souckova D, Zivna L, Kroca M, Rudolf E, et al. Interaction of B cells with intracellular pathogen Francisella tularensis. Microb Pathog. 2008;45(2):79-85. doi: 10.1016/j.micpath.2008.01.010. PubMed PMID: 18524531.

226. Cole LE, Yang Y, Elkins KL, Fernandez ET, Qureshi N, Shlomchik MJ, et al. Antigen-specific B-1a antibodies induced by Francisella tularensis LPS provide long-term protection against F. tularensis LVS challenge. Proc Natl Acad Sci U S A. 2009;106(11):4343-8. doi: 10.1073/pnas.0813411106. PubMed PMID: 19251656; PubMed Central PMCID: PMC2657382.

227. Dreisbach VC, Cowley S, Elkins KL. Purified lipopolysaccharide from Francisella tularensis live vaccine strain (LVS) induces protective immunity against LVS infection that requires B cells and gamma interferon. Infect Immun. 2000;68(4):1988-96. PubMed PMID: 10722593; PubMed Central PMCID: PMC97377.

228. Crane DD, Griffin AJ, Wehrly TD, Bosio CM. B1a Cells Enhance Susceptibility to Infection with Virulent Francisella tularensis via Modulation of NK/NKT Cell Responses. J Immunol. 2013;190(6):2756-66. doi: 10.4049/jimmunol.1202697. PubMed PMID: 23378429; PubMed Central PMCID: PMC3594638.

229. Koskela P, Salminen A. Humoral immunity against Francisella tularensis after natural infection. J Clin Microbiol. 1985;22(6):973-9. Epub 1985/12/01. PubMed PMID: 4066925; PubMed Central PMCID: PMCPMC271862.

230. Francis E, Evans A. Agglutination, cross-agglutination, and agglutination absorption in tularemia. Public Health Rep. 1926;41:1273-95.

231. Ransmeier J, Ewing C. The agglutination reaction in tularemia. The Journal of infectious diseases. 1941;69(193-205).

232. Ericsson M, Sandstrom G, Sjostedt A, Tarnvik A. Persistence of cell-mediated immunity and decline of humoral immunity to the intracellular bacterium Francisella tularensis 25 years after natural infection. J Infect Dis. 1994;170(1):110-4. Epub 1994/07/01. PubMed PMID: 8014484.

233. Koskela P, Herva E. Cell-mediated and humoral immunity induced by a live Francisella tularensis vaccine. Infect Immun. 1982;36(3):983-9. Epub 1982/06/01. PubMed PMID: 7095859; PubMed Central PMCID: PMCPMC551428.

234. Waag DM, McKee KT, Jr., Sandstrom G, Pratt LL, Bolt CR, England MJ, et al. Cell-mediated and humoral immune responses after vaccination of human volunteers with the live vaccine strain of Francisella tularensis. Clin Diagn Lab Immunol. 1995;2(2):143-8. Epub 1995/03/01. PubMed PMID: 7697521; PubMed Central PMCID: PMCPMC170117.

235. Thorpe BD, Marcus S. Phagocytosis and intracellular fate of Pasteurella tularensis: in vitro effects of exudate stimulants and streptomycin on phagocytic cells. Journal of the Reticuloendothelial Society. 1967;4(1):10-23. PubMed PMID: 6030546.

236. Fulop M, Mastroeni P, Green M, Titball RW. Role of antibody to lipopolysaccharide in protection against low- and high-virulence strains of Francisella tularensis. Vaccine. 2001;19(31):4465-72. PubMed PMID: 11483272.

237. Stenmark S, Lindgren H, Tarnvik A, Sjostedt A. Specific antibodies contribute to the host protection against strains of Francisella tularensis subspecies holarctica. Microb Pathog. 2003;35(2):73-80. PubMed PMID: 12901846.

238. Kirimanjeswara GS, Golden JM, Bakshi CS, Metzger DW. Prophylactic and therapeutic use of antibodies for protection against respiratory infection with Francisella tularensis. J Immunol. 2007;179(1):532-9. PubMed PMID: 17579074.

239. Lavine CL, Clinton SR, Angelova-Fischer I, Marion TN, Bina XR, Bina JE, et al. Immunization with heat-killed Francisella tularensis LVS elicits protective antibody-mediated immunity. European journal of immunology. 2007;37(11):3007-20. doi: 10.1002/eji.200737620. PubMed PMID: 17960662.

240. Klimpel GR, Eaves-Pyles T, Moen ST, Taormina J, Peterson JW, Chopra AK, et al. Levofloxacin rescues mice from lethal intra-nasal infections with virulent Francisella tularensis and induces immunity and production of protective antibody. Vaccine. 2008;26(52):6874-82. doi: 10.1016/j.vaccine.2008.09.077. PubMed PMID: 18930100; PubMed Central PMCID: PMC2630585.

241. Conlan JW, Shen H, Webb A, Perry MB. Mice vaccinated with the O-antigen of Francisella tularensis LVS lipopolysaccharide conjugated to bovine serum albumin develop varying degrees of protective immunity against systemic or aerosol challenge with virulent type A and type B strains of the pathogen. Vaccine. 2002;20(29-30):3465-71. PubMed PMID: 12297391.

242. Fulop M, Manchee R, Titball R. Role of lipopolysaccharide and a major outer membrane protein from Francisella tularensis in the induction of immunity against tularemia. Vaccine. 1995;13(13):1220-5. PubMed PMID: 8578807.

243. Conlan JW, Vinogradov E, Monteiro MA, Perry MB. Mice intradermally-inoculated with the intact lipopolysaccharide, but not the lipid A or O-chain, from Francisella tularensis LVS rapidly acquire varying degrees of enhanced resistance against systemic or aerogenic challenge with virulent strains of the pathogen. Microb Pathog. 2003;34(1):39-45. PubMed PMID: 12620383.

244. Baron SD, Singh R, Metzger DW. Inactivated Francisella tularensis live vaccine strain protects against respiratory tularemia by intranasal vaccination in an immunoglobulin A-dependent fashion. Infect Immun. 2007;75(5):2152-62. doi: 10.1128/IAI.01606-06. PubMed PMID: 17296747; PubMed Central PMCID: PMC1865787.

245. Bitsaktsis C, Rawool DB, Li Y, Kurkure NV, Iglesias B, Gosselin EJ. Differential requirements for protection against mucosal challenge with Francisella tularensis in the

presence versus absence of cholera toxin B and inactivated F. tularensis. J Immunol. 2009;182(8):4899-909. doi: 10.4049/jimmunol.0803242. PubMed PMID: 19342669; PubMed Central PMCID: PMC2720832.

246. Eyles JE, Hartley MG, Laws TR, Oyston PC, Griffin KF, Titball RW. Protection afforded against aerosol challenge by systemic immunisation with inactivated Francisella tularensis live vaccine strain (LVS). Microb Pathog. 2008;44(2):164-8. doi: 10.1016/j.micpath.2007.08.009. PubMed PMID: 17904793.

247. Huntley JF, Conley PG, Rasko DA, Hagman KE, Apicella MA, Norgard MV. Native outer membrane proteins protect mice against pulmonary challenge with virulent type A Francisella tularensis. Infect Immun. 2008;76(8):3664-71. doi: 10.1128/IAI.00374-08. PubMed PMID: 18505805; PubMed Central PMCID: PMC2493219.

248. Ray HJ, Cong Y, Murthy AK, Selby DM, Klose KE, Barker JR, et al. Oral live vaccine strain-induced protective immunity against pulmonary Francisella tularensis challenge is mediated by CD4+ T cells and antibodies, including immunoglobulin A. Clinical and vaccine immunology : CVI. 2009;16(4):444-52. doi: 10.1128/CVI.00405-08. PubMed PMID: 19211773; PubMed Central PMCID: PMC2668291.

249. Elkins KL, Rhinehart-Jones TR, Culkin SJ, Yee D, Winegar RK. Minimal requirements for murine resistance to infection with Francisella tularensis LVS. Infect Immun. 1996;64(8):3288-93. Epub 1996/08/01. PubMed PMID: 8757866; PubMed Central PMCID: PMC174220.

250. Elkins KL, Rhinehart-Jones T, Nacy CA, Winegar RK, Fortier AH. T-cell-independent resistance to infection and generation of immunity to Francisella tularensis. Infect Immun. 1993;61(3):823-9. Epub 1993/03/01. PubMed PMID: 8432603; PubMed Central PMCID: PMCPMC302807.

251. Cowley SC, Hamilton E, Frelinger JA, Su J, Forman J, Elkins KL. CD4-CD8- T cells control intracellular bacterial infections both in vitro and in vivo. J Exp Med. 2005. p. 309-19.

252. Cowley SC, Meierovics AI, Frelinger JA, Iwakura Y, Elkins KL. Lung CD4-CD8- double-negative T cells are prominent producers of IL-17A and IFN-gamma during primary respiratory murine infection with Francisella tularensis live vaccine strain. J Immunol. 2010. p. 5791-801.

253. Chen W, Kuolee R, Austin JW, Shen H, Che Y, Conlan JW. Low dose aerosol infection of mice with virulent type A Francisella tularensis induces severe thymus atrophy and CD4+CD8+ thymocyte depletion. Microb Pathog. 2005;39(5-6):189-96. Epub 2005/11/01. doi: S0882-4010(05)00096-3 [pii] 10.1016/j.micpath.2005.08.005. PubMed PMID: 16257504; PubMed Central PMCID: PMC1564440.

254. Sjostedt A, North RJ, Conlan JW. The requirement of tumour necrosis factor-alpha and interferon-gamma for the expression of protective immunity to secondary murine tularaemia depends on the size of the challenge inoculum. Microbiology. 1996;142 ( Pt 6):1369-74. PubMed PMID: 8704976.

255. Anthony LS, Ghadirian E, Nestel FP, Kongshavn PA. The requirement for gamma interferon in resistance of mice to experimental tularemia. Microb Pathog. 1989;7(6):421-8. Epub 1989/12/01. PubMed PMID: 2516219.

256. Cowley SC, Elkins KL. Multiple T cell subsets control Francisella tularensis LVS intracellular growth without stimulation through macrophage interferon gamma receptors. J Exp Med. 2003. p. 379-89.

257. Cowley SC, Sedgwick JD, Elkins KL. Differential requirements by CD4+ and CD8+ T cells for soluble and membrane TNF in control of Francisella tularensis live vaccine strain intramacrophage growth. J Immunol. 2007. p. 7709-19.

258. Barrigan LM, Tuladhar S, Brunton JC, Woolard MD, Chen C, Saini D, et al. Infection with Francisella tularensis clpB leads to an altered yet protective immune response. Infection and Immunity. 2013;in press.

259. Pepper M, Linehan JL, Pagan AJ, Zell T, Dileepan T, Cleary PP, et al. Different routes of bacterial infection induce long-lived TH1 memory cells and short-lived TH17 cells. Nat Immunol. 2010. p. 83-9.

260. Kurtulus S, Hildeman D. Assessment of CD4(+) and CD8 (+) T cell responses using MHC class I and II tetramers. Methods in molecular biology. 2013;979:71-9. doi: 10.1007/978-1-62703-290-2_8. PubMed PMID: 23397390.

261. Valentino MD, Hensley LL, Skrombolas D, McPherson PL, Woolard MD, Kawula TH, et al. Identification of a dominant CD4 T cell epitope in the membrane lipoprotein Tul4 from Francisella tularensis LVS. Mol Immunol. 2009;46(8-9):1830-8. Epub 2009/02/24. doi: S0161-5890(09)00038-8 [pii] 10.1016/j.molimm.2009.01.008. PubMed PMID: 19233475; PubMed Central PMCID: PMC2709240.

262. Lee BY, Horwitz MA, Clemens DL. Identification, recombinant expression, immunolocalization in macrophages, and T-cell responsiveness of the major extracellular proteins of Francisella tularensis. Infect Immun. 2006;74(7):4002-13. doi: 10.1128/IAI.00257-06. PubMed PMID: 16790773; PubMed Central PMCID: PMC1489726.

263. Yu JJ, Goluguri T, Guentzel MN, Chambers JP, Murthy AK, Klose KE, et al. Francisella tularensis T-cell antigen identification using humanized HLA-DR4 transgenic mice. Clinical and vaccine immunology : CVI. 2010;17(2):215-22. doi: 10.1128/CVI.00361-09. PubMed PMID: 20016043; PubMed Central PMCID: PMC2815527.

264. McMurry JA, Gregory SH, Moise L, Rivera D, Buus S, De Groot AS. Diversity of Francisella tularensis Schu4 antigens recognized by T lymphocytes after natural infections in humans: identification of candidate epitopes for inclusion in a rationally designed tularemia vaccine. Vaccine. 2007;25(16):3179-91. doi: 10.1016/j.vaccine.2007.01.039. PubMed PMID: 17291638.

265. Gregory SH, Mott S, Phung J, Lee J, Moise L, McMurry JA, et al. Epitope-based vaccination against pneumonic tularemia. Vaccine. 2009;27(39):5299-306. doi: 10.1016/j.vaccine.2009.06.101. PubMed PMID: 19616492; PubMed Central PMCID: PMC2772204.

266. Woolard MD, Barrigan LM, Fuller JR, Buntzman AS, Bryan J, Manoil C, et al. Identification of *Francisella novicida* mutants that fail to induce prostaglandin $E_2$ synthesis by infected macrophages. Front Microbiol. 2013;4. doi: 10.3389/fmicb.2013.00016.

267. Elkins KL, Colombini SM, Meierovics AI, Chu MC, Chou AY, Cowley SC. Survival of secondary lethal systemic Francisella LVS challenge depends largely on interferon gamma. Microbes Infect. 2010;12(1):28-36. doi: 10.1016/j.micinf.2009.09.012. PubMed PMID: 19781659.

268. Conlan W, Shen H, Kuolee R, Zhao X, Chen W. Aerosol-, but not intradermal-immunization with the live vaccine strain of Francisella tularensis protects mice against subsequent aerosol challenge with a highly virulent type A strain of the pathogen by an alphabeta T cell- and interferon gamma- dependent mechanism. Vaccine. 2005;23(19):2477-85. doi: 10.1016/j.vaccine.2004.10.034. PubMed PMID: 15752834.

269. Bakshi CS, Malik M, Mahawar M, Kirimanjeswara GS, Hazlett KR, Palmer LE, et al. An improved vaccine for prevention of respiratory tularemia caused by Francisella tularensis SchuS4 strain. Vaccine. 2008;26(41):5276-88. doi: 10.1016/j.vaccine.2008.07.051. PubMed PMID: 18692537; PubMed Central PMCID: PMC2652725.

270. Shen H, Harris G, Chen W, Sjostedt A, Ryden P, Conlan W. Molecular immune responses to aerosol challenge with Francisella tularensis in mice inoculated with live vaccine candidates of varying efficacy. PLoS One. 2010;5(10):e13349. doi: 10.1371/journal.pone.0013349. PubMed PMID: 20967278; PubMed Central PMCID: PMC2953512.

271. Karttunen R, Surcel HM, Andersson G, Ekre HP, Herva E. Francisella tularensis-induced in vitro gamma interferon, tumor necrosis factor alpha, and interleukin 2 responses appear within 2 weeks of tularemia vaccination in human beings. J Clin Microbiol. 1991;29(4):753-6. PubMed PMID: 1909711; PubMed Central PMCID: PMC269865.

272. Surcel HM, Syrjala H, Karttunen R, Tapaninaho S, Herva E. Development of Francisella tularensis antigen responses measured as T-lymphocyte proliferation and cytokine production (tumor necrosis factor alpha, gamma interferon, and interleukin-2 and -

4) during human tularemia. Infect Immun. 1991;59(6):1948-53. PubMed PMID: 1674737; PubMed Central PMCID: PMC257948.

273. Salerno-Goncalves R, Hepburn MJ, Bavari S, Sztein MB. Generation of heterogeneous memory T cells by live attenuated tularemia vaccine in humans. Vaccine. 2009;28(1):195-206. doi: 10.1016/j.vaccine.2009.09.100. PubMed PMID: 19799845; PubMed Central PMCID: PMC2788084.

274. Paranavitana C, Zelazowska E, DaSilva L, Pittman PR, Nikolich M. Th17 cytokines in recall responses against Francisella tularensis in humans. Journal of interferon & cytokine research : the official journal of the International Society for Interferon and Cytokine Research. 2010;30(7):471-6. doi: 10.1089/jir.2009.0108. PubMed PMID: 20626289.

275. Eneslatt K, Rietz C, Ryden P, Stoven S, House RV, Wolfraim LA, et al. Persistence of cell-mediated immunity three decades after vaccination with the live vaccine strain of Francisella tularensis. European journal of immunology. 2011;41(4):974-80. doi: 10.1002/eji.201040923. PubMed PMID: 21442618; PubMed Central PMCID: PMC3516913.

# CHAPTER 2

# INFECTION WITH *FRANCISELLA TULARENSIS* LVS *CLPB* LEADS TO AN ALTERED YET PROTECTIVE IMMUNE RESPONSE[1,2]

## OVERVIEW

Bacterial attenuation is typically thought of as reduced bacterial growth in the presence of constant immune pressure. Infection with *Francisella tularensis* elicits innate and adaptive immune responses. Several in vivo screens have identified *F. tularensis* genes necessary for virulence. Many of these mutations render *F. tularensis* defective for intracellular growth. However, some mutations have no impact on intracellular growth leading us to hypothesize that these *F. tularensis* mutants are attenuated because they induce an altered host immune response. We were particularly interested in the *F. tularensis* LVS mutant *clpB* (FTL_0094) because this strain was attenuated in pneumonic tularemia yet induced a protective immune response. LVS *clpB*'s attenuation was not due to an intracellular growth defect as LVS *clpB* grew similarly to LVS in primary bone marrow derived macrophages and a variety of cell lines. We therefore determined whether LVS *clpB* induced an altered immune response compared to LVS in vivo. We found that LVS *clpB*

[1] Contributing authors: Lydia M. Barrigan, Shraddha Tuladhar, Jason C. Brunton, Matthew D. Woolard, Ching-ju Chen, Divey Saini, Richard Frothingham, Gregory D. Sempowski, Thomas H. Kawula, and Jeffrey A. Frelinger

[2] Portions of this chapter were published in *Infection and Immunity*. Barrigan, et al. 2013 Jun;81(6):2028-42. 

induced pro-inflammatory cytokine production in the lung early after infection, a process not observed during LVS infection. LVS *clpB* provoked a robust adaptive immune response similar in magnitude to LVS, but with increased IFN-γ and IL-17A production as measured by mean fluorescence intensity. Altogether, our results indicate that LVS *clpB* is attenuated due to altered host immunity and not an intrinsic growth defect. These results also indicate that disruption of non-essential gene(s) that are involved in bacterial immune evasion, like *F. tularensis clpB*, can serve as a model for the rational design of attenuated vaccines.

## INTRODUCTION

Enormous efforts have gone into detecting bacterial mutations that result in diminished growth in vivo. Many of these mutations are the result of a failure of the pathogen to grow in vitro, and can be attributed to defects in critical aspects of bacterial metabolism. Mutations, for example, that result in auxotrophy render the bacteria incapable of synthesizing essential nutrients such as purines or co-enzymes and therefore cause a growth defect. Relatively few mutations that cause bacterial attenuation have been demonstrated to be the result of a failure of the pathogen to interfere with host immune responses. In this manuscript, we focus on one mutation that likely falls into this class of altered host immunity.

*Francisella tularensis* is a gram negative coccobacillus and the causative agent of the zoonotic disease tularemia. Inhalation of as few as 10 virulent type A *F. tularensis* organisms can cause fatal disease in humans (1). This low infectious dose, ability to persist in the environment, ease of aerosolization, and high morbidity and mortality has earned *F. tularensis* a Category A Select Agent classification (2). In fact, *F. tularensis* has been used

as the infectious agent in bioweapons and continues to present a real threat today (3, 4). It is therefore critical to understand both infection and pathogenesis. Many attenuating mutations of *Francisella* have been described (5-7), but little information is available on the immune response to attenuated mutants, beyond whether they can protect from secondary challenge with wild-type bacteria.

Experiments utilizing *F. tularensis* as the infectious agent typically use three strains that differ widely for virulence in humans and mice. *F. tularensis* subsp. *tularensis* SchuS4 (SchuS4) is a type A strain and must be handled at BSL-3 conditions because of its low infectious dose and its ability to be transmitted via aerosol. SchuS4 is highly pathogenic in mice with an $LD_{100}$ of <10 CFU (8). Mice inoculated with SchuS4 succumb to infection within 6 days of inoculation (9) making studies of the adaptive immune response in non-manipulated mice impossible. For our experiments, we used the type B strain, *F. tularensis* subsp. *holartica* live vaccine strain (LVS). LVS is attenuated in humans and mice compared to SchuS4. Although LVS was widely used in Eastern Europe as a vaccine, it is unlikely to ever be licensed in the United States. LVS's intranasal $LD_{50}$ is approximately 1000 CFU in mice (8) allowing us to examine aspects of adaptive immunity using an intranasal inoculation dose of 500 CFU. The third strain commonly used is *F. novicida* U112 (U112) which is avirulent in immunocompetent humans but is highly virulent in mice with a low infectious dose and rapid death similar to SchuS4.

The immune response to *F. tularensis* is multi-layered and complex, requiring components of both innate and adaptive immunity. The bacterium has evolved several strategies to evade or subvert the host's immune response so that it can persist in the host. First, *F. tularensis* infects a variety of innate immune cells during infection in the lung

including macrophages, dendritic cells, monocytes, and neutrophils (10, 11). *F. tularensis* also expresses a form of LPS that does not efficiently stimulate TLR4 (12). LVS does not stimulate functional maturation (cytokine production) of dendritic cells but does promote phenotypic maturation through the up-regulation of CD80 and CD86 (11). SchuS4 does not induce phenotypic or functional maturation of dendritic cells, allowing the bacterium to persist in an immunosuppressed environment (13). Finally, *F. tularensis* lives intracellularly, allowing the bacterium to avoid antibody and complement-mediated destruction (14).

Because *F. tularensis* replicates within host cells, the T cell response is a critical component for bacterial clearance. Indeed, T cells are required for clearance of *F. tularensis* and the development of protective immunity (15). In particular, IFN-γ is required for controlling *F. tularensis* infection. When IFN-γ is blocked by antibody, there is an increase in bacterial burden and mice deficient in IFN-γ succumb to an LVS inoculum dose that is sublethal in wild-type mice (16, 17). Administration of recombinant IFN-γ to infected mice decreases bacterial burdens confirming this cytokine's importance in control of the infection (18). Th17 cells are also induced in the lung following intranasal inoculation (19). IL-17A deficient mice have increased bacterial burdens compared to wild-type mice and administration of IL-17 neutralizing antibody also increased bacterial burdens highlighting this cytokine's importance during respiratory tularemia (20, 21).

Several in vivo screens have identified *F. tularensis* virulence determinants in U112, LVS, and SchuS4 (5-7). A *F. tularensis* mutant could be attenuated if the mutation disrupts expression of a gene necessary for intracellular growth such as the genes within the pathogenicity island (22). A *F. tularensis* mutant could also be attenuated if the disrupted gene causes the strain to become an auxotroph (5-7). When a mutation does not cause an

intracellular growth defect, a strain's attenuation could be the result of the failure to evade the host's immune response. We were interested in characterizing the immune response to an attenuated LVS mutant, LVS *clpB* (FTL_0094). *clpB* encodes a highly conserved chaperone protein of the AAA+ superfamily of ATPases. *F. tularensis* ClpB is involved in the response to oxidative, ethanol, and acid stresses (23). LVS *clpB* and SchuS4 *clpB* strains are attenuated when delivered using intradermal, intraperitoneal, or oral inoculation routes (23-25). Previous infection with LVS *clpB* and SchuS4 *clpB* provided protection during wild-type challenge (23-25). However, the host's primary immune response to LVS *clpB* that elicits protection during wild-type challenge has not yet been examined.

In this study, we examined the innate and adaptive immune response following intranasal infection with LVS or LVS *clpB*. Our LVS *clpB* strain did not show any defects in intracellular growth in primary bone marrow derived macrophages or several cell lines. Because there were no differences in growth, we hypothesized that LVS *clpB*'s attenuation was due to an altered immune response. Indeed, LVS *clpB* induced altered innate and adaptive immune responses compared to LVS. Other groups have shown SchuS4 *clpB* and LVS *clpB* are attenuated in vivo, but potential mechanism(s) causing attenuation have not been described (23-25). The work presented here describes the immune response that contributes to LVS *clpB*'s attenuation. The studies also highlight the potential use of *clpB* as a target for attenuation because milder disease is caused while still inducing a robust protective immune response in the lung.

## MATERIALS AND METHODS

### Bacteria

The live vaccine strain of *Francisella tularensis* subsp. *holartica* (LVS) was obtained from the CDC (Atlanta, GA). *F. tularensis* subsp. *tularensis* (SchuS4) was obtained from BEI Resources (Manassas, VA). Bacteria were grown on chocolate agar supplemented with 1% IsoVitalex (Becton-Dickinson), brain heart infusion (BHI) broth supplemented with 1% IsoVitalex, or Chamberlain's defined media (CDM) (26). When necessary, kanamycin (10 μg/mL) or hygromycin (200 μg/mL) was added for antibiotic selection. Bacteria were grown at 37˚C. To prepare bacterial inoculations, bacteria were removed from a lawn grown on chocolate agar and resuspended in sterile PBS at an $OD_{600}$=1 (equivalent to $1x10^{10}$ CFU/mL). Appropriate dilutions were made in sterile PBS to obtain the desired bacterial dose. The number of viable bacteria was quantified by serial dilution and plating on chocolate agar. The LVS *clpB*::Tn strain was generated using the EZ-Tn5 system (Epicentre). Insertion in *clpB* mapped to nucleotide 89763. The LVS *clpB* (FTL_0094) and LVS *dotU* (FTL_0119) deletion strains were generated using the suicide vector pMP812 (27) containing an amplified region of *clpB* or *dotU*.

### Bacterial growth curves

In a 96-well plate, CDM or BHI broth was inoculated with LVS, LVS *clpB*, or LVS *dotU* so that the starting $OD_{600}$=0.01. The $OD_{600}$ was measured every 15 minutes for 48 hours using a TECAN Infinite M200 plate reader (TECAN) capable of maintaining 37˚C and 5% $CO_2$ while shaking.

**Mice**

C57Bl/6J (B6), B6.SJL-*Ptprc*$^{a}$*Pepc*$^{b}$/BoyJ (B6-CD45.1), and BALB/cByJ (BALB/c) mice were obtained from The Jackson Laboratory (Bar Harbor, ME). B6.129S7-*Rag1*$^{tm1Mom}$/J (Rag$^{-/-}$) were purchased from The Jackson Laboratory and then bred in-house. All mice were housed in specific-pathogen free conditions at the University of Arizona or Duke University in accordance with their respective Institutional Animal Care and Use Committees. Female B6 and BALB/c mice used for infections were between 7 to 12 weeks of age.

**Cell lines and BMDM generation**

J774.1, MH-S, and A549 cells were obtained from ATCC (Manassas, VA). J774.1 and A549 cells were cultured in DMEM supplemented with 10% fetal bovine serum (Atlas), L-glutamine (HyClone), sodium pyruvate (HyClone), and penicillin/streptomycin (Life). MH-S cells were cultured in RPMI 1640 supplemental with 10% fetal bovine serum (Atlas), L-glutamine (HyClone), sodium pyruvate (HyClone), and penicillin/streptomycin (Life). Media was replaced with antibiotic free media 24 hours prior to inoculation with *F. tularensis*. BMDMs were generated from B6 bone marrow as previously described (28).

**In vitro growth assays**

1x10$^{6}$ cells/well (BMDM, J774, and MH-S) or 0.5x10$^{6}$ cells/well (A549) were seeded into a 24 well plate for intracellular growth assays and given 2 hours to adhere to the plate. Cells were inoculated at a multiplicity of infection (MOI) of 25:1. Infection was facilitated by centrifugation at 300xg for 5 minutes. Cells were incubated for 2 hours with bacteria and then media was removed. Media containing 50 μg/mL gentamicin (Sigma) was added to kill extracellular bacteria. One hour after gentamicin addition, media was removed and the cells

were washed twice before the addition of fresh media. To determine intracellular growth, media was removed 4 or 24 hours post-infection and 1 mL of PBS was added to the cells. Cells were removed from the plate by scraping and pipeting vigorously up and down. Cells were lysed by vortexing at maximal speed for 1 minute. Serial 1:10 dilutions of the lysate were made and plated on chocolate agar. Resulting colonies were counted 72 hours later.

**Inoculation of Mice**

Mice were anesthetized with 575 mg/kg tribromomethanol (Avertin) (Sigma) administered intraperitoneally. Mice were then intranasally inoculated with 5 x $10^2$ CFU LVS, 5x$10^4$ CFU LVS *clpB*, or 5x$10^5$ CFU LVS *dotU* suspended in 50 μL PBS. For high dose LVS challenge experiments, mice were anesthetized with 0.25 mL of 7.5 mg/mL ketamine and 0.5 mg/mL xylazine cocktail in PBS. Mice were then intranasally inoculated with 5x$10^3$ CFU LVS. For SchuS4 challenge, approximately 30 CFUs of SchuS4 were administered via the aerosol route in a BSL-3 chamber. Mice were weighed daily following all inoculations. Mice were sacrificed if they lost more than 25% of their starting weight as indicated in our UA and Duke IACUC protocols.

**Determination of bacterial burdens**

Spleens, livers, and lungs were homogenized in sterile PBS using a Biojector (Bioject). 10-fold serial dilutions were made and plated on chocolate agar. Resulting colonies were counted 72 hours later. The limit of detection is 50 CFU per organ.

**Collection of broncheoalverolar lavage fluid**

Mice were sacrificed and the trachea exposed. A 22 gauge catheter was inserted into the trachea and secured with suture. The lungs were fully inflated with 800 μL of PBS and

washed three times. Cells were removed from the lavage fluid by centrifugation. Collected lavage fluid was frozen at -80˚C until Luminex analysis.

**Luminex analysis**

A multiplex luminex bead-based approach was used to quantify cytokines/chemokines in BAL fluid or clarified tissue homogenate. A 20-analyte assay panel was performed according to the manufacturer's protocol (Invitrogen) using a BioPlex array reader (Bio-Rad Laboratories). Using integrated cytokine/chemokine standard curves, the assay reports pg/mL of the following analytes: FGF basic, GM-CSF, IFN-γ, IL-1α, IL-1β, IL-2, IL-4, IL-5, IL-6, IL-10, IL-12 (p40/p70), IL-13, IL-17, KC, MCP-1, MIG, MIP-1α, TNF-α, and VEGF. A five-parameter non-linear logistic regression model was used to establish standard curve and to estimate the probability of occurrence of a concentration at a given point. Standard outliers were removed from the analysis if the observed/expected % recovery was outside of the acceptable limits (70-130%). Upper and lower levels of quantification were determined by the BioPlex Manager software based on goodness of fit and percent recovery. Calculated pg/mL for experimental specimens were multiplied by the inherent assay dilution factor (df=2) and reported as final observed pg/mL.

**Depletion of IFN-γ**

Purified XMG1.2 (anti-IFN-γ) antibody was a generous gift from Mary Ann Accavitti-Loper at the SERCEB Mouse Monoclonal Antibody Core (University of Alabama-Birmingham). Rat IgG1 isotype control antibody (anti-HRPN) was purchased from BioXCell (West Lebanon, NH). Mice were administered 500 μg of depleting or control antibody in 200 μL PBS via intraperitoneal injection on days 0 and 2 post-inoculation.

**Gating strategy for BALF analysis**

The gating scheme is shown in figure 1. Single cells were discriminated from doublets by plotting side scatter height (SSC-H) versus side scatter area (SSC-A). Cells were then gated on by plotting SSC-A versus forward scatter area (FSC-A). Live cells were then gated by plotting the live/dead stain on a 1-D histogram. Cells from the BALF were discriminated from the CFSE-labeled splenocyte carries by plotting an empty channel versus CFSE. $CD3^+$, $CD19^+$, and not B and T cells were gated on by plotting CD3 versus CD19. From the not B and T gate, GR-1 versus CD11b was plotted to distinguish neutrophils from not neutrophils. From the not neutrophils gate, SSC-A versus F4/80 was plotted to distinguish $F4/80^+$ from $F4/80^-$ cells. From the $F4/80^-$ gate, CD11c versus FSC-A was plotted and dendritic cells were gated on. From the $F4/80^+$ gate, CD11c versus CD11b was plotted to distinguish alveolar macrophages (AMs) from interstitial macrophages (IMs).

**Collection of spleen and lung cells**

Spleens were harvested from mice and made into a single cell suspension. Red blood cells were lysed using ammonium chloride-potassium carbonate lysis buffer. Lungs were perfused with PBS to remove blood and then finely minced. Minced lung was placed in 10 mL of digestion buffer containing 0.5 mg/mL collagenase I (Worthington Biochemical), 0.02 mg/mL DNase (Sigma), and 125 U/mL elastase (Worthington Biochemical) in RPMI1640 (HyClone). Lungs were digested for 30 minutes at 37˚C and then vigorously pipetted prior to filtering through a 100 μM filter. Mononuclear cells were isolated from the single cell suspension by density gradient centrifugation over Lympholyte M (Cedarlane Labs). Viable cells from spleen and lung were determined by trypan blue exclusion using a hemacytometer.

**Antibodies**

The following directly conjugated antibodies were utilized for flow cytometry analysis: CD3 AF488 (Clone 145-2C11, eBioscience); CD3 Pacific Blue (Clone 17A2, Biolegend); CD4 AF700 (Clone GK1.5, Biolegend); CD8a V500 (Clone 53-6.7, BD Biosciences); CD11b Pacific Blue (Clone M1/70, Biolegend); CD11b V500 (Clone M1/70, BD Horizon); CD11c Pacific Blue (Clone N418, Biolegend); CD11c PE-Cy7 (Clone N418, Biolegend); CD19 Pacific Blue (Clone 6D5, Biolegend); CD19 PerCP-Cy5.5 (Clone 6D5, Biolegend); CD45.1 PE-Cy7 (Clone A20, Biolegend); F4/80 Pacific Blue (Clone BM8, Biolegend); F4/80 PE (Clone BM8, eBioscience); GR-1 (Ly-6G) eFluor 450 (Clone RB6-8C5, eBioscience); GR-1 AF700 (clone RB6-8C5, eBioscience); IFN-γ PE (Clone XMG1.2, BD Biosciences); IL-17A AF647 (Clone TC11-18H10.1, Biolegend); NK1.1 Pacific Blue (Clone PK136, Biolegend); TCR γδ PerCP-Cy5.5 (Clone GL3, Biolegend). All antibodies were titrated on normal B6 splenocytes prior to use.

**Intracellular cytokine staining**

Splenocytes from B6-CD45.1 mice were used as antigen presenting cells. B6-CD45.1 cells were added at $2x10^6$/well in a 24 well plate or $0.5x10^6$/well in a 48 well plate and infected with LVS at an MOI of 200:1 or mock infected. Two hours post-infection, the media was removed and 5 μg/mL gentamicin was added to kill any extracellular bacteria. Splenocytes were cultured overnight in the presence of gentamicin. Prior to co-culture with cells isolated from infected mice, antigen presenting cells were washed extensively to remove any cytokine or $PGE_2$ that could interfere with the co-culture. Cells isolated from mice were co-cultured at a 1:1 ratio with infected or mock infected splenocytes for 24 hours. During the last 4 hours of culture, 10 μg/mL Brefeldin A (Sigma) was added to each well to

stop cytokine secretion. Cells were removed from the plate and stained with Pacific Blue succimidyl ester (Invitrogen) to distinguish live and dead cells. Cells were then stained with antibodies for surface markers. Following fixation and permeabilization of the cells, cells were stained for IFN-γ and IL-17A. Cells were washed extensively after each staining step to remove residual unbound antibody.

**Gating strategy for intracellular cytokine staining analysis**

The gating scheme is shown in figure 2. Single cells were discriminated from doublets by plotting side scatter linear versus side scatter area. Cells were then selected by plotting side scatter area versus forward scatter area. Live $CD3^+$ T cells were then selected by plotting CD3 versus the Pacific Blue channel which included the live/dead stain and markers for antigen presenting cells. From the $CD3^+$ gate, $CD4^+$ and $CD8^+$ T cells were selected. Gates for IFN-γ and IL-17A positive cells were set based on isotype control staining. Delta mean fluorescent intensity (ΔMFI) for each sample was determined by subtracting the cytokine negative population from the cytokine positive population. FlowJo v7.6 (Treestar) was used for all flow cytometry analysis.

**Determination of IFN-γ and IL-17A secretion by purified $CD4^+$ T cells**

B6 splenocytes were depleted of T cells using Mouse Thy1.2 Dynabeads (Life Technologies) and used as antigen presenting cells. $5x10^4$/well T cell depleted splenocytes were seeded in a 96 well plate and then infected with LVS at an MOI of 200:1 or mock infected. Two hours post-infection, the media was removed and 5 μg/mL gentamicin was added to kill any extracellular bacteria. T cell depleted splenocytes were cultured overnight in the presence of gentamicin. Prior to co-culture with purified $CD4^+$ T cells from infected mice, antigen presenting cells were washed extensively to remove any cytokine or $PGE_2$ that

could interfere with the co-culture. $CD4^+$ T cells were enriched from single cell suspension of lung cells or splenocytes using a Dynabeads Untouched Mouse CD4 Cells Kit (Life Technologies). Enriched $CD4^+$ T cells were co-cultured at a 1:1 ratio with T cell depleted LVS infected or mock infected splenocytes for 24 hours. Culture supernatant was then removed and stored at -20°C until ELISA analysis. Each sample was tested in triplicate. IFN-γ concentration was determined using a Mouse IFN-γ Instant ELISA (eBioscience) and IL-17A concentration was determined using a Mouse IL-17A Ready-Set-Go ELISA (eBioscience). T cell depletion and $CD4^+$ T cell enrichment was determined using flow cytometry analysis. IFN-γ and IL-17A concentrations were normalized based on the number of $CD4^+$ T cells in the culture as determined by flow cytometry.

**Statistical analysis**

Data were analyzed using a one-way ANOVA with Tukey's post-test for cytokine levels and flow cytometry results. Bacterial burdens were log transformed and then a Student's t-test or ANOVA with Tukey's post-test was applied. For LVS protection studies, a Chi-square test with Yates' correction was applied. GraphPad Prism (v5.04) was used for analysis. Error bars show standard error of the mean. Significance levels are indicated as follows: * $p < 0.05$; ** $p < 0.01$, *** $p < 0.001$, **** $p < 0.0001$.

## RESULTS

**LVS *clpB* is attenuated in mouse pneumonic tularemia**

Several groups have shown that LVS *clpB* or SchuS4 *clpB* strains are attenuated following either intradermal, intraperitoneal, or oral inoculation in either BALB/c or C3H/HeN mice (23-25). We were interested in determining whether LVS *clpB* was also

attenuated in a pneumonic tularemia model in C57Bl/6J (B6) mice. For this study, we produced two LVS *clpB* mutant strains. One strain carried a transposon (Tn) insertion in the *clpB* gene and the other was an in frame deletion of the *clpB* coding sequence. The mutations were confirmed by DNA sequencing. Although transposon mutations can have polar effects, we did not expect any from the transposon insertion in *clpB* because bioinformatic analysis indicated that *clpB* is not located in an operon (23). Indeed, we found the *clpB*::Tn mutant and the deletion strain behaved identically in all experiments. We have therefore combined all data and will simply refer to infection with either strain as LVS *clpB*.

Initial experiments demonstrated that LVS *clpB* did not disseminate to the spleen and liver in all mice when an inoculation dose of 500 CFU was used, despite this dose causing disease following LVS inoculation (figure 3). We therefore conducted preliminary experiments to establish the dose of LVS *clpB* that produced a similar peak bacteremia in the spleen so that mice were exposed to similar antigen levels. Similar antigen load is important because in other infection models, the magnitude of the primary adaptive immune response was influenced by the peak bacterial load and not the duration of infection (29-31). As a control for inoculation with a bacterial strain that failed to grow intracellularly, we selected LVS *dotU* (32). We achieved similar burdens for LVS and LVS *clpB* but since LVS *dotU* fails to grow intracellularly (32), this strain was inoculated at the highest practical dose. Seven to twelve week old B6 mice were intranasally inoculated with $5x10^2$ CFU LVS, $5x10^4$ CFU LVS *clpB*, or $5x10^5$ CFU LVS *dotU*. To determine bacterial growth in vivo, mice were euthanized on days 3, 7, and 10 post-inoculation and bacterial burdens were determined in the spleen, liver, and lung by plating serial dilutions of tissue homogenate on chocolate agar (figure 4A-C). While LVS *clpB* and LVS bacterial burdens were not significantly different 3

days post-inoculation in the spleen and liver, LVS *clpB* was cleared much faster than LVS from all organs tested. Few LVS *clpB* colonies were recovered 10 days post-inoculation while LVS-infected mice still had high bacterial loads, particularly in the lung. LVS *clpB* was also attenuated in BALB/c mice compared to LVS (figure 5A-C). Like B6 mice, LVS and LVS *clpB* burdens are similar in the spleen and liver of BALB/c mice on day 3 post-inoculation and LVS *clpB* is cleared faster than LVS.

Despite the 1000-fold higher dose of LVS *dotU* compared to LVS, the number of colonies recovered from the lungs 3 days post-inoculation was 1000-fold less than LVS. Viable LVS *dotU* organisms were recovered from isolated lung cells from LVS *dotU* infected mice harvested 3 days post-inoculation cultured in gentamicin for 1 hour demonstrating that LVS *dotU* was internalized and the bacteria had not simply persisted in the extracellular space (figure 6). Despite its intracellular location, LVS *dotU* failed to leave the lung and transit to the spleen and liver and was effectively cleared by 7 days post-inoculation in all organs tested. Because LVS *dotU* was not found in distal organs on day 3 post-inoculation, but infected cells were still present in the lung, these data suggest that infected cells were not the primary method of dissemination. Alternatively, the LVS *dotU* infected cells were not activated in a manner that caused them to leave the primary site of infection. To confirm that rapid clearance of LVS *clpB* and LVS *dotU* was specifically due to the absence of these genes, the strains were trans-complemented. B6 mice were intranasally inoculated with $5x10^2$ CFU of LVS *clpB* complement or LVS *dotU* complement. We used the same dose as LVS since transcomplementation should return these strains to wild-type LVS virulence levels. Indeed, transcomplementation of LVS *clpB* and LVS *dotU* led to bacterial burdens comparable to LVS in the spleen, liver, and lungs 3 days post-

inoculation (figure 7). Overall, these results demonstrate that LVS *clpB* is attenuated in a pneumonic model of tularemia, just as other groups have shown for LVS *clpB* and SchuS4 *clpB* by different routes of inoculation (23-25).

We also wanted to understand if the extent of disease caused by LVS *clpB* was similar to LVS induced disease. As a measure of overall health, body weight change is a reasonable measure of clinical status. Infected B6 and BALB/c mice were weighed daily and weight loss as a percentage of starting weight is reported (figure 8). LVS infected mice lost approximately 15% of their starting weight by day 7 and then slowly regained weight. In contrast to LVS, LVS *clpB* infected mice only lost approximately 10% of their starting weight and began to regain weight 5 days post-inoculation. LVS *clpB* mice regained their lost weight more rapidly than LVS infected mice which correlated with faster bacterial clearance. Mice infected with LVS *dotU* did not lose any weight, an expected result given the bacteria failed to grow in vivo. Together these results indicate the LVS *clpB* is attenuated in pneumonic tularemia and lead to a weight loss profile that differed from LVS infection.

**Previous infection with LVS *clpB* protects against lethal LVS intranasal challenge**

We next sought to determine whether previous intranasal inoculation with LVS, LVS *clpB*, or LVS *dotU* elicits an immune response that was protective against subsequent lethal LVS intranasal challenge. Mice were intranasally inoculated with $5x10^2$ CFU LVS, $5x10^4$ CFU LVS *clpB*, or $5x10^5$ CFU LVS *dotU*. To examine the early memory response, mice were challenged with $5x10^3$ CFU (approximately 5 $LD_{50}$ (8)) LVS intranasally 28 days after the initial infection. All mice vaccinated with LVS or LVS *clpB* survived lethal LVS challenge (figure 9A). LVS and LVS *clpB* vaccinated mice lost little weight following lethal LVS challenge and quickly returned to their starting weight (figure 9B). Naïve and LVS

*dotU* vaccinated mice continued to lose weight after LVS and LVS *clpB* vaccinated mice began their recovery. The abrupt change in the weight loss curve for the LVS *dotU* group is due to the one surviving mouse. Naïve mice fell below the weight loss threshold 6 or 7 days post-re-challenge. 5 of 6 LVS *dotU* vaccinated mice succumbed to infection 6 days after the lethal dose challenge. There was no significant difference in survival when LVS *dotU* vaccinated mice were compared to the naïve group. The surviving LVS *dotU* vaccinated mouse lost more than 20% of its starting weight, but never fell below the 25% threshold after challenge with LVS. Despite sustained illness indicated by weight loss in this mouse, there were no colonies recovered from the spleen, liver, or lung 14 days following the lethal challenge, similar to mice following primary exposure to LVS.

When naïve and LVS *dotU* vaccinated mice were sacrificed upon losing >25% of their starting weight (day 6 post-re-challenge), we harvested spleen, liver, and lung and determined bacterial burdens (figure 9C-E). We also harvested spleen, liver, and lungs from LVS and LVS *clpB* vaccinated mice on day 6 post-infection and determined bacterial burdens for comparison purposes (figure 9C-E). Naïve and LVS *dotU* vaccinated mice had high bacterial burdens in the spleen and liver with means exceeding $10^5$ CFU. Even higher bacterial burdens were observed in the lungs of naïve and LVS *dotU* vaccinated mice (means $>10^7$ CFU). LVS and LVS *clpB* vaccinated mice had few or no colonies recovered from the spleen, liver, and lung. For example, no colonies were recovered from the lungs of LVS vaccinated mice and 4 of 6 LVS *clpB* vaccinated mice.

We were also interested in whether LVS *clpB* would confer long-lived protection against lethal LVS challenge. Mice were intranasally innoculated with $5x10^2$ CFU LVS, $5x10^4$ CFU LVS *clpB*, or $5x10^5$ CFU LVS *dotU* and then challenged with $5x10^3$ CFU LVS

intranasally 120 days after the initial infection. All LVS and LVS *clpB* vaccinated mice survived lethal LVS challenge (figure 10A). All naïve mice succumbed to their infection by day 7. Over half of the LVS *dotU* vaccinated mice succumbed to their infection by day 7 and all but one mouse succumbed by day 14. The surviving LVS *dotU* vaccinated mouse lost more than 20% of its starting weight but never fell below the 25% threshold for sacrifice. This mouse was sacrificed on day 14 and the bacterial burdens were determined in the spleen, liver, and lung. 125 CFUs were recovered from the spleen, zero CFUs were recovered in the liver, and 425 CFUs were recovered from the lung indicating this mouse was clearing the high dose LVS challenge. When mice were challenged 120 days after vaccination, the LVS and LVS *clpB* vaccinated groups lost more weight (approximately 10-15% of starting weight) compared to the same groups challenged 28 days after vaccination (figure 10B). LVS and LVS *clpB* vaccinated mice not only showed equivalent weight loss after high-dose LVS challenge but also regained their lost weight at a similar pace. Naïve and LVS *dotU* vaccinated mice also show similar weight loss profiles compared to each other. Figure 2E also shows the surviving LVS *dotU* vaccinated mouse exhibited extreme weight loss but did rapidly gain weight on days 13 and 14.

When naïve and LVS *dotU* vaccinated mice fell below the weight loss threshold on day 6, four mice per group were sacrificed and bacterial burdens were determined for the spleen, liver and lung (figure 10C-E). Naïve and LVS *dotU* vaccinated mice had high bacterial burdens that were comparable to the burdens found when mice were challenged 28 days after vaccination with means exceeding $10^5$ in the spleen and liver and $10^7$ in the lung.. LVS and LVS *clpB* vaccinated mice had approximately $10^4$ CFU in their lungs on day 6 after

the high-dose LVS challenge but few, if any, CFUs in the spleen and liver. These results clearly indicate that LVS *clpB* protects against subsequent lethal LVS challenge.

Since LVS *clpB* induced a robust adaptive immune response that protected against a lethal LVS challenge, we next wanted to determine whether LVS *clpB* could protect against aerosolized highly virulent SchuS4. Mice were intranasally innoculated with $5x10^2$ CFU LVS, $5x10^4$ CFU LVS *clpB*, or $5x10^5$ CFU LVS *dotU* and then challenged with 30 CFU SchuS4 (measured as dose retained in the lungs at one hour, approximately 30 $LD_{100}$ (8)) via the aerosol route 28 days after the initial infection. The use of aerosolized SchuS4 in B6 mice is a very stringent test of whether LVS *clpB* infection confers protection. Previous vaccination with LVS protected 2 of 7 mice and LVS *clpB* vaccination protected 1 of 8. These results are consistent with the findings of others who have also shown that previous LVS infection does not fully protect against SchuS4 challenge in B6 mice (33, 34). Naïve and LVS *dotU* vaccinated mice succumbed to SchuS4 infection 5 days post-infection. While neither LVS nor LVS *clpB* vaccination provided complete protection against subsequent SchuS4 infection, these infections significantly increased the median survival time from 5 days (naïve) to 9 (LVS *clpB*) or 10 (LVS) days (figure 11). A Mantel-Cox log-rank test was used to compare survival of the vaccinated groups to the naïve group. LVS *dotU* vaccination was not statistically different from the naïve group but LVS and LVS *clpB* vaccination significantly increased survival after SchuS4 challenge ($p \leq 0.001$).

**LVS *clpB* does not exhibit an intracellular growth defect**

A bacterial strain's attenuation could be the result of a growth defect or an altered immune response that is more effective at bacterial clearance. We therefore sought to determine whether our LVS *clpB* or LVS *dotU* strains had a growth defect in broth or

intracellularly that could explain their attenuation in vivo. We initially examined the ability of LVS, LVS *clpB*, and LVS *dotU* to grow in either CDM (minimal) or BHI (rich) broth. We inoculated cultures with log phase bacteria and monitored the $OD_{600}$ every 15 minutes for 48 hours. The growth rates of the three strains in CDM and BHI are nearly identical (figure 12A-B). Therefore, there is no inherent growth difference in vitro.

We next determined whether LVS *clpB* or LVS *dotU* had an intracellular growth defect in primary BMDMs or the cell lines: A549 (human alveolar type II epithelial), J774 (mouse macrophage), and MH-S (mouse alveolar macrophage). Cells were inoculated with LVS or LVS *clpB* at an MOI of 25:1 for 120 minutes to allow internalization. Cells were then treated with gentamicin to kill extracellular bacteria. To determine bacterial internalization, cells were lysed 4 hours after inoculation and serial dilutions of the lysate were plated on chocolate agar. We recovered a similar number of both LVS and LVS *clpB* CFUs within each different cell type at 4 hours post-inoculation indicating that LVS *clpB* is not defective for internalization (figure 13A-D). To determine the ability of LVS *clpB* to grow in BMDMs, we lysed infected cells 24 hours post-inoculation and plated serial dilutions of the lysate on chocolate agar. We found a similar increase in the number of CFUs recovered for LVS and LVS *clpB* within each cell line indicating LVS *clpB* has no intracellular growth defect (figure 13A-D). Because LVS *clpB* grows in a variety of cell lines, these data indicate the ability of LVS *clpB* to grow intracellularly is generalizable and not specific to a certain cell type. Although LVS *dotU* infects all cells tested so that it is protected from gentamicin similarly to LVS 4 hours post-inoculation, this strain failed to grow and a similar number or even fewer CFUs were recovered 24 hours post-inoculation (figure 13A-D). We can rescue the intracellular growth defect seen with LVS *dotU* by trans-

complementation (figure 14). These results indicate the in vivo attenuation of LVS *dotU* is likely a consequence of this strain's inability to grow intracellularly. Indeed, LVS *dotU* and U112 *dotU* fail to escape the phagosome (32, 35) to reach the cytosol- *Francisella*'s replicative niche. However, since LVS *clpB* has no intracellular growth defect, its attenuation may be caused by an altered immune response that is more effective at bacterial clearance.

**LVS *clpB* fails to inhibit early pro-inflammatory cytokine production in the lung**

Because LVS *clpB* did not exhibit an intracellular growth defect, we hypothesized that this strain's attenuation was due to an altered immune response that was more effective at bacterial clearance. To test our hypothesis, we first examined cytokine production in the lung BALF on day 3 post-inoculation using a 20-plex mouse cytokine Luminex assay. Despite higher lung bacterial burdens in LVS infected B6 mice on day 3 post-inoculation compared to LVS *clpB* infected B6 mice (figure 4A), the BALF of LVS infected B6 mice contained less pro-inflammatory cytokines and chemokines compared to LVS *clpB* infected B6 mice (figure 15). LVS *clpB* also induced a similar profile of pro-inflammatory cytokines and chemokines in the lungs of BALB/c mice on day 3 post-inoculation whereas LVS did not (figure 15). BALB/c mice also had significantly higher day 3 post-inoculation lung LVS burdens compared to LVS *clpB* (figure 5A). Clearly, LVS *clpB* failed to suppress early pro-inflammatory cytokine production in the lung which is in stark contrast to LVS infection which does not induce pro-inflammatory cytokine production in the lung (figure 15 and (11)). Additionally, the failure of LVS *clpB* to suppress pro-inflammatory cytokine production is not specific to a particular mouse strain as the same effect is seen in B6 and BALB/c mice. Despite the high inoculum dose of LVS *dotU*, this strain did not elicit any

detectable pro-inflammatory cytokine production in the lungs of B6 or BALB/c infected mice (data not shown).

**Depletion of IFN-γ early after LVS *clpB* inoculation increases bacterial burdens**

To confirm that pro-inflammatory cytokine production early after LVS *clpB* inoculation was important innate-mediated bacterial clearance, we treated B6 mice with 500 μg of XMG1.2 (anti-IFN-γ) or rat IgG1 isotype antibody on day 0 and day 2 post-inoculation. On day 3 post-inoculation, mice were sacrificed and bacterial burdens were determined in the spleen, liver, and lung. Mice receiving IFN-γ depleting antibody had significantly higher bacterial burdens than mice receiving isotype control antibody in all organs (figure 16A-C). We confirmed IFN-γ depletion by subjecting clarified tissue homogenates to Luminex analysis. All mice receiving anti-IFN-γ depleting antibody had IFN-γ levels below the detection limit whereas isotype control animals had high levels of lung IFN-γ (figure 16D). These data indicate pro-inflammatory cytokine production, such as IFN-γ, early after LVS *clpB* inoculation help control bacterial replication.

**LVS *clpB* infection alters the cellular composition of the BALF**

The presence of pro-inflammatory cytokines/chemokines in the BALF on day 3 post-inoculation suggested that the cellular composition of the BALF could be altered in LVS *clpB* infected mice. First, we determined the overall cellularity of the BALF for uninfected, LVS, LVS *clpB*, or LVS *dotU* infected B6 mice. LVS *clpB* infected mice have significantly more cells in the BALF compared to uninfected, LVS, and LVS *dotU* infected mice (figure 17A). We then used flow cytometry to identify alveolar macrophages, dendritic cells, interstitial macrophages, and neutrophils. Because the total cellularity of LVS *clpB* BALF was significantly higher than all other groups, the total number of each individual cell

population is also increased. We therefore focused on whether the composition of the response is changing (figure 17B-E). We did not detect a significant increase in any of the analyzed cell populations except for neutrophils. In LVS *clpB* infected mice, neutrophils comprise approximately 40% of all BALF cells; neutrophils are only approximately 10% of BALF cells in LVS infected mice. The difference in the composition is not surprising given the presence of neutrophil chemoattractants like MIG and KC in the BALF of LVS *clpB* infected mice (figure 15).

We also determined the BALF cellularity of uninfected, LVS, LVS *clpB*, or LVS *dotU* infected BALB/c mice on day 3 post-inoculation. Like B6 mice infected with LVS *clpB*, BALB/c mice also had significantly more cells in the BALF upon LVS *clpB* infection (figure 18). BALB/c mice express high levels of GR-1 on all myeloid cells; therefore, we could not unambiguously define the cellular composition of the BALF as we did in B6 mice. Despite being unable to define the cellular composition of BALB/c BALF, we did observe increased cellularity in LVS *clpB* infected mice, data consistent with increased pro-inflammatory cytokine and chemokine levels as determined by Luminex (figure 15).

**MyD88 and TLR2 signaling are required for LVS *clpB* clearance**

We next sought to determine the signaling pathways involved in mediating LVS *clpB* clearance. Signaling through MyD88 is required for survival during LVS infection (16, 36). To determine whether MyD88 signaling is required for clearance of LVS *clpB*, we intranasally inoculated MyD88$^{-/-}$ or B6 mice with 5x10$^4$ CFU LVS *clpB* and determined bacterial burdens in the spleen, liver, and lung on days 3 and 7 post-inoculation. MyD88$^{-/-}$ mice have significantly higher bacterial burden in the lung, but not the spleen or liver, on day 3 post-inoculation (figure 19A-C). These data suggest that MyD88 signaling is necessary for

control of bacterial growth at the site of primary infection, but not distal sites, early after inoculation. On day 7 post-inoculation, bacterial burdens in all three organs exceeded $10^8$ CFU (figure 19A-C). This increase in bacterial burdens indicates MyD88 signaling is necessary for a productive innate immune response capable of controlling LVS *clpB* infection. Despite the high bacterial burdens, MyD88$^{-/-}$ mice do not lose any weight until days 6 and 7 post-inoculation when bacterial burdens are very high (figure 19D). The absence of weight loss in earlier after inoculation in MyD88$^{-/-}$ mice suggests there is little production of cytokines like IL-1, IL-6, and TNF-α.

TLR2 signaling is required for survival following intranasal or intradermal inoculation with LVS (36). TLR2 requires MyD88 to progagate the signaling cascade (37). To determine whether the failure of MyD88$^{-/-}$ mice to control LVS *clpB* infection was due solely to the failure to propagate signals initiated by TLR2, we infected TLR2$^{-/-}$ or B6 mice with $5x10^4$ CFU LVS *clpB* and determined bacterial burdens in the spleen, liver, and lung on days 3 and 7 post-inoculation. On day 3 post-inoculation, B6 and TLR2$^{-/-}$ had identical burdens in the spleen, liver, and lung indicating TLR2 signaling is not necessary for early control of LVS *clpB* (figure 20A-C). On day 7 post-inoculation, TLR2$^{-/-}$ mice have significantly higher bacterial burdens in the lung and liver compared to B6 mice; spleen bacterial burdens are not different between the two groups (figure 20A-C). Lung TLR2 signaling is particularly important for controlling the infection because bacterial burdens are approximately 100-fold increased in the lungs of TLR2$^{-/-}$ mice compared to B6 (figure 20C). TLR2$^{-/-}$ mice have similar weight loss profiles as B6 mice until days 6 and 7 post-inoculation where they fail to gain weight at the same rate as B6 mice (figure 20D). These weight loss

data suggest that there are TLR2-independent pathways mediating cytokine production that causes weight loss early after inoculation.

**TLR2 signaling is required for production of some pro-inflammatory cytokines after LVS *clpB* infection**

Three *Francisella* lipoproteins have been identified as TLR2 ligands- LpnA, FTT_1103, and FTL_0645 (38-40). TLR2 signaling is necessary for the production of pro-inflammatory cytokines in peritoneal macrophages infected with LVS (36, 41). Therefore, it was possible that TLR2$^{-/-}$ mice fail to control LVS *clpB* infection because of defective cytokine/chemokine production. We isolated BALF from uninfected or LVS *clpB* infected B6 and TLR2$^{-/-}$ mice on day 3 post-inoculation and determined cytokine and chemokine concentrations using Luminex analysis. TLR2$^{-/-}$ mice were able to produce several pro-inflammatory cytokines/chemokines after LVS *clpB* infection at significantly higher levels compared to uninfected mice (IL-12, IP-10, KC, MIG, and GM-CSF) (figure 21). Despite the ability of TLR2$^{-/-}$ mice to produce these cytokines/chemokines, they did not produce as much cytokine/chemokine as B6 mice (with the exception of GM-CSF where equivalent amounts were produced) (figure 21). These data suggest that LVS *clpB* stimulates both TLR2-independent and TLR2-dependent pathways that lead to pro-inflammatory cytokine production. The production of IL-1α, IL-1β, IL-2, IL-6, IL-17, MIP-1α, and TNF-α required TLR2 signaling as these cytokines/chemokines were not found at significantly higher levels in LVS *clpB* infected TLR2$^{-/-}$ mice compared to uninfected mice (figure 21). Of note, IFN-γ was 28-fold higher in LVS *clpB* infected TLR2$^{-/-}$ mice compared to uninfected mice but this was not a statistically significant increase (figure 21). Although GM-CSF and IFN-γ were produced at higher levels in B6 and TLR2$^{-/-}$ mice than uninfected mice, there was no

difference between the LVS *clpB* infected B6 and TLR2$^{-/-}$ mice suggesting their induction is TLR2-independent. Altogether, these data indicate that LVS *clpB* stimulates the innate immune system via TLR2-independent and -dependent mechanisms that lead to pro-inflammatory cytokine and chemokine production.

**TLR2 signaling is not required for neutrophil influx into the BALF**

The differential cytokine and chemokine concentrations in the BALF of LVS *clpB* infected B6 and TLR2$^{-/-}$ mice could affect cellular recruitment to the lungs and therefore the cellular composition of the BALF. We first determined the total number of cells present in the BALF and found LVS *clpB* infected B6 mice had significantly more BALF cells than both uninfected and LVS *clpB* infected TLR2$^{-/-}$ mice (figure 22A). LVS *clpB* infected TLR2$^{-/-}$ mice did have significantly more BALF cells than uninfected mice indicating TLR2-independent pathways are involved in cellular recruitment (figure 22A). These data are consistent with decreased, but not absent, cytokines and chemokines in the BALF which could cause a decrease in cellular recruitment (figure 21). Despite recovering fewer cells from the BALF of LVS *clpB* infected TLR2$^{-/-}$ mice, the cellular composition is nearly identical to B6 mice in terms of the percentage of BALF cells that are alveolar macrophages, dendritic cells, or neutrophils (figure 22B-E). There was a statistically significant increase in the percentage of interstitial macrophages in LVS *clpB* infected TLR2$^{-/-}$ mice compared to B6 mice (figure 22D). While statistically significant, we do not believe the increase to be biologically significant because the percentage of all cells is low and amounts to just a few hundred cells. Together, these data indicate that while TLR2$^{-/-}$ mice have decreased total BALF cellularity compared to B6 mice, the composition of the BALF is equivalent.

**Adaptive immunity is required for LVS *clpB* clearance**

LVS clearance requires adaptive immunity (15). Because LVS *clpB* induced a robust innate immune response and was nearly cleared from the host prior to the peak of the adaptive immune response (day 10 post-inoculation (19)), this raised the possibility that the innate immune system alone was capable of controlling the infection and mediating bacterial clearance without the requirement of adaptive immunity even though the adaptive response was vigorous (see below). To test this possibility, we infected B6 and $Rag^{-/-}$ with $5x10^4$ CFU LVS *clpB*. On days 3 and 7 post-infection, B6 and $Rag^{-/-}$ mice had equivalent bacterial burdens in the lung indicating that innate immunity was capable of controlling the infection initially (figure 23A). We next infected $Rag^{-/-}$ and B6 mice with $5x10^4$ CFU LVS *clpB* and harvested organs 28 days post-inoculation. No bacteria were recovered from the B6 mice but LVS *clpB* persisted in the lungs of $Rag^{-/-}$ mice (figure 23A). The same trend was seen in the spleen and liver (figure 23B-C). Despite persistent bacteremia with LVS *clpB* in $Rag^{-/-}$ mice, weight loss profiles were identical in $Rag^{-/-}$ and B6 mice (figure 23D). Since LVS *clpB* persisted in $Rag^{-/-}$ mice, this result indicates that adaptive immunity is required for LVS *clpB* clearance similar to LVS (15); the robust innate response is not sufficient to clear LVS *clpB*. It further suggests that the innate immune response is responsible for the early weight loss profile observed in LVS *clpB* inoculated mice.

**LVS *clpB* infection induces altered immune expansion**

After determining that adaptive immunity is required for LVS *clpB* clearance, we characterized the adaptive immune response to this strain. First we determined the total number of cells recovered from the spleen and lung on days 7 and 10 post-inoculation (figure 24). LVS and LVS *clpB* infected mice had similar increases in spleen cellularity with an

approximately 2-3 fold increase in total cells compared to uninfected mice on days 7 and 10 post-inoculation (figure 24A-B). LVS and LVS *clpB* infected mice also had increased lung cellularity of 2-5 fold over uninfected mice on days 7 and 10 post-inoculation (figure 24C-D). When spleen cellularity of LVS and LVS *clpB* infected mice was compared, there was no significant difference on day 7 or 10 post-inoculation (figure 24A-B). However, lung cellularity was decreased significantly in LVS *clpB* infected mice compared to LVS infected mice on days 7 and 10 post-inoculation (figure 24C-D). The difference in lung cellularity is likely due to the contraction of the immune response following LVS *clpB* clearance. While the LVS *clpB* infection was nearly cleared on day 10 post-inoculation, LVS infected mice still had high bacterial burdens and an on-going infection likely drives sustained lung cellularity. Because LVS *dotU* failed to grow in vivo, it was not surprising that LVS *dotU* infected mice did not have any increase in spleen or lung cellularity compared to uninfected mice and exhibited no immune expansion from day 7 to 10 (figure 24A-D).

**LVS *clpB* infection induced a robust IFN-γ mediated immune response similar in magnitude to LVS infection**

Given the strong innate response, we suspected that in spite of the earlier clearance of LVS *clpB*, we would still observe a robust adaptive response. We therefore examined whether IFN-γ production by $CD4^+$ T cells was altered after LVS *clpB* infection in terms of absolute number and frequency (Figure 25A-H). We identified IFN-γ producing T cells using intracellular cytokine staining following co-culture with LVS infected congenic B6-CD45.1 splenocytes as antigen presenting cells. The gating scheme used for all flow cytometry analysis is shown in figure 2. We found no statistically significant difference in the number of $CD4^+$ T cells producing IFN-γ in LVS and LVS *clpB* infected mice on day 7 in

the spleen and lung (figure 25A-B). On day 10 post-inoculation, the number of splenic $CD4^+$ IFN-$\gamma^+$ T cells was not significantly different between LVS and LVS *clpB* infected mice in spite of lower bacterial burdens in LVS *clpB* infected mice (figure 25C). In the lung, however, there was a significant decrease in the number of $CD4^+$ IFN-$\gamma^+$ T cells in LVS *clpB* infected mice compared to LVS infected mice (figure 25D). While the frequency of IFN-$\gamma^+$ cells in the $CD4^+$ T cell pool in LVS *clpB* infected mice was higher than LVS infected mice (41.6% versus 35.8%), the difference did not reach statistical significance (figure 25H). Because the frequency of IFN-$\gamma^+$ cells of $CD4^+$ T cells was similar in the lungs of LVS and LVS *clpB* infected mice, the difference in the absolute number was due to fewer total cells in the lungs of LVS *clpB* infected mice on day 10 post-inoculation (figure 24D). The frequency of splenic IFN-$\gamma^+$ $CD4^+$ T cells in LVS infected mice was significantly increased compared uninfected and LVS *dotU* infected mice on days 7 and 10 post-inoculation (figure 25E, G). LVS *clpB* infected mice did not have a statistically significant increase in the frequency of IFN-$\gamma^+$ $CD4^+$ T cells compared to uninfected mice in the spleen on day 7 or 10 post-inoculation, but the frequency trends higher (figure 25E, G). LVS and LVS *clpB* infected mice had significantly more IFN-$\gamma^+$ $CD4^+$ T cells in the lung on day 7 post-inoculation compared to uninfected and LVS *dotU* infected mice (figure 25F). We did not detect an increase in the number or frequency of splenic or lung $CD4^+$ IFN-$\gamma^+$ cells in LVS *dotU* infected mice compared to uninfected mice (figure 25A-H).

$CD8^+$ T cells showed a similar pattern of IFN-γ production as $CD4^+$ T cells (figure 26A-H). There was no statistical difference in the number of $CD8^+$ IFN-$\gamma^+$ T cells in the spleen or lungs of LVS and LVS *clpB* infected mice on day 7 post-inoculation (figure 26A-B). On day 10 post-inoculation, there were equivalent numbers of $CD8^+$ T cells producing

IFN-γ in the spleens of LVS *clpB* and LVS infected mice (figure 26C). There was, however, a significant decrease in the number of IFN-$\gamma^+$ $CD8^+$ T cells in the lungs of LVS *clpB* infected mice on day 10 post-inoculation compared to LVS infected mice (figure 26D). Again, the percentages of IFN-$\gamma^+$ cells in the $CD8^+$ T cell pool remained the same, therefore any decrease in absolute number on day 10 is due to decreased lung cellularity in LVS *clpB* infected mice (figure 26H). There was a significant decrease in the frequency of IFN-$\gamma^+$ $CD8^+$ T cells in the lungs of LVS *clpB* infected mice compared to LVS infected mice on day 7 post-inoculation in the lung (figure 26F). The difference in the frequency of IFN-$\gamma^+$ $CD8^+$ T cells between LVS and LVS *clpB* infected mice in the lung on day 7 post-inoculation has been overcome by LVS *clpB* infected mice by day 10 post-inoculation (figure 26F, H). In the spleen, the frequency of IFN-$\gamma^+$ $CD8^+$ T cells are similar for all groups on day 7 post-inoculation (figure 26E). By day 10 post-infection, LVS and LVS *clpB* infected mice have significantly higher frequencies of IFN-$\gamma^+$ $CD8^+$ T cells compared to uninfected or LVS *dotU* infected mice (figure 26G). Uninfected and LVS *dotU* infected mice were similar to each other in terms of the absolute number and frequency of $CD8^+$ IFN-$\gamma^+$ cells in the spleen and lungs on days 7 and 10 post-inoculation (figure 26A-D).

We found an approximate 2-fold increase in the number of IFN- $\gamma^+$ $CD4^+$ T cells in the spleens of LVS and LVS *clpB* infected mice between days 7 and 10 post-inoculation (figure 25A, C). There was at least a 10-fold expansion of IFN- $\gamma^+$ $CD4^+$ T cells in the lungs of LVS and LVS *clpB* infected mice between days 7 and 10 post-inoculation (figure 25B, D). LVS *clpB* infected mice, however, did not show the degree of expansion seen in LVS infected mice (10-fold versus 35-fold). The frequency of IFN-$\gamma^+$ $CD4^+$ T cells also increased from day 7 to day 10 post-inoculation in the lungs of LVS and LVS *clpB* infected mice

(figure 25F, H). There was no change in the number of IFN-$\gamma^+$ $CD8^+$ T cells in the spleens of LVS or LVS *clpB* infected mice between days 7 and 10 post-inoculation (figure 26A, C). There was, however, an approximate 10-fold increase in the number of responding IFN-$\gamma^+$ $CD8^+$ T cells in the lungs of both LVS and LVS *clpB* infected mice between days 7 and 10 (figure 26B, D). Like $CD4^+$ T cells, the frequency of IFN-$\gamma^+$ $CD8^+$ T cells increased in the lungs of LVS and LVS *clpB* infected mice from day 7 to day 10 post-inoculation (figure 26F, H) Together these results indicate that LVS *clpB* infection induced a similar number and frequency of IFN- $\gamma^+$ $CD4^+$ and $CD8^+$ T cells as LVS infection.

**LVS *clpB* infection led to increased IFN-γ expression by responding T cells compared to LVS infection**

We next measured the mean fluorescent intensity (MFI) of $CD4^+$ IFN-$\gamma^+$ cells because MFI is an indication of how much IFN-γ is expressed on a per cell basis. We normalized the data by subtracting the MFI of the IFN-$\gamma^-$ population from the MFI of the IFN-$\gamma^+$ population to give a change in MFI (ΔMFI). Figure 27A-D shows data for $CD4^+$ IFN-$\gamma^+$ ΔMFI combined from 4 independent experiments. The differences in ΔMFI for $CD4^+$ IFN-$\gamma^+$ T cells on day 10 were consistent from experiment to experiment and representative histograms derived from the same experiment are shown (figure 27E-H). There was a significant increase in the ΔMFI of $CD4^+$ cells producing IFN-γ in the spleens and lungs from LVS and LVS *clpB* infected mice compared to either uninfected mice on day 7 and 10 post-inoculation (figure 27A-D). On day 7 post-inoculation, there was no significant difference in $CD4^+$ IFN-γ ΔMFI from LVS infected mice as compared to LVS *clpB* infected mice for both the spleen and lung (figure 27A-B). However, on day 10, there was a significant increase in IFN-γ ΔMFI from LVS *clpB* infected mice compared to LVS infected

mice in both the spleen and lung (figure 27C-D). To further investigate IFN-γ production by $CD4^+$ T cells, we enriched $CD4^+$ T cells from the spleen and lung on day 10 post-inoculation. We chose day 10 because this time point had more responding $CD4^+$ T cells than day 7 and also exhibited differences in IFN-γ expression as measured by ΔMFI. Enriched lung and spleen $CD4^+$ T cells were re-stimulated using LVS infected T cell-depleted splenocytes. The concentration of IFN-γ in the culture supernatant was determined by ELISA 24 hours after the start of the co-culture and normalized to the number of $CD4^+$ T cells in each sample (figure 28). There was no difference in the IFN-γ concentration following re-stimulation of enriched lung or spleen $CD4^+$ T cells from LVS or LVS *clpB* infected mice. It is possible that we did not see the difference in IFN-γ production by $CD4^+$ T cells because of IFN-γ turnover during the culture. Additionally, intracellular cytokine staining is a much more sensitive technique than ELISA analysis of culture supernatant.

The IFN-γ ΔMFI trend for $CD8^+$ T cells is similar to the $CD4^+$ T cell subset. Measurement of IFN-γ ΔMFI in the spleen and lung showed similar expression of IFN-γ on 7 days post-inoculation in LVS and LVS *clpB* infected mice (figure 29A-B). There was a significant increase in the ΔMFI of IFN-$\gamma^+$ in the $CD8^+$ T cells in LVS *clpB* infected mice compared to LVS infected mice in the spleen and lung on day 10 post-inoculation (figure 29C-D). Representative histograms derived from the same experiment for IFN-$\gamma^+$ $CD8^+$ T cells from LVS and LVS *clpB* infected mice are shown (figure 29E-H). The IFN-γ ΔMFI in $CD8^+$ T cells indicates that like $CD4^+$ T cells, the cells from LVS *clpB* infected mice express more IFN-γ than cells isolated from LVS infected mice, even though fewer cells are present.

**LVS *clpB* infection increases IL-17 expression compared to LVS infection**

Th17 cells are also involved in the immune response during pneumonic tularemia (19, 20). Although there was no significant change on day 7 post-inoculation, by day 10 post-inoculation there was a significant increase in the absolute number of $CD4^+$ IL-$17A^+$ T cells in the lungs of LVS infected mice compared to uninfected mice (figure 30C, D). LVS *clpB* infected mice trended towards more $CD4^+$ IL-$17A^+$ T cells in the lungs on day 10 post-inoculation than uninfected mice but the difference did not reach statistical significance (figure 30D). There was no significant difference in the absolute number of Th17 cells in the lungs of LVS and LVS *clpB* infected mice on day 10 post-inoculation (figure 30D). There was also an expansion of Th17 cells in the lung between days 7 and 10 post-inoculation for LVS and LVS *clpB* infected mice with nearly a 10-fold increase in cell number (figure 30C-D). The absolute number and frequency of splenic $CD4^+$ T cells producing IL-17A was similar on days 7 and 10 post-inoculation among uninfected, LVS, LVS *clpB*, and LVS *dotU* infected mice indicating Th17 cells are not responding to infection in the spleen (figure 30A-B). On day 7 post-inoculation, the lungs of LVS infected mice have a significant increase in the frequency of IL-$17A^+$ $CD4^+$ T cells compared to uninfected mice (figure 30G). LVS *clpB* infected mice have a significant increase in the frequency of IL-$17A^+$ $CD4^+$ T cells in the lung on day 10 post-inoculation compared to uninfected and LVS *dotU* infected mice (figure 30H).

There was a significant increase in IL-17A ΔMFI in the lung of LVS *clpB* infected mice on day 10 post-inoculation in the lung compared to LVS (figure 31D). There was also no significant difference in the splenic IL-17A ΔMFI when all groups of mice are compared (figure 31A-B). Representative histograms of IL-$17A^+$ $CD4^+$ T cells are shown (figure 31E-

H). We also determined IL-17 secretion by enriched $CD4^+$ T cells from the lung and spleen on day 10. These cells were re-stimulated with LVS infected T cell depleted splenocytes and the concentration of IL-17 was determined using ELISA (figure 32). Enriched $CD4^+$ T cells from the lungs of LVS and LVS *clpB* infected mice secreted similar amounts of IL-17A. Overall, our results suggest that Th17 expansion largely occurs at the site of primary infection.

**LVS *clpB* induces an altered innate and adaptive immune response compared to LVS infection**

Altogether, our results demonstrate that LVS *clpB* infection induces altered host immunity compared to wild-type LVS infection. First, we saw early pro-inflammatory cytokine production in the lungs of LVS *clpB* infected mice, a process that was inhibited during LVS infection. The production of these pro-inflammatory cytokines was partially dependent on TLR2 signaling. Additionally, LVS *clpB* infected mice produced at least equivalent expansion of Th1, Th17, and $CD8^+$ T cell responses as LVS infected mice, with lower bacterial burdens and a shorter duration of infection.

## DISCUSSION

Bacterial attenuation can be the consequence of a strain's failure to grow, as in the case of auxotrophs, or by a strain's failure to inhibit components of host immunity. Both in vitro and in vivo screens have identified *Francisella* virulence determinants and several of those screens identified *clpB* as a gene required for virulence (5-7, 42). While several groups describe a slight intracellular growth defect for *clpB* strains (23, 43, 44), we did not see an intracellular growth defect for our LVS *clpB* strains in the cell types we tested. This result

suggested that something else was responsible for *clpB*'s attenuation in animal models of infection (23-25). We therefore hypothesized that LVS *clpB* induces an altered immune response that mediates faster bacterial clearance.

To test our hypothesis, we first confirmed that our LVS *clpB* strain was attenuated in a pneumonic model of tularemia. In order to achieve similar bacterial burdens early after infection, we inoculated mice with a 100-fold higher dose of LVS *clpB* compared to LVS. Ideally, we would have used the same inoculation dose for both bacterial strains. However, LVS *clpB* not only failed to disseminate to the spleen and liver in all mice but the bacterial burdens were also significantly lower in all organs tested on day 3 post-inoculation at an inoculation dose of $5x10^2$ CFU. An inoculation dose of $5x10^4$ CFU of LVS *clpB* led to similar bacterial burdens as LVS 3 days post-inoculation and allowed us to examine differences in the adaptive immune response in the absence of large differences in overall antigen load. Despite similar bacterial burdens early after inoculation, we observed rapid clearance of LVS *clpB*. Even though LVS *clpB* was cleared rapidly from the host, this strain did elicit an adaptive immune response that developed into protective memory. Importantly, previous infection with LVS *clpB* provided equivalent protection as LVS against subsequent lethal LVS intranasal inoculation. The bacterial burdens in LVS and LVS *clpB* vaccinated mice infected 120 days after vaccination were higher than the same groups challenged 28 days after vaccination. The increase in bacterial burden was consistent with the increased weight loss seen when mice were challenged 120 days after vaccination. Because the number of antigen-specific T cells decreases over time, we hypothesize the increased bacterial burdens seen upon challenge 120 days after vaccination was due to fewer responding T cells compared to day 28. However, we cannot directly address this hypothesis

by quantifying the number of *Francisella*-specific T cells because MHCI or MHCII tetramer is not yet available. Previous LVS *clpB* infection did not provide complete protection against aerosolized SchuS4 administered 28 days after LVS *clpB* infection. LVS *clpB* infection did however, increase the median survival time. One mouse previously inoculated with LVS *dotU* survived lethal LVS challenge; however, we do not know if that was the result of a secondary immune response. This result was surprising given that our intracellular cytokine staining showed LVS *dotU* infected mice behaved much like naïve mice with similar low numbers of IFN-γ producing T cells. However, LVS *dotU* persisted intracellularly in some mice until at least day 7 post-inoculation, allowing time for a *F. tularensis* specific T cell response to be primed. The protection was incomplete and indicates a LVS *dotU* mutant would not be effective vaccine. Overall, our LVS *clpB* strain was attenuated in pneumonic tularemia while providing 100% protection against subsequent lethal infection just as other groups had shown using other models of tularemia (23-25).

After confirming the attenuation of LVS *clpB* in pneumonic tularemia, we examined the innate immune response in the lung. LVS infection does not elicit a pro-inflammatory cytokine response in the lung despite promoting phenotypic maturation of dendritic cells (11). We also found that LVS infection did not elicit a pro-inflammatory cytokine response in the lung despite very high bacterial burdens on day 3 post-inoculation. LVS *clpB*, in contrast, did elicit a robust pro-inflammatory cytokine response in the lungs of both B6 and BALB/c mice. The failure of LVS *clpB* to inhibit early cytokine production could explain why lower inoculation doses resulted in poor dissemination to the spleen and liver, in spite of no intracellular growth defect. Because antibody depletion of IFN-γ increased lung LVS *clpB* burdens, these data suggest that the high concentration of pro-inflammatory cytokines

and chemokines in the lung are responsible for the decrease in bacterial burdens compared to LVS we observe on day 3 post-inoculation.

Maximal weight loss occurs two days earlier in LVS *clpB* infected mice compared to LVS infected mice and corresponds to the same time period where there are high levels of pro-inflammatory cytokines in the BALF. We therefore hypothesize that the earlier weight loss in LVS *clpB* infected mice is caused by the pro-inflammatory cytokine response and not bacterial burdens or the adaptive immune response. $Rag^{-/-}$ mice infected with LVS *clpB* have identical weight loss profiles as B6 mice, despite the presence of a chronic infection, suggesting weight loss is not caused by bacterial burdens. We have not determined whether $Rag^{-/-}$ mice are capable of producing pro-inflammatory cytokines/chemokines after LVS *clpB* infection, however, $Rag^{-/-}$ mice have an intact innate immune system so we predict these mice would produce cytokines upon infection. LVS *clpB* infected $MyD88^{-/-}$ mice do not lose weight between days 2-5 post-inoculation and only begin to lose weight when they have extremely high bacterial burdens and are therefore likely experiencing organ failure. We have not determined whether $MyD88^{-/-}$ mice can produce pro-inflammatory cytokines/chemokines after LVS *clpB* infection, however we predict that they cannot based on their failure to lose weight and the requirement of MyD88 for all TLR signaling, except TLR3. The production of pro-inflammatory cytokines during LVS *clpB* infection was only partially dependent on TLR2 signaling. *Francisella* has three identified TLR2 ligands and TLR2-signalling has been reported to be important for survival during intranasal and intradermal inoculation with LVS (36, 38-40). $TLR2^{-/-}$ mice were able to produce some pro-inflammatory cytokines and chemokines in response to LVS *clpB* infection but did not induce the levels that were found in wild-type mice inoculated with LVS *clpB*. LVS *clpB*

infected TLR2$^{-/-}$ mice fail to regain weight at the same rate as B6 mice and have higher bacterial burdens on day 7 post-inoculation. These data suggest that TLR2$^{-/-}$ mice have a defect in the development of adaptive immunity. To support this idea, LVS *clpB* infected TLR2$^{-/-}$ mice had a significantly lower concentration of IL-12 in the BALF on day 3 post-inoculation compared to LVS infected mice. IL-12 production by dendritic cells or macrophages directs naïve T cells towards a Th1 (IFN-γ producing) fate upon antigen encounter (45, 46). This question could be addressed in the context of LVS *clpB* infection with simple intracellular cytokine staining experiments to determine whether TLR2$^{-/-}$ mice have an altered T cell response compared to B6 mice.

Despite a robust pro-inflammatory innate immune response to LVS *clpB*, the innate response was not sufficient to mediate bacterial clearance alone. Additionally, we knew from our protection studies that there was priming of the adaptive immune response because mice previously infected with LVS *clpB* were protected from lethal LVS challenge. We then began to characterize the adaptive immune response to LVS *clpB*. When overall immune expansion is compared, LVS and LVS *clpB* infection led to a similar increase in the number of cells found in the spleen on days 7 and 10. We found a significant decrease in the number of cells isolated from the lungs of LVS *clpB* infected mice on days 7 and 10 post-inoculation compared to LVS infected mice. This decrease was likely due to contraction of the immune response as LVS *clpB* was rapidly cleared from the host while LVS infected mice maintain high bacterial burdens. To further support this, the percentages of CD4$^{+}$ and CD8$^{+}$ T cells in the lungs were the same in LVS and LVS *clpB* infected mice indicating that while the magnitude of the response was changing, the composition of the response remained unchanged. When we examined the effector function of cells in the spleen, we found

equivalent numbers of $CD4^+$ and $CD8^+$ T cells producing IFN-γ in LVS and LVS *clpB* infected mice. The absolute number of $CD4^+$ and $CD8^+$ T cells in the lung of LVS *clpB* infected mice was decreased compared to LVS infected mice but the percentage of cells producing IFN-γ remained the same.

Although we found similar frequencies of IFN-γ producing $CD4^+$ and $CD8^+$ T cells after LVS or LVS *clpB* infection, we did find altered expression levels of IFN-γ as measured by ΔMFI. There was a significant increase in the amount of IFN-γ expressed by T cells from LVS *clpB* infected mice compared to LVS infected mice in both the spleen and lung as measured by ΔMFI. Since IFN-γ is critical for LVS clearance and administration of recombinant IFN-γ decreased bacterial burdens, the increased production of IFN-γ by T cells in LVS *clpB* infected mice is consistent with faster clearance of LVS *clpB* (18).

The IL-17 response is also important during pneumonic tularemia. We have previously shown that LVS intranasal, but not intradermal, inoculation induces Th17 cells in the lung (19). IL-17 production following *F. tularensis* infection has been shown to promote IL-12 production by dendritic cells and indirectly promote a Th1 immune response (20). Although infection with LVS or LVS *clpB* led to similar numbers of Th17 cells in the lungs of infected mice, Th17 cells from LVS *clpB* infected mice expressed significantly more IL-17A as measured by ΔMFI. The increase in IL-17 expression by LVS *clpB* infected mice is consistent with the finding by Lin *et al*, where the Th1 response was promoted by IL-17 (20).

We also measured IFN-γ and IL-17 concentration in the BALF, 7 and 10 days post-inoculation. We did not detect increased concentration of either cytokine in BALF from LVS *clpB* infected mice compared to LVS mice. Although these data are not in agreement with the flow ΔMFI data, we attribute the difference to differential distribution of immune

cells between airspace and lung parenchyma. Cytokines in the BALF are secreted predominantly by cells within the airspace, and represent production by a variety of immune cells. In contrast, our intracellular cytokine staining experiments measure IFN-γ and IL-17 in the entire lung, but this analysis is limited only to T cells. When we enriched $CD4^+$ T cells from the lung and spleen on day 10 post-inoculation and re-stimulated them ex vivo with LVS infected T cell-depleted splenocytes, we did not detect differences in IFN-γ or IL-17A secretion into the culture supernatant. Differences between the read-out of the flow cytometry and ELISA assays could also account for disparate result. At a minimum, however, $CD4^+$ T cells isolated from LVS *clpB* infected mice are able to produce equivalent amounts of cytokine compared to T cells from LVS infected mice.

The increase in IFN-γ production by T cells in LVS *clpB* infected mice could be caused by differences in lung prostaglandin $E_2$ ($PGE_2$) concentration. $PGE_2$ suppresses IFN-γ production by T cells in LVS infected mice (19). U112 *clpB* fails to induce $PGE_2$ in BMDMs (35) and LVS *clpB* induced significantly less $PGE_2$ than wild-type LVS in BMDMs (figure 33). LVS *clpB* infected mice have significantly lower $PGE_2$ concentrations in the lavage fluid on day 7 and 10 post-inoculation compared to LVS infected mice (figure 34). The high concentration of $PGE_2$ in LVS infected mice decreases IFN-γ production by responding T cells, an inhibitory process not present in LVS *clpB* infected mice. Increased IFN-γ production in LVS *clpB* infected mice is also consistent with increased IL-17 expression by T cells in LVS *clpB* infected mice based on the finding by Lin *et al* where the Th1 response was promoted by IL-17 (20). However, $PGE_2$ has been shown to promote IL-23 production which drives the development of Th17 cells (47-50). In LVS *clpB* infected mice, there was little $PGE_2$ present in the BALF suggesting there is another mechanism

driving Th17 accumulation since this cell subset was present in equivalent numbers in LVS and LVS *clpB* infected mice despite dramatic differences in $PGE_2$ levels.

Although we are still in the process of identifying the *F. tularensis* effector molecule responsible for inducing $PGE_2$, it seems unlikely that ClpB directly induces $PGE_2$. ClpB is an intracellular chaperone protein that is unlikely to be sensed by the host. Proteomic analysis by Meibom, *et al* of a membrane-enriched protein fraction from a LVS *clpB* mutant identified 5 proteins with decreased expression compared to LVS at elevated temperature conditions (23). None of the identified targets of ClpB are required for $PGE_2$ induction (35) therefore ClpB must have another target that is involved in $PGE_2$ induction. We speculate *clpB* was identified as a gene necessary for $PGE_2$ induction because ClpB plays a role in assembly of the type VI secretion system that is responsible for secreting the unknown $PGE_2$ inducer. Studies to identify the mechanim(s) utilized by *F. tularensis* to induce $PGE_2$ synthesis are ongoing.

ClpB is a highly conserved chaperone protein present not only in prokaryotes but also in eukaryotes and plants (51). Due to ClpB's conserved nature and the finding that disruption of *clpB* attenuates *F. tularensis* as well as other bacteria (52-56), this gene is an excellent candidate target for attenuation of pathogenic bacteria for vaccine development. In the case of *F. tularensis*, LVS *clpB* infection was cleared faster than LVS yet induced a robust IFN-γ mediated immune response that was protective in both short- and long-term secondary infections. Therefore, *clpB* serves as an advantageous target for *F. tularensis* attenuation for future vaccine development. This work also highlights the importance of examining the immune response to attenuated mutants, particularly in the course of vaccine development.

**Figure 1**

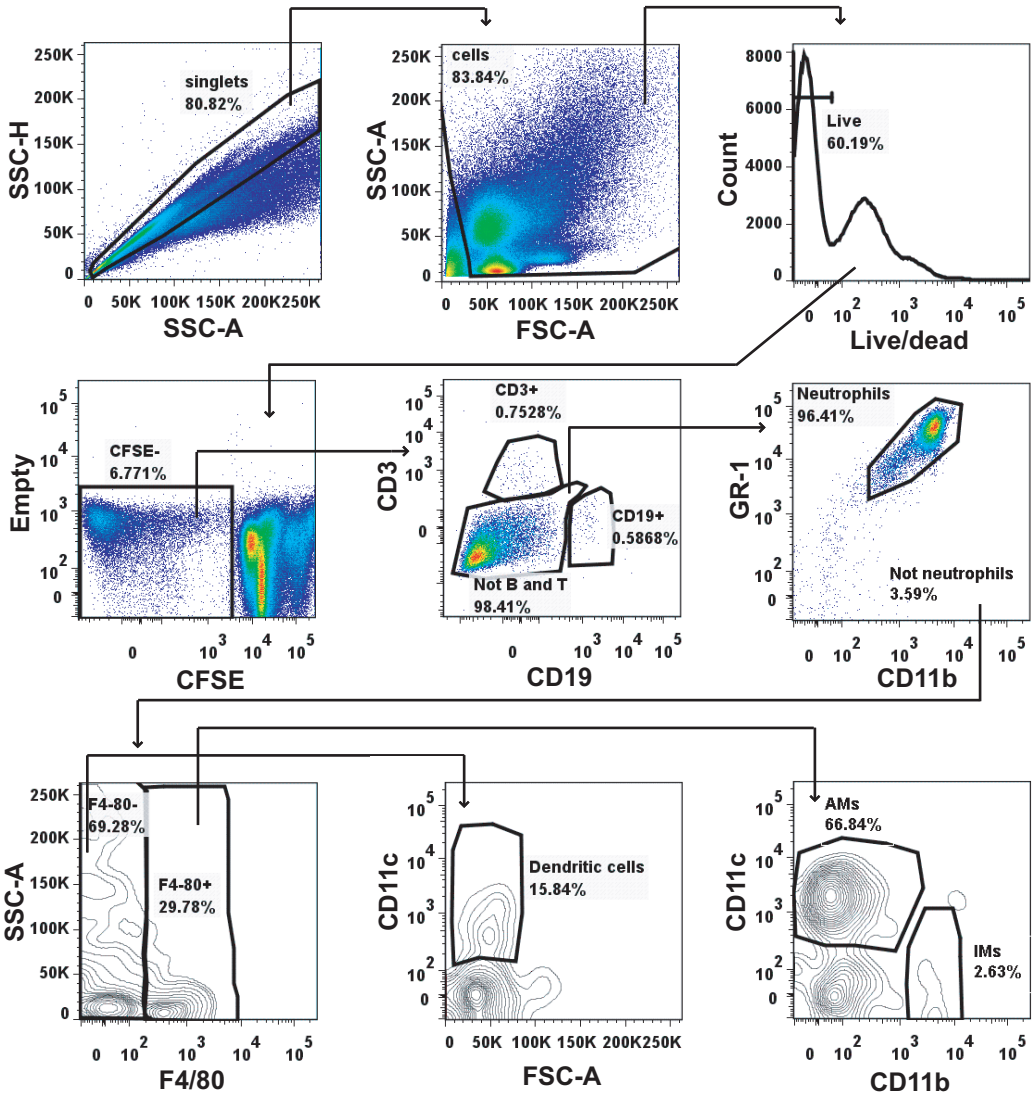


**Figure 1.** ***Gating scheme for BALF analysis.*** Single cells were discriminated from doublets by plotting side scatter height (SSC-H) versus side scatter area (SSC-A). Cells were then gated on by plotting SSC-A versus forward scatter area (FSC-A). Live cells were then gated by plotting the live/dead stain on a 1-D histogram. Cells from the BALF were discriminated from the CFSE-labeled splenocyte carries by plotting an empty channel versus CFSE. $CD3^+$, $CD19^+$, and not B and T cells were gated on by plotting CD3 versus CD19. From the not B and T gate, GR-1 versus CD11b was plotted to distinguish neutrophils from not neutrophils. From the not neutrophils gate, SSC-A versus F4/80 was plotted to distinguish $F4/80^+$ from $F4/80^-$ cells. From the $F4/80^-$ gate, CD11c versus FSC-A was plotted and dendritic cells were gated on. From the $F4/80^+$ gate, CD11c versus CD11b was plotted to distinguish alveolar macrophages (AMs) from interstitial macrophages (IMs). For each gate, the percent of the parent gate is indicated in bold (for example, AMs are 66.84% of the $F4/80^+$ gate).

**Figure 2**

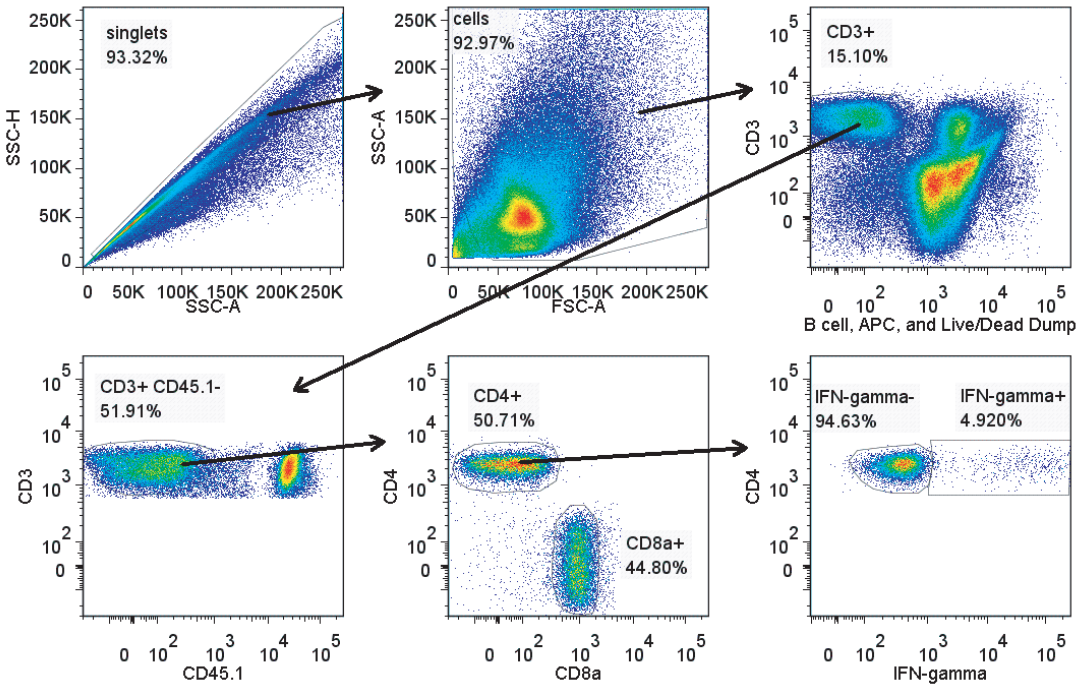


**Figure 2.** ***Gating scheme for intracellular cytokine staining analysis.*** Single cells were discriminated from doublets by plotting side scatter linear versus side scatter area. Cells were then selected by plotting side scatter area versus forward scatter area. Live $CD3^+$ T cells were then selected by plotting CD3 versus the Pacific Blue channel which included the live/dead stain and markers for antigen presenting cells. $CD45.1^-$ $CD3^+$ cells were gated on by plotting CD3 versus CD45.1. From the $CD45.1^-$ $CD3^+$ gate, $CD4^+$ and $CD8^+$ T cells were selected. Gates for IFN-γ and IL-17A positive cells were set based on isotype control staining. For simplicity, only $CD4^+$ IFN-γ is shown. Change in mean fluorescent intensity (ΔMFI) for each sample was determined by subtracting the cytokine negative population from the cytokine positive population. For each gate, the percent of the parent gate is indicated in bold (for example, $CD3^+$ cells are 15.10% of the cells gate).

**Figure 3**

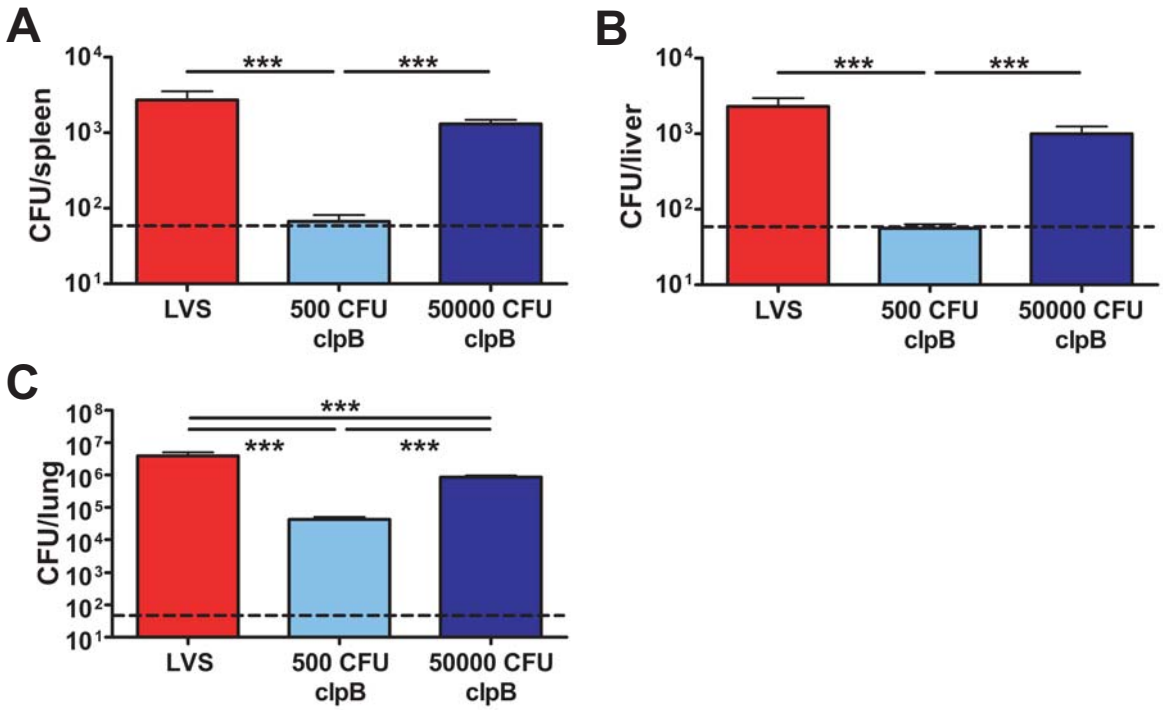


**Figure 3.** ***LVS* clpB *does not disseminate when a low inoculation dose is used.*** B6 mice were intranasally inoculated with $5x10^2$ CFU LVS, $5x10^2$ CFU LVS *clpB*, or $5x10^4$ CFU LVS *clpB*. On day 3 post-inoculation, bacterial burdens were determined in the A) spleen, B) liver, and C) lung by plating serial dilutions of organ homogenate on chocolate agar. n=6-10 mice/group. Data are combined from at least 2 independent experiments. The dashed line indicates the limit of detection of 50 CFUs. Statistical significance was determined on log-transformed data using ANOVA with Tukey's post-test.

**Figure 4**

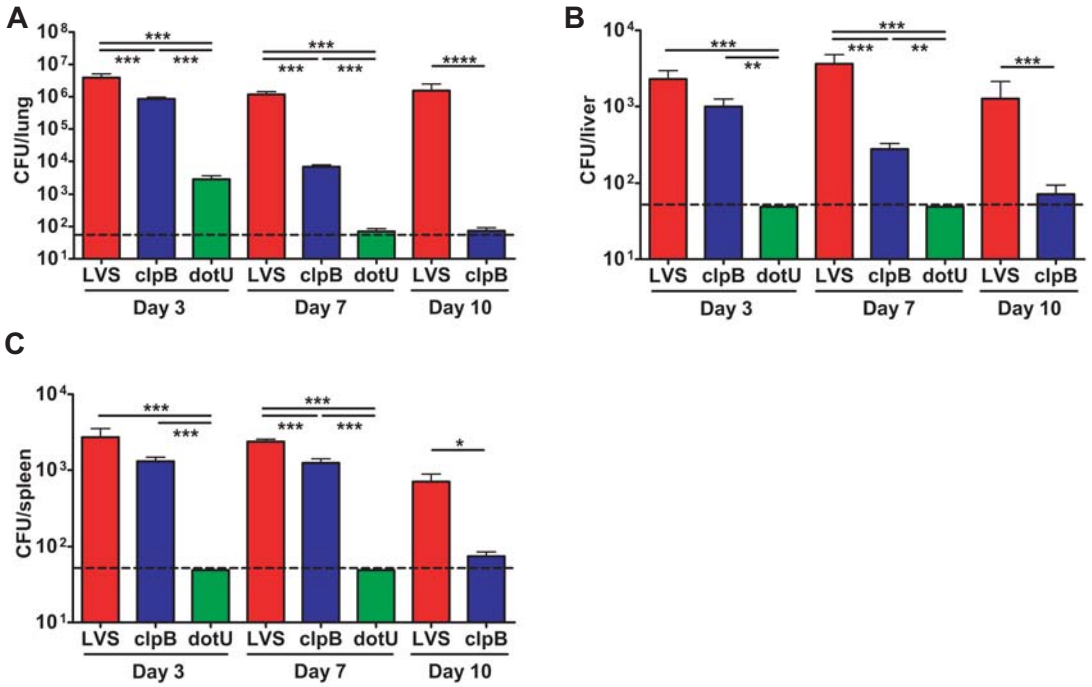


**Figure 4.** ***LVS* clpB *infected B6 mice clear bacteria faster.*** B6 mice were intranasally inoculated with LVS (5x10$^2$ CFU), LVS *clpB* (5x10$^4$ CFU), or LVS *dotU* (5x10$^5$ CFU). On days 3, 7, and 10 post-inoculation, bacterial burdens were determined in the A) lung, B) liver, and C) spleen by plating serial dilutions of organ homogenate on chocolate agar. n=5-12 mice/group. Data are combined from at least 4 independent experiments per time point. The dashed line indicates the limit of detection of 50 CFUs. Statistical significance was determined on log-transformed data using ANOVA with Tukey's post-test (day 3 and 7) or a Student's t-test (day 10).

**Figure 5**

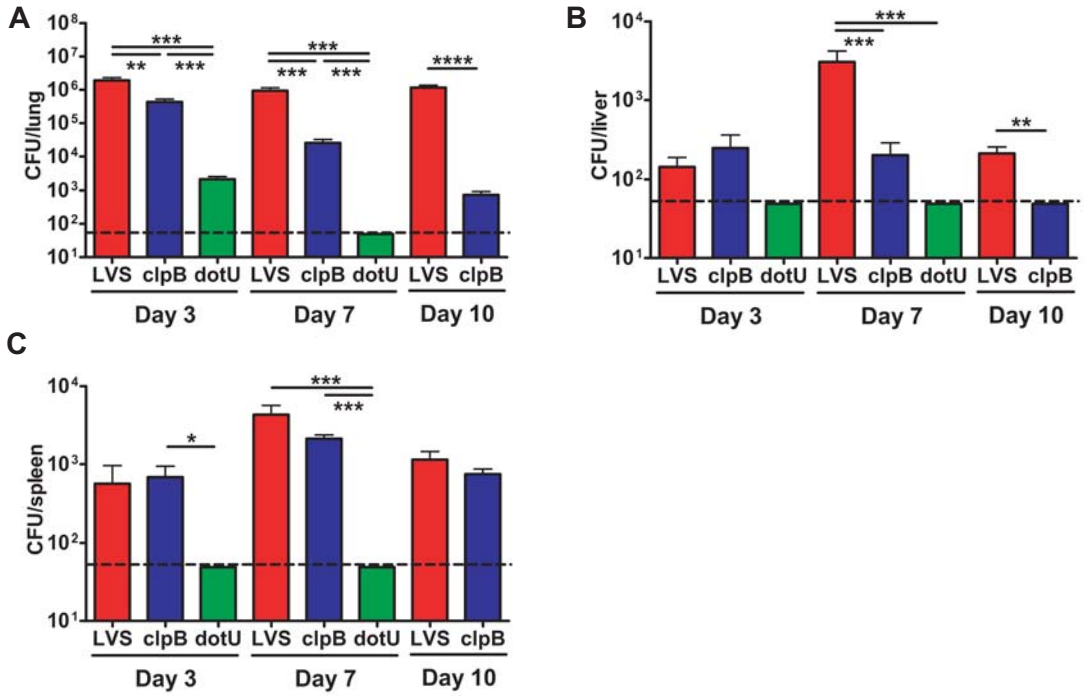


**Figure 5.** ***LVS* clpB *infected BALB/c mice clear bacteria faster.*** BALB/c mice were intranasally inoculated with LVS ($5x10^2$ CFU), LVS *clpB* ($5x10^4$ CFU), or LVS *dotU* ($5x10^5$ CFU). On days 3, 7, and 10 post-inoculation, bacterial burdens were determined in the A) lung, B) liver, and C) spleen by plating serial dilutions of organ homogenate on chocolate agar. n=4-6 mice/group. Data are combined from 2 independent experiments per time point. The dashed line indicates the limit of detection of 50 CFUs. Statistical significance was determined on log-transformed data using ANOVA with Tukey's post-test (day 3 and 7) or a Student's t-test (day 10).

**Figure 6**

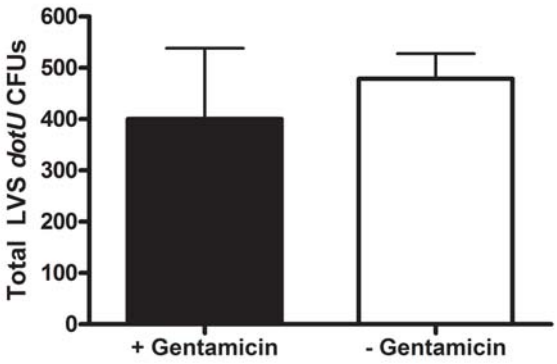


**Figure 6.** ***LVS* dotU *is internalized by lung cells following intranasal inoculation.*** B6 mice were intranasally inoculated with $5x10^5$ CFU LVS *dotU*. 3 days post-inoculation, lungs were removed and digested into a single cell suspension. Samples were then divided in half and one half was treated with 50 μg/mL gentamicin for 45 minutes to kill extracellular bacteria. Cells were washed to remove antibiotic and then plated directly on chocolate agar without lysis. The number of bacterial colonies in the untreated half and gentamicin-treated half were determined. n=3 mice. Data are from 1 experiment.

**Figure 7**

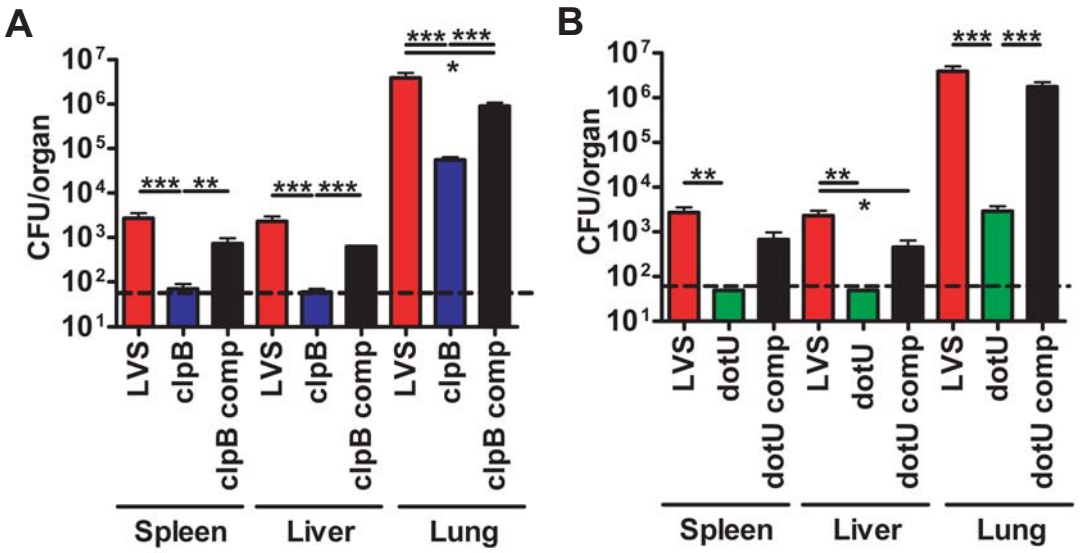


**Figure 7.** ***Trans-complementation of LVS* clpB *or LVS* dotU *restores bacterial virulence to LVS levels.*** B6 mice were intranasally inoculated with $5x10^2$ CFU LVS, LVS *clpB*, LVS *clpB* complement, or LVS *dotU* complement or $5x10^5$ LVS *dotU*. Bacterial burdens were determined in the lung for A) LVS *clpB* or B) LVS *dotU* on days 3 post-inoculation by plating serial dilutions of organ homogenate on chocolate agar. The dashed line indicates the limit of detection of 50 CFUs. Statistical significance was determined using an ANOVA with Tukey's post-test on log-transformed data. n=3-4 mice/group. Data are from 1 experiment.

**Figure 8**

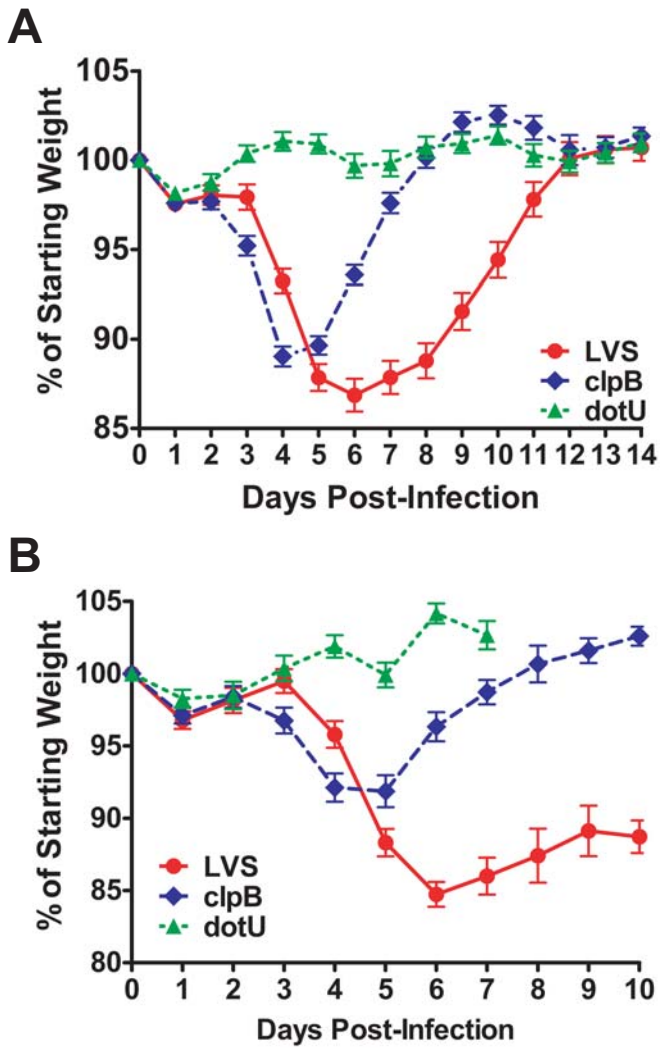


**Figure 8.** ***LVS* clpB *infected B6 and BALB/c mice exhibit less disease.*** B6 and BALB/c mice were intranasally inoculated with LVS ($5x10^2$ CFU), LVS *clpB* ($5x10^4$ CFU), or LVS *dotU* ($5x10^5$ CFU). Mouse weight was determined daily and is reported as the percentage of starting weight for A) B6 or B) BALB/c mice. n=25-32 mice/group (B6) or n=4-6 mice/group (BALB/c).

**Figure 9**

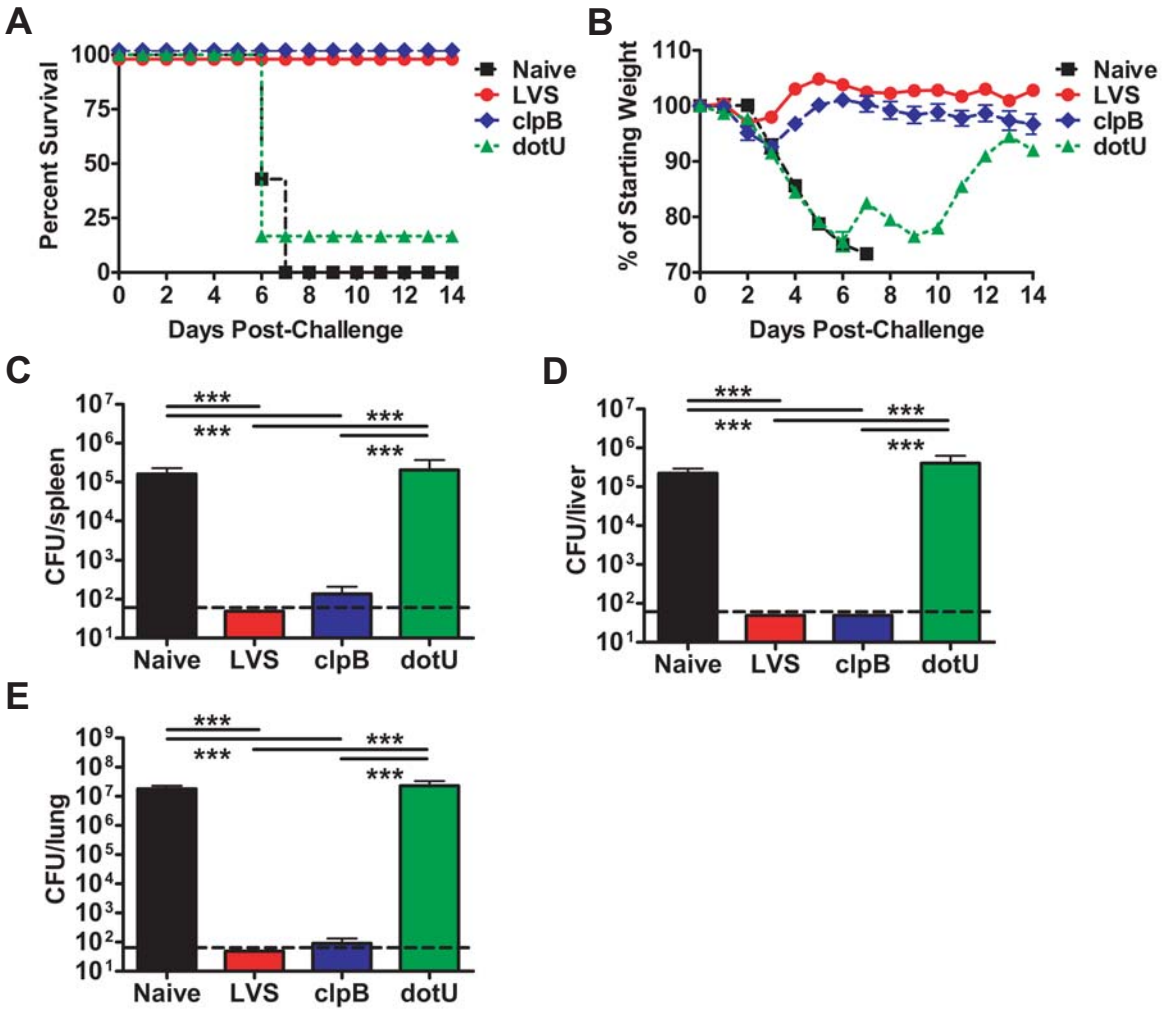


**Figure 9.** ***LVS* clpB *protects against a lethal LVS secondary challenge 28 after primary infection.*** B6 mice were intranasally inoculated with LVS ($5x10^2$ CFU), LVS *clpB* ($5x10^4$ CFU), or LVS *dotU* ($5x10^5$ CFU), or left uninfected. A) 28 days after primary infection, mice were challenged intranasally with $5x10^3$ CFU LVS and survival was measured. n=6-12 mice/group. Data are combined from 2 independent experiments. A Chi-square test with Yate's correction was used to compare survival of the vaccinated groups to the naïve group: Naïve versus LVS: $p \leq 0.001$; Naïve versus LVS *clpB*: $p \leq 0.0001$; Naïve versus LVS *dotU*: ns. B) Mice were weighed daily following secondary infection with LVS and weight loss is reported as a percentage of starting weight. Weight loss by the surviving LVS *dotU* vaccinated mouse is reported. n=6-12 mice/group. Data are combined from 2 independent experiments. Bacterial burdens in the C) spleen, D) liver, and E) lung on day 6 post-rechallenge were determined by plating serial dilutions of tissue homogenate on chocolate agar. n=5-7 mice/group. Data are combined from 2 independent experiments. The dashed line indicates the limit of detection of 50 CFUs. Statistical significance was determined on log-transformed data using ANOVA with Tukey's post-test.

**Figure 10**

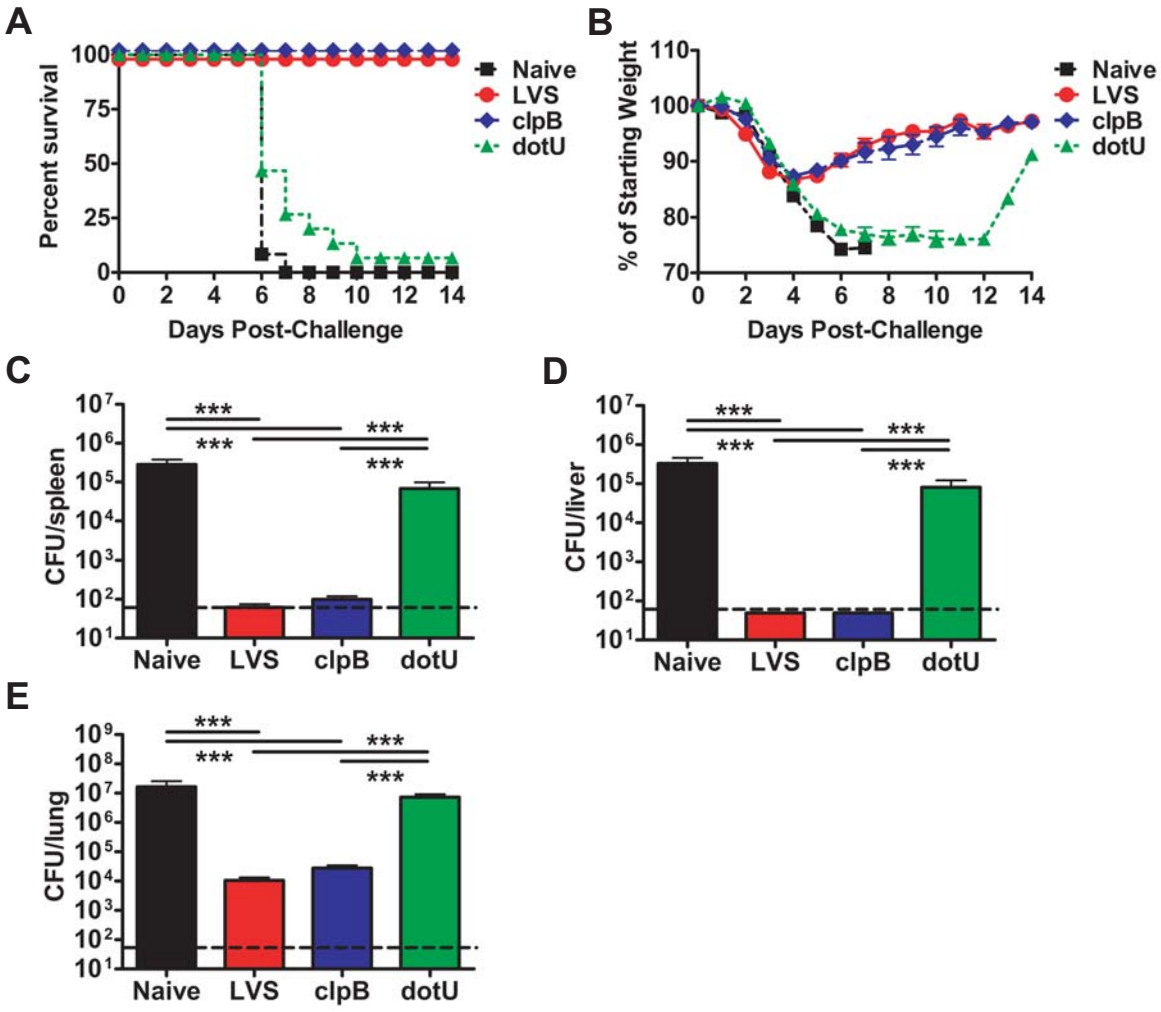


**Figure 10.** ***LVS* clpB *protects against a lethal LVS secondary challenge 120 after primary infection.*** B6 mice were intranasally inoculated with LVS ($5x10^2$ CFU), LVS *clpB* ($5x10^4$ CFU), or LVS *dotU* ($5x10^5$ CFU), or left uninfected. A) 120 days after primary infection, mice were challenged intranasally with $5x10^3$ CFU LVS and survival was measured. n=6-12 mice/group. Data are combined from 2 independent experiments. A Chi-square test with Yate's correction was used to compare survival of the vaccinated groups to the naïve group: Naïve versus LVS: $p \leq 0.001$; Naïve versus LVS *clpB*: $p \leq 0.0001$; Naïve versus LVS *dotU*: ns. B) Mice were weighed daily following secondary infection with LVS and weight loss is reported as a percentage of starting weight. Weight loss by the surviving LVS *dotU* vaccinated mouse is reported. n=12-15 mice/group. Data are combined from 2 independent experiments. Bacterial burdens in the C) spleen, D) liver, and E) lung on day 6 post-rechallenge were determined by plating serial dilutions of tissue homogenate on chocolate agar. n=6-8 mice/group. Data are combined from 2 independent experiments. The dashed line indicates the limit of detection of 50 CFUs. Statistical significance was determined on log-transformed data using ANOVA with Tukey's post-test.

**Figure 11**

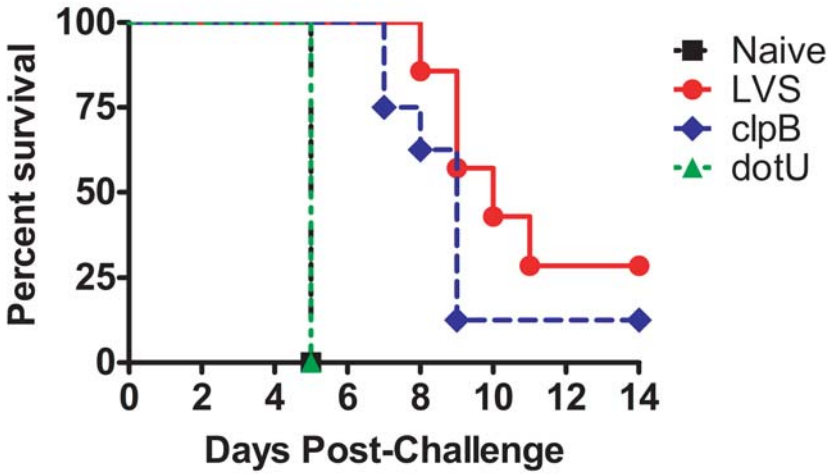


**Figure 11.** ***Previous infection with LVS* clpB *increases median survival time after lethal SchuS4 aerosol challenge.*** B6 mice were intranasally inoculated with LVS ($5x10^2$ CFU), LVS *clpB* ($5x10^4$ CFU), or LVS *dotU* ($5x10^5$ CFU), or left uninfected. 28 days after primary infection, mice were challenged with 30 CFU of aerosolized SchuS4. A Mantel-Cox log-rank test was used to compare survival of the vaccinated groups to the naïve group. n=8 mice/group. Data are from 1 experiment. Naïve versus LVS: $p \leq 0.001$; Naïve versus LVS *clpB*: $p \leq 0.0001$; Naïve versus LVS *dotU*: ns.

**Figure 12**

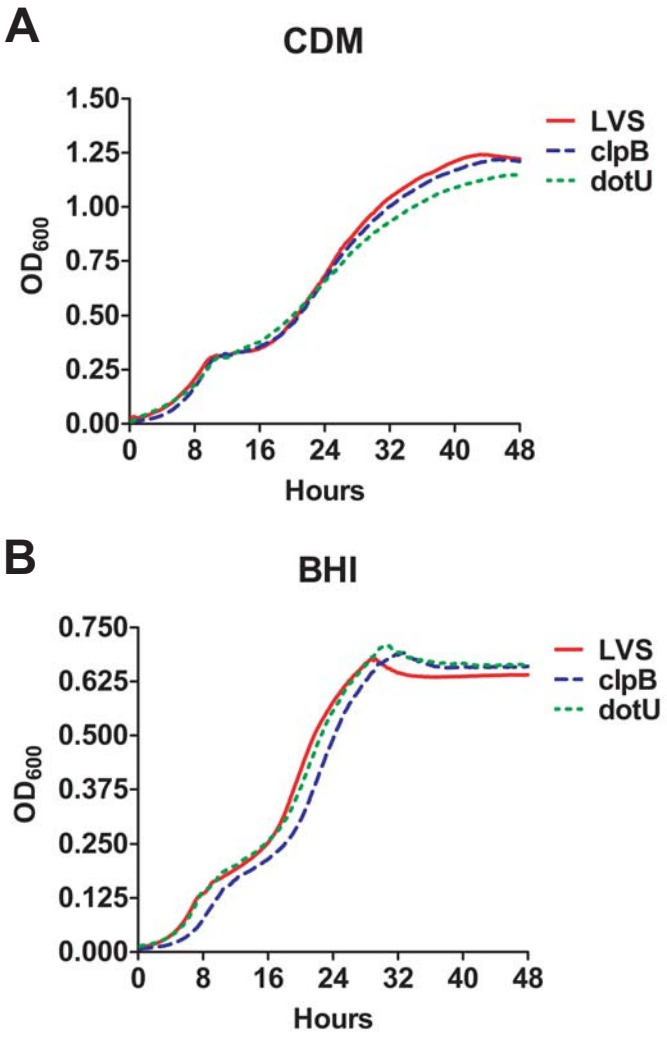


**Figure 12.** ***LVS* clpB *does not exhibit a broth growth defect.*** LVS, LVS *clpB* and LVS *dotU* growth in A) CDM or B) BHI broth was determined using a TECAN Infinite M200 plate reader by measuring the $OD_{600}$ every 15 minutes for 48 hours. Data shown are the average of triplicate wells and are representative of at least 3 independent experiments per strain.

**Figure 13**

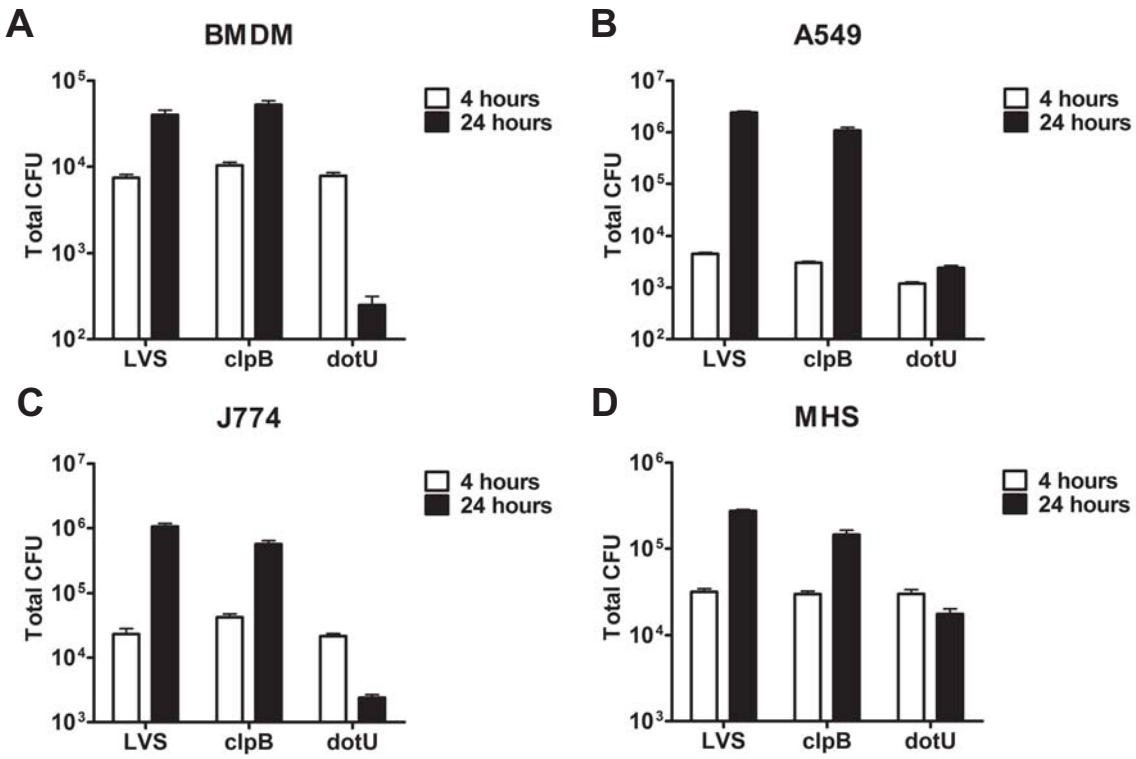


**Figure 13.** ***LVS* clpB *does not exhibit an intracellular growth defect.*** A) B6 bone marrow derived macrophages (BMDMs), B) A549, C) J774, or D) MHS cells were infected with LVS, LVS *clpB*, or LVS *dotU* at an MOI of 25:1. Cells were lysed either 4 or 24 hours post-infection and serial dilutions of the lysate were plated on chocolate agar to determine the number of bacteria present. Cells were infected with each strain in triplicate and lysates from each sample were plated in duplicate. Data are representative of at least 2 independent experiments.

**Figure 14**

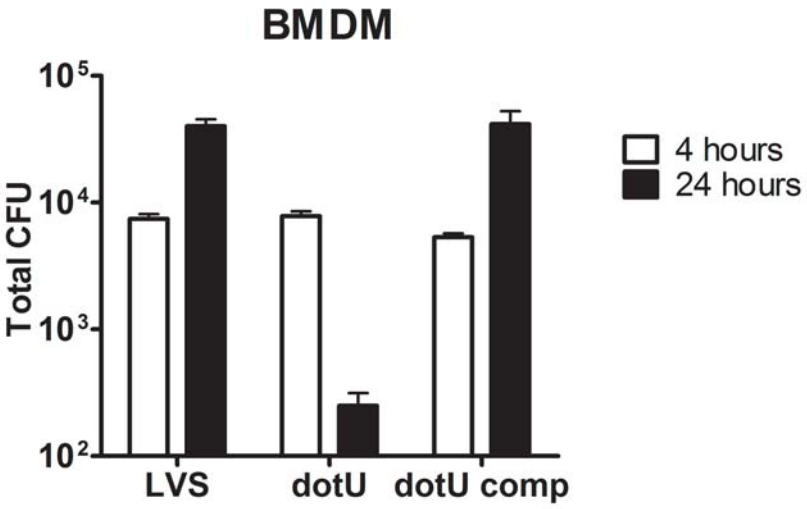


**Figure 14.** ***Trans-complementation of LVS*** **dotU** ***restores intracellular growth.*** B6 bone marrow derived macrophages (BMDMs) were inoculated with LVS, LVS *dotU*, or LVS *dotU* complement at an MOI of 25:1. BMDMs were lysed either 4 or 24 hours post-inoculation and serial dilutions of the lysate were plated on chocolate agar to determine the number of bacteria present. BMDMs were inoculated with each strain in triplicate and lysates from each sample were plated in duplicate. Data are representative of 3 independent experiments.

**Figure 15**

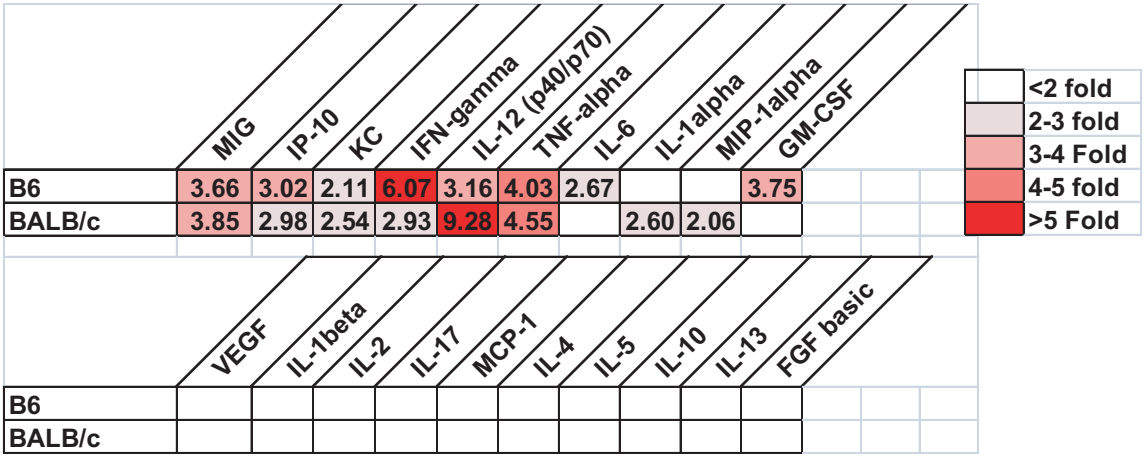


**Figure 15.** ***LVS* clpB *induces a pro-inflammatory response in the lung early after infection.*** B6 or BALB/c mice were intranasally inoculated with LVS ($5x10^2$ CFU) or LVS *clpB* ($5x10^4$ CFU), or left uninfected. 3 days post-inoculation, BALF was collected and cytokine and chemokine concentrations were determined using a Luminex-based assay. Cytokine and chemokines levels were first normalized to the levels in uninfected mice and then the fold increase in cytokine or chemokine concentration from LVS *clpB* infected mice over LVS infected mice was determined for each infected group and values are indicated in bold if they exceeded 2 fold. n=4-7 mice/group. Data are combined from at least 2 independent experiments per mouse strain. ANOVA with Tukey's post-test was used to determine significant changes in cytokine and chemokine concentrations within each mouse strain. LVS *clpB* levels were significantly higher ($p \leq 0.05$) than LVS in both mouse strains for IP-10, KC, IL-12, and TNF-$\alpha$. LVS *clpB* levels were significantly higher ($p \leq 0.05$) than LVS levels in B6 mice for IFN-$\gamma$, IL-6, and GM-CSF. LVS *clpB* levels were significantly higher ($p \leq 0.05$) than LVS levels in BALB/c mice for MIG.

**Figure 16**

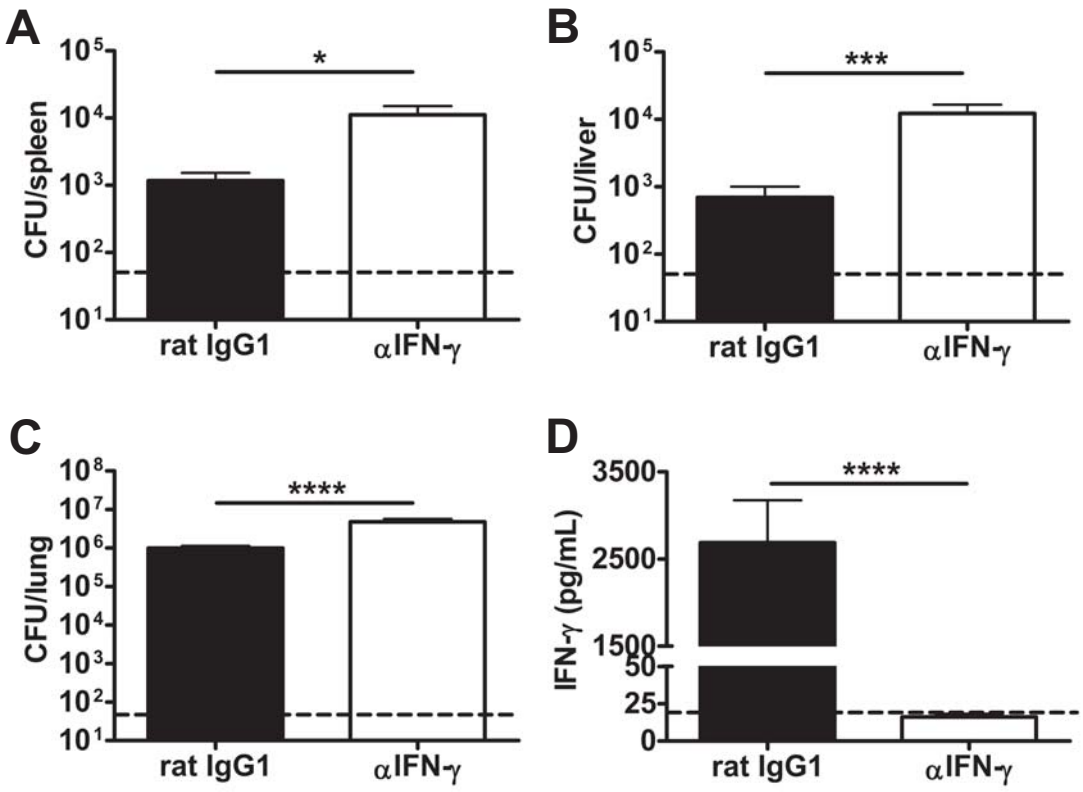


**Figure 16.** ***IFN-γ depletion increases bacterial burdens after LVS* clpB *inoculation.*** B6 mice were intranasally inoculated with LVS *clpB* ($5x10^4$ CFU). Mice were treated with 500 μg anti-IFN-γ or rat IgG1 isotype control antibody on day 0 and 2 post-inoculation. Bacterial burdens in the A) spleen, B) liver, and C) lung were determined on day 3 post-inoculation by plating serial dilutions of tissue homogenate on chocolate agar. n=8 mice/group. Data are compiled from 2 independent experiments. The dashed line indicates the limit of detection of 50 CFUs. Statistical significance was determined on log-transformed data using a Student's t-test. D) Lung tissue homogenate was clarified and IFN-γ concentration determined by Luminex analysis. n=8 mice/group. Data are compiled from 2 independent experiments. The dashed line indicates the limit of detection of 20 pg/mL. Statistical significance was determined using a Student's t-test.

**Figure 17**

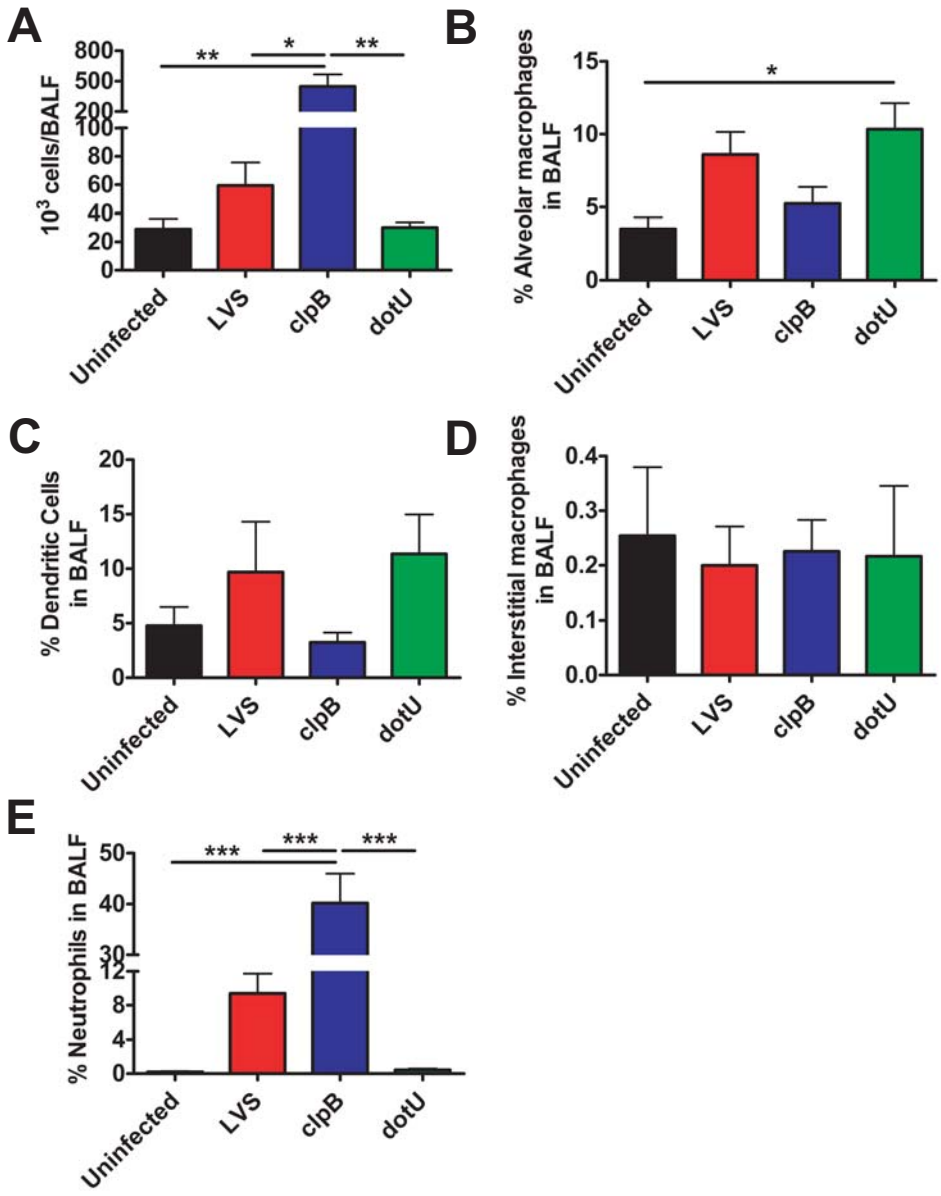


**Figure 17.** ***LVS* clpB *infection of B6 mice leads to increased mBAL cellularity and altered mBAL cellular composition.*** B6 mice were intranasally inoculated with LVS ($5x10^2$ CFU), LVS *clpB* ($5x10^4$ CFU), or LVS *dotU* ($5x10^5$ CFU), or left uninfected. A) On day 3 post-inoculation, the total number of cells in the mBAL was determined. The % B) alveolar macrophages, C) dendritic cells, D) interstitial macrophages, and e) neutrophils of all cells in the mBAL was determined by flow cytometry. n=4-7 mice/group. Data are combined from 2 independent experiments.

**Figure 18**

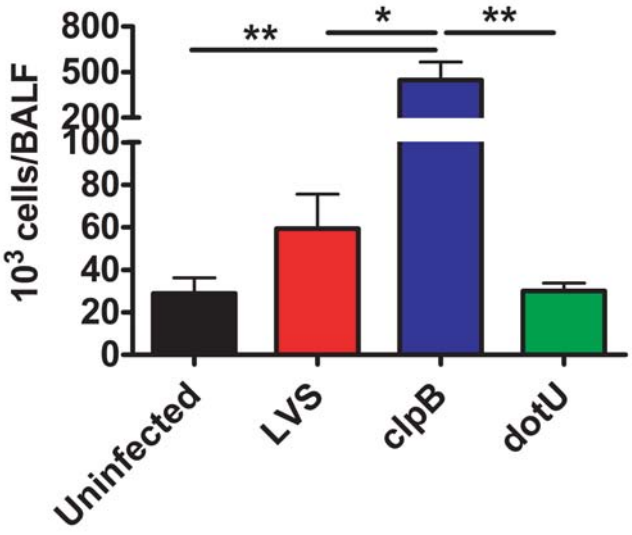


**Figure 18.** ***LVS* clpB *infection of BALB/c mice leads to increased mBAL cellularity.*** BALB/c mice were intranasally inoculated with LVS ($5x10^2$ CFU), LVS *clpB* ($5x10^4$ CFU), or LVS *dotU* ($5x10^5$ CFU), or left uninfected. On day 3 post-inoculation, the total number of cells in the mBAL was determined. n=5-7 mice/group. Data are combined from 2 independent experiments.

**Figure 19**

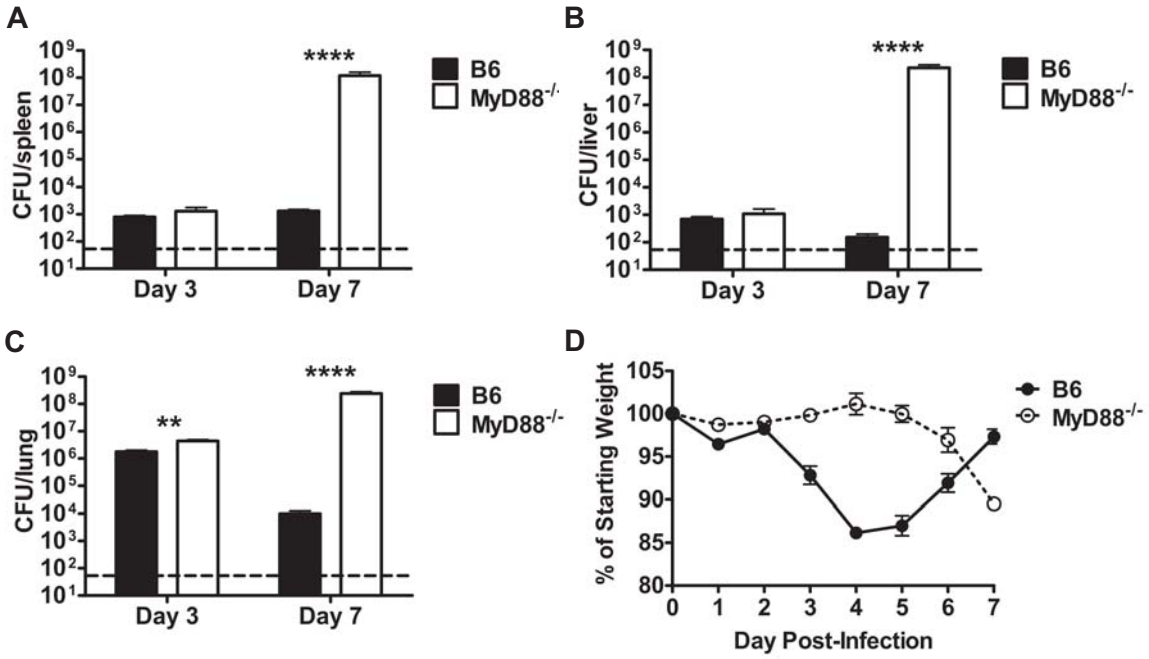


**Figure 19.** ***MyD88 signaling is required to control LVS*** **clpB** ***infection.*** B6 or MyD88$^{-/-}$ mice were intranasally inoculated with LVS *clpB* (5x10$^4$ CFU). On days 3 and 7 post-inoculation, bacterial burdens were determined in the A) spleen, B) liver, and C) lung by plating serial dilutions of organ homogenate on chocolate agar. n=5-9 mice/group. Data are combined from 2 independent experiments per time point. The dashed line indicates the limit of detection of 50 CFUs. Statistical significance was determined on log-transformed data using a Student's t-test.

**Figure 20**

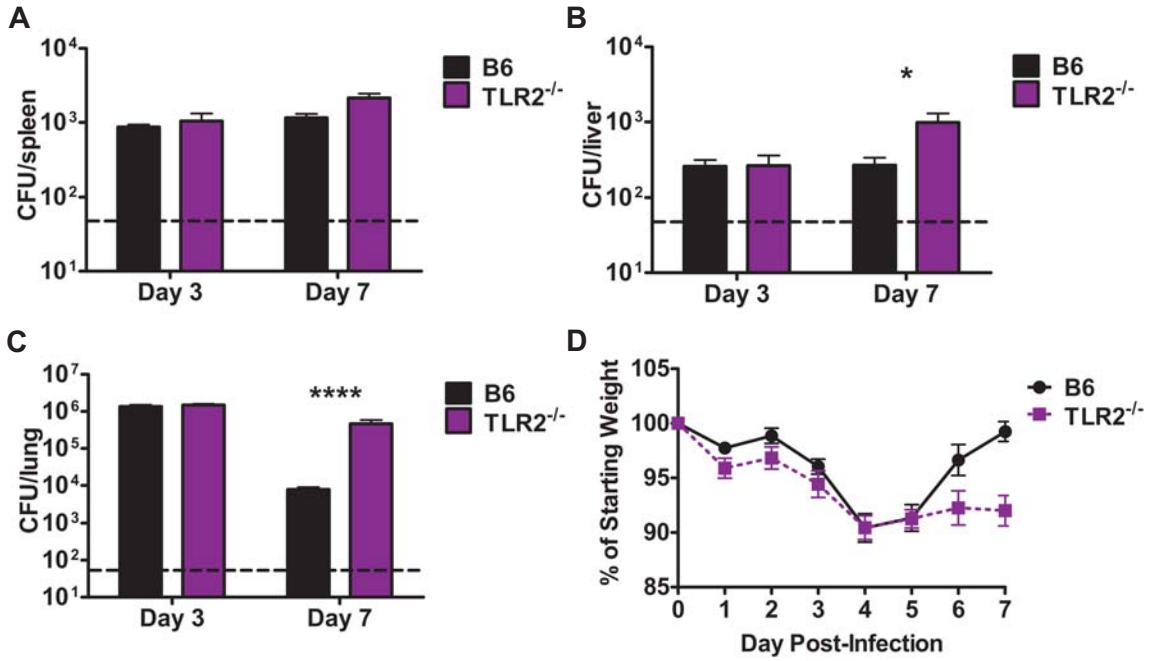


**Figure 20.** ***TLR2 signaling is required to control LVS* clpB *infection.*** B6 or TLR2$^{-/-}$ mice were intranasally inoculated with LVS *clpB* (5x10$^4$ CFU). On days 3 and 7 post-inoculation, bacterial burdens were determined in the A) spleen, B) liver, and C) lung by plating serial dilutions of organ homogenate on chocolate agar. n=3-8 mice/group. Data are from 1 experiment for day 3 and combined from 2 independent experiments for day 7. The dashed line indicates the limit of detection of 50 CFUs. Statistical significance was determined on log-transformed data using a Student's t-test. D) Weight loss was determined daily and is reported as a percentage of the starting weight.

**Figure 21**

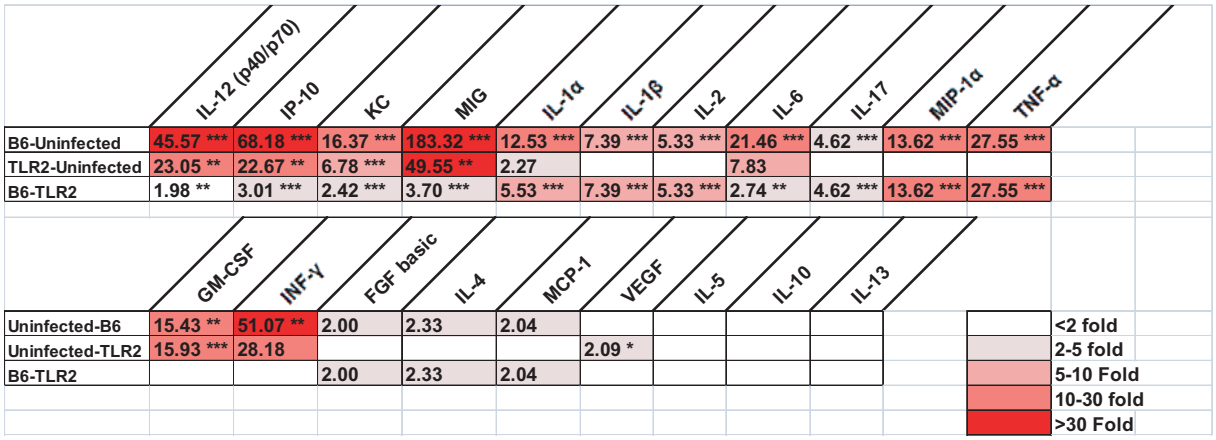

| | IL-12 (p40/p70) | IP-10 | KC | MIG | IL-1α | IL-1β | IL-2 | IL-6 | IL-17 | MIP-1α | TNF-α |
|---|---|---|---|---|---|---|---|---|---|---|---|
| B6-Uninfected | 45.57 *** | 68.18 *** | 16.37 *** | 183.32 *** | 12.53 *** | 7.39 *** | 5.33 *** | 21.46 *** | 4.62 *** | 13.62 *** | 27.55 *** |
| TLR2-Uninfected | 23.05 ** | 22.67 ** | 6.78 *** | 49.55 ** | 2.27 | | | 7.83 | | | |
| B6-TLR2 | 1.98 ** | 3.01 *** | 2.42 *** | 3.70 *** | 5.53 *** | 7.39 *** | 5.33 *** | 2.74 ** | 4.62 *** | 13.62 *** | 27.55 *** |

| | GM-CSF | INF-γ | FGF basic | IL-4 | MCP-1 | VEGF | IL-5 | IL-10 | IL-13 |
|---|---|---|---|---|---|---|---|---|---|
| Uninfected-B6 | 15.43 ** | 51.07 ** | 2.00 | 2.33 | 2.04 | | | | |
| Uninfected-TLR2 | 15.93 *** | 28.18 | | | | 2.09 * | | | |
| B6-TLR2 | | | 2.00 | 2.33 | 2.04 | | | | |

<2 fold
2-5 fold
5-10 Fold
10-30 fold
>30 Fold

**Figure 21.** ***TLR2 signaling is required for maximal pro-inflammatory cytokine production following LVS* clpB *infection.*** B6 or TLR2$^{-/-}$ mice were intranasally inoculated with LVS *clpB* (5x10$^4$ CFU). On day 3 post-inoculation, BALF was collected and cytokine and chemokine concentrations were determined using a Luminex-based assay and fold increases for each pair of groups is reported. n=3-5 mice/group. Uninfected mice are combined B6 and TLR2$^{-/-}$. Data are from 1 experiment. An ANOVA with Tukey's post-test was used to determine statisical significance for each cytokine or chemokine. Statistical significance is indicated by stars after the fold change when two groups differed.

**Figure 22**

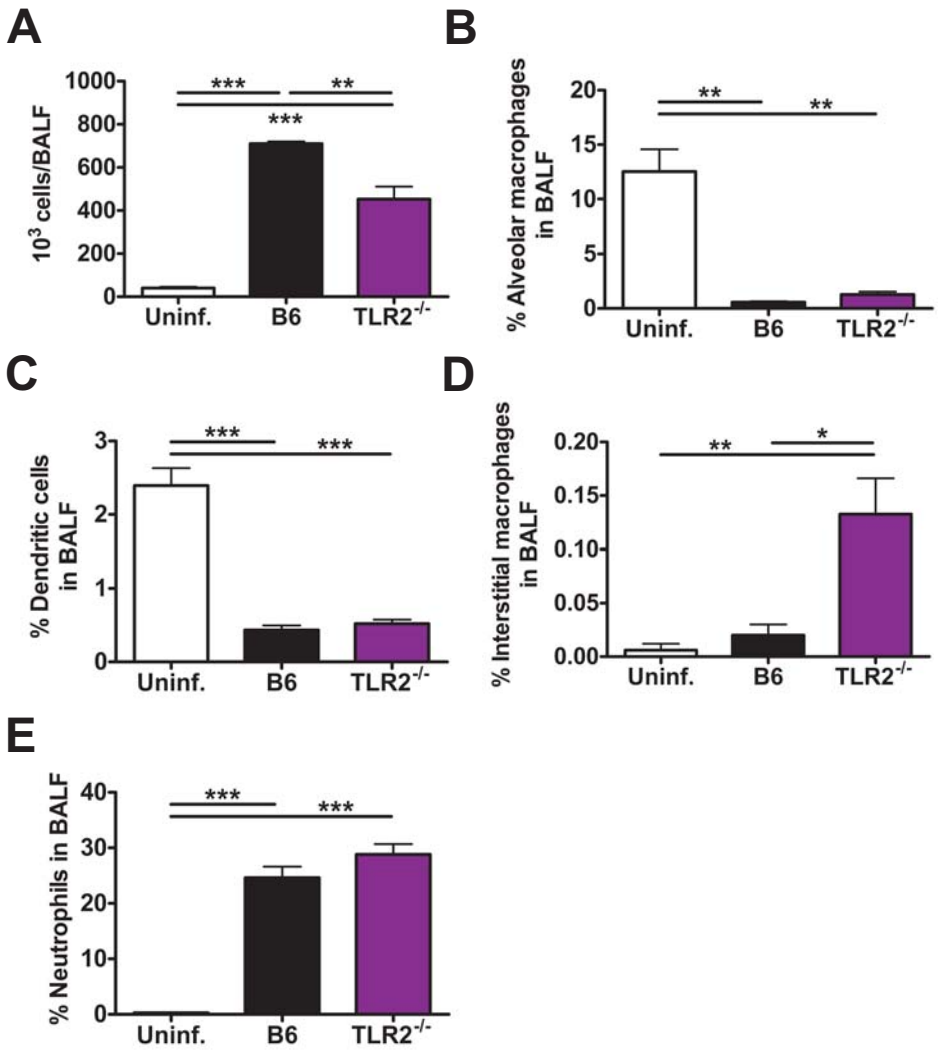


**Figure 22.** ***LVS* clpB *infection of B6 and TLR2$^{-/-}$ mice leads to increased BALF cellularity and altered BALF cellular composition.*** B6 or TLR2$^{-/-}$ mice were intranasally inoculated with LVS *clpB* (5x10$^4$ CFU) or left uninfected. A) On day 3 post-inoculation, the total number of cells in the BALF was determined. The % B) alveolar macrophages, C) dendritic cells, D) interstitial macrophages, and e) neutrophils of all cells in the BALF was determined by flow cytometry. n=3-5 mice/group. Data are from 1 experiment. Statistical significance was determined using ANOVA with Tukey's post-test.

**Figure 23**

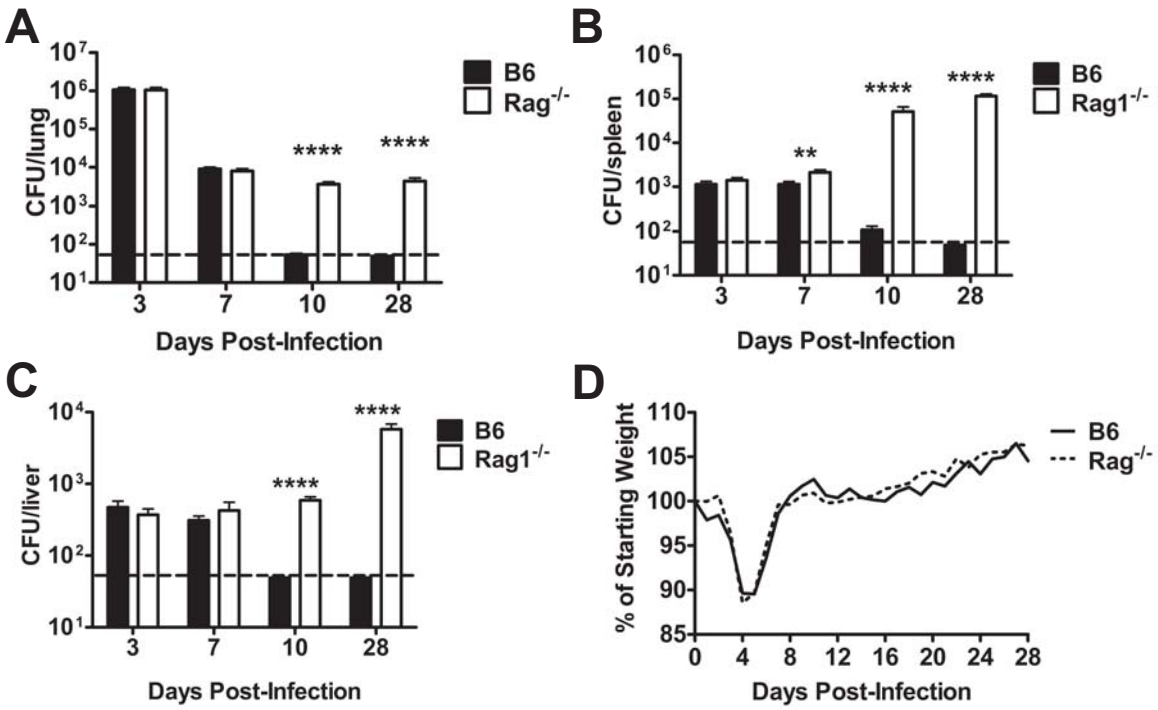


**Figure 23.** ***Adaptive immunity is required for LVS* clpB *clearance.*** B6 or Rag$^{-/-}$ mice were intranasally inoculated with 5x10$^4$ CFU LVS *clpB*. Bacterial burdens were determined in the A) lung, B) spleen, and C) liver on days 3, 7, 10, and 28 post-inoculation by plating serial dilutions of organ homogenate on chocolate agar. n=6-8 mice/group for each time point. Data are combined from 2 independent experiments for each time point. The dashed line indicates the limit of detection of 50 CFUs. Statistical significance was determined on log-transformed data using a Student's t-test. D) Mouse weight was determined daily and is reported as the percentage of starting weight. n=6-8 mice/group. Data are combined from 2 independent experiments.

**Figure 24**

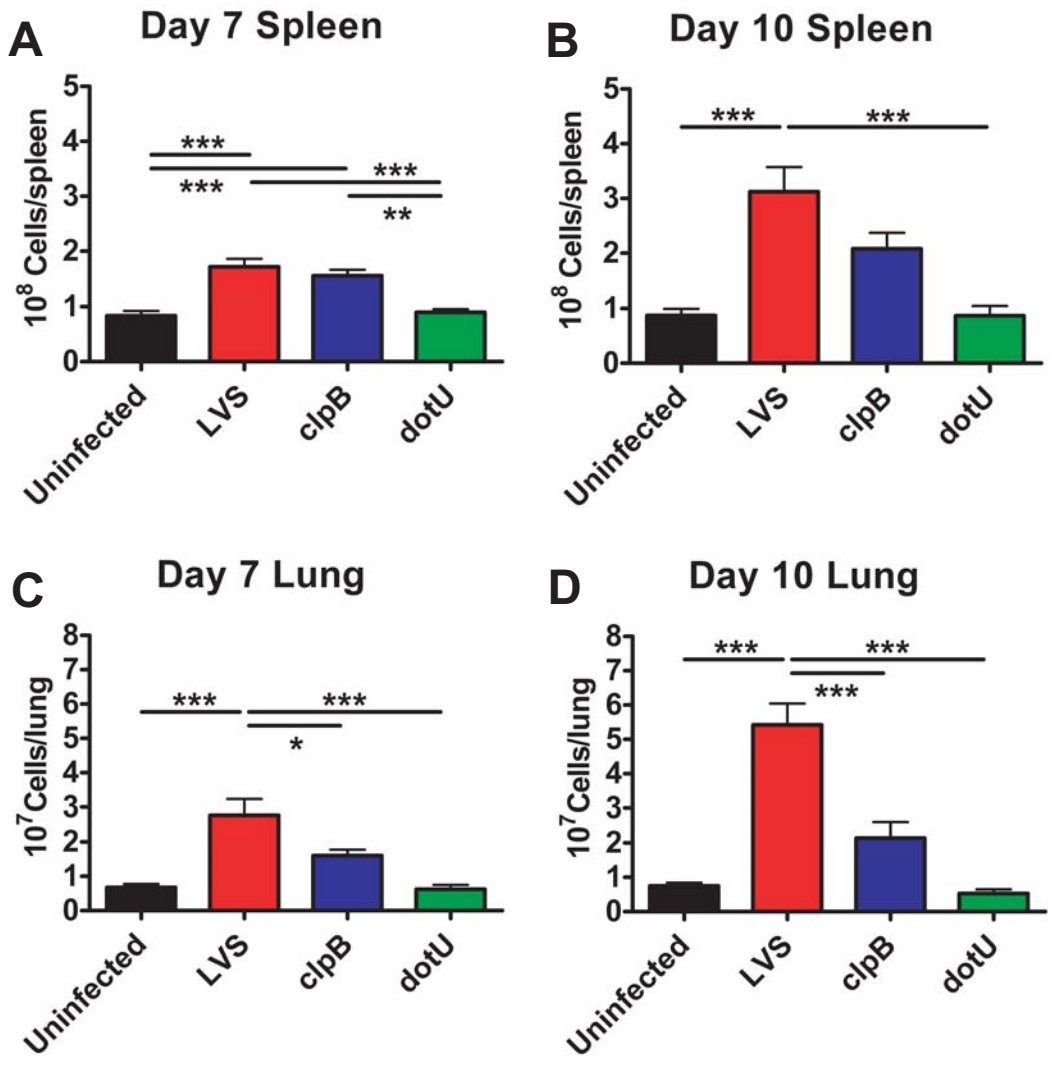


**Figure 24.** ***LVS and LVS* clpB *infection leads to increased spleen and lung cellularity.*** B6 mice were intranasally inoculated with LVS ($5x10^2$ CFU), LVS *clpB* ($5x10^4$ CFU), or LVS *dotU* ($5x10^5$ CFU), or left uninfected. The total number of cells in the spleen or lung was determined on day 7 and 10 post-inoculation by trypan blue exclusion. Total number of cells in the spleen on day A) 7 or B) 10 post-inoculation. Total number of cells in the lung on day C) 7 or D) 10 post-inoculation. n=4-9 mice/group. Data are combined from at least 4 independent experiments. Statistical significance was determined using an ANOVA with Tukey's post-test.

**Figure 25**

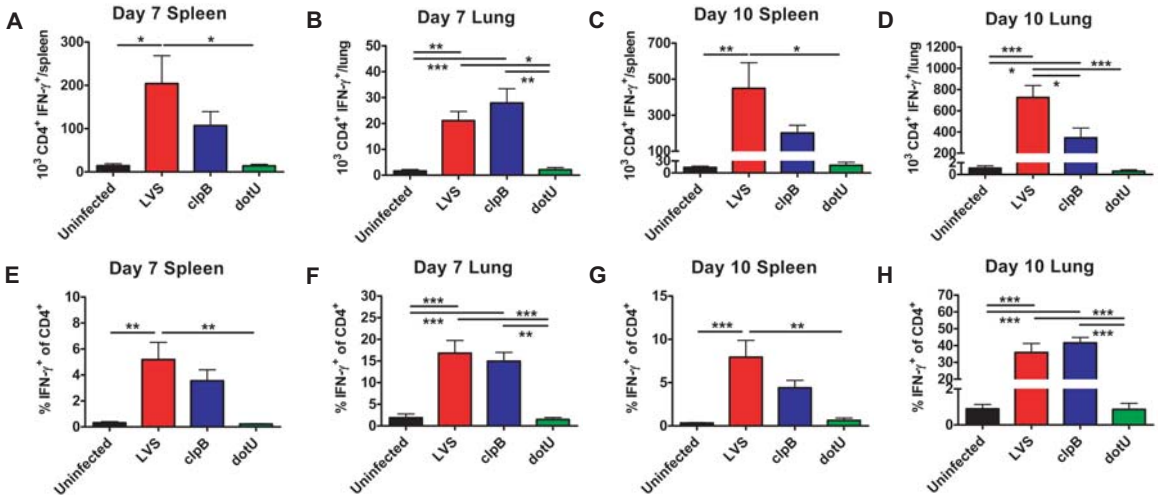


**Figure 25.** ***LVS and LVS* clpB *infection leads to increased IFN-γ$^+$ CD4$^+$ T cells.*** B6 mice were intranasally inoculated with LVS (5x10$^2$ CFU), LVS *clpB* (5x10$^4$ CFU), or LVS *dotU* (5x10$^5$ CFU), or left uninfected. On days 7 and 10 post-inoculation, splenocytes or isolated lung cells were re-stimulated with LVS infected B6-CD45.1 antigen presenting cells for 24 hours. Brefeldin A was added during the last 4 hours of co-culture. n=4-9 mice/group. Data are combined from at least 4 independent experiments. Statistical significance was determined using an ANOVA with Tukey's post-test. Number of IFN-γ producing CD4$^+$ in the A) spleen or B) lung on day 7 post-inoculation. Number of IFN-γ producing CD4$^+$ in the C) spleen or D) lung on day 10 post-inoculation. % IFN-γ$^+$ of CD4$^+$ in the E) spleen or F) lung on day 7 post-inoculation. % IFN-γ$^+$ of CD4$^+$ in the G) spleen or H) lung on day 10 post-inoculation.

**Figure 26**

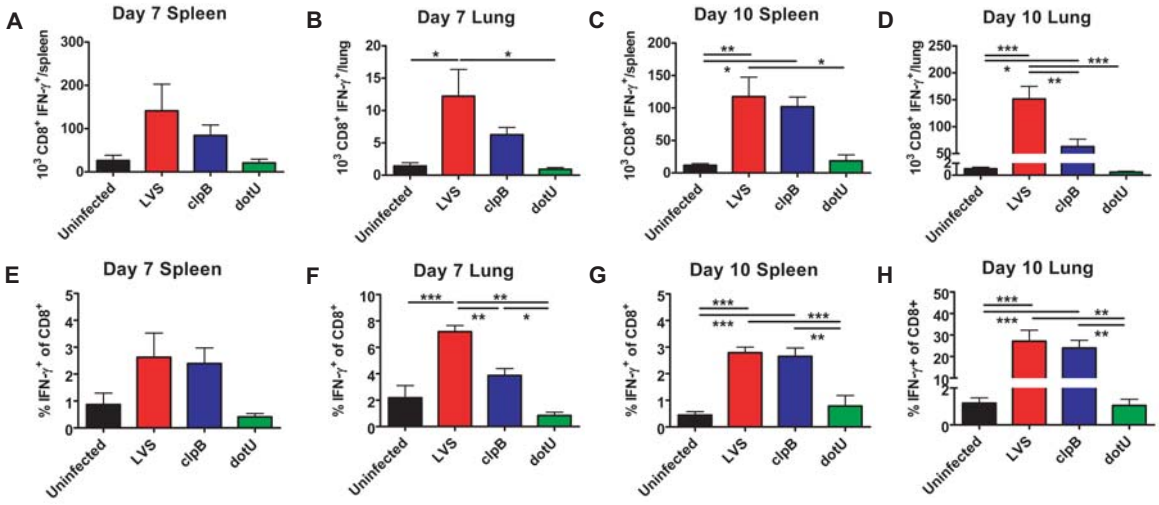


**Figure 26.** ***LVS and LVS* clpB *infection leads to increased IFN-γ$^+$ CD8$^+$ T cells.*** B6 mice were intranasally inoculated with LVS (5x10$^2$ CFU), LVS *clpB* (5x10$^4$ CFU), or LVS *dotU* (5x10$^5$ CFU), or left uninfected. On days 7 and 10 post-inoculation, splenocytes or isolated lung cells were re-stimulated with LVS infected B6-CD45.1 antigen presenting cells for 24 hours. Brefeldin A was added during the last 4 hours of co-culture. n=4-9 mice/group. Data are combined from at least 4 independent experiments. Statistical significance was determined using an ANOVA with Tukey's post-test. Number of IFN-γ producing CD8$^+$ in the A) spleen or B) lung on day 7 post-inoculation. Number of IFN-γ producing CD8$^+$ in the C) spleen or D) lung on day 10 post-inoculation. % IFN-γ$^+$ of CD8$^+$ in the E) spleen or F) lung on day 7 post-inoculation. % IFN-γ$^+$ of CD8$^+$ in the G) spleen or H) lung on day 10 post-inoculation.

**Figure 27**

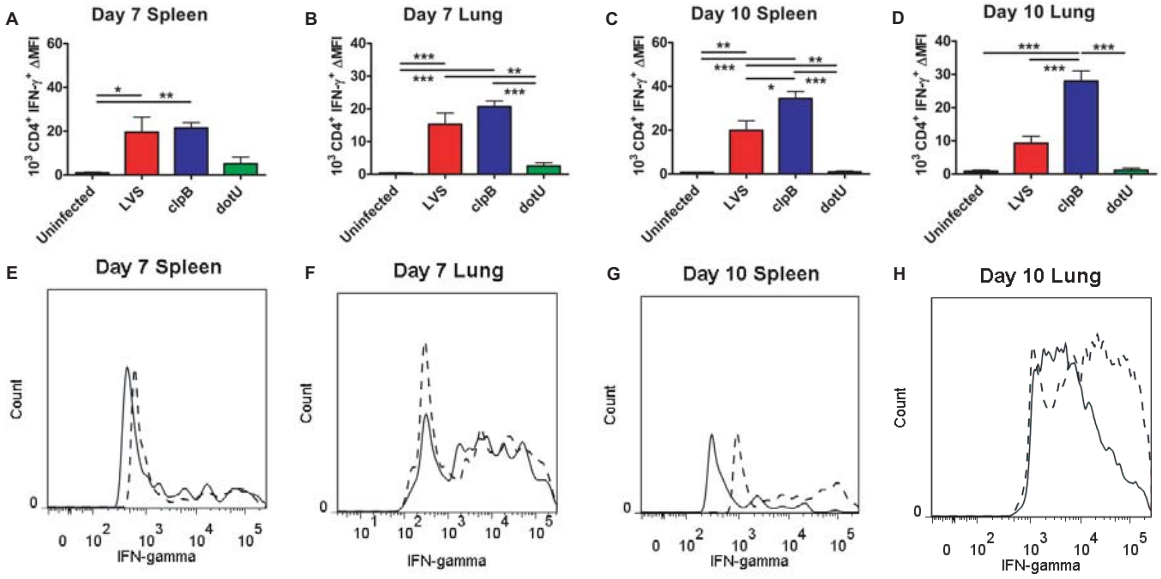


**Figure 27.** ***CD4$^+$ T cells from LVS* clpB *infected mice express more IFN-γ per cell than LVS infected mice.*** B6 mice were intranasally inoculated with LVS (5x10$^2$ CFU), LVS *clpB* (5x10$^4$ CFU), or LVS *dotU* (5x10$^5$ CFU), or left uninfected. On days 7 and 10 post-inoculation, splenocytes or isolated lung cells were re-stimulated with LVS infected B6-CD45.1 antigen presenting cells for 24 hours. Brefeldin A was added during the last 4 hours of co-culture. To determine the change in mean fluorescent intensity (ΔMFI) for each sample, the MFI of the IFN-γ negative population was subtracted from the MFI of the IFN-γ positive population. n=4-9 mice/group. Data are combined from at least 4 independent experiments. Statistical significance was determined using an ANOVA with Tukey's post-test. IFN-γ ΔMFI for CD4$^+$ T cells in the A) spleen or B) lung on day 7 post-inoculation. IFN-γ ΔMFI for CD4$^+$ T cells in the C) spleen or D) lung on day 10 post-inoculation. Representative histograms of the IFN-γ$^+$ CD4$^+$ T cells from LVS (solid line) and LVS *clpB* (dotted line) infected mice in the E) spleen or F) lung on day 7 post-inoculation. Representative histograms of the IFN-γ$^+$ CD4$^+$ T cells from LVS (solid line) and LVS *clpB* (dotted line) infected mice in the G) spleen or H) lung on day 10 post-inoculation.

**Figure 28**

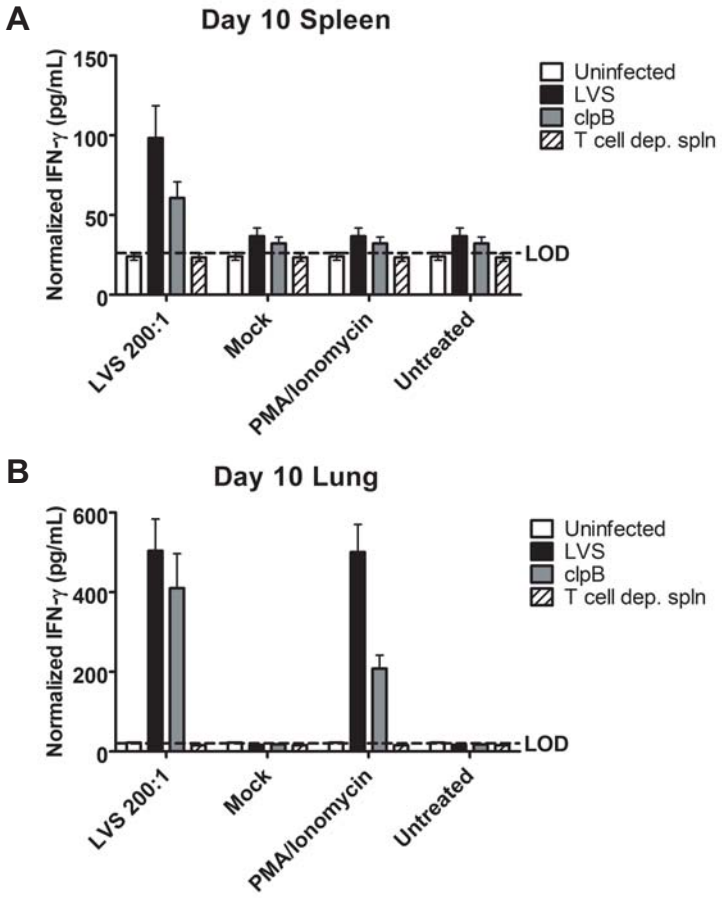


**Figure 28.** ***CD4$^+$ T cells from LVS or LVS* clpB *infected mice secrete similar amounts of IFN-γ.*** B6 mice were intranasally inoculated with LVS (5x10$^2$ CFU), LVS *clpB* (5x10$^4$ CFU), or left uninfected. 10 days post-infection, CD4$^+$ T cells were enriched from the A) spleen and B) lung and re-stimulated with LVS or mock infected T cell-depleted splenocytes. Cells were stimulated with PMA/Ionomycin as a positive control or left untreated as a negative control. IFN-γ secretion into the culture supernatant was measured by ELISA. Each sample was analyzed in triplicate. n=4 mice/group. Data are combined from two independent experiments.

**Figure 29**

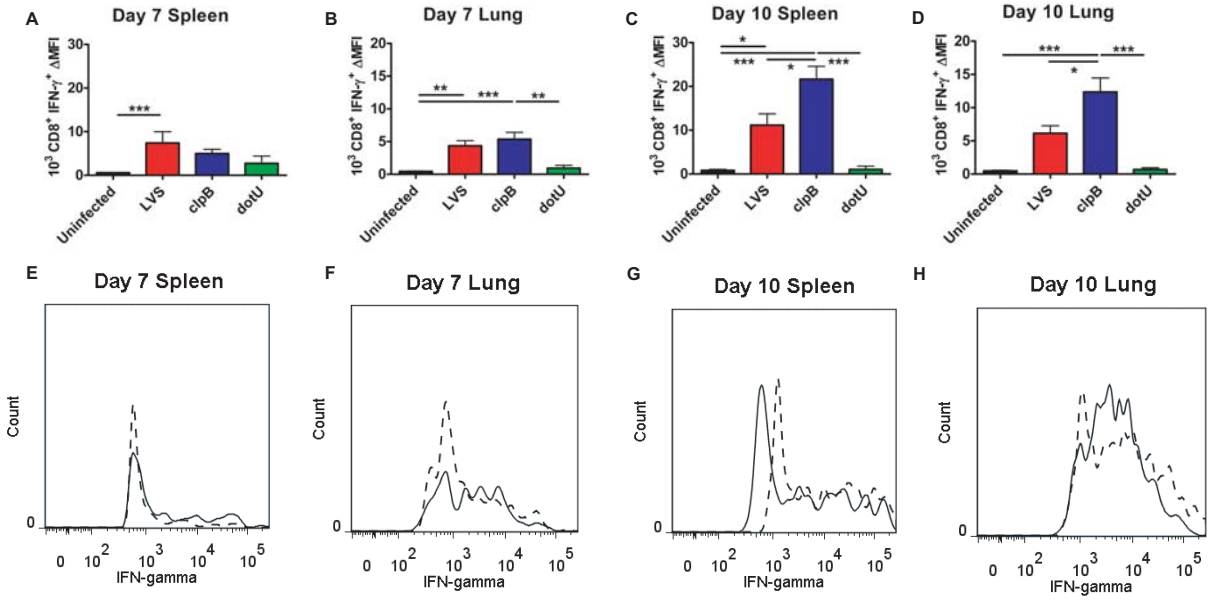


**Figure 29.** ***CD8$^+$ T cells from LVS* clpB *infected mice express more IFN-γ per cell than LVS infected mice.*** B6 mice were intranasally inoculated with LVS (5x10$^2$ CFU), LVS *clpB* (5x10$^4$ CFU), or LVS *dotU* (5x10$^5$ CFU), or left uninfected. On days 7 and 10 post-inoculation, splenocytes or isolated lung cells were re-stimulated with LVS infected B6-CD45.1 antigen presenting cells for 24 hours. Brefeldin A was added during the last 4 hours of co-culture. To determine the change in mean fluorescent intensity (ΔMFI) for each sample, the MFI of the IFN-γ negative population was subtracted from the MFI of the IFN-γ positive population. n=4-9 mice/group. Data are combined from at least 4 independent experiments. Statistical significance was determined using an ANOVA with Tukey's post-test. IFN-γ ΔMFI for CD8$^+$ T cells in the A) spleen or B) lung on day 7 post-inoculation. IFN-γ ΔMFI for CD8$^+$ T cells in the C) spleen or D) lung on day 10 post-inoculation. Representative histograms of the IFN-γ$^+$ CD8$^+$ T cells from LVS (solid line) and LVS *clpB* (dotted line) infected mice in the E) spleen or F) lung on day 7 post-inoculation. Representative histograms of the IFN-γ$^+$ CD8$^+$ T cells from LVS (solid line) and LVS *clpB* (dotted line) infected mice in the G) spleen or H) lung on day 10 post-inoculation.

**Figure 30**

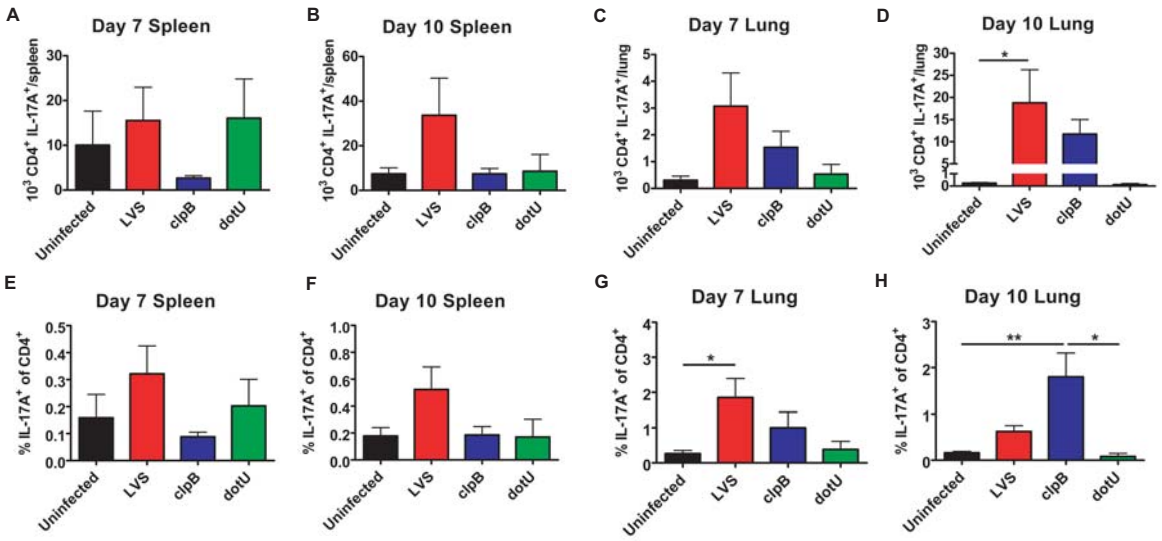


**Figure 30.** ***Th17 cells expand in the lungs of LVS and LVS*** **clpB** ***infected mice.*** B6 mice were intranasally inoculated with LVS (5x$10^2$ CFU), LVS *clpB* (5x$10^4$ CFU), or LVS *dotU* (5x$10^5$ CFU), or left uninfected. On days 7 and 10 post-infection, splenocytes or isolated lung cells were re-stimulated with LVS infected B6-CD45.1 antigen presenting cells for 24 hours. Brefeldin A was added during the last 4 hours of co-culture. n=4-9 mice/group. Data are combined from at least 4 independent experiments. Statistical significance was determined using an ANOVA with Tukey's post-test. Number of IL-17A producing $CD4^+$ in the spleen on A) day 7 or B) day 10 post-infection. Number of IL-17A producing $CD4^+$ in the lung on C) day 7 or D) day 10 post-infection. % IL-$17A^+$ of $CD4^+$ in the spleen on E) day 7 or F) day 10 post-inoculation. % IL-$17A^+$ of $CD4^+$ in the lung on G) day 7 or H) day 10 post-inoculation.

**Figure 31**

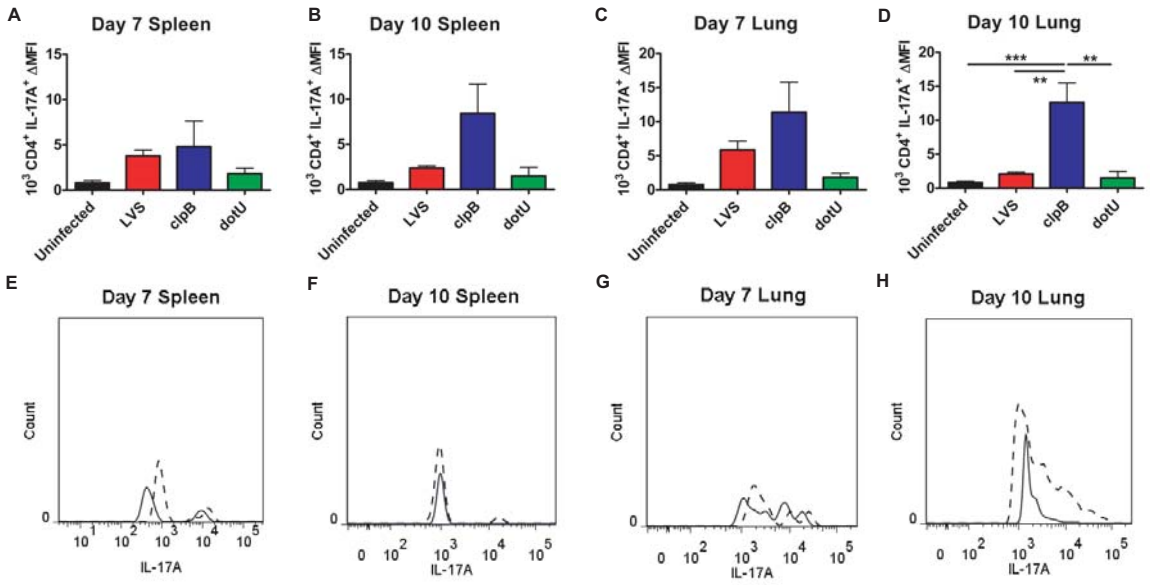


**Figure 31.** ***Th17 cells from LVS* clpB *infected mice express more IL-17 than cells from LVS infected mice.*** B6 mice were intranasally inoculated with LVS ($5x10^2$ CFU), LVS *clpB* ($5x10^4$ CFU), or LVS *dotU* ($5x10^5$ CFU), or left uninfected. On days 7 and 10 post-infection, splenocytes or isolated lung cells were re-stimulated with LVS infected B6-CD45.1 antigen presenting cells for 24 hours. Brefeldin A was added during the last 4 hours of co-culture. To determine the change in mean fluorescent intensity (ΔMFI), the MFI of the IL-17A negative population was subtracted from the MFI of the IL-17A positive population. n=4-9 mice/group. Data are combined from at least 4 independent experiments. Statistical significance was determined using an ANOVA with Tukey's post-test. IL-17A ΔMFI for $CD4^+$ T cells in the spleen on A) day 7 or B) day 10 post-infection. IL-17A ΔMFI for $CD4^+$ T cells in the lung on C) day 7 or D) day 10 post-infection. Representative histograms of the IL-$17A^+$ $CD4^+$ T cells from LVS (solid line) and LVS *clpB* (dotted line) infected mice in the spleen on E) day 7 or F) day 10 post-infection. Representative histograms of the IL-$17A^+$ $CD4^+$ T cells from LVS (solid line) and LVS *clpB* (dotted line) infected mice in the lung on G) day 7 or H) day 10 post-infection.

**Figure 32**

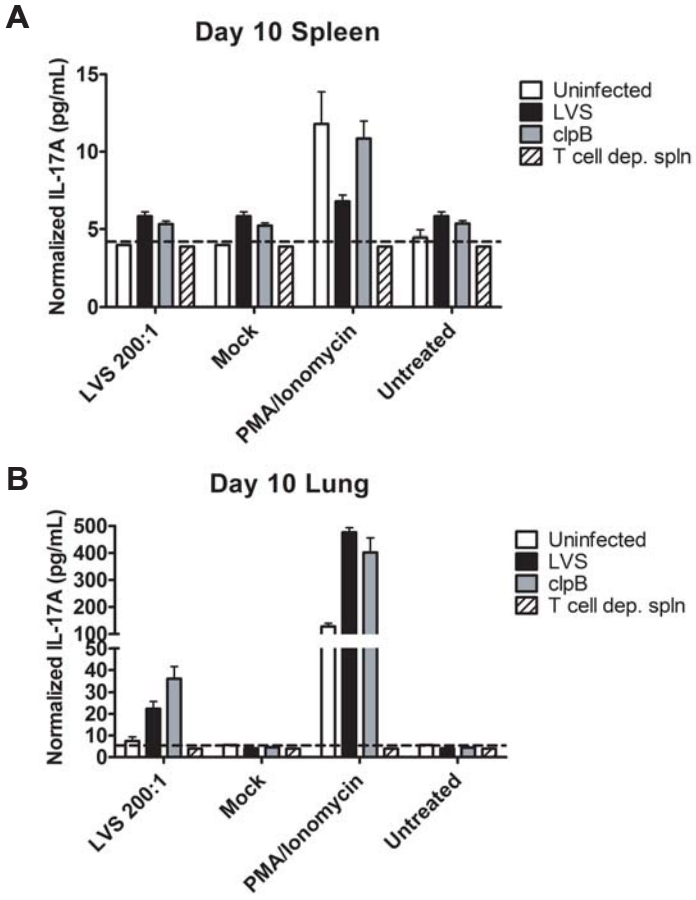


**Figure 32.** ***CD4$^+$ T cells from LVS or LVS* clpB *infected mice secrete similar amounts of IL-17A.*** B6 mice were intranasally inoculated with LVS ($5x10^2$ CFU), LVS *clpB* ($5x10^4$ CFU), or left uninfected. 10 days post-inoculation, CD4$^+$ T cells were enriched from the A) spleen and B) lung and re-stimulated with LVS or mock infected T cell-depleted splenocytes. Cells were stimulated with PMA/Ionomycin as a positive control or left untreated as a negative control. IL-17A secretion into the culture supernatant was measured by ELISA. The dashed line indicates the limit of detection of 6 pg/mL. Each sample was analyzed in triplicate. n=4 mice/group. Data are combined from two independent experiments.

**Figure 33**

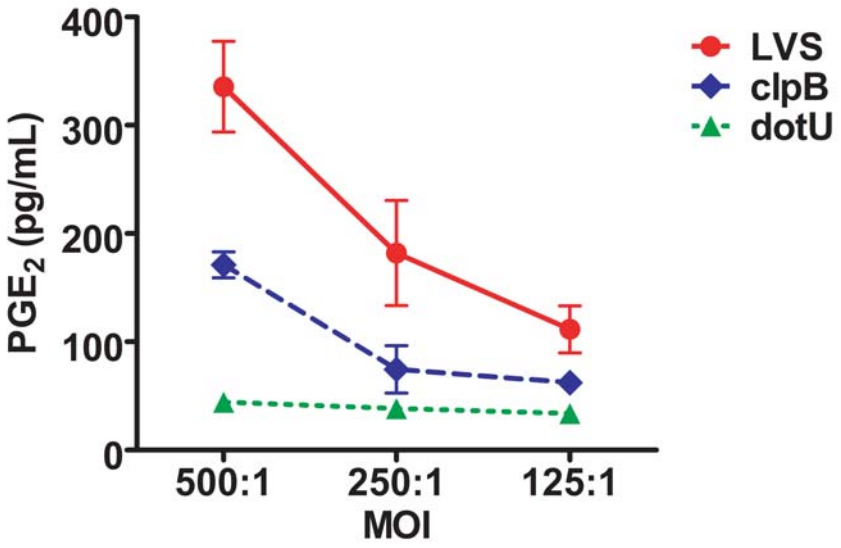


**Figure 33.** ***LVS* clpB *induces less PGE$_2$ synthesis and secretion from bone marrow-derived macrophages compared to LVS.*** 1x10$^5$ B6 BMDMs were inoculated at an MOI of 500:1, 250:1, or 125:1 with LVS, LVS *clpB*, or LVS *dotU*. 24 hours post-inoculation, culture supernatants were collected and the concentration of PGE$_2$ was determined using an ELISA. BMDMs were infected with each strain in triplicate. Uninfected BMDMs produced 38.58 +/- 1.62 pg/mL PGE$_2$ and LPS treated BMDMs (positive control) produced 672.58 +/- 172.01 pg/mL PGE$_2$. Data are representative of 3 independent experiments. Statistical significance was determined using ANOVA with Tukey's post-test to compare the strains at each MOI: 500:1: LVS versus LVS *clpB*: $p \leq 0.001$; LVS versus LVS *dotU*: $p \leq 0.001$; LVS *clpB* versus LVS *dotU*: $p \leq 0.01$. 250:1: LVS versus LVS *clpB*: $p \leq 0.05$; LVS versus LVS *dotU*: $p \leq 0.01$; LVS *clpB* versus LVS *dotU*: ns. 125:1: LVS versus LVS *clpB*: $p \leq 0.01$; LVS versus LVS *dotU*: $p \leq 0.001$; LVS *clpB* versus LVS *dotU*: ns.

**Figure 34**

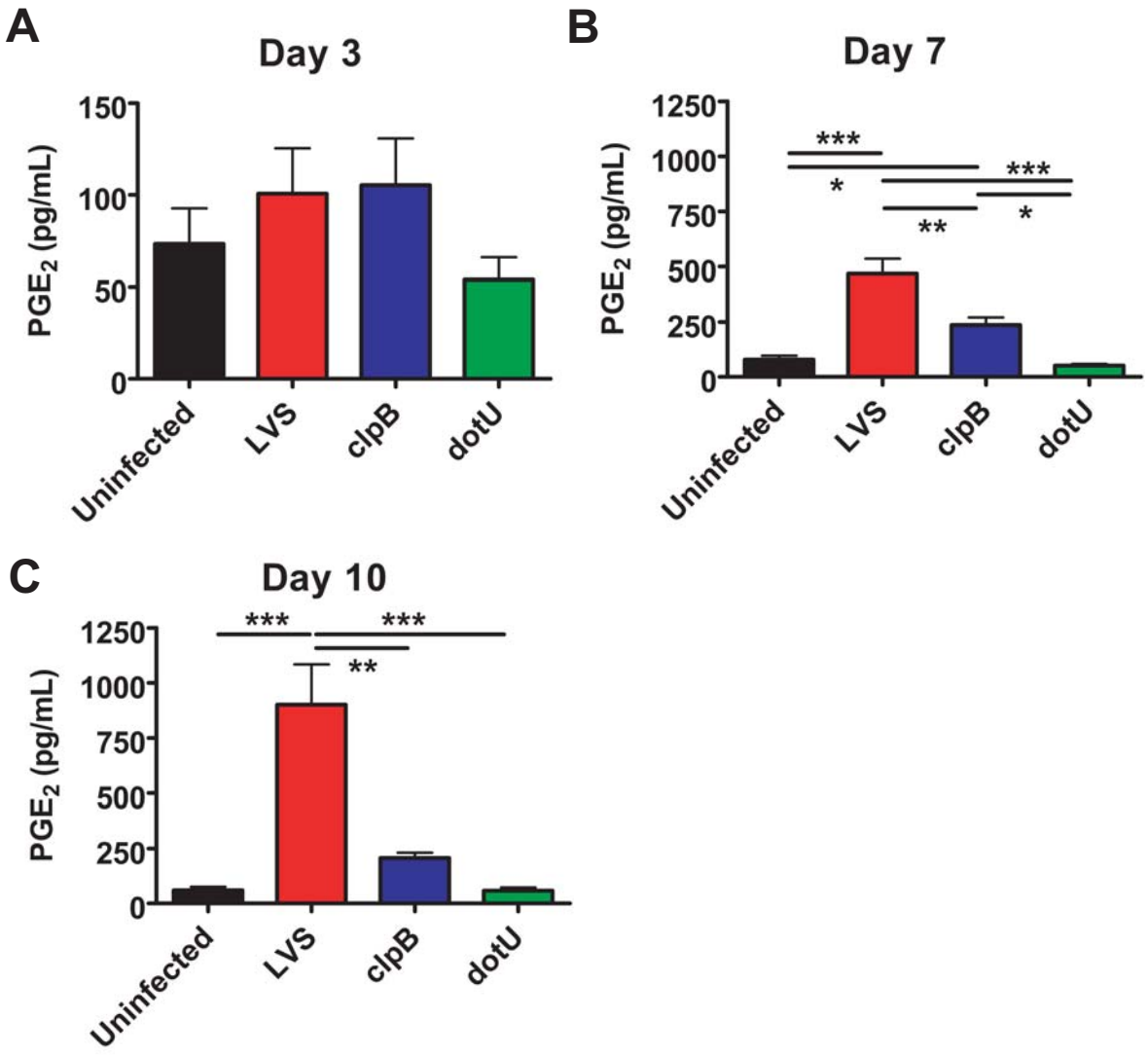


**Figure 34.** ***LVS* clpB *infected mice produce less $PGE_2$ than LVS infected mice.*** B6 mice were intranasally inoculated with LVS ($5x10^2$ CFU), LVS *clpB* ($5x10^4$ CFU), or left uninfected. On days A) 3, B) 7, and C) 10 days post-inoculation BALF was collected and the concentration of $PGE_2$ was determined by ELISA. n=5-10 mice/group for each time point. Data are combined from at least two independent experiments per time point. Statistical significance was determined using ANOVA with Tukey's post-test.

## REFERENCES


1. Pechous RD, McCarthy TR, Zahrt TC. Working toward the future: insights into Francisella tularensis pathogenesis and vaccine development. Microbiol Mol Biol Rev. 2009;73(4):684-711. Epub 2009/12/01. doi: 73/4/684 [pii] 10.1128/MMBR.00028-09. PubMed PMID: 19946137; PubMed Central PMCID: PMC2786580.

2. Dennis DT, Inglesby TV, Henderson DA, Bartlett JG, Ascher MS, Eitzen E, et al. Tularemia as a biological weapon: medical and public health management. JAMA. 2001;285(21):2763-73. Epub 2001/06/21. doi: jst10001 [pii]. PubMed PMID: 11386933.

3. Christopher GW, Cieslak TJ, Pavlin JA, Eitzen EM, Jr. Biological warfare. A historical perspective. JAMA. 1997;278(5):412-7. Epub 1997/08/06. PubMed PMID: 9244333.

4. Alibek K, Handelman S. Biohazard : the chilling true story of the largest covert biological weapons program in the world, told from the inside by the man who ran it. 1st ed. New York: Random House; 1999. xi, 319 p., 8 p. of plates p.

5. Kadzhaev K, Zingmark C, Golovliov I, Bolanowski M, Shen H, Conlan W, et al. Identification of genes contributing to the virulence of Francisella tularensis SCHU S4 in a mouse intradermal infection model. PLoS One. 2009;4(5):e5463. Epub 2009/05/09. doi: 10.1371/journal.pone.0005463. PubMed PMID: 19424499; PubMed Central PMCID: PMC2675058.

6. Su J, Yang J, Zhao D, Kawula TH, Banas JA, Zhang JR. Genome-wide identification of Francisella tularensis virulence determinants. Infect Immun. 2007;75(6):3089-101. Epub 2007/04/11. doi: IAI.01865-06 [pii] 10.1128/IAI.01865-06. PubMed PMID: 17420240; PubMed Central PMCID: PMC1932872.

7. Weiss DS, Brotcke A, Henry T, Margolis JJ, Chan K, Monack DM. In vivo negative selection screen identifies genes required for Francisella virulence. Proc Natl Acad Sci U S A. 2007;104(14):6037-42. Epub 2007/03/29. doi: 0609675104 [pii] 10.1073/pnas.0609675104. PubMed PMID: 17389372; PubMed Central PMCID: PMC1832217.

8. Metzger DW, Bakshi CS, Kirimanjeswara G. Mucosal immunopathogenesis of Francisella tularensis. Ann N Y Acad Sci. 2007;1105:266-83. Epub 2007/03/31. doi: annals.1409.007 [pii] 10.1196/annals.1409.007. PubMed PMID: 17395728.

9. Conlan JW, Chen W, Shen H, Webb A, KuoLee R. Experimental tularemia in mice challenged by aerosol or intradermally with virulent strains of Francisella tularensis: bacteriologic and histopathologic studies. Microb Pathog. 2003;34(5):239-48. PubMed PMID: 12732472.

10. Hall JD, Woolard MD, Gunn BM, Craven RR, Taft-Benz S, Frelinger JA, et al. Infected-host-cell repertoire and cellular response in the lung following inhalation of Francisella tularensis Schu S4, LVS, or U112. Infect Immun. 2008;76(12):5843-52. Epub 2008/10/15. doi: IAI.01176-08 [pii] 10.1128/IAI.01176-08. PubMed PMID: 18852251; PubMed Central PMCID: PMC2583552.

11. Bosio CM, Dow SW. Francisella tularensis induces aberrant activation of pulmonary dendritic cells. J Immunol. 2005;175(10):6792-801. Epub 2005/11/08. doi: 175/10/6792 [pii]. PubMed PMID: 16272336.

12. Hajjar AM, Harvey MD, Shaffer SA, Goodlett DR, Sjostedt A, Edebro H, et al. Lack of in vitro and in vivo recognition of Francisella tularensis subspecies lipopolysaccharide by Toll-like receptors. Infect Immun. 2006;74(12):6730-8. Epub 2006/09/20. doi: IAI.00934-06 [pii] 10.1128/IAI.00934-06. PubMed PMID: 16982824; PubMed Central PMCID: PMC1698081.

13. Bosio CM, Bielefeldt-Ohmann H, Belisle JT. Active suppression of the pulmonary immune response by Francisella tularensis Schu4. J Immunol. 2007;178(7):4538-47. Epub 2007/03/21. doi: 178/7/4538 [pii]. PubMed PMID: 17372012.

14. Chong A, Celli J. The francisella intracellular life cycle: toward molecular mechanisms of intracellular survival and proliferation. Front Microbiol. 2010;1:138. Epub 2010/01/01. doi: 10.3389/fmicb.2010.00138. PubMed PMID: 21687806; PubMed Central PMCID: PMC3109316.

15. Yee D, Rhinehart-Jones TR, Elkins KL. Loss of either CD4+ or CD8+ T cells does not affect the magnitude of protective immunity to an intracellular pathogen, Francisella tularensis strain LVS. J Immunol. 1996;157(11):5042-8. Epub 1996/12/01. PubMed PMID: 8943413.

16. Collazo CM, Sher A, Meierovics AI, Elkins KL. Myeloid differentiation factor-88 (MyD88) is essential for control of primary in vivo Francisella tularensis LVS infection, but not for control of intra-macrophage bacterial replication. Microbes Infect. 2006;8(3):779-90. Epub 2006/03/04. doi: S1286-4579(05)00364-3 [pii] 10.1016/j.micinf.2005.09.014. PubMed PMID: 16513388.

17. Leiby DA, Fortier AH, Crawford RM, Schreiber RD, Nacy CA. In vivo modulation of the murine immune response to Francisella tularensis LVS by administration of anticytokine antibodies. Infect Immun. 1992;60(1):84-9. Epub 1992/01/01. PubMed PMID: 1729199; PubMed Central PMCID: PMC257506.

18. Anthony LS, Ghadirian E, Nestel FP, Kongshavn PA. The requirement for gamma interferon in resistance of mice to experimental tularemia. Microb Pathog. 1989;7(6):421-8. Epub 1989/12/01. PubMed PMID: 2516219.

19. Woolard MD, Hensley LL, Kawula TH, Frelinger JA. Respiratory Francisella tularensis live vaccine strain infection induces Th17 cells and prostaglandin E2, which inhibits generation of gamma interferon-positive T cells. Infect Immun. 2008;76(6):2651-9. Epub 2008/04/09. doi: IAI.01412-07 [pii] 10.1128/IAI.01412-07. PubMed PMID: 18391003; PubMed Central PMCID: PMC2423094.

20. Lin Y, Ritchea S, Logar A, Slight S, Messmer M, Rangel-Moreno J, et al. Interleukin-17 is required for T helper 1 cell immunity and host resistance to the intracellular pathogen Francisella tularensis. Immunity. 2009;31(5):799-810. Epub 2009/10/27. doi: S1074-7613(09)00448-8 [pii] 10.1016/j.immuni.2009.08.025. PubMed PMID: 19853481; PubMed Central PMCID: PMC2789998.

21. Markel G, Bar-Haim E, Zahavy E, Cohen H, Cohen O, Shafferman A, et al. The involvement of IL-17A in the murine response to sub-lethal inhalational infection with Francisella tularensis. PLoS One. 2010;5(6):e11176. doi: 10.1371/journal.pone.0011176. PubMed PMID: 20585449; PubMed Central PMCID: PMC2887844.

22. Nano FE, Zhang N, Cowley SC, Klose KE, Cheung KK, Roberts MJ, et al. A Francisella tularensis pathogenicity island required for intramacrophage growth. J Bacteriol. 2004;186(19):6430-6. Epub 2004/09/18. doi: 10.1128/JB.186.19.6430-6436.2004 186/19/6430 [pii]. PubMed PMID: 15375123; PubMed Central PMCID: PMC516616.

23. Meibom KL, Dubail I, Dupuis M, Barel M, Lenco J, Stulik J, et al. The heat-shock protein ClpB of Francisella tularensis is involved in stress tolerance and is required for multiplication in target organs of infected mice. Mol Microbiol. 2008;67(6):1384-401. Epub 2008/02/21. doi: MMI6139 [pii] 10.1111/j.1365-2958.2008.06139.x [doi]. PubMed PMID: 18284578.

24. Conlan JW, Shen H, Golovliov I, Zingmark C, Oyston PC, Chen W, et al. Differential ability of novel attenuated targeted deletion mutants of Francisella tularensis subspecies tularensis strain SCHU S4 to protect mice against aerosol challenge with virulent bacteria: effects of host background and route of immunization. Vaccine. 2010;28(7):1824-31. Epub 2009/12/19. doi: S0264-410X(09)01904-5 [pii] 10.1016/j.vaccine.2009.12.001. PubMed PMID: 20018266; PubMed Central PMCID: PMC2822029.

25. Twine S, Shen H, Harris G, Chen W, Sjostedt A, Ryden P, et al. BALB/c mice, but not C57BL/6 mice immunized with a DeltaclpB mutant of Francisella tularensis subspecies tularensis are protected against respiratory challenge with wild-type bacteria: Association of protection with post-vaccination and post-challenge immune responses. Vaccine. 2012;30(24):3634-45. Epub 2012/04/10. doi: S0264-410X(12)00412-4 [pii] 10.1016/j.vaccine.2012.03.036. PubMed PMID: 22484348.

26. Chamberlain RE. Evaluation of Live Tularemia Vaccine Prepared in a Chemically Defined Medium. Appl Microbiol. 1965;13:232-5. Epub 1965/03/01. PubMed PMID: 14325885; PubMed Central PMCID: PMC1058227.

27. LoVullo ED, Molins-Schneekloth CR, Schweizer HP, Pavelka MS, Jr. Single-copy chromosomal integration systems for Francisella tularensis. Microbiology. 2009;155(Pt 4):1152-63. Epub 2009/04/01. doi: 155/4/1152 [pii] 10.1099/mic.0.022491-0. PubMed PMID: 19332817.

28. Woolard MD, Wilson JE, Hensley LL, Jania LA, Kawula TH, Drake JR, et al. Francisella tularensis-infected macrophages release prostaglandin E2 that blocks T cell proliferation and promotes a Th2-like response. J Immunol. 2007;178(4):2065-74. Epub 2007/02/06. doi: 178/4/2065 [pii]. PubMed PMID: 17277110.

29. Porter BB, Harty JT. The onset of CD8+-T-cell contraction is influenced by the peak of Listeria monocytogenes infection and antigen display. Infect Immun. 2006;74(3):1528-36. doi: 10.1128/IAI.74.3.1528-1536.2006. PubMed PMID: 16495523; PubMed Central PMCID: PMC1418632.

30. Williams MA, Bevan MJ. Shortening the infectious period does not alter expansion of CD8 T cells but diminishes their capacity to differentiate into memory cells. J Immunol. 2004;173(11):6694-702. PubMed PMID: 15557161.

31. Wong P, Pamer EG. Cutting edge: antigen-independent CD8 T cell proliferation. J Immunol. 2001;166(10):5864-8. PubMed PMID: 11342598.

32. Broms JE, Meyer L, Lavander M, Larsson P, Sjostedt A. DotU and VgrG, Core Components of Type VI Secretion Systems, Are Essential for Francisella LVS Pathogenicity. PLoS One. 2012;7(4):e34639. Epub 2012/04/20. doi: 10.1371/journal.pone.0034639 PONE-D-12-02842 [pii]. PubMed PMID: 22514651; PubMed Central PMCID: PMC3326028.

33. Chen W, Shen H, Webb A, KuoLee R, Conlan JW. Tularemia in BALB/c and C57BL/6 mice vaccinated with Francisella tularensis LVS and challenged intradermally, or by aerosol with virulent isolates of the pathogen: protection varies depending on pathogen virulence, route of exposure, and host genetic background. Vaccine. 2003;21(25-26):3690-700. Epub 2003/08/19. doi: S0264410X03003864 [pii]. PubMed PMID: 12922099.

34. Schmitt DM, O'Dee DM, Horzempa J, Carlson PE, Jr., Russo BC, Bales JM, et al. A Francisella tularensis live vaccine strain that improves stimulation of antigen-presenting cells does not enhance vaccine efficacy. PLoS One. 2012;7(2):e31172. Epub 2012/02/23. doi: 10.1371/journal.pone.0031172 PONE-D-11-07219 [pii]. PubMed PMID: 22355343; PubMed Central PMCID: PMC3280287.

35. Woolard MD, Barrigan LM, Fuller JR, Buntzman AS, Bryan J, Manoil C, et al. Identification of *Francisella novicida* mutants that fail to induce prostaglandin $E_2$ synthesis by infected macrophages. Front Microbiol. 2013;4. doi: 10.3389/fmicb.2013.00016.

36. Abplanalp AL, Morris IR, Parida BK, Teale JM, Berton MT. TLR-dependent control of Francisella tularensis infection and host inflammatory responses. PLoS One. 2009;4(11):e7920. doi: 10.1371/journal.pone.0007920. PubMed PMID: 19936231.

37. Medzhitov R, Preston-Hurlburt P, Kopp E, Stadlen A, Chen C, Ghosh S, et al. MyD88 is an adaptor protein in the hToll/IL-1 receptor family signaling pathways. Molecular cell. 1998;2(2):253-8. PubMed PMID: 9734363.

38. Thakran S, Li H, Lavine CL, Miller MA, Bina JE, Bina XR, et al. Identification of Francisella tularensis lipoproteins that stimulate the toll-like receptor (TLR) 2/TLR1 heterodimer. J Biol Chem. 2008;283(7):3751-60. doi: M706854200 [pii] 10.1074/jbc.M706854200. PubMed PMID: 18079113.

39. Forestal CA, Gil H, Monfett M, Noah CE, Platz GJ, Thanassi DG, et al. A conserved and immunodominant lipoprotein of Francisella tularensis is proinflammatory but not essential for virulence. Microb Pathog. 2008;44(6):512-23. doi: S0882-4010(08)00003-X [pii] 10.1016/j.micpath.2008.01.003. PubMed PMID: 18304778.

40. Parra MC, Shaffer SA, Hajjar AM, Gallis BM, Hager A, Goodlett DR, et al. Identification, cloning, expression, and purification of Francisella lpp3: an immunogenic lipoprotein. Microbiol Res. Germany: 2009 Elsevier GmbH; 2010. p. 531-45.

41. Cole LE, Shirey KA, Barry E, Santiago A, Rallabhandi P, Elkins KL, et al. Toll-like receptor 2-mediated signaling requirements for Francisella tularensis live vaccine strain infection of murine macrophages. Infect Immun. 2007;75(8):4127-37. doi: 10.1128/IAI.01868-06. PubMed PMID: 17517865; PubMed Central PMCID: PMC1951974.

42. Maier TM, Pechous R, Casey M, Zahrt TC, Frank DW. In vivo Himar1-based transposon mutagenesis of Francisella tularensis. Appl Environ Microbiol. 2006;72(3):1878-85. Epub 2006/03/07. doi: 72/3/1878 [pii] 10.1128/AEM.72.3.1878-1885.2006. PubMed PMID: 16517634; PubMed Central PMCID: PMC1393221.

43. Gray CG, Cowley SC, Cheung KK, Nano FE. The identification of five genetic loci of Francisella novicida associated with intracellular growth. FEMS Microbiol Lett. 2002;215(1):53-6. Epub 2002/10/24. doi: S0378109702009114 [pii]. PubMed PMID: 12393200.

44. Tempel R, Lai XH, Crosa L, Kozlowicz B, Heffron F. Attenuated Francisella novicida transposon mutants protect mice against wild-type challenge. Infect Immun. 2006;74(9):5095-105. Epub 2006/08/24. doi: 74/9/5095 [pii] 10.1128/IAI.00598-06. PubMed PMID: 16926401; PubMed Central PMCID: PMC1594869.

45. Hsieh CS, Macatonia SE, Tripp CS, Wolf SF, O'Garra A, Murphy KM. Development of TH1 CD4+ T cells through IL-12 produced by Listeria-induced macrophages. Science. 1993;260(5107):547-9. Epub 1993/04/23. PubMed PMID: 8097338.

46. Seder RA, Gazzinelli R, Sher A, Paul WE. Interleukin 12 acts directly on CD4+ T cells to enhance priming for interferon gamma production and diminishes interleukin 4

inhibition of such priming. Proc Natl Acad Sci U S A. 1993;90(21):10188-92. Epub 1993/11/01. PubMed PMID: 7901851; PubMed Central PMCID: PMCPMC47739.

47. Kalinski P, Vieira PL, Schuitemaker JH, de Jong EC, Kapsenberg ML. Prostaglandin E(2) is a selective inducer of interleukin-12 p40 (IL-12p40) production and an inhibitor of bioactive IL-12p70 heterodimer. Blood. 2001;97(11):3466-9. Epub 2001/05/23. PubMed PMID: 11369638.

48. Schnurr M, Toy T, Shin A, Wagner M, Cebon J, Maraskovsky E. Extracellular nucleotide signaling by P2 receptors inhibits IL-12 and enhances IL-23 expression in human dendritic cells: a novel role for the cAMP pathway. Blood. 2005;105(4):1582-9. Epub 2004/10/16. doi: 2004-05-1718 [pii] 10.1182/blood-2004-05-1718. PubMed PMID: 15486065.

49. Sheibanie AF, Tadmori I, Jing H, Vassiliou E, Ganea D. Prostaglandin E2 induces IL-23 production in bone marrow-derived dendritic cells. FASEB J. 2004;18(11):1318-20. Epub 2004/06/08. doi: 10.1096/fj.03-1367fje 03-1367fje [pii]. PubMed PMID: 15180965.

50. Hunter CA. New IL-12-family members: IL-23 and IL-27, cytokines with divergent functions. Nat Rev Immunol. 2005;5(7):521-31. Epub 2005/07/07. doi: nri1648 [pii] 10.1038/nri1648. PubMed PMID: 15999093.

51. Zolkiewski M. A camel passes through the eye of a needle: protein unfolding activity of Clp ATPases. Mol Microbiol. 2006;61(5):1094-100. Epub 2006/08/02. doi: MMI5309 [pii] 10.1111/j.1365-2958.2006.05309.x. PubMed PMID: 16879409; PubMed Central PMCID: PMC1852505.

52. Chastanet A, Derre I, Nair S, Msadek T. clpB, a novel member of the Listeria monocytogenes CtsR regulon, is involved in virulence but not in general stress tolerance. J Bacteriol. 2004;186(4):1165-74. Epub 2004/02/06. PubMed PMID: 14762012; PubMed Central PMCID: PMC344206.

53. Lourdault K, Cerqueira GM, Wunder EA, Jr., Picardeau M. Inactivation of clpB in the pathogen Leptospira interrogans reduces virulence and resistance to stress conditions. Infect Immun. 2011;79(9):3711-7. Epub 2011/07/07. doi: IAI.05168-11 [pii] 10.1128/IAI.05168-11. PubMed PMID: 21730091; PubMed Central PMCID: PMC3165490.

54. Capestany CA, Tribble GD, Maeda K, Demuth DR, Lamont RJ. Role of the Clp system in stress tolerance, Biofilm formation, and intracellular invasion in Porphyromonas gingivalis. Journal of Bacteriology. 2008;190(4):1436-46. doi: Doi 10.1128/Jb.01632-07. PubMed PMID: ISI:000253005800033.

55. Kannan TR, Musatovova O, Gowda P, Baseman JB. Characterization of a unique ClpB protein of Mycoplasma pneumoniae and its impact on growth. Infect Immun. 2008;76(11):5082-92. Epub 2008/09/10. doi: IAI.00698-08 [pii] 10.1128/IAI.00698-08. PubMed PMID: 18779336; PubMed Central PMCID: PMC2573332.

56. Turner AK, Lovell MA, Hulme SD, Zhang-Barber L, Barrow PA. Identification of Salmonella typhimurium genes required for colonization of the chicken alimentary tract and for virulence in newly hatched chicks. Infect Immun. 1998;66(5):2099-106. Epub 1998/05/09. PubMed PMID: 9573095; PubMed Central PMCID: PMC108169.

# CHAPTER 3

# IFN-γ, BUT NOT IL-17A, IS REQUIRED FOR SURVIVAL DURING SECONDARY PULMONARY *FRANCISELLA TULARENSIS* LVS INFECTION[1]

## OVERVIEW

IL-17 production by T cells is critical following intranasal inoculation with the highly pathogenic bacterium, *Francisella tularensis* Live Vaccine Strain (LVS). In the absence of IL-17, mice have higher bacterial burdens and produce less IFN-γ, a cytokine required for *F. tularensis* clearance. While the importance of both Th1 and Th17 cells during primary intranasal *F. tularensis* infection is clear, the importance of these cells isn't understood during the memory response. Using intracellular cytokine staining, we measured the number of $CD4^+$ T cells producing IFN-γ or IL-17 in vaccinated mice on day 4 of the secondary response. Because there were so few bacteria in the spleen after secondary challenge, we also measured the local immune response in the lung where bacterial loads were higher. Although there was a robust Th1 response, Th17 cells are not present at higher numbers in the lungs of vaccinated mice compared to unvaccinated mice. These data show that the lung is the dominant site of the secondary infection and the immune response. Furthermore, these data suggest Th17 cells are not required for survival after secondary challenge. To further investigate the importance of IFN-γ and IL-17 during the secondary response to *F. tularensis*, we depleted either IFN-γ or IL-17 in vivo using monoclonal antibody treatment. Vaccinated mice treated with IFN-γ depleting antibody lost more weight and had higher bacterial burdens compared to vaccinated mice treated with isotype control antibody. In contrast, treatment with anti-IL-17 antibody did not alter

[1] Contributing authors: Lydia Barrigan, Shraddha Tuladhar, Deepa Jamwal, and Jeffrey Frelinger

weight loss profiles or bacterial burdens compared to mice treated with isotype control antibody. Altogether, these results suggest that IFN-γ is required both during primary and secondary intranasal *F. tularensis* infection. IL-17, on the other hand, is critical during the primary response to intranasal *F. tularensis* but dispensable during the secondary response.

## INTRODUCTION

Tularemia, or rabbit fever, is caused by the gram negative coccobacillus, *Francisella tularensis*. *Francisella* is highly pathogenic and causes severe disease in humans, leading the U.S. government to categorize *Francisella* as a Tier 1 Select Agent (1). While the CDC reports approximately 120 cases of naturally-acquired tularemia each year in the U.S., *Francisella* has been used as the infectious agent in bioweapons and continues to pose a realistic threat today (2-4). The potential of a bioterrorism attack utilizing *F. tularensis* as the infection agent underscores the need for an effective vaccine. Although the *Francisella* Live Vaccine Strain (LVS) was widely used as a vaccine in Europe where tularemia is much more common, the mechanisms of attenuation are undefined, preventing the FDA from licensing this vaccine in the U.S. (1).

Three different strains of *Francisella* are commonly studied in the laboratory. *F. tularensis* subsp. *tularensis* SchuS4 (SchuS4) is a highly virulent Type A strain. As few as 10 organisms can cause severe disease in humans with a 30-60% fatality rate if antibiotics are not administered (5). The $LD_{100}$ in mice is <10 CFU for all inoculation routes and mice succumb to infection within 5-6 days (6, 7). SchuS4 is handled at BSL-3 due to its ease of aersolization and low infectious dose in humans. Because unmanipulated mice succumb to SchuS4 infection before the development of an adaptive immune response, *F. tularensis* subsp. *holartica* LVS is used to study components of adaptive immunity. LVS is less

virulent in both mouse and man; the $LD_{50}$ for mice varies widely depending on the inoculation route. The $LD_{50}$ for intraperitoneal inoculation is <1 CFU, intranasal inoculation is $10^3$ CFU, and intradermal inoculation has an $LD_{50}$ of $>10^5$ CFU (8). The final commonly studied strain of *Francisella* is *F. novicida* U112 (U112). U112 is avirulent in immunocompetent humans but highly virulent in mice with a low infectious dose ($LD_{100}$ < 10 CFU) and rapid death similar to SchuS4.

The T cell response is required to mediate *F. tularensis* clearance because the bacterium lives within infected cells (9). IFN-γ is required to control LVS infection. IFN-γ depletion increases systemic bacterial burdens and mice deficient in IFN-γ succumb to an otherwise sublethal LVS infection for wild-type mice (10, 11). Treatment with exogenous recombinant IFN-γ decreases bacterial burdens further confirming the importance of IFN-γ for bacterial control (12). The route of primary infection influences the T cell response. When B6 mice are inoculated intranasally with LVS, there are significantly fewer responding T cells producing IFN-γ in the lung compared to intradermally inoculated mice even though bacterial burdens (i.e. antigen loads) are similar early after infection (13). The increased IFN-γ production observed in intradermally inoculated mice correlates with faster bacterial clearance compared to mice inoculated intranasally. Intranasal inoculation with LVS also induces expansion of lung Th17 cells, a response not seen in intradermally inoculated mice (13). IL-17A is also important for bacterial control following intranasal inoculation as $IL17^{-/-}$ mice have increased lung LVS burdens compared to wild-type B6 mice (14). In primary infections with LVS, treatment with IL-17A depleting antibody increases lung bacterial burdens compared to mice treated with isotype control antibody and decreases the mean time to death (14, 15).

Previous infection with LVS or the attenuated mutant, LVS *clpB*, provides 100% protection against lethal LVS challenge and T cells are required for the development of protective immunity (9, 16). While the importance of IFN-γ and IL-17A during primary pneumonic tularemia are clear (10-12, 14, 15), the nature of the T cell response during secondary pneumonic tularemia remains unknown. We sought to determine whether IFN-γ producing $CD4^+$ and $CD8^+$ T cells and/or Th17 cells are elicited during the secondary response using intracellular cytokine staining. We further determined if IFN-γ and/or IL-17A are important during the secondary response using antibody depletion. Additionally, we were interested in comparing the memory responses in LVS and LVS *clpB* vaccinated mice because both strains completely protected during a lethal challenge, despite differences in the primary T cell response. We found LVS and LVS *clpB* vaccinated mice have nearly identical T cell responses during a secondary infection and that IFN-γ is absolutely required for survival during re-challenge whereas IL-17A is dispensable. Understanding what T cell responses are crucial for protective memory will inform further vaccine development.

## MATERIALS AND METHODS

### Bacteria

The live vaccine strain of *Francisella tularensis* subsp. *holartica* (LVS) was obtained from the CDC (Atlanta, GA). Bacteria were grown at 37˚C on chocolate agar supplemented with 1% IsoVitalex (Becton-Dickinson). To prepare bacterial inoculations, bacteria were removed from a lawn grown on chocolate agar and resuspended in sterile PBS at an $OD_{600}$=1 (equivalent to $1x10^{10}$ CFU/mL). Appropriate dilutions were made in sterile PBS to obtain the desired bacterial dose. The actual number of viable bacteria was determined by serial

dilution and plating on chocolate agar. The LVS *clpB* (FTL_0094) deletion strain was generated using the suicide vector pMP812 (17) containing an amplified region of *clpB*.

**Mice**

C57Bl/6J (B6) and B6.SJL-*Ptprc*$^{a}$*Pepc*$^{b}$/BoyJ (B6-CD45.1) mice were obtained from The Jackson Laboratory (Bar Harbor, ME). All mice were housed in specific-pathogen free conditions at the University of Arizona in accordance with the Institutional Animal Care and Use Committee (IACUC). Female B6 mice used for infections were between 7 to 12 weeks of age.

**Inoculation of Mice**

Mice were anesthetized with 575 mg/kg tribromomethanol (Avertin) (Sigma) administered intraperitoneally. Mice were then intranasally inoculated with 5 x $10^2$ CFU LVS or 5x$10^4$ CFU LVS *clpB* suspended in 50 µL PBS. Mice were weighed daily following all inoculations. For lethal LVS challenge experiments, mice were anesthetized with 0.25 mL of 7.5 mg/mL ketamine and 0.5 mg/mL xylazine cocktail in PBS. Mice were then intranasally inoculated with 5x$10^3$ CFU (5 x $LD_{50}$) LVS in 50 µL PBS. Mice were weighed daily following all inoculations. Mice were sacrificed if they lost more than 25% of their starting weight as indicated in our IACUC protocol.

**Determination of serum IgG titers**

LVS lysate was made by lysing mid-log phase LVS grown in brain heart infusion (BHI) broth using RIPA buffer. The amount of protein in the LVS lysate was quantified using a Bio-Rad DC Protein Assay (Bio-Rad). High binding ELISA plates (Costar) were coated overnight with 0.25 µg/well LVS lysate in 100 mM sodium carbonate/bicarbonate buffer (pH 9.6). Coated plates were washed with 1x PBS containing 0.05% Tween-20 and

then blocked with 5% BSA (w/v) in PBS for 1 hour at room temperature. 100 µL/well of 1:2 serial dilutions of mouse serum starting at 1:100 was added to the plate and incubated at room temperature for 2 hours. Plates were then washed with 1x PBS containing 0.05% Tween-20. 100 µL/well of anti-mouse IgG conjugated to alkaline phosphatase (1:1000) (Life) was added to the plate and incubated at room temperature for 1 hour. Plates were washed with 1x PBS containing 0.05% Tween-20. 100 µL/well para –Nitrophenylphosphate (pNpp) (Life) was added to the plate and incubated for 30 minutes at room temperature. $A_{405}$ and $A_{570}$ were measured using a plate reader (Molecular Devices). $A_{570}$ was subtracted from $A_{405}$ to normalize and half-maximal titers were determined for each mouse. Each serum sample was analyzed in duplicate.

**Western blots detecting LVS specific antibodies**

10, 20, and 40 µg of LVS lysate were loaded in a 4-12% Bis-Tris SDS polyacrylamide gel (Life). A molecular weight marker ranging from 10-250 kDa was also loaded on the gel (Licor). Proteins were separated by subjecting the gel to 150 volts for approximately 2 hours. Proteins were then transferred onto a PVDF membrane by subjecting the transfer apparatus to 25 volts for 60 minutes. The membrane was then blocked with 5% BSA in TBST buffer (w/v) for 1 hour at room temperature. Mouse sera from naïve, LVS, or LVS *clpB* infected mice collected 28 days post-inoculation was diluted 1:2000 in 5% BSA in TBST buffer (w/v) and incubated on the membrane overnight at 4°C. The membrane was then washed thoroughly with TBST buffer. Goat anti-mouse IgG conjugated to IRDye 800CW (Licor) was diluted 1:5000 in 5% milk in TBST and incubated with the membrane for 1 hour at room temperature. The membrane was then washed thoroughly and then bands were visualized using the Odyssey Infrared Imaging System (Licor).

**Determination of bacterial burdens**

Spleens, livers, and lungs were homogenized in sterile PBS using a Biojector (Bioject) as previously described (13). 10-fold serial dilutions were made and plated on chocolate agar. Resulting colonies were counted 72 hours later. The limit of detection is 50 CFU per organ.

**Collection of spleen and lung cells**

Spleens were harvested from mice and made into a single cell suspension. Red blood cells were lysed using ammonium chloride-potassium carbonate lysis buffer. Lungs were perfused with PBS to remove blood and then finely minced. Minced lung was placed in 10 mL of digestion buffer containing 0.5 mg/mL collagenase I (Worthington Biochemical), 0.02 mg/mL DNase (Sigma), and 125 U/mL elastase (Worthington Biochemical) in RPMI1640 (HyClone). Lungs were digested for 30 minutes at 37˚C and then vigorously pipetted prior to filtering through a 100 μM filter. Mononuclear cells were isolated from the single cell suspension by density gradient centrifugation over Lympholyte M (Cedarlane Labs). Viable cells from spleen and lung were determined by trypan blue exclusion using a hemacytometer.

**Antibodies**

The following directly conjugated antibodies were utilized for flow cytometry analysis: CD3 AF488 (Clone 145-2C11, eBioscience); CD4 AF700 (Clone GK1.5, Biolegend); CD8a V500 (Clone 53-6.7, BD Biosciences); CD45.1 PE-Cy7 (Clone A20, Biolegend); TCR γδ PerCP-Cy5.5 (Clone GL3, Biolegend); IFN-γ PE (Clone XMG1.2, BD Biosciences); IL-17A AF647 (Clone TC11-18H10.1, Biolegend); CD11b Pacific Blue (Clone M1/70, Biolegend); CD11c Pacific Blue (Clone N418, Biolegend); CD19 Pacific Blue (Clone 6D5, Biolegend); F4/80 Pacific Blue (Clone BM8, Biolegend); GR-1 (Ly-6G) eFluor

450 (Clone RB6-8C5, eBioscience); NK1.1 Pacific Blue (Clone PK136, Biolegend). All antibodies were titrated on normal B6 splenocytes prior to use.

**Intracellular cytokine staining**

Splenocytes from B6-CD45.1 were used as antigen presenting cells. B6-CD45.1 cells were added at $2x10^6$/well in a 24 well plate or $0.5x10^6$/well in a 48 well plate and infected with LVS at an MOI of 200:1 or mock infected. Two hours post-infection, the media was removed and 5 μg/mL gentamicin was added to kill any extracellular bacteria. Splenocytes were cultured overnight in the presence of gentamicin to allow antigen processing and presentation. Prior to co-culture with cells isolated from infected mice, antigen presenting cells were washed extensively to remove any cytokine or $PGE_2$ that could interfere with the co-culture. Cells isolated from mice were co-cultured at a 1:1 ratio with infected or mock infected splenocytes for 24 hours. During the last 4 hours of culture, 10 μg/mL Brefeldin A (Sigma) was added to each well to stop cytokine secretion. Cells were removed from the plate and stained with Pacific Blue succimidyl ester (Invitrogen) to distinguish live and dead cells. Cells were then stained with antibodies for surface markers. Following fixation and permeabilization of the cells, cells were stained for IFN-γ and IL-17A. Cells were washed extensively after each staining step to remove residual unbound antibody.

**Gating Strategy for T cell Analysis**

The gating scheme is shown in figure 1. Single cells were discriminated from doublets by plotting side scatter linear versus side scatter area. Cells were then selected by plotting side scatter area versus forward scatter area. Live $CD3^+$ T cells were then selected by plotting CD3 versus the Pacific Blue channel which included the live/dead stain and markers for antigen presenting cells. From the $CD3^+$ gate, $CD4^+$ and $CD8^+$ T cells were

selected. Gates for IFN-γ and IL-17A positive cells were set based on isotype control staining. Change in mean fluorescent intensity (ΔMFI) for each sample was determined by subtracting the cytokine negative population from the cytokine positive population. FlowJo v7.6 (Treestar) was used for all flow cytometry analysis.

**Depletion of IFN-γ or IL-17A**

Anti-IFN-γ (clone XMG1.2) was a generous gift from Mary Ann Accavitti-Loper (University of Alabama- Birmingham). Rat IgG1 isotype control antibody (clone HRPN), anti-IL-17A (clone 17F3), and mouse IgG1 isotype control antibody (clone MOPC-21) were purchased from BioXCell (West Lebanon, NH). Mice were administered 500 μg of anti-IFN-γ or rat IgG1 isotype control or 100 ug of anti-IL-17A or mouse IgG1 in 200 μL PBS via intraperitoneal injection on days 0, 2, and 4 post-inoculation.

**Luminex analysis**

A multiplex luminex bead-based approach was used to quantify cytokines/chemokines in BAL fluid or clarified tissue homogenate. A 20-analyte assay panel was performed according to the manufacturer's protocol (Invitrogen) using a BioPlex array reader (Bio-Rad Laboratories). Using integrated cytokine/chemokine standard curves, the assay reports pg/mL of the following analytes: FGF basic, GM-CSF, IFN-γ, IL-1α, IL-1β, IL-2, IL-4, IL-5, IL-6, IL-10, IL-12 (p40/p70), IL-13, IL-17, KC, MCP-1, MIG, MIP-1α, TNF-α, and VEGF. A five-parameter non-linear logistic regression model was used to establish standard curve and to estimate the probability of occurrence of a concentration at a given point. Standard outliers were removed from the analysis if the observed/expected % recovery was outside of the acceptable limits (70-130%). Upper and lower levels of quantification were determined by the BioPlex Manager software based on goodness of fit

and percent recovery. Calculated pg/mL for experimental specimens were multiplied by the inherent assay dilution factor (df=2) and reported as final observed pg/mL.

**Statistical analysis**

Statistical significance of flow cytometry data was determined using a Kruskal-Wallis with Dunn's post-test. Bacterial burdens were log transformed and then a one-way ANOVA with Tukey's post-test was applied. A Mann-Whitney test was used for IgG titer data. GraphPad Prism (v5.04) was used for analysis. Error bars show standard error of the mean. Significance levels are indicated as follows: * $p < 0.05$; ** $p < 0.01$, *** $p < 0.001$, **** $p < 0.0001$.

## RESULTS

**Do differences in the adaptive immune response to LVS and LVS *clpB* translate to differences in the memory response?**

We have previously shown that LVS *clpB* is attenuated, not because of an intrinsic growth defect, but instead by inducing altered innate and adaptive immunity (16). The kinetics of the T cell response during primary infection with LVS and LVS *clpB* differs (16). To briefly summarize, LVS and LVS *clpB* infected mice have similar immune responses on day 7 post-inoculation, i.e. the total spleen and lung cellularity are similar as are the number of $CD4^+$ T cells producing IFN-γ or IL-17A or $CD8^+$ T cells producing IFN-γ (Chapter 2 figures 24-26). Additionally, the amount of cytokine produced by responding T cells is similar on day 7 post-inoculation as measured by delta mean fluorescence intensity (ΔMFI) (Chapter 2 figures 27 and 29). The immune responses between LVS and LVS *clpB* infected mice differ 10 days post-inoculation. LVS infected mice have significantly higher spleen and

lung cellularity on day 10 post-inoculation than LVS *clpB* infection (Chapter 2 figure 24). The differences in cellularity are likely a consequence of immune response contraction because LVS *clpB* was nearly cleared from the host on day 10 post-inoculation (Chapter 2 figure 4). Although there is a significant decrease in the number of T cells responding in LVS *clpB* infected mice, the responding T cells produced significantly more IFN-γ and IL-17A as measured by ΔMFI (Chapter 2 figures 25-27, 29-31). Despite LVS *clpB*'s attenuation, inoculation with this strain induced a robust adaptive immune response that was required for bacterial clearance (Chapter 2 figure 23). Previous infection with LVS or LVS *clpB* induced a protective immune response during lethal LVS challenge early (day 28) or late (day 120) post-initial infection (Chapter 2 figures 9, 10). We next sought to determine whether the secondary immune response was similar in LVS and LVS *clpB* vaccinated mice.

**LVS and LVS *clpB* infected mice have similar antibody responses**

B cell deficient mice are not more susceptible to primary infection with LVS, however they are 100-fold more susceptible during secondary infection (18). Therefore, while differences in the primary antibody response to LVS or LVS *clpB* were unlikely to affect bacterial clearance during the first infection, differences in the antibody response may impact clearance, and therefore survival, during a second infection. We therefore determined anti-*Francisella* IgG titers in LVS and LVS clpB infected mice 28 and 120 days post-inoculation. Mice were inoculated with $5x10^2$ CFU LVS or $5x10^4$ CFU LVS *clpB*. On days 28 and 120 post-inoculation, sera was obtained from naïve, LVS or LVS *clpB* vaccinated mice and half-maximal IgG titers were determined by ELISA. LVS and LVS *clpB* vaccinated mice had similar IgG titers on day 28 or day 120 post-inoculation (figure 2A-D). Naïve mouse sera did not contain LVS-specific IgG antibodies (figure 2A, C). In addition to

similar IgG titers, sera from LVS and LVS *clpB* infected mice produced similar, but not identical, banding patterns when used to probe LVS lysate indicating infection with LVS or LVS *clpB* results in recognition of similar *Francisella* antigens (figure 2E). Together, these data indicate that infection with either LVS or LVS *clpB* elicits a similar antibody response in terms of total IgG levels as well as antibody specificity. Additionally, these data suggested that survival of LVS and LVS *clpB* vaccinated mice during lethal LVS challenge is not a consequence of a more robust B cell response in one vaccinated group compared to the other.

**Previous infection with LVS and LVS *clpB* decreases bacterial burdens during secondary infection**

We next examined the T cell response in LVS and LVS *clpB* vaccinated mice to determine whether differences in the primary response translated to differences in the memory response. We chose to look at the T cell memory response on day 4 post-rechallenge because the secondary response occurs more rapidly than the primary response and this time point was also before unvaccinated mice began to succumb to infection (16). We first determined bacterial burdens in the spleen, liver, and lung on day 4 post-rechallenge to quantitate the amount of antigen present in each tissue. Mice were inoculated with $5x10^2$ CFU LVS or $5x10^4$ CFU LVS *clpB* and then challenged with $5x10^3$ CFU LVS 120 days after the initial infection. Age-matched unvaccinated mice were also inoculated with $5x10^3$ CFU LVS. As expected, bacterial burdens were significantly lower in the spleen, liver, and lung of LVS and LVS *clpB* vaccinated mice compared to unvaccinated mice (figure 3A-C). These data indicate that prior infection with LVS or LVS *clpB* elicits an immune response that

controls bacterial growth at the site of primary infection (lung) as well as distal sites (spleen and liver).

**Spleen and lung cellularity is similar irrespective of vaccination status**

We next examined the secondary T cell response in LVS or LVS *clpB* vaccinated mice. Mice were inoculated with $5x10^2$ CFU LVS or $5x10^4$ CFU LVS *clpB* and then challenged with $5x10^3$ CFU LVS 120 days after the initial infection. Age-matched unvaccinated mice were also inoculated with $5x10^3$ CFU LVS. On day 4 post-re-challenge, mice were sacrificed and the number of live cells in the spleen and lung were determined by trypan blue exclusion. Unvaccinated, LVS vaccinated, and LVS *clpB* vaccinated mice had similar spleen and lung cellularity (figure 4). It is likely that the cellular composition of unvaccinated and vaccinated mice is different; however, quantification of individual cell populations using flow cytometry was not performed.

**LVS and LVS *clpB* vaccinated mice have an increased lung IFN-γ-mediated immune response compared to unvaccinated mice**

IFN-$\gamma^+$ $CD4^+$ and $CD8^+$ T cells respond in the lung during the primary immune response to LVS and LVS *clpB* (16). We next determined whether memory $CD4^+$ and/or $CD8^+$ T cells were responding during the secondary infection in LVS and LVS *clpB* vaccinated mice by quantifying the number of $CD4^+$ and $CD8^+$ T cells producing IFN-γ in the lung on day 4 post-re-challenge. LVS and LVS *clpB* vaccinated mice had significantly more IFN-γ producing $CD4^+$ and $CD8^+$ T cells than unvaccinated mice (figure 5A, B). There was no significant difference in the number of IFN-γ producing $CD4^+$ or $CD8^+$ T cells in the lungs of LVS or LVS *clpB* vaccinated mice during re-challenge. Additionally, responding $CD4^+$ and $CD8^+$ T cells from the lungs of LVS and LVS *clpB* vaccinated mice produced

significantly more IFN-γ as measured by ΔMFI compared to unvaccinated mice (figure 5C, D). The IFN-γ ΔMFI for $CD4^+$ and $CD8^+$ T cells from LVS and LVS *clpB* vaccinated mice were not significantly different. Together these data indicate that LVS or LVS *clpB* vaccination leads to a similar IFN-γ response in the lung during lethal re-challenge that is greater in magnitude than the IFN-γ response in unvaccinated mice.

**LVS and LVS *clpB* vaccinated mice have a similar lung IL-17A-mediated immune response compared to unvaccinated mice**

Primary infection with LVS and LVS *clpB* induces Th17 expansion in the lung (13, 16). We next examined whether memory Th17 cells were responding during re-challenge as we found for IFN-γ producing T cells (figure 5). Using ICS, we determined the number of Th17 cells in the lung on day 4 post-re-challenge and found similar numbers of Th17 cells irrespective of vaccination status (figure 6A). Additionally, IL-17A expression did not increase in vaccinated mice compared to unvaccinated mice as measured by ΔMFI (figure 6B). These data indicate that despite the importance of Th17 cells during the primary response, Th17 cells do not appear to be an important component of the memory response on day 4 post-re-challenge because the response in vaccinated mice is similar to unvaccinated mice.

**The secondary response is nearly absent in the spleens of LVS and LVS *clpB* vaccinated mice**

Bacterial burdens were near the detection limit in the spleen on day 4 post-re-challenge (figure 3A). It is possible that bacterial burdens were low in the spleen because there was a robust T cell response that controlled the infection. Alternatively, the robust T cell memory response in the lung could decrease bacterial dissemination to distal organs and

low antigen loads will not drive a local memory response. To distinguish between these two possibilities, we examined the secondary immune response in the spleen on day 4 post-re-challenge using ICS. Additionally, examination of the secondary response in the spleen would indicate whether the memory response was systemic or limited to the primary site of infection (lung). There were similar absolute numbers of IFN-γ producing $CD4^+$ or $CD8^+$ T cells in LVS or LVS *clpB* vaccinated mice compared to unvaccinated mice (figure 7A, B). IFN-γ ΔMFI was significantly higher in $CD4^+$ T cells from vaccinated mice compared to unvaccinated mice (figure 7C) but a significant increase in IFN-γ ΔMFI for $CD8^+$ T cells was not observed in vaccinated mice compared to unvaccinated mice (figure 7D).

Primary intranasal infection with LVS or LVS *clpB* does not elicit expansion of Th17 cells in the spleen (13, 16). Similarly, the absolute number of Th17 cells in the spleens of LVS or LVS *clpB* vaccinated mice was similar to unvaccinated mice (figure 8A). Additionally, IL-17A expression was not increased in vaccinated mice compared to unvaccinated mice as measured by ΔMFI (figure 8B). These data indicate that, like a primary infection with LVS or LVS clpB, Th17 cells are not involved in the immune response in the spleen.

Because we observed similar numbers of $CD4^+$ IFN-$\gamma^+$, $CD8^+$ IFN-$\gamma^+$, and Th17 cells in the spleens of vaccinated and unvaccinated mice on day 4 post-re-challenge, these data suggest that the low bacterial burdens were not a consequence of a robust T cell response. Instead, these data suggest that low bacterial burdens in the spleen did not drive splenic memory T cell expansion and that a systemic immune response does not occur following intranasal secondary challenge of immune mice.

**IFN-γ production is required during the secondary response to LVS**

The secondary response in LVS and LVS *clpB* vaccinated mice induced IFN-γ producing $CD4^+$ and $CD8^+$ T cells in the lungs as determined by ICS. To determine whether IFN-γ was required during the secondary response, we treated mice with 500 μg XMG1.2 (anti-IFN-γ) or rat IgG1 isotype control on days 0, 2, and 4 post-re-challenge. On day 0 mice were intranasally inoculated with $5x10^3$ CFU LVS, approximately 1 hour after antibody treatment. Mice were weighed daily and weight loss reported as % of starting weight (figure 9A). Weight loss is monitored because we have found it is a nearly perfect indicator of clinical status. The weight loss profiles of LVS and LVS *clpB* vaccinated mice receiving anti-IFN-γ was similar to unvaccinated mice receiving either anti-IFN-γ or isotype control (figure 9A). LVS or LVS *clpB* vaccinated mice receiving isotype control antibody did not lose as much weight as those receiving anti-IFN-γ and had begun to regain lost weight on day 5 post-re-challenge (figure 9A) indicating they are recovering from their infection and will survive. We sacrificed all vaccinated mice receiving isotype control antibody on day 6 post-re-challenge to determine bacterial burdens and therefore could not explicitly demonstrate that these mice would survive the lethal challenge. However, the weight loss profiles of vaccinated mice receiving isotype control antibody are nearly identical to untreated vaccinated mice in Barrigan, et al that did recover all lost weight and survive the same lethal challenge dose (16). Therefore, we are confident that the isotype control treated vaccinated mice would have survived the lethal challenge.

We next examined bacterial burdens in the spleen, liver, and lung on day 6 post-re-challenge following administration of anti-IFN-γ or isotype control antibody. We selected day 6 because unvaccinated mice begin to succumb to the lethal LVS inoculation at this time

point. LVS and LVS *clpB* vaccinated mice receiving anti-IFN-γ had significantly higher bacterial burdens than vaccinated mice receiving isotype control antibody in the spleen, liver, and lung (figure 9B-D). Vaccinated mice depleted of IFN-γ not only have higher bacterial burdens than vaccinated mice receiving isotype control antibody, they also have similar bacterial burdens as unvaccinated mice receiving anti-IFN-γ (figure 9B-D). Unvaccinated mice receiving anti-IFN-γ had significantly higher bacterial burdens in all organs tested compared to unvaccinated mice receiving isotype control antibody and two of the unvaccinated mice administered anti-IFN-γ succumbed to the infection on day 5 post-inoculation (figure 9B-D). All mice receiving anti-IFN-γ have lung IFN-γ levels near the limit of detection (21.6 pg/mL) while mice receiving isotype control antibody have between 1-5 ng/mL IFN-γ concentrations in the lung as measured by Luminex (data not shown) confirming successful depletion of IFN-γ. These data indicate that IFN-γ production is critical during an intranasal secondary infection just as has previously been shown for primary infections with LVS (10, 11).

**IL-17A is dispensable during the secondary response to LVS**

Lethal secondary infection in LVS or LVS *clpB* vaccinated mice did not elicit a Th17 response that was greater in magnitude compared to unvaccinated mice as determined by ICS. We therefore hypothesized that IL-17A was not required for protection during secondary infection. To test this hypothesis, we treated unvaccinated, LVS vaccinated, or LVS *clpB* vaccinated mice with 100 μg 17F3 (anti-IL-17A) or mouse IgG1 isotype control on day 0, 2, and 4 post-rechallenge. Mice were then intranasally inoculated with $5x10^3$ CFU LVS. Mice were weighed daily and weight loss was reported as % of starting weight (figure 10A). The weight loss profiles of LVS and LVS *clpB* vaccinated mice were identical

regardless of treatment with anti-IL-17A or isotype control (figure 10A). Unvaccinated mice also had identical weight loss profiles irrespective of antibody treatment (figure 10A). We then determined bacterial burdens in the spleen, liver, and lung on day 6 post-rechallenge. LVS and LVS *clpB* vaccinated mice had spleen and liver bacterial burdens near the limit of detection for both treatment groups (figure 10B-C). In the lung, bacterial burdens were similar in LVS and LVS *clpB* vaccinated mice receiving anti-IL-17A compared to isotype control (figure 10D). Bacterial burdens in the spleen, liver, and lung of unvaccinated mice were similar irrespective of antibody depletion (figure 10B-D). Luminex analysis of clarified tissue homogenates determined IL-17A levels are below the detection limit in the spleen and lungs of mice receiving anti-IL-17A and isotype control antibody, irrespective of vaccination status (data not shown). To confirm the Luminex results, we tested the clarified lung homogenate by IL-17A ELISA and found vaccinated mice had similar levels of IL-17A (70-80 pg/mL) irrespective of antibody treatment. Unvaccinated mice had slightly higher IL-17A levels (130-150 pg/mL), but again there was no difference in concentration between anti-IL-17A and isotype treated mice. These data indicate IL-17A is produced at low levels in our model during the secondary infection, further supporting our conclusion that IL-17A is dispensable during a recall response.

Altogether, our results indicate that the secondary immune response in LVS and LVS *clpB* vaccinated mice is nearly identical in terms of the absolute numbers of responding cells as well as the amount of cytokine produced. These data indicate that primary infection with attenuated LVS *clpB* primes the immune system equivalently as LVS despite eliciting an altered primary response (16). We also determined the importance of IFN-γ and IL-17A

during the secondary response and found IL-17A is dispensable while IFN-γ is absolutely required for survival during intranasal re-challenge.

## DISCUSSION

Primary intranasal inoculation with LVS or LVS *clpB* elicits a robust IFN-γ and IL-17A response in the lungs of infected mice (16). Both of these cytokines are critical for controlling the primary infection. IFN-$\gamma^{-/-}$ and IL-$17^{-/-}$ mice have increased bacterial burdens compared to wild-type mice and antibody depletion of either IFN-γ or IL-17A also increases bacterial burdens (10-12, 14, 15). While the roles of IFN-γ and IL-17A during primary pneumonic tularemia are clear, it remains unknown whether these cytokines are also important during secondary infection.

**Route of primary infection influences survival during lethal secondary infection**

Intradermal vaccination with LVS does not provide protection during lethal aerosol challenge with SchuS4 or another lethal Type A strain (19, 20). In order to achieve protective immunity for future intranasal challenge, mice must be inoculated intranasally (19, 21). Intradermal inoculation with LVS leads to a robust IFN-γ response in the lung by both $CD4^+$ and $CD8^+$ T cells that is greater in magnitude than mice inoculated intranasally (13). Despite eliciting a robust IFN-γ mediated immune response in the lung, intradermally inoculated mice are not protected during lethal intranasal challenge with SchuS4 (21). Because Th17 cells expand in the lung following LVS intranasal inoculation but not intradermal inoculation (13), one could hypothesize that memory Th17 cells are critical to the development of protective immunity in the lung. Th17 cells are a critical component of the primary immune response to *Francisella* and other pathogens ((14) and reviewed in (22)).

**The T cell response on day 4 post-re-challenge is dominated by IFN-γ producing T cells**

Using ICS, we identified IFN-γ and IL-17A producing T cells on day 4 post-re-challenge. In the lung, there were significantly more $CD4^+$ and $CD8^+$ T cells producing IFN-γ in LVS and LVS *clpB* vaccinated mice compared to unvaccinated mice. ΔMFI was used as a measure of how much IFN-γ is produced per cell, LVS and LVS *clpB* vaccinated mice have significantly higher IFN-γ ΔMFIs for $CD4^+$ and $CD8^+$ T cells compared to unvaccinated mice. Clearly, previous infection with either LVS or LVS *clpB* primes both $CD4^+$ and $CD8^+$ T cells that produce IFN-γ in the lung upon re-challenge. We also quantified the number of Th17 cells in the lungs and although there is a trend toward an increased number of Th17 cells in LVS or LVS *clpB* vaccinated mice compared to unvaccinated mice, it does not reach statistical significance. The IL-17A ΔMFIs were also not increased in LVS or LVS *clpB* vaccinated mice compared to unvaccinated mice. These data suggest that Th17 cells do not play a critical role in the lung during secondary infection with LVS. Instead, responding T cells in the lung produce IFN-γ.

**IFN-γ depletion in vaccinated mice worsens disease and increases bacterial burdens**

The intracellular cytokine staining experiments demonstrate that the secondary response to an intranasal infection is mediated by both $CD4^+$ and $CD8^+$ T cells producing IFN-γ. Although Th17 cells in the lung are an important component of the lung's primary immune response (13, 15, 23), this cell subset does not expand during secondary infection, suggesting that these cells are dispensable. To further interrogate the importance of IFN-γ and IL-17A during secondary infection, we antibody depleted each cytokine during secondary infection. LVS and LVS *clpB* vaccinated mice depleted of IFN-γ had significantly higher bacterial burdens and experienced increased weight loss compared to mice receiving

isotype antibody during re-challenge. IFN-γ depletion in vaccinated mice caused them to behave like unvaccinated mice for both experimental read-outs. This result demonstrated that IFN-γ is absolutely required for protective immunity during a secondary intranasal infection. The requirement of IFN-γ during secondary infection has also been shown using several routes of LVS vaccination and then lethal challenge with LVS, SchuS4, or another Type A strain (19, 24, 25).

**IL-17A depletion in vaccinated mice does not alter disease course or increase bacterial burdens**

Depletion of IL-17A had no impact on weight loss in LVS and LVS *clpB* vaccinated mice compared to mice treated with isotype control antibody. IL-17A depletion in LVS and LVS *clpB* vaccinated mice also did not alter bacterial burdens suggesting that IL-17A is dispensable for bacterial control during the secondary response. Surprisingly, we did not observe an increase in bacterial burdens or weight loss profiles for unvaccinated mice receiving IL-17A depleting antibody compared to mice receiving isotype control antibody as other groups have shown using the very similar depletion regimens (14, 15). This could suggest that the depletion antibody we used was not effective. To test whether the anti-IL-17A antibody could bind IL-17A, we performed an in vitro depletion experiment and found the antibody was capable of depleting IL-17A. Additionally, we determined the concentration of anti-IL-17A and found the concentration we determined was almost identical to the one reported by the vendor. Together, these data suggest the anti-IL-17A antibody was functional and should bind IL-17A in vivo. Additionally, the dose administered to the mice was correct based on independent verification of the antibody concentration.

Because we have ruled out non-functional antibody, there are several possible alternative explanations for the observed result where naïve mice do not have increased bacterial burdens upon IL-17A depletion. First, we used a different inoculation dose and delivery route (5000 CFU intranasally versus 1000 CFU intratracheally (14)). Second, the unvaccinated mice were age matched with the vaccinated mice and were 7-8 months old when they were inoculated while the other groups used young (6-8 weeks old) mice (14, 15). Finally, not all laboratory LVS stocks are identical thereby raising the possibility that slight differences in the infecting strain could affect virulence and/or impact the immune response. We could test the function of the in-hand depleting antibody by treating young mice during a primary LVS infection to recapitulate experiments described by Lin, et al and Markel, et al (15, 23). We confirmed cytokine depletion by clarifying tissue homogenates used to determine bacterial burdens and subjecting these samples to Luminex analysis. IL-17A levels were below detection limit for mice receiving IL-17A depleting antibody or isotype control. These data indicate there was little IL-17A present in the lung irrespective of vaccination status and therefore little antigen for the anti-IL-17A antibody to deplete. We also tested the clarified tissue homogenates by ELISA for a more sensitive determination of IL-17A concentration and found similar IL-17A concentrations in vaccinated mice irrespective of antibody treatment. Unvaccinated mice had slightly higher IL-17A concentrations than the vaccinated mice (2-fold), but there were no differences between anti-IL-17A and isotype control treatment. We confirmed the antibody was functional and administered at the desired dose therefore, little IL-17A was produced in the lung of unvaccinated or vaccinated mice.

During lethal SchuS4 secondary challenge following intradermal vaccination with SchuS4 *clpB*, high levels of IL-17A are detectable in the lung during secondary aerosol infection and high IL-17 levels correlate with protection (26). However, depletion of IL-17A did not significantly increase bacterial burdens compared to mice given isotype control antibody, suggesting this cytokine is not necessary for protective immunity in our experiments (26). The authors did not examine whether IFN-γ was required for protection despite also detecting this cytokine at high levels in the lung and also finding it correlated with protection (26). The primary T cell response to SchuS4 cannot be described in unmanipulated mice because they rapidly succumb to infection. The Bosio laboratory has developed a convalescent model of SchuS4 infection where mice are intraperitoneally administered levofloxacin daily from day 3 until day 14 post-inoculation (27). This model allowed the examination of the T cell response in the lung following primary intranasal inoculation with SchuS4. They detected IFN-$\gamma^+$ $CD4^+$ and $CD8^+$ T cells in the lung and spleens, with the peak response occurring on day 7 post-inoculation (27). IL-17A was undetectable in lung and spleen tissue homogenates, indicating this cytokine is not produced at detectable levels in this model of primary SchuS4 infection (27). More sensitive techniques, such as ICS, may allow the detection of Th17 cells and should be explored further in this model to determine whether primary intranasal inoculation with SchuS4 induces a Th17 response. This model could also be utilized to ask similar questions such as the requirement of IFN-γ and IL-17A for survival during secondary intranasal challenge with SchuS4.

**Does the expression of lung T cell homing receptors differ in mice vaccinated intranasally or intradermally?**

Combined, our ICS and IL-17A depletion data suggest Th17 cells are not contributing to protective immunity to re-infection in the lung. Because the presence of Th17 cells was a key difference during intranasal and intradermal primary infection, there must be an alternative explanation for why intradermally vaccinated mice are not protected during lethal intranasal challenge. It is possible that intradermally vaccinated mice are not protected during an intranasal challenge because the site of T cell priming is critical for expression of lung homing receptors. Therefore, despite the ability to produce large amounts of IFN-γ in response to *Francisella* antigens, T cells from intradermally vaccinated mice do not express the correct receptors to allow the T cells to traffic to the lung and control the secondary infection. While skin and gut T cell homing receptors are well characterized, lung T cell homing receptors are less well defined. Human lung resident memory T cells express the β1 integrin, VLA-1, and the addressin, PSGL-1 (28). It is unclear whether these homing receptors are expressed on mouse lung T cells. These questions would be easier to answer in a system with MHCI or MHCII tetramer to examine homing receptor expression by *Francisella*-specific T cells. We have identified an immunodominant $CD4^+$ epitope and collaborators are in the process of cloning and expressing $IA^b$ presenting the LpnA peptide that can be used to identify *Francisella*-specific $CD4^+$ T cells (29). A $CD8^+$ immunodominant epitope has not yet been identified. In the absence of MHCI and/or MHCII tetramer, we could identify antigen experienced T cells by $CD44^{hi}$ and IFN-γ or IL-17A expression. It is highly likely that $CD44^{hi}$ T cells producing either IFN-γ or IL-17A following re-stimulation by LVS infected APCs are responding to LVS infection. We could

then determine what homing receptor(s) these cells express and compare intranasally and intradermally infected mice.

**Conventional T cell transfer experiments using T cells from immune mice do not confer protection**

To identify T cell population(s) that are required for protective immunity, immunologists transfer purified cell populations into naïve mice and challenge with the pathogen of interest. Much effort has gone into developing a transfer system in a variety of *Francisella* models of infection (Karen Elkins, personal communication). The only published adoptive transfer system that has successfully protected naïve mice during rechallenge is intraperitoneal injection of T cells followed 2 hours later by intraperitoneal injection of bacteria (ref). While this system does distinguish between T cells isolated from naïve and immune mice, the peritoneum of the mouse has essentially been turned into a petri dish. This system doesn't require proper T cell trafficking as T cells encounter infected peritoneal macrophages and control the infection before bacteria can disseminate (Karen Elkins, personal communication). If conventional T cell transfers were successful in our *Francisella* model, experiments could be designed to identify cell types critical for secondary protection. For instance, $CD4^+$ and/or $CD8^+$ T cells could be purified from a specific tissue of an immune mouse and transferred into a naïve replete recipient that is subsequently lethally challenged. This type of experiment would allow questions of where resident memory is located following primary intranasal or intradermal inoculation.

Because conventional T cell transfers do not confer protection, yet those same T cells are required for protection if the mouse was left intact, we hypothesize the T cells fail to traffic properly following transfer. We could begin to address T cell trafficking questions by

transferring T cells from an immune mouse into a congenically-marked recipient. The presence of donor T cells in the spleen, lung, and lymph nodes would be determined by flow cytometry 24 hours after transfer. These experiments would be improved if we could identify *Francisella*-specific T cells using tetramer. This way, we would not be examining the ability of all T cells to home but could specifically address where *Francisella*-specific T cells traffic.

As an alternative approach to avoid issues of T cell trafficking during transfer experiments, we could use parabiosis experiments to determine whether T cells could migrate between a pair consisting of an immune and naïve mouse through existing architecture. For example, we predict that intransal inoculation of an immune mouse attached to a naïve mouse would confer protection on the naïve animal because the immune mouse would control the infection in their lung and decrease dissemination. We found that LVS and LVS *clpB* vaccinated mice had spleen and liver bacterial burdens near the limit of detection. These data, along with the near absence of a memory T cell response in the spleen indicates the infection is primarily contained in the lung. Similarly, an immune mouse would control the infection and decrease the number of bacteria that disseminate to the attached naïve mouse. Another potential experiment would involve challenging the naïve mouse in the pair intranasally. If memory T cells had already or could traffic to the naïve mouse, we expect the naïve mouse to be protected. If the memory T cells do not traffic properly, we expect the naïve mouse to succumb to the lethal infection. If the naïve mouse was protected by trafficking memory T cells, we could also separate the mice prior to lethal infection to determine whether the T cells that conferred protection had already trafficked to the naïve mouse or if they migrated after infection.

**The degree of IFN-$\gamma^+$ $CD4^+$ and $CD8^+$ T cells and Th17 cell expansion during re-challenge remains unclear**

We cannot state with certainty whether IFN-γ or IL-17 producing T cells expanded in the lungs or spleens of LVS and LVS *clpB* vaccinated mice because we haven't definitively determined the number of resting memory T cells. A preliminary experiment examining IFN-γ and IL-17A production in resting memory T cells stimulated ex vivo by LVS-infected CD45.1 splenocytes suggested the presence of IFN-γ producing memory T cells but not Th17 cells in the lung. These data are consistent with the ICS findings on day 4 post-re-challenge where IFN-$\gamma^+$ $CD4^+$ and $CD8^+$ T cells were found at significantly higher numbers in LVS or LVS *clpB* vaccinated mice compared to unvaccinated mice and Th17 cells aren't found at increased numbers. It is possible that we examined the secondary T cell response at a time point before Th17 cells have expanded and are detectable using ICS. Future studies should examine the T cell response at several time points post-re-challenge to determine the kinetics of the secondary response. The antibody depletion experiments suggest that even if Th17 cells do expand later in the secondary infection, this cell type isn't required for survival. Future experiments should also examine the presence of resting memory T cells in the spleen and lung following primary intranasal and intradermal inoculation with LVS. These data will allow a clearer understanding of whether T cell expansion occurs in the lung and spleen during secondary infection.

**Antibody responses are similar in LVS and LVS *clpB* vaccinated mice**

In addition to examining the T cell response, we determined whether primary infection with LVS or LVS *clpB* induced altered B cell responses that could impact survival during re-challenge. LVS and LVS *clpB* vaccinated mice did not have significantly different

FT-specific IgG titers on day 28 or 120 post-inoculation suggesting the B cell response primed during both infections is similar. Additionally, the banding patters were similar in LVS and LVS *clpB* vaccinated mice when LVS lysate was probed indicating similar antigens were recognized during both infections. The patterns are not, however, identical (figure 2E). The differences could be explained by altered protein expression in LVS or LVS *clpB* bacteria during infection. ClpB is a highly conserved chaperone protein involved in the stress response. In its absence, protein expression could be altered because the bacteria cannot properly respond to stresses caused by the infection environment and therefore the host would be exposed to two different sets of antigens.

Because *Francisella* lives intracellularly, the antibody response is not required for protection. Indeed, CD4 knock-out mice have poor antibody responses (i.e. low titers) in the absence of T cell help, yet these mice still survive the primary infection and subsequent lethal secondary challenge (9). B cell knock-out mice (BKO), which lack mature B cells, survive primary intradermal inoculation with LVS but have a lower $LD_{50}$ than wild-type mice (18). During a secondary infection, B cell deficiency give a more pronounced phenotype with a two-log decrease in the $LD_{50}$ compared to immune wild-type mice (18). Transfer of immune serum into BKO mice does not ameliorate protection but transfer of B cells from immune mice does (18). Together, these data suggest that the protection mediated by B cells is not antibody-dependent and instead is a consequence of another intrinsic function of B cells. In human cases of tularemia, there is no correlation between antibody titers and protection during a secondary infection (30). Therefore, while LVS infection in humans and mice does elicit an antibody response, this response is not required for protective immunity.

**Model of primary and secondary immune response to LVS infection**

Overall, we propose the following model: during primary intranasal infection with LVS, IL-17A produced by innate and adaptive cells in the lung initially controls the infection until IFN-γ production by $CD4^+$ and $CD8^+$ T cells levels increase and clear the infection. Th17 cells do not expand in the spleen during primary infection in spite of the rapid dissemination of bacteria following inoculation (16). During secondary intranasal infection with LVS, $CD4^+$ and $CD8^+$ T cells in the lung expand and produce IFN-γ. Th17 cells do not expand in the lung during secondary infection. The secondary response in the lung controls the infection and bacteria do not spread to distal organs like the spleen and the T cell response is not significantly different than unvaccinated mice. Another important finding from these experiments was that there were no statistically significant differences between LVS and LVS *clpB* vaccinated mice for all parameters measured. These data indicated that the protective immune response elicited by previous infection with either strain is nearly identical. Because LVS *clpB* provides 100% protection during lethal challenge while causing less overall disease, this strain is an excellent vaccine candidate.

**Figure 1**

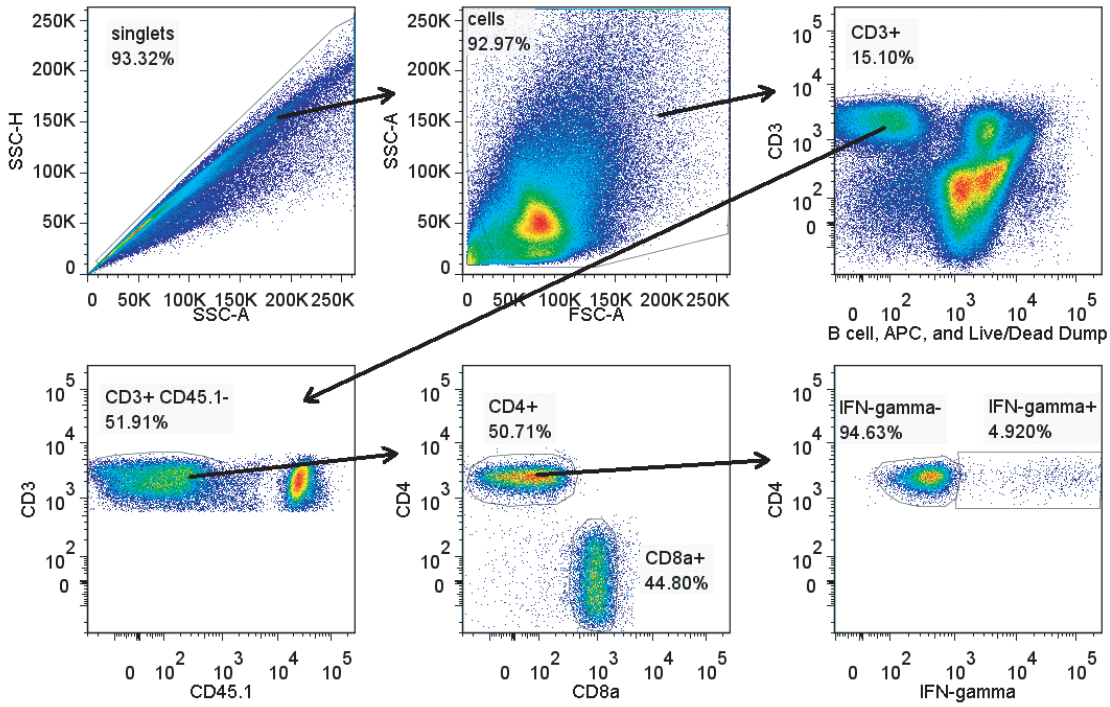


**Figure 1.** ***Gating scheme for flow cytometry analysis.*** Single cells were discriminated from doublets by plotting side scatter height (SSC-H) versus side scatter area (SSC-A). Cells were then selected by plotting SSC-A versus forward scatter area (FSC-A). Live $CD3^+$ T cells were then selected by plotting CD3 versus the Pacific Blue channel which included the live/dead stain and markers for antigen presenting cells. $CD45.1^-$ T cellls were the gated on by plotting CD3 versus CD45.1. From the $CD45.1^-$ gate, $CD4^+$ and $CD8^+$ T cells were selected. Gates for IFN-γ and IL-17A positive cells were set based on isotype control staining. For simplicity, only $CD4^+$ IFN-γ is shown. Change in mean fluorescent intensity (ΔMFI) for each sample was determined by subtracting the cytokine negative population from the cytokine positive population. For each gate, the percent of the parent gate is indicated in bold (for example, $CD3^+$ cells are 15.10% of the cells gate).

**Figure 2**

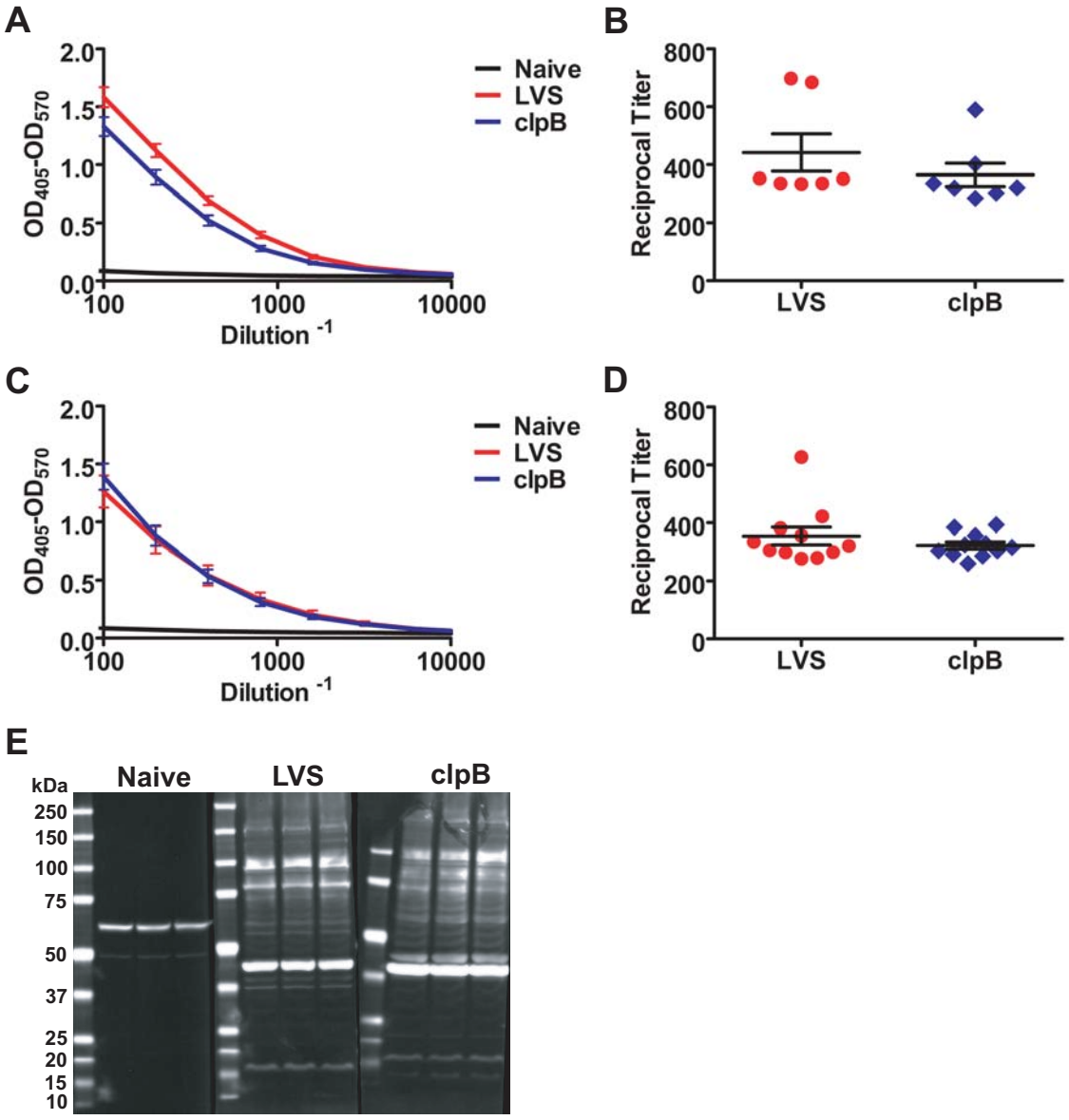


**Figure 2.** ***Antibody responses are similar in LVS and LVS* clpB *infected mice.*** B6 mice were intranasally inoculated with $5x10^2$ CFU LVS or $5x10^4$ CFU LVS *clpB*, or left uninfected. On day 28 (A, B) or 120 (C, D) post-inoculation, sera was collected and the amount of LVS-specific IgG antibodies were determined using an ELISA. Half-maximal titers were calculated for LVS and LVS *clpB* infected mice. n=7-11 mice/group. Data are combined from 2 independent experiments. Each sample was analyzed in duplicate. A Mann-Whitney test was used to determine statistical significance. E) LVS whole cell lysate was probed with sera from naïve, LVS, or LVS *clpB* mice collected 28 days post-inoculation. LVS-specific antibodies were detected using goat anti-mouse IgG secondary antibody.

**Figure 3**

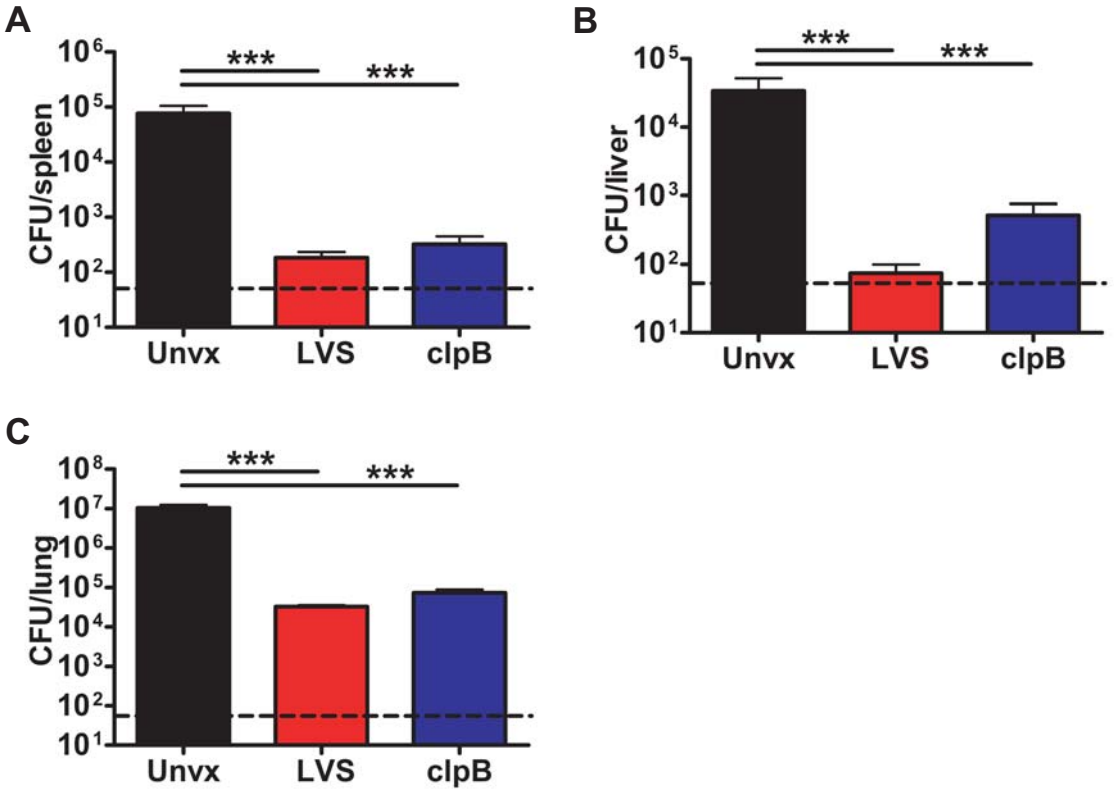


**Figure 3.** ***Previous infection with LVS or LVS*** **clpB** ***decreases bacterial burdens on day 4 post-rechallenge.*** B6 mice were intranasally inoculated with $5x10^2$ CFU LVS or $5x10^4$ CFU LVS *clpB*, or left unvaccinated (Unvx). On day 120 post-inoculation, all mice were challenged with $5x10^3$ CFU LVS. On day 4 post-rechallenge, bacterial burdens were determined in the A) spleen, B) liver, and C) lung by plating serial dilutions of organ homogenate on chocolate agar. n=3-4 mice/group. Data are combined from 2 independent experiments. The dashed line indicates the limit of detection of 50 CFUs. Statistical significance was determined on log-transformed data using a one-way ANOVA with Tukey's post-test.

**Figure 4**

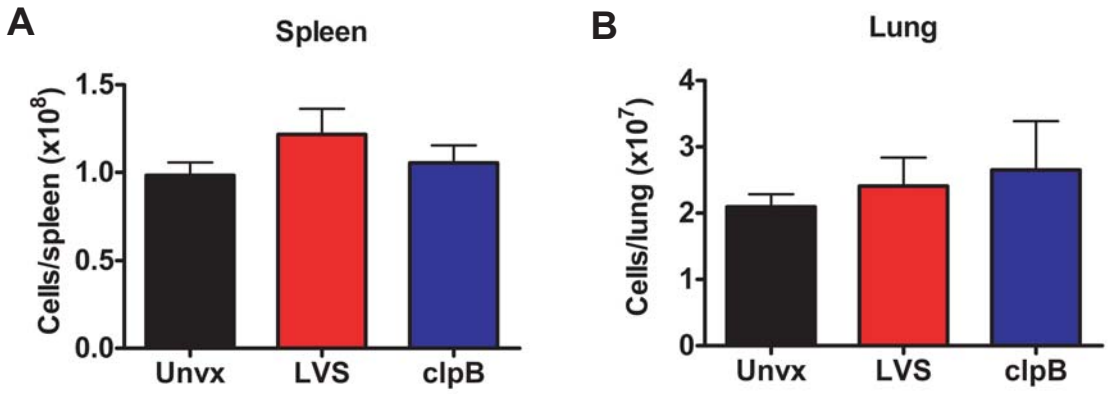


**Figure 4.** ***LVS and LVS* clpB *vaccinated mice have similar spleen and lung cellularity as unvaccinated mice on day 4 post-rechallenge.*** B6 mice were intranasally inoculated with $5x10^2$ CFU LVS or $5x10^4$ CFU LVS *clpB*, or left unvaccinated (Unvx). On day 120 post-inoculation, all mice were challenged with $5x10^3$ CFU LVS. On day 4 post-rechallenge, total cellularity was determined in the A) spleen or B) lung by trypan blue exclusion. n=6 mice/group. Data are combined from 3 independent experiments. Statistical significance was determined using a Kruskal-Wallis test with Dunn's correction.

**Figure 5**

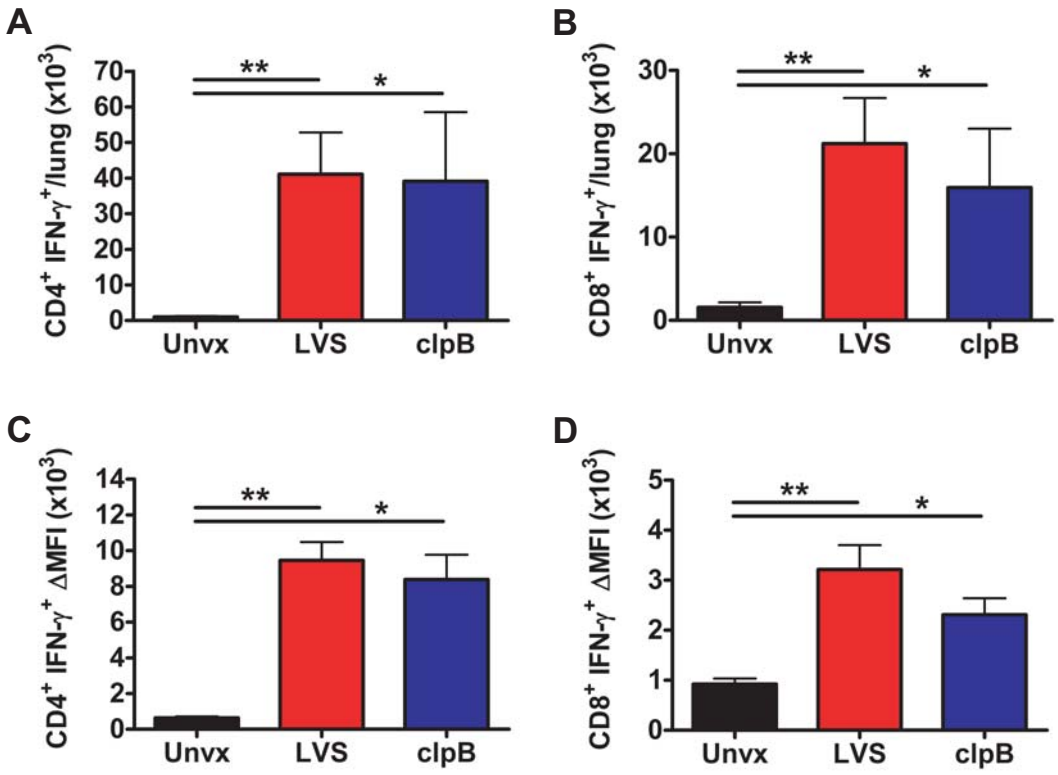


**Figure 5.** ***Vaccinated mice have increased numbers of lung IFN-γ producing CD4$^+$ and CD8$^+$ T cells compared to unvaccinated mice.*** B6 mice were intranasally inoculated with 5x10$^2$ CFU LVS or 5x10$^4$ CFU LVS *clpB*, or left unvaccinated (Unvx). On day 120 post-inoculation, all mice were challenged with 5x10$^3$ CFU LVS. On day 4 post-rechallenge, lung cells were restimulated with LVS infected B6-CD45.1 antigen presenting cells for 24 hours. Brefeldin A was added during the last 4 hours of culture. The number of A) CD4$^+$ IFN-γ$^+$ or B) CD8$^+$ IFN-γ$^+$ T cells in the lung was determined by flow cytometry. To determine change in mean fluorescent intensity (ΔMFI) for each sample, the MFI of the IFN-γ negative population was subtracted from the MFI of the IFN-γ positive population for C) CD4$^+$ or D) CD8$^+$ T cells. n=6 mice/group. Data are combined from 3 independent experiments. Statistical significance was determined using a Kruskal-Wallis test with Dunn's correction.

**Figure 6**

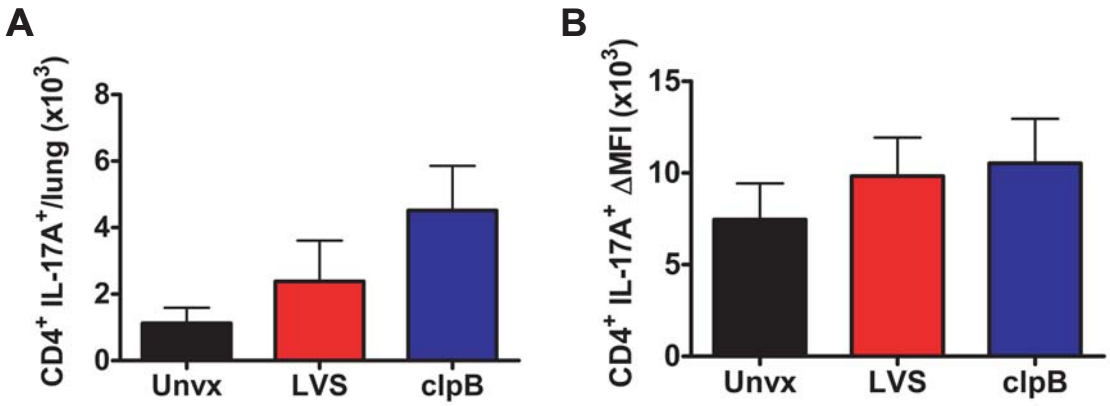


**Figure 6.** ***Vaccinated mice do not have increased numbers of lung Th17 cells compared to unvaccinated mice.*** B6 mice were intranasally inoculated with $5x10^2$ CFU LVS or $5x10^4$ CFU LVS *clpB*, or left unvaccinated (Unvx). On day 120 post-inoculation, all mice were challenged with $5x10^3$ CFU LVS. On day 4 post-rechallenge, lung cells were restimulated with LVS infected B6-CD45.1 antigen presenting cells for 24 hours. Brefeldin A was added during the last 4 hours of culture. A) Number of $CD4^+$ $IL\text{-}17A^+$ T cells in the lung were determined by flow cytometry. B) Change in mean fluorescent intensity (ΔMFI) for each sample was determined by subtracting the MFI of the IL-17A negative population from the MFI of the IL-17A positive population. n=6 mice/group. Data are combined from 3 independent experiments. Statistical significance was determined using a Kruskal-Wallis test with Dunn's correction.

**Figure 7**

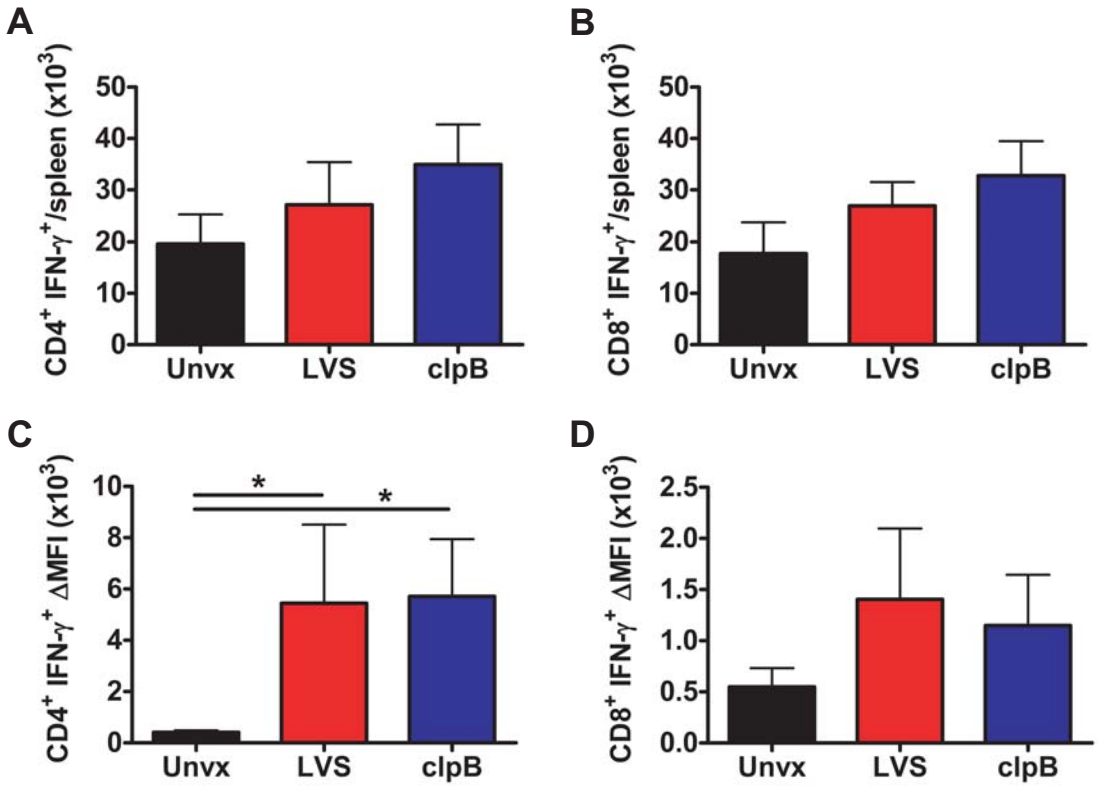


**Figure 7.** ***The IFN-γ mediated secondary response is nearly absent in the spleen.*** B6 mice were intranasally inoculated with $5x10^2$ CFU LVS or $5x10^4$ CFU LVS *clpB*, or left unvaccinated (Unvx). On day 120 post-inoculation, all mice were challenged with $5x10^3$ CFU LVS. On day 4 post-rechallenge, spleen cells were restimulated with LVS infected B6-CD45.1 antigen presenting cells for 24 hours. Brefeldin A was added during the last 4 hours of culture. The number of A) $CD4^+$ IFN-$\gamma^+$ or B) $CD8^+$ IFN-$\gamma^+$ T cells in the spleen was determined by flow cytometry. To determine change in mean fluorescent intensity (ΔMFI) for each sample, the MFI of the IFN-γ negative population was subtracted from the MFI of the IFN-γ positive population for C) $CD4^+$ or D) $CD8^+$ T cells. n=6 mice/group. Data are combined from 3 independent experiments. Statistical significance was determined using a Kruskal-Wallis test with Dunn's correction.

**Figure 8**

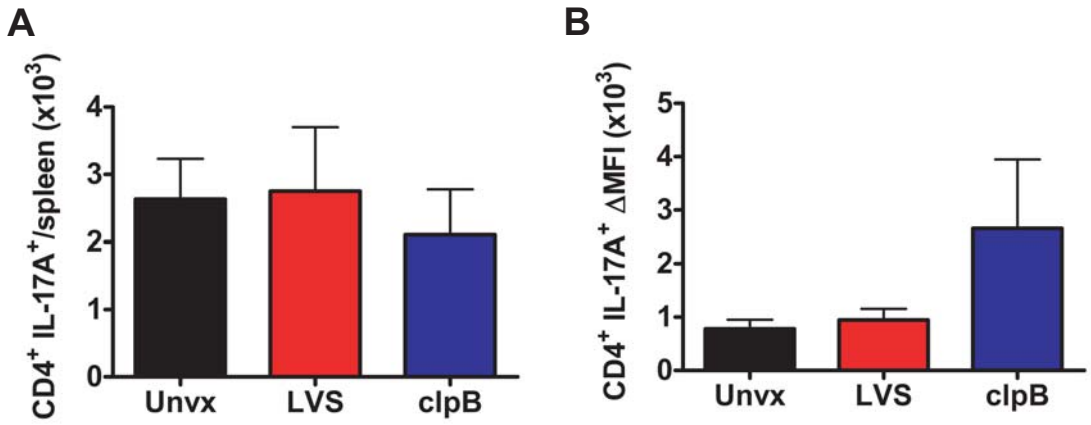


**Figure 8.** ***The IL-17A mediated secondary response is absent in the spleen.*** B6 mice were intranasally inoculated with $5x10^2$ CFU LVS or $5x10^4$ CFU LVS *clpB*, or left unvaccinated (Unvx). On day 120 post-inoculation, all mice were challenged with $5x10^3$ CFU LVS. On day 4 post-rechallenge, spleen cells were restimulated with LVS infected B6-CD45.1 antigen presenting cells for 24 hours. Brefeldin A was added during the last 4 hours of culture. A) Number of $CD4^+$ $IL\text{-}17A^+$ T cells in the spleen were determined by flow cytometry. B) Change in mean fluorescent intensity (ΔMFI) for each sample was determined by subtracting the MFI of the IL-17A negative population from the MFI of the IL-17A positive population. n=6 mice/group. Data are combined from 3 independent experiments. Statistical significance was determined using a Kruskal-Wallis test with Dunn's correction.

**Figure 9**

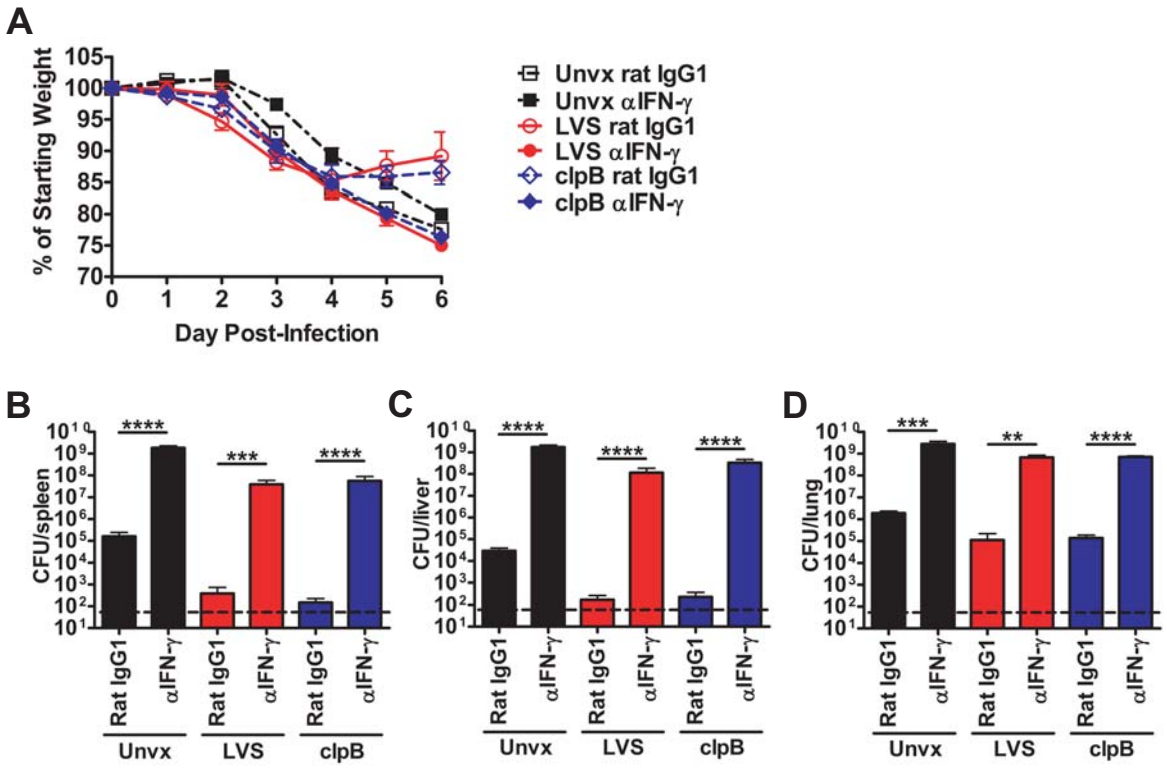


**Figure 9.** ***IFN-γ depletion increases bacterial burdens.*** B6 mice were intranasally inoculated with $5x10^2$ CFU LVS or $5x10^4$ CFU LVS *clpB*, or left unvaccinated (Unvx). On day 120 post-inoculation, all mice were challenged with $5x10^3$ CFU LVS. A) Mouse weight was determined daily and is reported as the percentage of starting weight. n=3-5 mice/group. Data are combined from 2 independent experiments. On day 6 post-re-challenge, bacterial burdens were determined in the B) spleen, C) liver, and D) lung by plating serial dilutions of organ homogenate on chocolate agar. n=3-5 mice/group. Data are combined from 2 independent experiments. The dashed line indicates the limit of detection of 50 CFUs. Statistical significance was determined on log-transformed data using a Student's t-test comparing anti-IFN-γ to isotype control within each group.

**Figure 10**

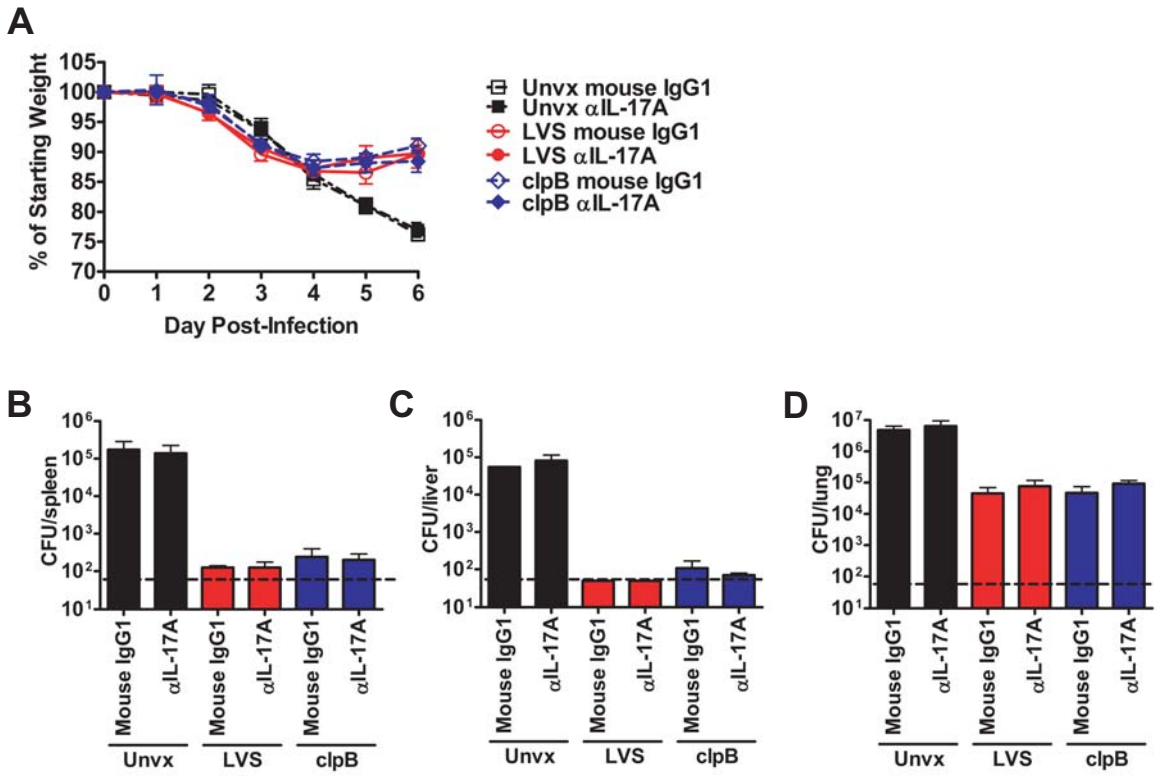


**Figure 10.** ***IL-17A depletion does not impact bacterial burdens.*** B6 mice were intranasally inoculated with $5x10^2$ CFU LVS or $5x10^4$ CFU LVS clpB, or left unvaccinated (Unvx). On day 120 post-inoculation, all mice were challenged with $5x10^3$ CFU LVS. A) Mouse weight was determined daily and is reported as the percentage of starting weight. n=3-5 mice/group. Data are combined from 2 independent experiments. On day 6 post-re-challenge, bacterial burdens were determined in the B) spleen, C) liver, and D) lung by plating serial dilutions of organ homogenate on chocolate agar. n=3-5 mice/group. Data are combined from 2 independent experiments. The dashed line indicates the limit of detection of 50 CFUs. Statistical significance was determined on log-transformed data using a Student's t-test comparing anti-IL-17A to isotype control within each group.

## REFERENCES


1. Dennis DT, Inglesby TV, Henderson DA, Bartlett JG, Ascher MS, Eitzen E, et al. Tularemia as a biological weapon: medical and public health management. JAMA. 2001;285(21):2763-73. Epub 2001/06/21. doi: jst10001 [pii]. PubMed PMID: 11386933.

2. Alibek K, Handelman S. Biohazard : the chilling true story of the largest covert biological weapons program in the world, told from the inside by the man who ran it. 1st ed. New York: Random House; 1999. xi, 319 p., 8 p. of plates p.

3. Christopher GW, Cieslak TJ, Pavlin JA, Eitzen EM, Jr. Biological warfare. A historical perspective. JAMA. 1997;278(5):412-7. Epub 1997/08/06. PubMed PMID: 9244333.

4. Centers for Disease Control and Prevention. Reported tularemia cases by state, United States, 2001-2010 2011 [cited 2011]. Available from: http://www.cdc.gov/tularemia/statistics/state.html.

5. Tarnvik A, Chu MC. New approaches to diagnosis and therapy of tularemia. Ann N Y Acad Sci. United States2007. p. 378-404.

6. Conlan JW, Chen W, Shen H, Webb A, KuoLee R. Experimental tularemia in mice challenged by aerosol or intradermally with virulent strains of Francisella tularensis: bacteriologic and histopathologic studies. Microb Pathog. 2003;34(5):239-48. PubMed PMID: 12732472.

7. Metzger DW, Bakshi CS, Kirimanjeswara G. Mucosal immunopathogenesis of Francisella tularensis. Ann N Y Acad Sci. 2007;1105:266-83. Epub 2007/03/31. doi: annals.1409.007 [pii] 10.1196/annals.1409.007. PubMed PMID: 17395728.

8. Fortier AH, Slayter MV, Ziemba R, Meltzer MS, Nacy CA. Live vaccine strain of Francisella tularensis: infection and immunity in mice. Infect Immun. 1991;59(9):2922-8. PubMed PMID: 1879918; PubMed Central PMCID: PMC258114.

9. Yee D, Rhinehart-Jones TR, Elkins KL. Loss of either CD4+ or CD8+ T cells does not affect the magnitude of protective immunity to an intracellular pathogen, Francisella tularensis strain LVS. J Immunol. 1996;157(11):5042-8. Epub 1996/12/01. PubMed PMID: 8943413.

10. Collazo CM, Sher A, Meierovics AI, Elkins KL. Myeloid differentiation factor-88 (MyD88) is essential for control of primary in vivo Francisella tularensis LVS infection, but not for control of intra-macrophage bacterial replication. Microbes Infect. 2006;8(3):779-90. Epub 2006/03/04. doi: S1286-4579(05)00364-3 [pii] 10.1016/j.micinf.2005.09.014. PubMed PMID: 16513388.

11. Leiby DA, Fortier AH, Crawford RM, Schreiber RD, Nacy CA. In vivo modulation of the murine immune response to Francisella tularensis LVS by administration of anticytokine antibodies. Infect Immun. 1992;60(1):84-9. Epub 1992/01/01. PubMed PMID: 1729199; PubMed Central PMCID: PMC257506.

12. Anthony LS, Ghadirian E, Nestel FP, Kongshavn PA. The requirement for gamma interferon in resistance of mice to experimental tularemia. Microb Pathog. 1989;7(6):421-8. Epub 1989/12/01. PubMed PMID: 2516219.

13. Woolard MD, Hensley LL, Kawula TH, Frelinger JA. Respiratory Francisella tularensis live vaccine strain infection induces Th17 cells and prostaglandin E2, which inhibits generation of gamma interferon-positive T cells. Infect Immun. 2008;76(6):2651-9. Epub 2008/04/09. doi: IAI.01412-07 [pii] 10.1128/IAI.01412-07. PubMed PMID: 18391003; PubMed Central PMCID: PMC2423094.

14. Lin Y, Ritchea S, Logar A, Slight S, Messmer M, Rangel-Moreno J, et al. Interleukin-17 Is Required for T Helper 1 Cell Immunity and Host Resistance to the Intracellular Pathogen Francisella tularensis. Immunity. 2009. Epub 2009/10/27. doi: S1074-7613(09)00448-8 [pii] 10.1016/j.immuni.2009.08.025. PubMed PMID: 19853481.

15. Markel G, Bar-Haim E, Zahavy E, Cohen H, Cohen O, Shafferman A, et al. The involvement of IL-17A in the murine response to sub-lethal inhalational infection with Francisella tularensis. PLoS One. 2010;5(6):e11176. doi: 10.1371/journal.pone.0011176. PubMed PMID: 20585449; PubMed Central PMCID: PMC2887844.

16. Barrigan LM, Tuladhar S, Brunton JC, Woolard MD, Chen C, Saini D, et al. Infection with *Francisella tularensis clpB* leads to an altered yet protective immune response. Infection and Immunity. 2013;in press.

17. LoVullo ED, Molins-Schneekloth CR, Schweizer HP, Pavelka MS, Jr. Single-copy chromosomal integration systems for Francisella tularensis. Microbiology. 2009;155(Pt 4):1152-63. Epub 2009/04/01. doi: 155/4/1152 [pii] 10.1099/mic.0.022491-0. PubMed PMID: 19332817.

18. Elkins KL, Bosio CM, Rhinehart-Jones TR. Importance of B cells, but not specific antibodies, in primary and secondary protective immunity to the intracellular bacterium Francisella tularensis live vaccine strain. Infect Immun. 1999;67(11):6002-7. PubMed PMID: 10531260; PubMed Central PMCID: PMC96986.

19. Conlan W, Shen H, Kuolee R, Zhao X, Chen W. Aerosol-, but not intradermal-immunization with the live vaccine strain of Francisella tularensis protects mice against subsequent aerosol challenge with a highly virulent type A strain of the pathogen by an alphabeta T cell- and interferon gamma- dependent mechanism. Vaccine. 2005;23(19):2477-85. doi: 10.1016/j.vaccine.2004.10.034. PubMed PMID: 15752834.

20. Shen H, Chen W, Conlan JW. Susceptibility of various mouse strains to systemically- or aerosol-initiated tularemia by virulent type A Francisella tularensis before and after immunization with the attenuated live vaccine strain of the pathogen. Vaccine. 2004;22(17-18):2116-21. doi: 10.1016/j.vaccine.2003.12.003. PubMed PMID: 15149767.

21. Wu TH, Hutt JA, Garrison KA, Berliba LS, Zhou Y, Lyons CR. Intranasal vaccination induces protective immunity against intranasal infection with virulent Francisella tularensis biovar A. Infect Immun. 2005;73(5):2644-54. Epub 2005/04/23. doi: 73/5/2644 [pii] 10.1128/IAI.73.5.2644-2654.2005. PubMed PMID: 15845466; PubMed Central PMCID: PMC1087315.

22. Curtis MM, Way SS. Interleukin-17 in host defence against bacterial, mycobacterial and fungal pathogens. Immunology. England2009. p. 177-85.

23. Lin Y, Ritchea S, Logar A, Slight S, Messmer M, Rangel-Moreno J, et al. Interleukin-17 is required for T helper 1 cell immunity and host resistance to the intracellular pathogen Francisella tularensis. Immunity. 2009;31(5):799-810. Epub 2009/10/27. doi: S1074-7613(09)00448-8 [pii] 10.1016/j.immuni.2009.08.025. PubMed PMID: 19853481; PubMed Central PMCID: PMC2789998.

24. Elkins KL, Colombini SM, Meierovics AI, Chu MC, Chou AY, Cowley SC. Survival of secondary lethal systemic Francisella LVS challenge depends largely on interferon gamma. Microbes Infect. 2010;12(1):28-36. doi: 10.1016/j.micinf.2009.09.012. PubMed PMID: 19781659.

25. Chen W, Shen H, Webb A, KuoLee R, Conlan JW. Tularemia in BALB/c and C57BL/6 mice vaccinated with Francisella tularensis LVS and challenged intradermally, or by aerosol with virulent isolates of the pathogen: protection varies depending on pathogen virulence, route of exposure, and host genetic background. Vaccine. 2003;21(25-26):3690-700. Epub 2003/08/19. doi: S0264410X03003864 [pii]. PubMed PMID: 12922099.

26. Shen H, Harris G, Chen W, Sjostedt A, Ryden P, Conlan W. Molecular immune responses to aerosol challenge with Francisella tularensis in mice inoculated with live vaccine candidates of varying efficacy. PLoS One. 2010;5(10):e13349. doi: 10.1371/journal.pone.0013349. PubMed PMID: 20967278; PubMed Central PMCID: PMC2953512.

27. Crane DD, Scott DP, Bosio CM. Generation of a convalescent model of virulent Francisella tularensis infection for assessment of host requirements for survival of tularemia. PLoS One. 2012;7(3):e33349. doi: 10.1371/journal.pone.0033349. PubMed PMID: 22428026; PubMed Central PMCID: PMC3299770.

28. Purwar R, Campbell J, Murphy G, Richards WG, Clark RA, Kupper TS. Resident memory T cells (T(RM)) are abundant in human lung: diversity, function, and antigen specificity. PLoS One. 2011;6(1):e16245. doi: 10.1371/journal.pone.0016245. PubMed PMID: 21298112; PubMed Central PMCID: PMC3027667.

29. Valentino MD, Hensley LL, Skrombolas D, McPherson PL, Woolard MD, Kawula TH, et al. Identification of a dominant CD4 T cell epitope in the membrane lipoprotein Tul4 from Francisella tularensis LVS. Mol Immunol. 2009;46(8-9):1830-8. doi: S0161-5890(09)00038-8 [pii] 10.1016/j.molimm.2009.01.008. PubMed PMID: 19233475.

30. Tarnvik A. Nature of protective immunity to Francisella tularensis. Reviews of infectious diseases. 1989;11(3):440-51. PubMed PMID: 2665002.

# CHAPTER 4

# IDENTIFICATION OF EARLY INTERACTIONS BETWEEN *FRANCISELLA* AND THE HOST[1]

## OVERVIEW

The host's adaptive immune response to *Francisella tularensis* is dependent on the route of inoculation. Intradermal inoculation with *F. tularensis* live vaccine strain (LVS) results in many IFN-$\gamma^+$ T cells in the lung whereas intranasal inoculation produces fewer IFN-$\gamma^+$ T cells and instead many IL-$17^+$ T cells in the lung. Interestingly, at one day post inoculation, bacterial loads are similar in the spleen and lung regardless of the route of inoculation. Due to the similar bacterial loads systemically, but very different host responses, we hypothesize that the adaptive immune response is influenced by local events at the site of infection immediately following inoculation. To test this hypothesis, we identified the first cell type infected in the lungs of mice intranasally inoculated with *F. novicida* U112, LVS, or the highly virulent SchuS4 strain of *F. tularensis* using flow cytometry. At four hours post-infection, we found that for all three strains of *Francisella*, alveolar macrophages are the primary cell type infected, to the exclusion of other myeloid cells and lung parenchyma. In the skin, neutrophils, macrophages, and dendritic cells are infected with U112 or LVS 4 hours post-inoculation. Following bacterial dissemination from the skin to

[1] Contributing authors: Lydia Barrigan, Shraddha Tulhadar, Shaun Steele, Kristina Reibe, Ching-ju Chen, Ian Cumming, John Whitesides, Sarah Seay, Richard Frothingham, Greg Sempowski, Tom Kawula, and Jeffrey Frelinger

the lung, interstitial macrophages or neutrophils are infected indicating different cell types are infected in the lung following intranasal and intradermal inoculation. The lung has a more pro-inflammatory milieu following intradermal inoculation compared to intranasal inoculation, consistent with the development of a robust IFN-γ-mediated immune response after intradermal inoculation. When alveolar macrophages are depleted using CD11c.DTR mice, lung bacterial burdens are higher on day 3 post-inoculation suggesting alveolar macrophages are necessary for controlling the infection early after inoculation. Overall, we identified the early interactions between *Francisella* and the host following two different routes of inoculation. We also identified the cytokines produced early after infection which likely play a role in shaping the subsequent adaptive immune response.

## INTRODUCTION

Immune responses following bacterial infections are influenced by the route of infection (1, 2). Cytokines produced by the innate immune response are critical in shaping the adaptive immune response (reviewed in (3)). For example, if a naïve $CD4^+$ T cell encounters antigen in the presence of IL-12, it will differentiate into Th1 effector T cell, but if it encounters IL-6 and TGF-β during antigen presentation, it will differentiate into a Th17 effector T cell (3). Our previous experiments in mice using intranasal or intradermal inoculation with *Francisella tularensis* subsp. *holartica* Live Vaccine Strain (LVS) demonstrated striking differences in the adaptive immune response in the lungs when these two inoculation routes were compared (2). Upon either intradermal or intranasal inoculation with LVS, bacteria rapidly disseminate and are found in the spleen, liver, and lung 24 hours after inoculation (2). After 3 days, equivalent bacterial burdens are found in the spleen and

lungs of mice inoculated via either route (2). Despite similar burdens early after inoculation, intradermally inoculated mice clear the infection more rapidly than intranasally inoculated mice and have an increased IFN-γ response. Intradermal inoculation leads to significantly more $CD4^+$ and $CD8^+$ T cells producing IFN-γ in both the spleen and lung on day 7 post-inoculation compared to intranasal inoculation (2). Faster bacterial clearance in intradermally inoculated mice correlates with the increased IFN-γ-mediated immune response. IFN-γ is required for controlling *F. tularensis* infection and administration of recombinant IFN-γ decreases bacterial burdens (4-6). Intranasal infection leads to an expansion of Th17 cells, a CD4+ T cell population not found in the lungs of intradermally inoculated mice (2). Altogether, we conclude T cell effector function is influenced by the inoculation route. Thus, it is important to understand the initiation of the immune response and identify the earliest cells infected by *Francisella* as well as the cytokine environment induced upon inoculation.

*Francisella tularensis* is a highly pathogenic, facultative intracellular, gram-negative coccobacillus. Infection with *F. tularensis* causes the zoonotic disease tularemia which is endemic in regions of the United States and Europe. *F. tularensis* subspecies *holartica* live vaccine strain (LVS) does not cause severe disease in humans (7). Murine infection with LVS most closely resembles human infection (8). The $LD_{50}$ for intranasal inoculations is approximately $10^3$ colony forming units (CFU) and approximately $10^6$ for intradermal inoculation (9, 10). While non-pathogenic in immunocompetent humans, *F. novicida* U112 (U112) is highly virulent in mice with an $LD_{50}$ for intranasal or intraperitoneal inoculation of <10 CFU (11, 12). *F. tularensis* subspecies *tularensis* SchuS4 (SchuS4) is highly pathogenic in both mice and humans. The route of *Francisella* infection contributes to the severity of

tularemia in humans. Approximately 90% of human tularemia cases are of the ulcerograndular type where bacteria are introduced through a cut in the skin or a bite from an arthropod vector (13). The most severe form of tularemia is pneumonic tularemia which results from bacterial inhalation. Before the use of antibiotics, pneumonic tularemia was fatal in 30-60% of cases when infection was caused by the highly virulent SchuS4 strain (13). Human disease can be caused by inhalation of as few as 10 organisms, highlighting the highly pathogenic nature of SchuS4 and intranasal infection (14).

Due to similar bacterial burdens early after inoculation but very different adaptive immune responses for each inoculation route, we hypothesized that the adaptive immune response was shaped by events early after inoculation. We therefore sought to identify host cells infected with *F. tularensis* early after inoculation. Previously, we found alveolar macrophages comprised between 50-80% of cells infected with U112 or LVS 24 hours after intranasal inoculation (15). Because infection for 24 hours had the potential of allowing for more than one round of infection, we were interested in identifying the infected cells 4 hours post-inoculation before any cell to cell spread. We found alveolar macrophages were the primary cell type infected after intranasal inoculation and interstitial macrophages were infected in the lung following intradermal inoculation and bacterial dissemination to the lung. We also identified cytokines and chemokines produced in the lung early after inoculation or bacterial dissemination as well has how disease course is altered in the absence of alveolar macrophages. Together, the work presented here helps us understand how events early after *F. tularensis* inoculation shape subsequent adaptive immunity.

## MATERIALS AND METHODS

### Bacteria

*Francisella novicida* U112 was obtained from Colin Manoil (University of Washington). *F. tularensis* subsp. *holartica* live vaccine strain (LVS) (29684) was obtained from American Type Culture Collection (Manassas, VA). *F. tularensis* subsp. *tularensis* SchuS4 (SchuS4) (NR-643) was obtained from BEI Resources (Manassas, VA) Bacteria were grown on chocolate agar supplemented with 1% IsoVitalex (Becton-Dickinson) at 37°C. Bacterial inoculations were prepared by removing bacteria from a lawn grown on chocolate agar and resuspended in sterile PBS at an $OD_{600}$=1 (equivalent to $1x10^7$CFU/μL). To achieve the desired dose, appropriate dilutions were made using sterile PBS. Viable bacteria in each preparation were quantified by serial dilution and plating on chocolate agar.

### Mice

C57Bl/6J (B6) mice were obtained from The Jackson Laboratory (Bar Harbor, ME). CD11c.diphtheria toxin receptor (CD11c.DTR) were obtained from Gunter Hammerling (German Cancer Research Center, Heidelberg, Germany) and then bred in-house. All mice were housed in specific-pathogen free conditions at the University of North Carolina- Chapel Hill, Duke University, or the University of Arizona in accordance with their respective Institutional Animal Care and Use Committees. Female mice used for experiments were between 7 to 12 weeks of age.

### Inoculation of Mice

For intranasal bacterial inoculations, mice were anesthetized with 575 mg/kg tribromomethanol (Avertin) (Sigma) administered intraperitoneally. Mice were then intranasally inoculated with 1 x $10^4$ CFU U112 or LVS suspended in 50 μL PBS. For

intradermal inoculations, mice were inoculated with 5 x $10^5$ CFU U112 or LVS in 25 µL at the base of the tail. The inoculum was divided between 3 injection sites along the tail. For diphtheria toxin (DT) treatment, CD11c.DTR mice were anesthetized with 0.25 mL of 7.5 mg/mL ketamine and 0.5 mg/mL xylazine cocktail in PBS administered intraperitoneally and then intranasally inoculated with 8 ng diphtheria toxin (Sigma, St. Louis, MO) in 50 µL PBS. Depletion of alveolar macrophages was confirmed by flow cytometry.

**Single Cell Suspension of Mouse Lung**

B6 lungs were finely minced and placed into a sterile-filtered digestion mix of RPMI 1640 (HyClone) containing L-glutamine (Gibco), sodium pyruvate (Gibco) and β-mercaptoethanol (Gibco), 0.05 mg/mL collagenase (Worthington Biochemicals), 0.02 mg/mL DNAse (Sigma), and 125 U/mL elastase (Worthington Biochemicals). For intranasally inoculated mice, 50 µg/mL gentamicin (Sigma) was added to the digestion mix to kill extracellular bacteria. The digestion mix was incubated in a 37°C water bath for 30 minutes with occasional shaking. The suspension was then strained through a 100 µM filter and cells pelleted by centrifugation at 300 x g for 5 minutes. Red blood cells were lysed using ammonium chloride potassium lysis buffer (Gibco) and washed with RMPI 1640 supplemented with 10% fetal calf serum (Atlas), L-glutamine, sodium pyruvate, and β-mercaptoethanol. The total number of viable cells was determined using a hemocytometer by trypan blue exclusion.

**Single Cell Suspension of Mouse Skin**

Tail skin was separated from the cartilage and placed dermis-side down in a petri dish containing 25 mg/mL trypsin (Invitrogen) and 50 µg/mL gentamicin. Tails were incubated 45 minutes at 37°C and then the dermal and epidermal layers separated. The epidermis was

placed back in the 25 mg/mL trypsin and allowed to incubate 15 additional minutes. Epidermal cells were removed from the epidermis by washing and passed through a 100 μm filter. The dermis was minced and placed in a sterile-filtered digestion mix composed of RPMI 1640, L-glutamine, sodium pyruvate, β-mercaptoethanol, 1000 U/mL collagenase (Worthington Biochemicals), 0.01 mg/mL DNAse (Sigma), 1000 U/mL hyluronidase (Worthington Biochemicals), and 25 μg/mL gentamicin (Sigma). The dermis was digested for 2 hours in a 37℃ water bath with occasional shaking. Dermal cells were then passed through a 100 μm filter and washed with RMPI 1640 supplemented with 10% fetal calf serum (Atlas), L-glutamine, sodium pyruvate, and β-mercaptoethanol. The total number of viable cells was determined using a hemocytometer by trypan blue exclusion.

**Bead Enrichment of $CD45^+$ cells**

Lung single cell suspensions were stained for 20 minutes on ice with CD45-APC (Clone 30-F11, Biolegend). After washing the cells to remove unbound antibody, IMag anti-APC magnetic particles (BD) were used to enrich CD45-APC positive cells according to the manufacturer's instructions. Cells that did not bind the magnetic beads were considered CD45-APC negative. CD45 enrichment was measured by flow cytometry. Enriched eukaryotic cells were directly plated on chocolate agar containing 10 μg/ml ampicillin (Sigma) and the number of CFUs counted 72 hours later.

**Identification of infected lung populations**

Lung cells in a single cell suspension after intranasal inoculation with *Francisella* had Fc receptors blocked with 2.4G2 to prevent non-specific staining and were then stained with F4/80 PE (Clone BM8, eBioscience), CD11b Pacific Blue (Clone M1/70, Biolegend), and CD11c APC (Clone N418, eBioscience). Lung cells from intradermally inoculated mice had

Fc receptors blocked with 2.4G2 and were then stained with F4/80 PE, CD11b Pacific Blue, CD11c APC, and GR-1 Pacific Orange (Clone, RB6-8C5, Invitrogen). The cells were sorted using a Reflection cell sorter (iCyt/Sony) or FACS Aria (BD) into four populations based on surface marker expression (Table 1). Sorted populations were plated directly on chocolate agar containing 10 μg/ml ampicillin without lysis and bacterial CFUs counted 24-72 hours later to enumerate the number of infected cells.

**Identification of infected epidermal and dermal populations**

Epidermal or dermal single cell suspensions after interdermal inoculation with *Francisella* were suspended in sterile PBS and then stained with 0.1 μg/mL Pacific Blue succimidyl ester (Invitrogen) for 8 minutes at room temperature. Cells had Fc receptors blocked with 2.4G2 and were then stained with F4/80 PE, CD45 PE-Cy7 (Clone 30-F11, Biolegend), CD11b FITC (Clone M1/80, eBioscience), CD11c PerCP-Cy5.5 (Clone N418, Biolegend), GR-1 Pacific Orange, and CD207 (Clone eBioRMUL.2, eBioscience). The cells were sorted using a FACS Aria (BD) based on surface marker expression (Table 2). $2x10^6$ naïve splenocytes were added to the sorted populations as carrier cells prior to centrifugation for 5 minutes at 300xg. Cells were then plated directly on chocolate agar containing 10 μg/ml ampicillin without lysis and bacterial CFUs counted 24-72 hours later to enumerate the number of infected cells.

**Lung, epidermal, or dermal tissue culture**

Lungs were minced finely and placed in 1 mL complete RPMI 1640 containing 50 μg/mL gentamicin in a 24 well plate. Tail skin was separated from the cartilage and placed dermis-side down in a petri dish containing 10X trypsin (Invitrogen) and 50 μg/mL gentamicin. Tails were incubated 45 minutes at 37°C and then the dermal and epidermal

layers separated. Intact epidermal or dermal cell layers were placed in 1 mL complete RPMI 1640 containing 50 μg/mL gentamicin in a 24 well plate. 1 hour after starting the culture, the gentamicin-containing media was removed and fresh media was added. Tissue was cultured for 24 hours and then culture supernatant was collected. Cells were removed by centrifugation at 300 x g for 5 minutes. Culture supernatants were stored at -80℃ until Luminex analysis was performed.

**Luminex analysis**

A multiplex luminex bead-based approach was used to quantify cytokines/chemokines in the culture supernatant. A 20-analyte assay panel was performed according to the manufacturer's protocol (Invitrogen) using a BioPlex array reader (Bio-Rad Laboratories). The assay reports pg/mL using integrated cytokine/chemokine standard curves. The concentrations of the following analytes were determined: FGF basic, GM-CSF, IFN-γ, IL-1α, IL-1β, IL-2, IL-4, IL-5, IL-6, IL-10, IL-12 (p40/p70), IL-13, IL-17, KC, MCP-1, MIG, MIP-1α, TNFα, and VEGF. A five-parameter non-linear logistic regression model was used to establish standard curve and to estimate the probability of occurrence of a concentration at a given point. Standard outliers were removed from the analysis if the observed/expected % recovery was outside of the acceptable limits (70-130%). Upper and lower levels of quantification were determined by the BioPlex Manager software based on goodness of fit and percent recovery. Calculated pg/mL for experimental specimens were multiplied by the inherent assay dilution factor (df=2) and reported as final observed pg/mL.

**Statistical analysis**

Data were analyzed using a one-way ANOVA with Tukey's post-test for cytokine levels. CFU levels were log-transformed and then a Student's t-test was used to determine

significance. GraphPad Prism (v5.04) was used for analysis. Error bars show standard error of the mean. Significance levels are indicated as follows: * $p < 0.05$; ** $p < 0.01$, *** $p < 0.001$, **** $p < 0.0001$.

## RESULTS

### Identification of infected host cells early after inoculation

The adaptive immune response to LVS is influenced by the route of infection despite similar bacterial burdens, and therefore antigen load, early after inoculation. We hypothesized the adaptive immune response was shaped by these events occurring early after inoculation. We therefore sought to identify infected cells early after inoculation. We chose to use 4 hours after inoculation so that *Francisella* had sufficient time to infect the cells it initially targets, but not time for cell to cell spread. We did not use GFP-expressing bacteria and flow cytometry to identify infected cells because there are few infected cells at 4 hours post-inoculation. For example, an intranasal inoculum dose of $1x10^4$ CFU yielded approximately 100 infected cells out of $1x10^7$ host lung cells. Additionally, intracellular replication of *Francisella* is just beginning at our chosen time point; therefore the GFP signal is low in infected cells. Instead of using GFP-expressing *Francisella* to identify infected cells by flow cytometry, we took another approach. The tissue of interest was digested into single cell suspensions in the presence of gentamicin to kill extracellular bacteria and stained with a variety of fluorophore-conjugated antibodies specific for surface markers that distinguish the cell populations of interest. We then utilized FACS to sort individual cell populations of interest. Purified cell populations were plated directly on chocolate agar

without eukaryotic cell lysis and the resulting colonies counted. A colony indicated a host cell of a specific type was infected with a live *Francisella* bacterium.

**LVS infects myeloid-derived cells after intranasal inoculation**

Previous experiments identified a variety of lung cell types were infected with *Francisella* 24 and 72 hours post-intranasal inoculation (16). Although the majority of infected cells 24 hours after intranasal inoculation with GFP-expressing *Francisella* strains were alveolar macrophages, alveolar type II epithelial cells were also identified as an infected cell type by flow cytometry (16). Our initial experiments, therefore, sought to determine whether cells initially targeted by LVS were of the myeloid or non-myeloid lineage. B6 mice were intranasally inoculated with $1x10^4$ CFU LVS and sacrificed 4 hours later. The lung single cell suspension was stained with anti-CD45-APC and anti-APC magnetic beads were used to positively select for myeloid-derived cells. Figure 1A shows representative flow cytometry histograms of CD45 staining within the pre-enrichment, negative selection ($CD45^-$), and positive selection ($CD45^+$) samples. Eukaryotic cells were directly plated on chocolate agar and the number of colonies within the $CD45^-$ and $CD45^+$ pools were counted (figure 1B). 99% of the resulting LVS colonies were on the $CD45^+$ plates indicating that LVS initially targets myeloid-derived cells for infection.

**Alveolar macrophages are the dominant infected cell type after intranasal inoculation**

Of the myeloid-derived cells in the lung, we selected alveolar macrophages, interstitial macrophages, and dendritic cells as the cell types most likely to be initially infected with *Francisella*. These cell types were distinguished from one another by surface expression of F4/80, CD11c, and CD11b as shown in Table 1. We also sorted an 'other' cell population that didn't fit within the gates for alveolar macrophages, interstitial macrophages,

or dendritic cells. The lung gating scheme used for the sorts is shown in figure 2. To identify infected cells in the lung early after intranasal inoculation, B6 mice were intranasally inoculated with $1x10^4$ CFU U112, LVS, or SchuS4 and sacrificed 4 hours post-inoculation. The lung single cell suspension was stained for F4/80, CD11c, and CD11b and cell populations sorted based on expression of these surface markers. Sorted eukaryotic cells were plated directly on chocolate agar and colonies counted (figure 3). Approximately 90% of all infected cells were alveolar macrophages indicating these cells were initially targeted by *Francisella* after intranasal inoculation. The remaining 10% of infected cells consisted of a mixture of interstitial macrophages, dendritic cells, and other. The results were consistent across individual mice. Alveolar macrophages were 86-96% of infected cells after U112 inoculation, 71-93% of infected cells after LVS inoculation, and 93-96% of infected cells after SchuS4 inoculation. Together, these data indicate alveolar macrophages are the dominant infected cell type after intranasal *Francisella* inoculation.

**Neutrophils are the dominant infected cell type in the skin after intradermal inoculation**

We next sought to determine what cells *Francisella* initially targets after intradermal inoculation. Of the myeloid-derived cells in the skin, we selected dendritic cells, macrophages, neutrophils, and langerhans as the cells as the cell types most likely to be target by *Francisella* after intradermal inoculation. Table 2 shows the surface markers used to distinguish these cell types. The gating scheme used during the sorts is shown in figure 4. Non-myeloid derived cells ($CD45^-$) were the majority of cells within the skin and were also sorted to determine whether they were targeted by *Francisella*. For intradermal inoculations, mice were inoculated with $5x10^5$ CFU U112 or LVS at the base of the tail spread over three injection sites. In order to recover approximately 100 infected cells, cells from two mice

were combined prior to the sort into one sample. In the epidermis, we found the majority of infected cells were neutrophils (figure 5). Dendritic cells were also targeted by *Francisella* in the epidermis (figure 5). In addition to neutrophils being the mostly likely cell typed infected with *Francisella* in the skin, neutrophils also had the highest percent infectivity of all sorted cell types by 10-100 fold. Neutrophils were also the dominant infected cell type in the dermis (figure 6). Macrophages were the other cell type targeted by *Francisella* in the dermis (figure 6). Again, dermal neutrophils had the highest percent infectivity of all cell types in the dermis. We had not expected naïve mouse skin to contain a large population of neutrophils but because so many neutrophils were infected after inoculation, we hypothesized that tissue damage and/or the presence of bacteria led to their recruitment. To test this hypothesis, we inoculated mice with 50 μL PBS and sacrificed the mice 4 hours later. We compared the % neutrophils of live $CD45^+$ cells in the epidermis and dermis of untouched, naïve mice to mice that had been inoculated with PBS (figure 7). We found a 3-4 fold increase in the % of neutrophils in the PBS inoculated mice suggesting that tissue damage caused by the injections leads to the recruitment of neutrophils to the skin. Recruited neutrophils can then become infected with *Francisella* in the intradermal space. Altogether, our data indicate neutrophils and dendritic cells are targeted by *Francisella* in the epidermis while neutrophils and macrophages are targeted by *Francisella* in the dermis. Langerhans cells were not targeted by *Francisella* in either the epidermis or dermis.

**Interstitial macrophages and neutrophils are the dominant infected cell types in the lung after intradermal inoculation**

Because we observed very different adaptive immune responses in the lung after intranasal or intradermal inoculation, we hypothesized that there were different events

occurring early after infection. One possibility was different infected cell types in the lung depending on the route of infection. We therefore sought to identify the infected cell type(s) after intradermal inoculation and bacterial dissemination to the lung. Mice were intradermally inoculated with $5x10^5$ CFU U112 or LVS. Lung harvests were carefully timed such that infected cells were reproducibly found in the lung but we were still examining infected cells as soon after infection as practical. Pilot experiments determined 48 hours post-inoculation was the time point that best fit these criteria. Lung single cell suspensions were stained for F4/80, CD11b, CD11c, and GR-1 and sorted into the populations shown in table 1 and figure 2. After intradermal inoculation and bacterial dissemination to the lung, interstitial macrophages and neutrophils are infected with *Francisella* (figure 8). Importantly, alveolar macrophages were not appreciably infected with *Francisella* in the lung after intradermal inoculation and bacterial dissemination. These results indicate that different cell types are targeted by *Francisella* in the lung depending on the inoculation route.

**Intradermal inoculation leads to a pro-inflammatory lung cytokine/chemokine environment**

Due to different cell types infected in the lung following intradermal or intranasal inoculation with LVS, we hypothesized that the cytokines and chemokines produced after inoculation would be different. We intranasally inoculated B6 mice with $1x10^4$ CFU LVS and harvested lung tissue 4 hours post-inoculation. Alternatively, B6 mice were intradermally inoculated with $5x10^5$ CFU and lungs were harvested 72 hours post-inoculation. Lungs were also harvested from naïve mice. All lungs were minced in the presence of 50 μg/mL gentamicin. Gentamicin was removed after 1 hour and the lung tissue was cultured overnight. Culture supernatant was collected 24 hours after harvest and

analyzed by Luminex. The average lung cytokine and chemokine concentrations for each group are shown in table 3. Intradermally inoculated mice had a pro-inflammatory lung milieu with significant increases in MIG, MCP-1, IP-10, and IFN-γ compared to naïve or intranasally inoculated mice (figure 9). Intranasally inoculated mice had a significant increase in IL-10 production compared to naïve mice (figure 9). These data indicate that the route of inoculation influences not only the types of cells that are initially infected but also the cytokine milieu of the lung.

By culturing whole lung tissue after inoculation, we identified cytokines and chemokines produced by all cell types in the lung, not just the cells infected with LVS. We attempted to determine the cytokines and chemokines produced specifically by alveolar macrophages after LVS inoculation using alveolar macrophages purified by flow cytometry sorting. Naïve sorted alveolar macrophages produced cytokine in the absence of LVS infection, indicating these cells had become activated during the tissue processing or sorting process. We were therefore unable to identify the cytokines and chemokines specifically produced by alveolar macrophages after intranasal inoculation.

We also attempted to determine whether cytokine and chemokines were produced in the skin following intradermal inoculation. 4 hours post-inoculation we isolated epidermis and dermis from naïve, mock (PBS injected), U112 inoculated, and LVS inoculated mice and cultured whole tissue for 24 hours. Luminex analysis of the culture supernatant showed that very little detectable cytokine or chemokine was produced by the epidermis or dermis. We did detect high levels of IL-1α in the epidermal cultures, however, IL-1α is constitutively produced by epidermal cells, so this result is expected (17, 18). We also detected FGF-basic (dermis), MIP-1α (epidermis), and VEGF (dermis), however all four groups of mice

(including naïve mice) had similar levels indicating these molecules are produced constitutively by the skin and were not being made in response to the infection.

**Depletion of alveolar macrophages increases bacterial burdens in the lung**

Since alveolar macrophages are the dominant infected cell type in the lung early after intranasal inoculation, we sought to determine how disease course would change in the absence of alveolar macrophages. To deplete alveolar macrophages, we utilized the CD11c.diphtheria toxin receptor (CD11c.DTR) mouse which expresses DTR under control of the CD11c promoter. Alveolar macrophages express high levels of CD11c and therefore would also express high levels of DTR, causing alveolar macrophages sensitive to diphtheria toxin depletion. We administered diphtheria toxin (DT) intranasally so that only alveolar macrophages were depleted and not systemic dendritic cells, which also express CD11c. We titrated the dose and timing of DT treatment so that alveolar macrophages were nearly absent prior to inoculation. Initial experiments indicated that nearly all alveolar macrophages were depleted 24 hours after DT treatment. However, when mice were inoculated with LVS 24 hours after DT treatment, mice succumbed within 3 days to neutrophilic pneumonia. We then re-analyzed our flow cytometry data from the initial titration experiments and found a 5-10 fold increase in neutrophils in DT-treated mice compared to PBS-treated mice. We then waited longer after DT treatment to allow time for the number of neutrophils to decrease. On day 5 post-DT-treatment, alveolar macrophages were still 95% depleted while neutrophils were increased only 2-fold (figure 10). Importantly, spleen and lung dendritic cells were present in similar frequencies as untreated mice indicating the DT-treatment did not deplete these populations 5 days post-treatment (figure 10). Therefore, we treated CD11c.DTR mice intranasally with DT 5 days prior to inoculation.

To determine whether the absence of alveolar macrophages affected bacterial burdens, we intranasally inoculated DT-treated CD11c.DTR mice with LVS and determined bacterial burdens in the spleen, liver, and lung on days 3, 7, and 10 post-inoculation (figure 11). On day 3 post-inoculation in the lung, DT-treated mice had significantly higher bacterial burdens compared to PBS-treated mice (figure 11A). Burdens continued to trend higher in the lung on days 7 and 10 post-inoculation in DT-treated mice compared to PBS-treated mice, but did not reach statistical significance (figure 11). Burdens also trended higher in the spleen in DT-treated mice compared to PBS-treated mice for all three time points, but statistical significance was not reached (figure 11). PBS- and DT-treated mice had similar liver burdens on days 3, 7, and 10 post-inoculation. These results indicate that the absence of alveolar macrophages does not significantly affect bacterial burdens in distal organs (spleen and liver). The increase in bacterial burdens in the lung on day 3 post-inoculation in mice lacking alveolar macrophages suggests that alveolar macrophages help control the initial infection.

**Interstitial macrophages are infected with LVS in the absence of alveolar macrophages**

We next sought to determine what cell type(s) were infected with LVS in the absence of alveolar macrophages in DT-treated CD11c.DTR mice. CD11c.DTR mice were treated with DT 5 days prior to intranasal inoculation with LVS. 4 hours post-inoculation, mice were sacrificed, lungs digested into a single cell suspension, and then single cells were stained for flow cytometry sorting. Alveolar macrophages, interstitial macrophages, dendritic cells, and neutrophils were sorted according to the markers described in table 1 and the gating scheme shown in figure 2. When alveolar macrophages are at greatly reduced numbers, interstitial macrophages are the dominant infected cell type 4 hours post-

inoculation (figure 12). However, even with significant alveolar macrophage depletion, nearly 10% of infected cells were alveolar macrophages indicating the remaining cells could still be infected with LVS. When alveolar macrophages were infected, they were infected at a higher rate (0.029% of sorted alveolar macrophages were infected) compared to interstitial macrophages which were present at much higher numbers (0.0059%) Neutrophils comprised a small percent of all infected cells and were only infected in 2 of 7 mice (figure 12). Alveolar macrophages were infected in 3 of 7 mice whereas interstitial macrophages were infected in all 7 mice indicating interstitial macrophages were the preferential target of LVS in the absence of abundant alveolar macrophages.

**The lung has a more pro-inflammatory milieu in the absence of alveolar macrophages**

We next sought to determine whether the cytokine milieu was altered in the absence of alveolar macrophages early after LVS inoculation. We hypothesized there would be an altered milieu because bacterial burdens were increased in the lungs in the absence of alveolar macrophages. B6 or DT-treated CD11c.DTR mice were intranasally inoculated with LVS and lungs harvested 4 hours post-inoculation. Lungs were minced and cultured for 24 hours before culture supernatant was collected and analyzed by Luminex. The average lung cytokine and chemokine concentrations for each group are shown in table 4. We found a significant increase in the concentrations of IL-12, MCP-1, MIG, and VEGF in mice CD11c.DTR mice treated with DT and therefore lacking alveolar macrophages compared to naïve B6 mice or LVS infected B6 mice (figure 13). IL-6 levels were significantly increased in LVS infected CD11c.DTR mice compared to B6 mice. GM-CSF was also elevated in CD11c.DTR mice but the increase did not reach statistical significance. Although we observed a different lung cytokine/chemokine milieu upon LVS inoculation in the absence of

alveolar macrophages, we did not isolate tissue from naïve, DT-treated CD11c.DTR mice to determine whether the changes we observe are due to the LVS infection or simply caused by the DT-treatment. For example, the high levels of GM-CSF could be driving monocyte differentiation into alveolar macrophages to re-populate the lung and may not be a consequence of LVS infection. Further studies are necessary to clearly address whether depletion of alveolar macrophages alters the lung environment prior to LVS inoculation.

## DISCUSSION

*Francisella* is capable of infecting a variety of cell types upon inoculation (15, 16, 19, 20). The early interactions between the host and pathogen set the stage for the adaptive immune response. We and others have shown the route of inoculation influences the type of adaptive immune response that develops (2, 21). We were particularly interested in the early interactions between *Francisella* and the host following intranasal and intradermal inoculation because of differential adaptive immune responses. Intranasal and intradermal inoculation with LVS leads to similar bacterial burdens early after inoculation, yet the adaptive immune responses are very different (2). We hypothesized early events after inoculation, such as the cells infected with *Francisella* immediately after inoculation, were shaping the adaptive immune response. We therefore sought to identify the cells that were infected with *Francisella* after inoculation that were likely responsible for shaping subsequent adaptive immunity.

We identified infected cells by sorting individual populations using flow cytometry. We did not use GFP-expressing bacteria because we had very few infected cells and it would therefore be difficult to identify dimly fluorescent cells among millions of host cells, many

with significant autofluorescence. This technique also only identified host cells infected with live *Francisella*. Experiments using flow cytometry and GFP-expressing bacteria do not determine whether the intracellular bacterium is alive. We had to intranasally inoculate mice with $1x10^4$ CFU to have detectable infected cells after sorting. This inoculum dose is 20-fold higher than our typical LVS intranasal inoculation dose. We do not believe the higher dose altered the distribution of infected cell types, the higher dose likely just increased the overall number of infected cells.

All three strains of *Francisella* predominantly infected alveolar macrophages following intranasal inoculation (figure 3). Alveolar macrophages are the resident macrophages of the airway and interact with inhaled antigens. It is therefore not surprising that inhalation of *Francisella* leads to infection of alveolar macrophages. Other pathogens, like *Mycobacterium tuberculosis*, *Mycoplasma pulmonis*, and *Legionella pneumophila,* target alveolar macrophages upon infection as well (22-25). Experiments conducted by the Dow group and reported in Bosio, et al. found that LVS infects pulmonary dendritic cells 1 hour post-intratracheal inoculation with $5x10^4$ CFU using flow cytometry to detect CFSE labeled bacteria inside of host cells (19). A potential explanation for the seemingly disparate results between the two experiments is the use of different surface markers to define airway dendritic cells and alveolar macrophages. Bosio, et al. defined dendritic cells as $CD11c^+$, $DEC\text{-}205^+$, $CD11b^-$, and $GR\text{-}1^-$ and alveolar macrophages as $CD11c^-$, $DEC\text{-}205^-$, $CD11b^+$, and $GR\text{-}1^+$ (19). We defined alveolar macrophages as $CD11c^{high}$ and $CD11b^{mid}$ (table 1). The markers described by Bosio, et al. for alveolar macrophages are a better fit with how we define interstitial macrophages (table 1). More recently, the Dow group reported in Guth, et al. that alveolar macrophages express high levels of DEC-205 and CD11c, giving this

macrophage cell subset a more dendritic cell-like surface phenotype (26). Therefore, the more recent work by the Dow group indicates that what they defined as dendritic cells in 2005 are actually alveolar macrophages. Thus, our results are consistent with the results described by Bosio, et al. where alveolar macrophages are the primary cell type targeted by *Francisella* after pulmonary infection.

Because alveolar macrophages were infected following intranasal inoculation with LVS, we sought to determine whether disease course was altered in the absence of alveolar macrophages. Alveolar macrophages express high levels of CD11c (figure 2) and can therefore be depleted in CD11c.DTR mice upon intranasal treatment with diphtheria toxin (DT). We chose to use CD11c.DTR mice so that alveolar macrophages are specifically depleted. Alveolar macrophages can also be depleted by intranasal administration of liposomal clodronate, however this treatment is non-specific and depletes >90% of lung and airway antigen presenting cells (19). Depletion of alveolar macrophages led to a significant increase in bacterial burdens in the lung on day 3 post-inoculation. Burdens continue to trend higher in the lung on days 7 and 10 post-inoculation but the increases did not reach statistical significance. Bacterial burdens were also not significantly increased in the spleen or liver at all three time points. These data suggest that alveolar macrophages help control bacterial burdens at the primary site of infection but do not play a role in bacterial dissemination.

Alveolar macrophages have been shown in other models to be either protective or detrimental during infection (19, 22, 27-29). CBA/J mice succumb rapidly (day 3) to *Klebsiella pneumoniae* in the absence of alveolar macrophages and have significantly higher bacterial burdens in the plasma and lung suggesting that alveolar macrophages control bacterial replication in the lung (27, 29). B6 mice, normally resistant to *Mycoplasma*

*pulmonis*, were more susceptible to infection in the absence of alveolar macrophages, indicating alveolar macrophages are important for host defense during *Mycoplasma* infection (28). In a *Mycobacterium tuberculosis* model, mice lacking alveolar macrophages were less susceptible to infection and had decreased mycobacterial burdens in the lung and liver suggesting the presence of alveolar macrophages is detrimental during infection (22). Bosio, et al. found depletion of alveolar macrophages with clodronate followed 18 hours later by intratracheal inoculation with a lethal dose of LVS led to decreased bacterial burdens and an increase in mean time to death (19). It is possible that the difference in bacterial burdens observed in untreated and clodronate treated mice was due to the absence of cells to infect because nearly all antigen-presenting cells were reported to be depleted (19). In our model of alveolar macrophage depletion, there are still other cells available for infection which could account for our different results. Additionally, Bosio, et la. inoculated mice with a high dose that killed untreated mice by 6 days, indicating there is little, if any, contribution of the adaptive immune response. In our model, the inoculation dose is half of the reported $LD_{50}$ for intranasal inoculation and all infected mice survive (9, 10). The increase in bacterial burdens on day 3 post-inoculation and then similar burdens on day 7 and 10 suggests that there are defects in the innate immune response in the absence of alveolar macrophages but that the adaptive immune response is able to mediate bacterial clearance whether or not mice had alveolar macrophages upon LVS inoculation. Future experiments should examine whether the adaptive immune response changes in the absence of alveolar macrophages during the primary response.

*Francisella* infects neutrophils, macrophages, and dendritic cells in the epidermis and dermis of the tail following intradermal inoculation (figure 5, 6). Neutrophils are recruited to

the skin upon tissue damage during PBS injection (figure 7). We therefore suggest a model where dendritic cells (epidermis) or macrophages (dermis) are resident cells infected with *Francisella* and that recruited neutrophils become infected with *Francisella* when they encounter bacteria in the intradermal space. It is not clear how *Francisella* disseminates from the site of inoculation on the tail to the lung. The long-held paradigm was that *Francisella* was strictly an intracellular pathogen in vivo and was carried to distal sites within host cells (30). Forestal, et al. was the first refute this dogma by describing cell-free LVS and SchuS4 in the plasma of infected mice (31). U112 has also been found non-cell associated in mouse plasma (32). To test whether *Francisella* disseminates as free bacteria in the bloodstream, mice could be treated with gentamicin to kill extracellular bacteria and bacterial burdens in distal organs monitored. If the time course of infection and bacterial burdens are similar in gentamicin and vehicle treated mice, these data would suggest that while *Francisella* can survive extracellularly, the bacteria disseminate within host cells. The dosage of gentamicin would need to be carefully titrated for such an experiment so that the dose is high enough to kill extracellular bacteria but low enough so that the gentamicin does not enter host cells and kill intracellular bacteria.

While we did not pursue experiments to determine the underlying mechanisms responsible for bacterial dissemination, we identified interstitial macrophages and neutrophils as the dominant infected cell types in the lung after intradermal inoculation and bacterial dissemination (figure 8). We carefully timed the lung harvest after intradermal inoculation so that we were identifying infected cells soon after bacteria disseminated to the lung. When the cytokine milieus were compared at time points early after bacterial entry into the lung (4 hours post-intranasal, 72 hours post-intradermal inoculation), we found intradermal

inoculation led to a more pro-inflammatory environment compared to naïve or intranasally inoculated mice (figure 9). These results are consistent with a more robust Th1 response in the lung during the adaptive immune response following intradermal inoculation (2).

If the cytokine and chemokines produced in DT-treated CD11c.DTR mice are due to the infection, the presence of a pro-inflammatory environment is consistent with the infection of interstitial macrophages (figures 8, 9, and 12). Intradermally inoculated mice did not have infected alveolar macrophages following bacterial dissemination (figure 8). Intradermally inoculated mice also had a more pro-inflammatory lung milieu compared to intranasally inoculated mice (figure 9). The presence of a pro-inflammatory lung milieu in DT-treated CD11c.DTR mice where interstitial macrophages are the dominant infected cell type (figure 12) is consistent with previous findings. However, if the lung milieu is more pro-inflammatory, we would expect better control of the infection which we did not observe on day 3 post-inoculation in the lung. It is possible that the lung milieu is initially pro-inflammatory, but changes by day 3. Additional experiments are necessary to determine whether the lung milieu is altered on day 3 post-inoculation in mice lacking alveolar macrophages. We also need to determine how the lung milieu changes upon depletion of alveolar macrophages because it is likely many of the changes observed were not due simply to the presence of LVS. For instance, we did observe an increase in GM-CSF concentration, but the increase did not reach statistical significance. GM-CSF is necessary for expressing high levels of CD11c and is therefore likely involved in the re-population of lung alveolar macrophages (26).

Overall, we have identified alveolar macrophages are initially infected with *Francisella* in the lung intranasal and macrophages, dendritic cells, and neutrophils are

infected in the skin after intradermal inoculation. We also determined interstitial macrophages are infected with *Francisella* in the lung following bacterial dissemination in the skin. We had previously observed a differential adaptive immune response following intranasal and intradermal inoculation, despite similar bacterial burdens early after inoculation. We predict there would be differences in the innate immune response in the lung that was contributing to the development of two distinct T cell responses and this was the case; different types of cells were infected following each inoculation route and the lung cytokine milieu was also different. We have begun to examine the immune response in the absence of alveolar macrophages during intranasal inoculation. Bacterial burdens are higher in the lung on day 3 post-inoculation in the absence of alveolar macrophages but are not increased later in infection. Additional experiments are necessary to determine whether the lung's cellular composition and cytokine milieu are altered on day 3 post-inoculation and whether this results in differences in the adaptive immune response. The work presented here does increase our understanding of the early interactions between the host and *Francisella* for two commonly studied routes of inoculation.

**Figure 1**

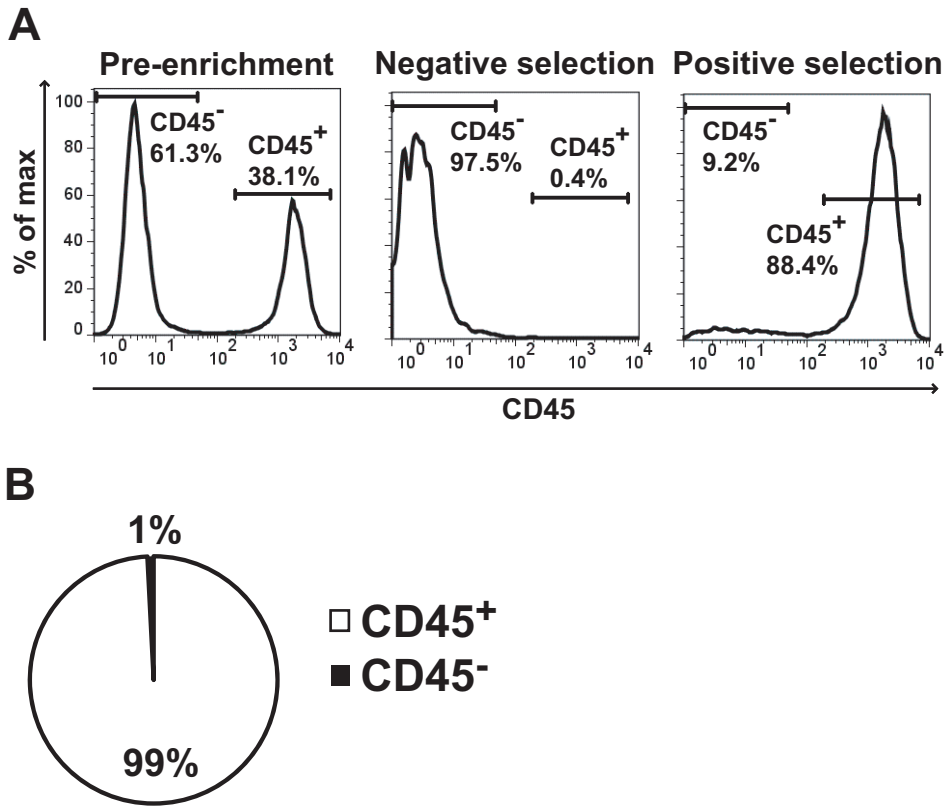


**Figure 1.** ***LVS infects myeloid-derived cells following intranasal inoculation.*** B6 mice were intranasally inoculated with $1x10^4$ CFU LVS. 4 hours post-infection mice were sacrificed and lungs were removed and digested into a single cell suspension. Cells were stained with CD45 APC and then $CD45^+$ cells were enriched using magnetic beads. A) Representative flow cytometry analysis of CD45 enrichment. B) $CD45^+$ and $CD45^-$ populations were directly plated on chocolate agar and the number of colonies were counted 72 hours later. Data are represented as the % of CFUs within a population out of all recovered colonies from 4 infected mice in 2 independent experiments.

**Table 1**

**Table 1. Identification of lung cell types**

| Cell type | Surface markers[a] |
|---|---|
| Alveolar macrophages | F4/80$^{high}$, CD11c$^{high}$, CD11b$^{mid}$ |
| Interstitial macrophages | F4/80$^{high}$, CD11c$^{var}$, CD11b$^{high}$ |
| Dendritic cells | F4/80$^{low}$, CD11c$^{high}$, CD11b$^{low}$ |
| Other | F4/80$^{low}$, CD11c$^{low}$, CD11b$^{var}$ |
| Neutrophils | F4/80$^{low}$,CD11b$^{high}$, GR-1$^{high}$ |

[a] mid, medium level; var, variable level

**Figure 2**

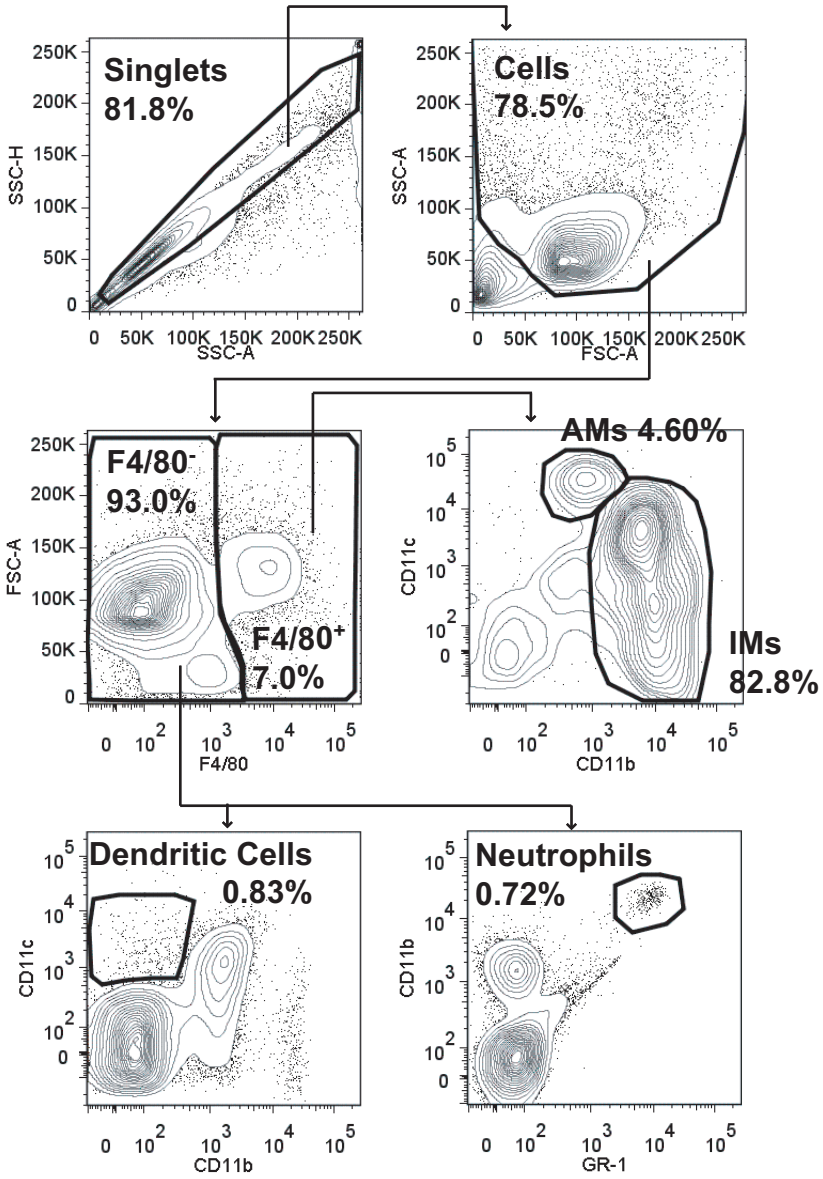


**Figure 2.** ***Lung gating scheme for sorting.*** Single cells were discriminated from doublets by plotting side scatter height (SSC-H) versus side scatter area (SSC-A). Cells were selected by plotting SSC-A versus forward scatter area (FSC-A). F4/80$^-$ and F4/80$^+$ cells were gated on by plotting FSC-A versus F4/80. From the F4/80$^+$ gate, alveolar macrophages (AMs) were discriminated from interstitial macrophages (IMs) by plotting CD11c versus CD11b. Of the F4/80$^-$ cells, dendritic cells were identified by plotting CD11c versus CD11b and neutrophils were identified by plotting CD11b versus GR-1. For each gate, the percent of the parent gate is indicated in bold (for example, AMs are 4.6% of the cells within the F4/80$^+$ gate).

**Figure 3**

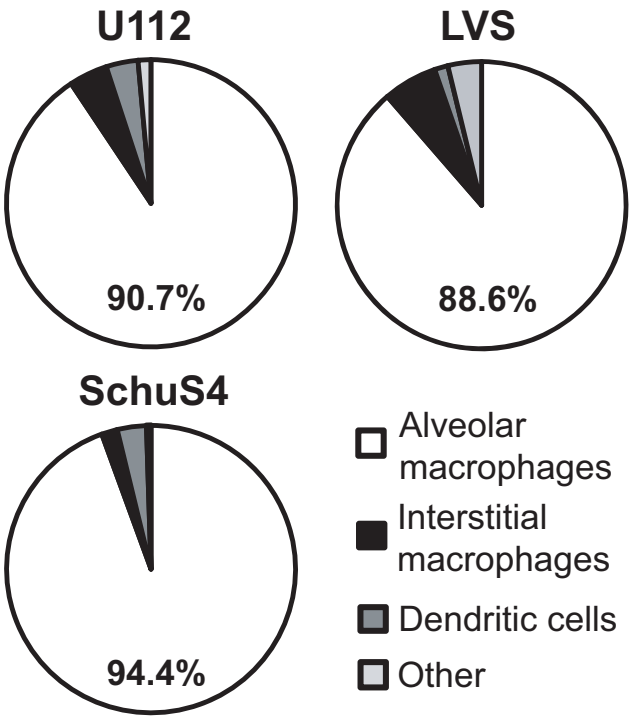


**Figure 3.** ***Alveolar macrophages are the primary infected cell type in the lung after intranasal inoculation with*** **Francisella.** B6 mice were intranasally inoculated with $1x10^4$ CFU U112, LVS, or SchuS4. 4 hours post-inoculation mice were sacrificed and lungs were removed and digested into a single cell suspension and stained for sorting. Alveolar macrophages, interstitial macrophages, dendritic cells, and other cell populations were sorted and directly plated on chocolate agar. Resulting colonies were counted 24-72 hours later. Data are represented as the % of CFUs within a population out of all recovered colonies from 2 mice (U112), 6 mice (LVS), or 3 mice (SchuS4) from 1 (U112), 3 (LVS), or 2 (SchuS4) independent experiments.

**Table 2**

**Table 2. Identification of skin cell types**

| Cell type | Surface markers |
|---|---|
| Dendritic cells | $CD45^{high}$, $F4/80^{low}$, $CD11c^{high}$ |
| Macrophages | $CD45^{high}$, $F4/80^{high}$, $CD11b^{high}$, $GR\text{-}1^{high}$ |
| Neutrophils | $CD45^{high}$, $F4/80^{low}$, $CD11b^{high}$, $GR\text{-}1^{high}$ |
| Langerhans | $CD45^{high}$, $F4/80^{high}$, $CD207^{high}$ |
| Non-myeloid | $CD45^{low}$ |

**Figure 4**

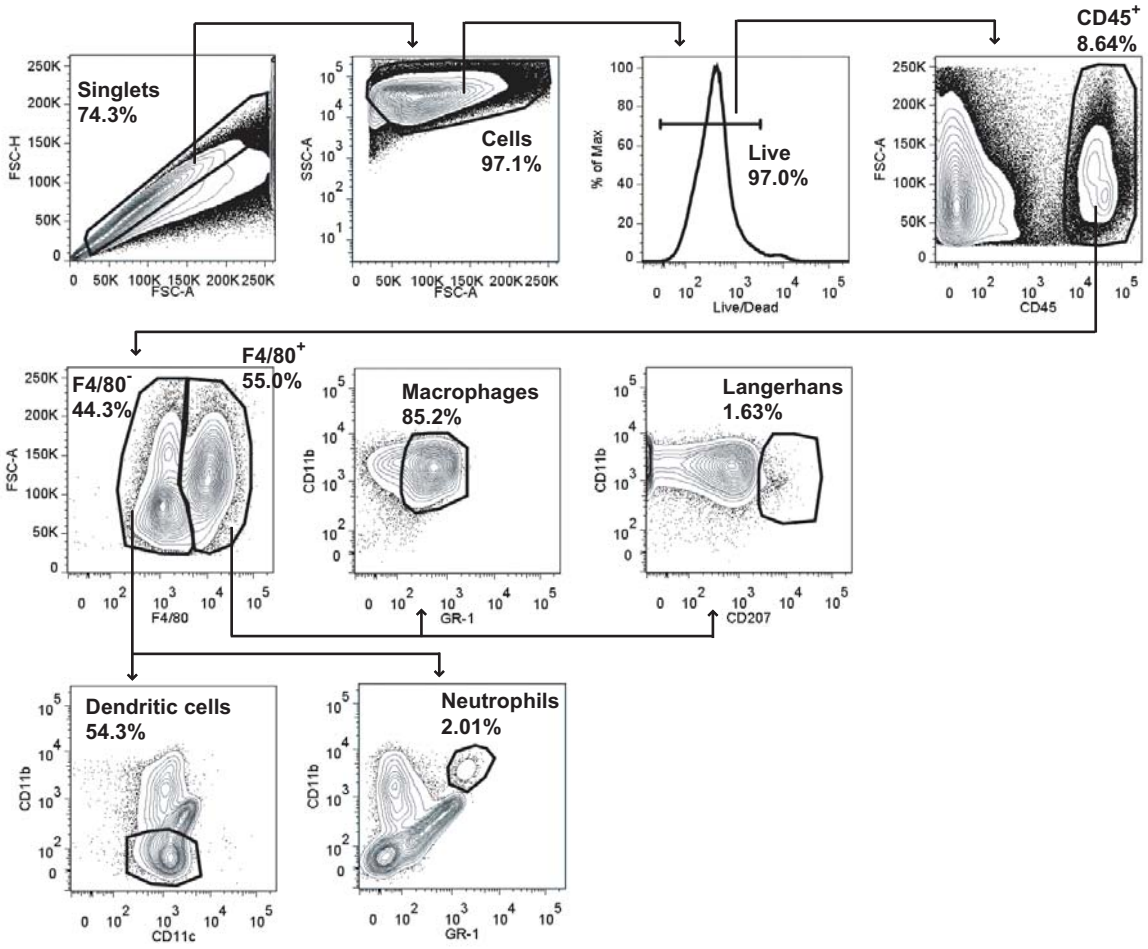


**Figure 4.** ***Epidermis and dermis gating scheme for sorting.*** Single cells were discriminated from doublets by plotting foward scatter height (FSC-H) versus forward scatter area (FSC-A). Cells were selected by plotting side scatter area (SSC-A) versus FSC-A. Live cells were selected using a 1-D histogram. CD45+ cells were gated on by plotting FSC-A versus CD45. F4/80$^-$ and F4/80$^+$ cells were gated on by plotting FSC-A versus F4/80. From the F4/80$^+$ gate, macrophages were gated on by plotting CD11b versus GR-1 and Langerhans were gated on by plotting CD11b versus CD207. Of the F4/80$^-$ cells, dendritic cells were identified by plotting CD11c versus CD11b and neutrophils were identified by plotting CD11b versus GR-1. For each gate, the percent of the parent gate is indicated in bold (for example, macrophages are 85.2% of the cells within the F4/80$^+$ gate).

**Figure 5**

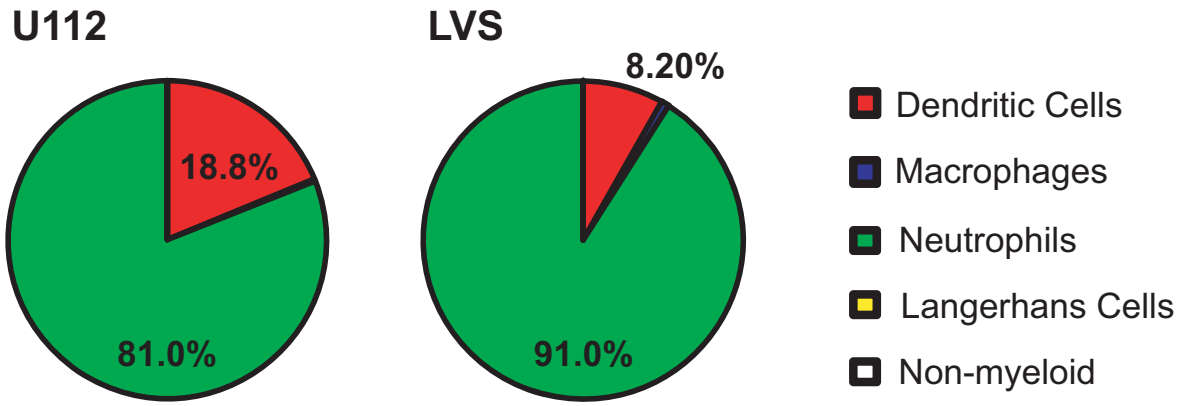


**Figure 5.** ***Neutrophils and dendritic cells are the primary cell types infected with U112 or LVS in the epidermis after intradermal inoculation.*** B6 mice were intradermally inoculated with $5x10^5$ CFU U112 or LVS in 50 µL PBS at the base of the tail. 4 hours post-inoculation, mice were sacrificed and the tails removed. Cells from two mice were combined for each sample. Epidermis and dermis layers were separated, digested into a single cell suspension, and stained for sorting. Dendritic cells, macrophages, neutrophils, Langerhans and non-myeloid cells were sorted and directly plated on chocolate agar. Resulting colonies were counted 24-72 hours later. Data are represented as the % of CFUs within a population out of all recovered colonies from 6 samples (U112 or LVS) from 2 (U112) or 3 (LVS) independent experiments.

**Figure 6**

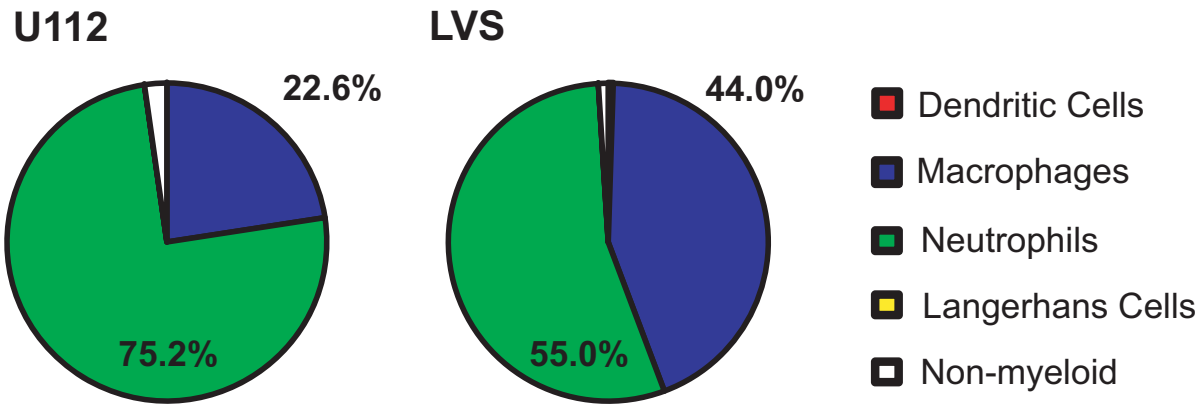


**Figure 6.** ***Neutrophils and macrophages are the primary cell types infected with U112 or LVS in the dermis after intradermal inoculation.*** B6 mice were intradermally inoculated with $5x10^5$ CFU U112 or LVS in 50 µL PBS at the base of the tail. 4 hours post-inoculation, mice were sacrificed and the tails removed. Cells from two mice were combined for each sample. Epidermis and dermis layers were separated, digested into a single cell suspension, and stained for sorting. Dendritic cells, macrophages, neutrophils, Langerhans and non-myeloid cells were sorted and directly plated on chocolate agar. Resulting colonies were counted 24-72 hours later. Data are represented as the % of CFUs within a population out of all recovered colonies from 6 samples (U112 or LVS) from 2 (U112) or 3 (LVS) independent experiments.

**Figure 7**

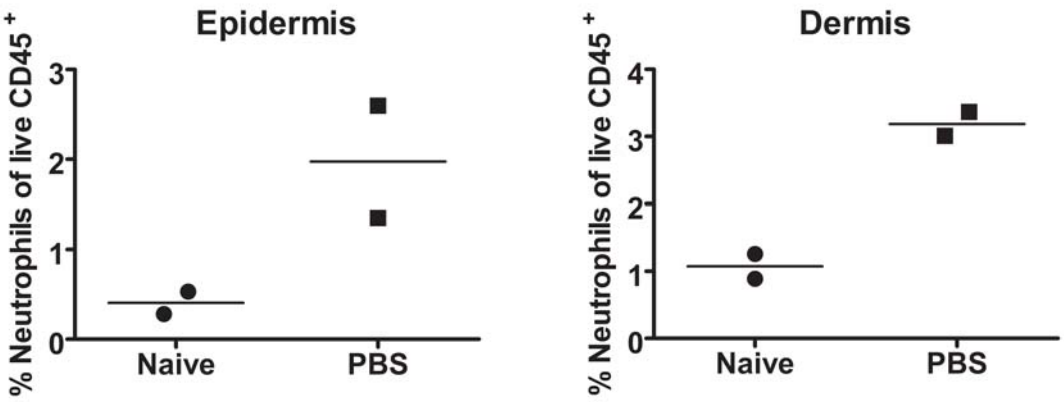


**Figure 7.** ***Neutrophils traffic to the skin following PBS inoculation.*** B6 mice were intradermally inoculated with 50 μL PBS at the base of the tail or left naive. 4 hours post-inoculation, mice were sacrificed and the tails removed. Epidermis and dermis layers were separated, digested into a single cell suspension, and stained for flow cytometry analysis. The % of neutrophils in the live $CD45^+$ gate was determined. n=2 mice. Data are from 1 experiment.

**Figure 8**

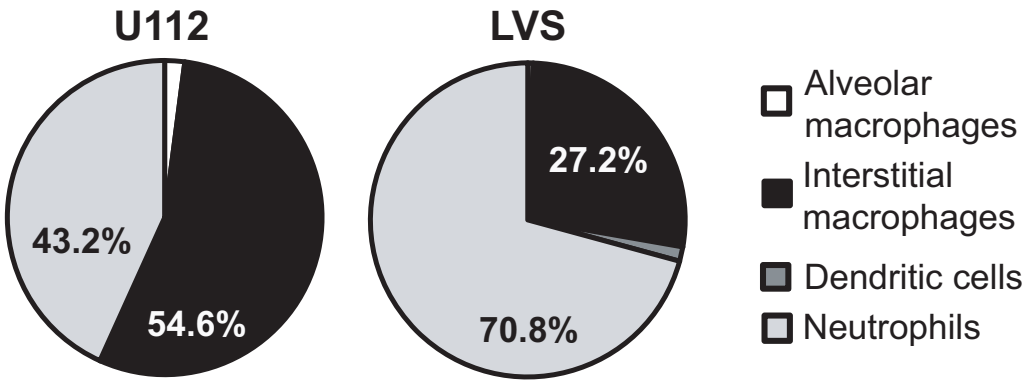


**Figure 8.** ***Interstitial macrophages and neutrophils are the primary cell types infected with U112 or LVS in the lung after intradermal inoculation.*** B6 mice were intradermally inoculated with $5x10^5$ CFU U112 or LVS in 50 μL PBS at the base of the tail. 48 hours post-inoculation mice were sacrificed and lungs were removed and digested into a single cell suspension and stained for sorting. Alveolar macrophages, interstitial macrophages, dendritic cells, and neutrophil cell populations were sorted and directly plated on chocolate agar. Resulting colonies were counted 24-72 hours later. Data are represented as the % of CFUs within a population out of all recovered colonies from 4 mice (U112 or LVS) from 1 (U112 or LVS) experiment per strain.

**Table 3**

**Table 3. Average lung cytokine and chemokine concentrations after two different routes of LVS inoculation (pg/mL)**

| | Intradermal[a] | Intranasal[b] | Naive |
|---|---|---|---|
| **FGF basic** | 69.47 | 69.47 | 69.47 |
| **GM-CSF** | 127.25 | 702.00 | 349.78 |
| **IFN-γ** | 137.30 | 17.21 | 17.21 |
| **IL-1α** | 28.55 | 28.55 | 28.55 |
| **IL-1β** | 24.51 | 24.51 | 24.51 |
| **IL-2** | 11.77 | 11.61 | 11.42 |
| **IL-4** | 30.93 | 30.93 | 30.93 |
| **IL-5** | 37.25 | 129.75 | 152.33 |
| **IL-6** | 549.35 | 823.18 | 600.25 |
| **IL-10** | 81.15 | 154.10 | 63.95 |
| **IL-12** | 10.87 | 11.03 | 16.78 |
| **IL-13** | 22.81 | 22.81 | 22.81 |
| **IL-17** | 3.54 | 3.54 | 3.54 |
| **IP-10** | 243.00 | 19.19 | 19.19 |
| **KC** | 1708.88 | 1785.48 | 1460.70 |
| **MCP-1** | 1025.65 | 102.65 | 47.79 |
| **MIG** | 1270.45 | 3.65 | 7.75 |
| **MIP-1α** | 32.10 | 45.60 | 42.38 |
| **TNF-α** | 17.42 | 17.42 | 17.42 |
| **VEGF** | 665.5 | 296.63 | 391.53 |

[a] Lungs harvested 72 post-intradermal inoculation

[b] Lungs harvested 4 hours post-intranasal inoculation

**Figure 9**

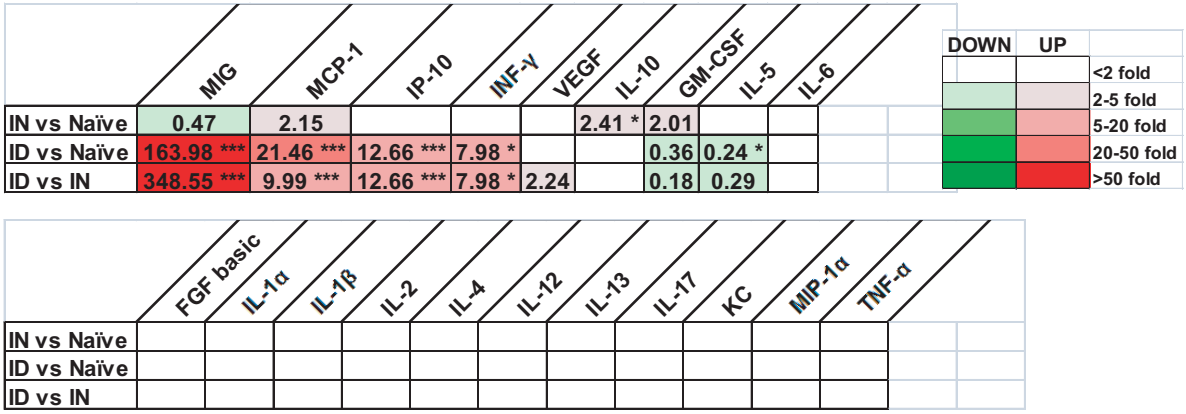


**Figure 9.** ***Intradermal inoculation induces a pro-inflammatory environment in the lung.*** B6 mice were intranasally inoculated with $1x10^4$ CFU LVS, intradermally inoculated with $5x10^5$ CFU LVS, or left naive. 4 hours post-intranasal inoculation or 72 hours post-intradermal inoculation, mice were sacrificed and lungs removed. Minced lungs were cultured for 24 hours. Culture supernatant was collected and analyzed using a Luminex-based assay. n=4 mice/group. Data are from 1 experiment. An ANOVA with Tukey's post-test was used to determine statisical significance for each cytokine or chemokine. Statistical significance is indicated by stars after the fold change when two groups differed.

**Figure 10**

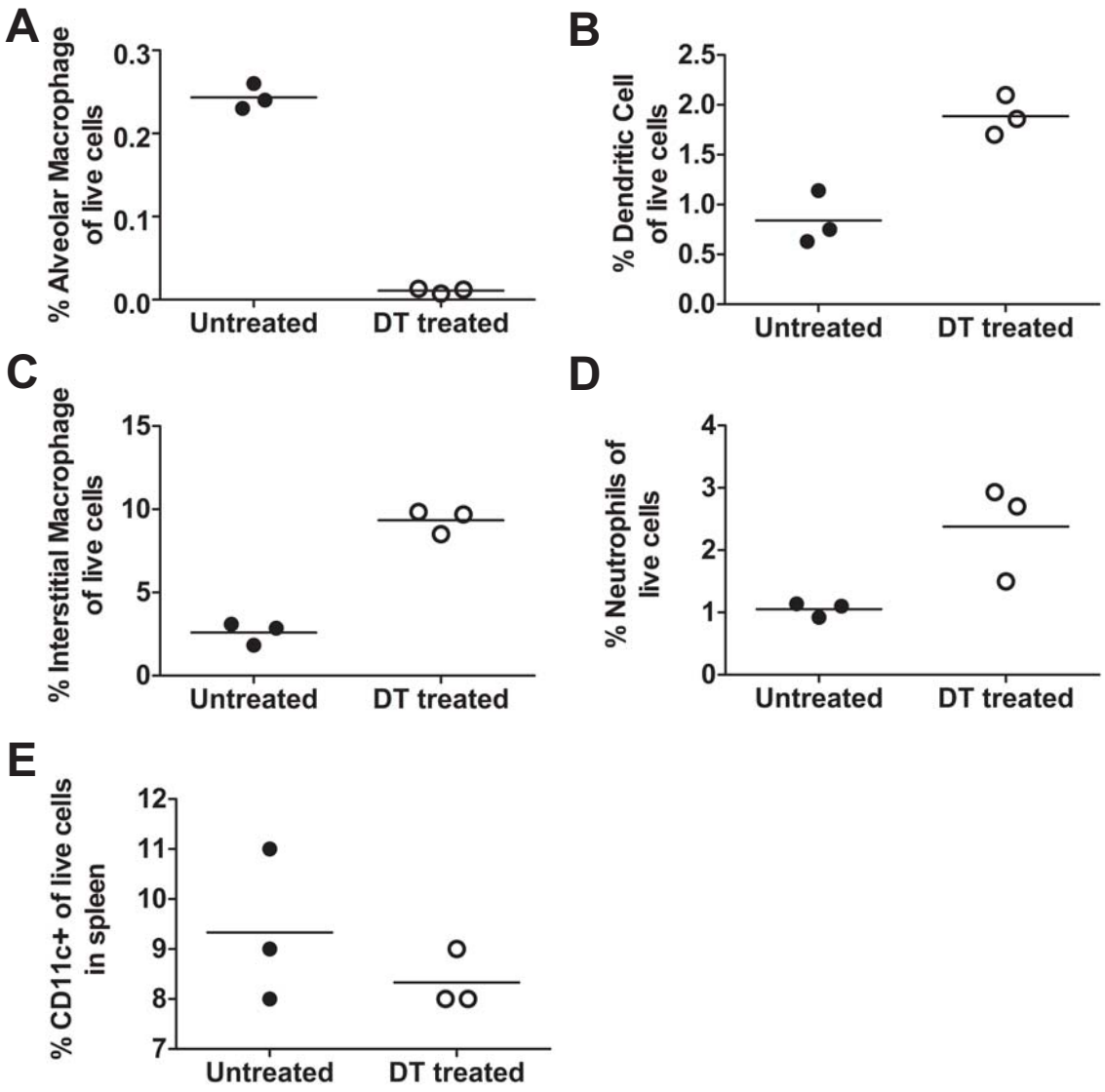


**Figure 10. Intranasal diphtheria toxin treatment depletes alveolar macrophages.** CD11c.DTR mice were intranasally inoculated with 8 ng of diphtheria toxin in 50 μL PBS. 5 days after treatment, lungs were removed, digested into a single cell suspension and strained for flow cytometry analysis. The % A) alveolar macrophages, B) dendritic cells, C) interstitial macrophages, D) neutrophils, and E) spleen dendritic cells was determined of live cells was determined. Each dot represents one mouse. Data are representative of 2 independent experiments.

**Figure 11**

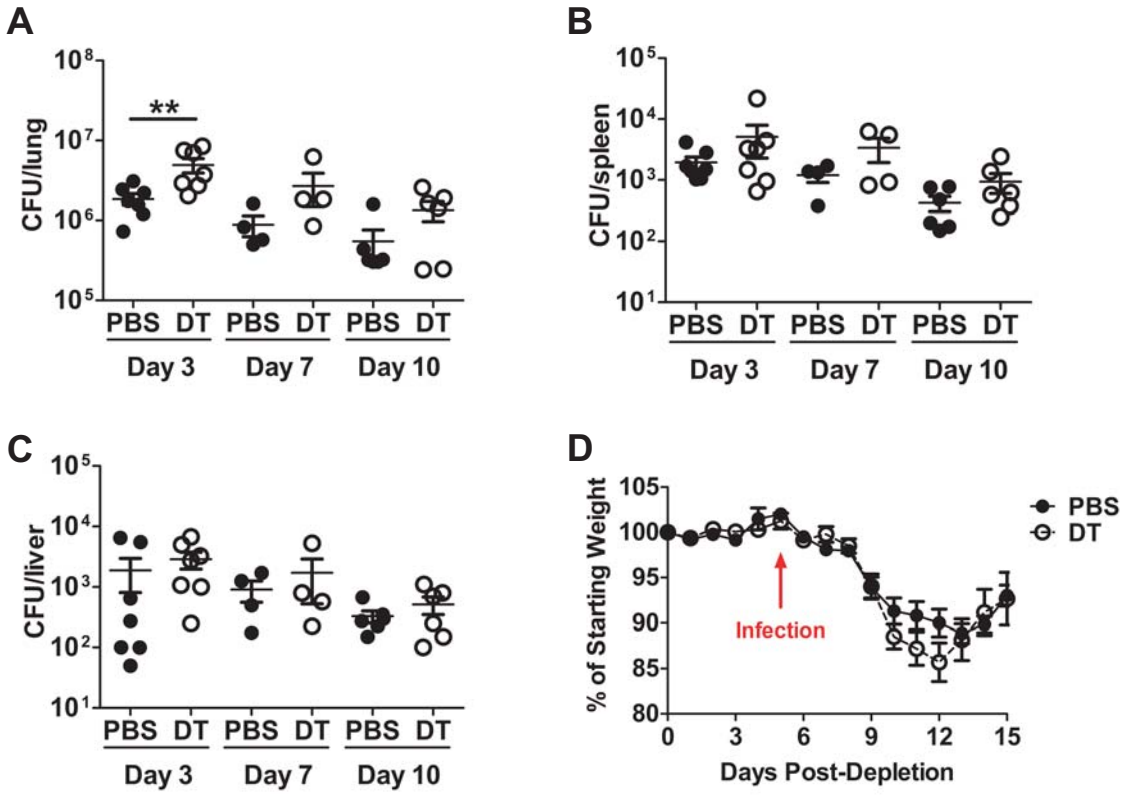


**Figure 11.** ***Bacterial burdens increase in the lung early after LVS inoculation in the absence of alveolar macrophages.*** B6 were intranasally inoculated with 50 µL PBS or CD11c.DTR mice were intranasally inoculated with 8 ng diphtheria toxin (DT) in 50 µL PBS. 5 days later, all mice intranasally inoculated with $5x10^2$ CFU LVS. On days 3, 7, and 10 post-inoculation, bacterial burdens were determined in the A) lung, B) spleen, and C) liver by plating serial dilutions of organ homogenate on chocolate agar. n=4-7 mice/group for each time point. Each dot represents one mouse. Data are from 1 experiment for day 7 and combined from 2 independent experiments for days 3 and 10. Statistical significance was determined on log-transformed data using a Student's t-test. D) Weight loss was determined daily and is reported as a percentage of the starting weight.

**Figure 12**

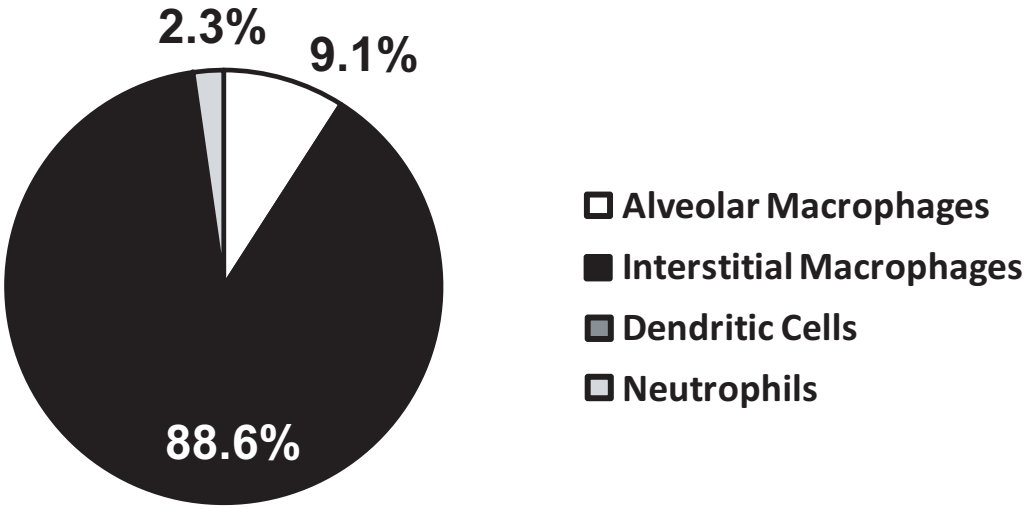


**Figure 12.** ***Interstitial macrophages are the dominant infected cell type in the absence of alveolar macrophages.*** CD11c.DTR mice were intranasally inoculated with 8 ng diphtheria toxin (DT) in 50 μL PBS. 5 days later, mice intranasally inoculated with $1x10^4$ CFU LVS. 4 hours post-inoculation were sacrificed and lungs removed and digested into a single cell suspension and stained for sorting. Alveolar macrophages, interstitial macrophages, dendritic cells, and neutrophils were sorted and directly plated on chocolate agar. Resulting colonies were counted 72 hours later. Data are represented as the % of CFUs within a population out of all recovered colonies from 7 mice from 2 independent experiments.

**Table 4**

**Table 4. Average lung cytokine and chemokine concentrations in the presence or absence of alveolar macrophages following intranasal LVS inoculation (pg/mL)**

| | Naïve B6 | LVS B6 (+ AMs) | LVS CD11c.DTR (-AMs) |
|---|---|---|---|
| **FGF basic** | 24.63 | 24.63 | 24.63 |
| **GM-CSF** | 348.66 | 286.62 | 2714.79 |
| **IFN-γ** | 10.80 | 10.80 | 10.80 |
| **IL-1α** | 14.40 | 14.40 | 14.40 |
| **IL-1β** | 11.80 | 11.80 | 11.80 |
| **IL-2** | 8.27 | 8.27 | 8.27 |
| **IL-4** | 14.59 | 14.59 | 20.38 |
| **IL-5** | 858.12 | 521.89 | 602.90 |
| **IL-6** | 2026.12 | 1030.81 | 2893.26 |
| **IL-10** | 6.26 | 6.26 | 6.26 |
| **IL-12** | 39.43 | 23.94 | 73.17 |
| **IL-13** | 11.56 | 11.56 | 11.56 |
| **IL-17** | 8.31 | 8.31 | 8.31 |
| **IP-10** | 147.98 | 74.19 | 108.30 |
| **KC** | 2111.13 | 2014.51 | 2167.38 |
| **MCP-1** | 183.79 | 163.37 | 369.29 |
| **MIG** | 2.44 | 3.64 | 33.48 |
| **MIP-1α** | 13.76 | 13.76 | 13.76 |
| **TNF-α** | 8.70 | 8.70 | 8.70 |
| **VEGF** | 101.72 | 115.97 | 624.17 |

**Figure 13**

| | IL-12 | MCP-1 | MIG | VEGF | IL-6 | GM-CSF | IP-10 | FGF basic | INF-γ |
|---|---|---|---|---|---|---|---|---|---|
| B6 LVS vs B6 Naïve | | | | | | | 0.50 | | |
| CD11c.DTR LVS vs B6 Naïve | 1.86 *** | 2.01 * | 13.74 ** | 6.14 *** | | 7.7863 | | | |
| CD11c.DTR LVS vs B6 LVS | 3.06 *** | 2.26 * | 9.20 ** | 5.38 *** | 2.81 * | 9.4719 | | | |

| | IL-α | IL-β | IL-2 | IL-4 | IL-5 | IL-10 | IL-13 | IL-17 | KC | MIP-1α | TNF α |
|---|---|---|---|---|---|---|---|---|---|---|---|
| B6 LVS vs B6 Naïve | | | | | | | | | | | |
| CD11c.DTR LVS vs B6 Naïve | | | | | | | | | | | |
| CD11c.DTR LVS vs B6 LVS | | | | | | | | | | | |

| DOWN | UP | |
|---|---|---|
| | | <2 fold |
| | | 2-3 fold |
| | | 3-4 fold |
| | | 4-5 fold |
| | | >5 fold |

**Figure 13.** ***LVS inoculation in the absence of alveolar macrophages induces a pro-inflammatory environment in the lung.*** B6 were intranasally inoculated with 50 µL PBS or CD11c.DTR mice were intranasally inoculated with 8 ng diphtheria toxin (DT) in 50 µL PBS. 5 days later, B6 and CD11c.DTR mice intranasally inoculated with $1x10^4$ CFU LVS or B6 mice were left naive. 4 hours post-intranasal inoculation, mice were sacrificed and lungs removed. Minced lungs were cultured for 24 hours. Culture supernatant was collected and analyzed using a Luminex-based assay. n=4 mice/group. Data are from 1 experiment. An ANOVA with Tukey's post-test was used to determine statisical significance for each cytokine or chemokine. Statistical significance is indicated by stars after the fold change when two groups differed.

## REFERENCES


1. Moon JJ, Chu HH, Pepper M, McSorley SJ, Jameson SC, Kedl RM, et al. Naive CD4(+) T cell frequency varies for different epitopes and predicts repertoire diversity and response magnitude. Immunity. 2007;27(2):203-13. doi: 10.1016/j.immuni.2007.07.007. PubMed PMID: 17707129; PubMed Central PMCID: PMC2200089.

2. Woolard MD, Hensley LL, Kawula TH, Frelinger JA. Respiratory Francisella tularensis live vaccine strain infection induces Th17 cells and prostaglandin E2, which inhibits generation of gamma interferon-positive T cells. Infect Immun. 2008;76(6):2651-9. Epub 2008/04/09. doi: IAI.01412-07 [pii] 10.1128/IAI.01412-07. PubMed PMID: 18391003; PubMed Central PMCID: PMC2423094.

3. Nurieva RI, Chung Y. Understanding the development and function of T follicular helper cells. Cellular & molecular immunology. 2010;7(3):190-7. doi: 10.1038/cmi.2010.24. PubMed PMID: 20383172.

4. Anthony LS, Ghadirian E, Nestel FP, Kongshavn PA. The requirement for gamma interferon in resistance of mice to experimental tularemia. Microb Pathog. 1989;7(6):421-8. Epub 1989/12/01. PubMed PMID: 2516219.

5. Collazo CM, Sher A, Meierovics AI, Elkins KL. Myeloid differentiation factor-88 (MyD88) is essential for control of primary in vivo Francisella tularensis LVS infection, but not for control of intra-macrophage bacterial replication. Microbes Infect. 2006;8(3):779-90. Epub 2006/03/04. doi: S1286-4579(05)00364-3 [pii] 10.1016/j.micinf.2005.09.014. PubMed PMID: 16513388.

6. Leiby DA, Fortier AH, Crawford RM, Schreiber RD, Nacy CA. In vivo modulation of the murine immune response to Francisella tularensis LVS by administration of anticytokine antibodies. Infect Immun. 1992;60(1):84-9. Epub 1992/01/01. PubMed PMID: 1729199; PubMed Central PMCID: PMC257506.

7. Oyston PC. Francisella tularensis vaccines. Vaccine. 2009;27 Suppl 4:D48-51. doi: 10.1016/j.vaccine.2009.07.090. PubMed PMID: 19837286.

8. Fortier AH, Green SJ, Polsinelli T, Jones TR, Crawford RM, Leiby DA, et al. Life and death of an intracellular pathogen: Francisella tularensis and the macrophage. Immunology series. 1994;60:349-61. Epub 1994/01/01. PubMed PMID: 8251580.

9. Metzger DW, Bakshi CS, Kirimanjeswara G. Mucosal immunopathogenesis of Francisella tularensis. Ann N Y Acad Sci. 2007;1105:266-83. Epub 2007/03/31. doi: annals.1409.007 [pii] 10.1196/annals.1409.007. PubMed PMID: 17395728.

10. Fortier AH, Slayter MV, Ziemba R, Meltzer MS, Nacy CA. Live vaccine strain of Francisella tularensis: infection and immunity in mice. Infect Immun. 1991;59(9):2922-8. PubMed PMID: 1879918; PubMed Central PMCID: PMC258114.

11. Kieffer TL, Cowley S, Nano FE, Elkins KL. Francisella novicida LPS has greater immunobiological activity in mice than F. tularensis LPS, and contributes to F. novicida murine pathogenesis. Microbes Infect. 2003;5(5):397-403. PubMed PMID: 12737995.

12. Lauriano CM, Barker JR, Yoon SS, Nano FE, Arulanandam BP, Hassett DJ, et al. MglA regulates transcription of virulence factors necessary for Francisella tularensis intraamoebae and intramacrophage survival. Proc Natl Acad Sci U S A. 2004;101(12):4246-9. Epub 2004/03/11. doi: 10.1073/pnas.0307690101 [doi] 0307690101 [pii]. PubMed PMID: 15010524; PubMed Central PMCID: PMC384726.

13. Tarnvik A, Berglund L. Tularaemia. Eur Respir J. 2003;21(2):361-73. Epub 2003/03/01. PubMed PMID: 12608453.

14. Saslaw S, Eigelsbach HT, Prior JA, Wilson HE, Carhart S. Tularemia vaccine study. II. Respiratory challenge. Arch Intern Med. 1961;107:702-14. Epub 1961/05/01. PubMed PMID: 13746667.

15. Hall JD, Woolard MD, Gunn BM, Craven RR, Taft-Benz S, Frelinger JA, et al. Infected-host-cell repertoire and cellular response in the lung following inhalation of Francisella tularensis Schu S4, LVS, or U112. Infect Immun. 2008;76(12):5843-52. Epub 2008/10/15. doi: IAI.01176-08 [pii] 10.1128/IAI.01176-08. PubMed PMID: 18852251; PubMed Central PMCID: PMC2583552.

16. Hall JD, Craven RR, Fuller JR, Pickles RJ, Kawula TH. Francisella tularensis replicates within alveolar type II epithelial cells in vitro and in vivo following inhalation. Infect Immun. 2007;75(2):1034-9. Epub 2006/11/08. doi: IAI.01254-06 [pii] 10.1128/IAI.01254-06. PubMed PMID: 17088343; PubMed Central PMCID: PMC1828526.

17. Hauser C, Saurat JH, Schmitt A, Jaunin F, Dayer JM. Interleukin 1 is present in normal human epidermis. J Immunol. 1986;136(9):3317-23. PubMed PMID: 3007615.

18. Schmitt A, Hauser C, Jaunin F, Dayer JM, Saurat JH. Normal epidermis contains high amounts of natural tissue IL 1 biochemical analysis by HPLC identifies a MW approximately 17 Kd form with a P1 5.7 and a MW approximately 30 Kd form. Lymphokine research. 1986;5(2):105-18. PubMed PMID: 3486328.

19. Bosio CM, Dow SW. Francisella tularensis induces aberrant activation of pulmonary dendritic cells. J Immunol. 2005;175(10):6792-801. Epub 2005/11/08. doi: 175/10/6792 [pii]. PubMed PMID: 16272336.

20. Bosio CM, Bielefeldt-Ohmann H, Belisle JT. Active suppression of the pulmonary immune response by Francisella tularensis Schu4. J Immunol. 2007;178(7):4538-47. Epub 2007/03/21. doi: 178/7/4538 [pii]. PubMed PMID: 17372012.

21. Pepper M, Linehan JL, Pagan AJ, Zell T, Dileepan T, Cleary PP, et al. Different routes of bacterial infection induce long-lived TH1 memory cells and short-lived TH17 cells. Nat Immunol. United States2010. p. 83-9.

22. Leemans JC, Juffermans NP, Florquin S, van Rooijen N, Vervoordeldonk MJ, Verbon A, et al. Depletion of alveolar macrophages exerts protective effects in pulmonary tuberculosis in mice. J Immunol. 2001;166(7):4604-11. PubMed PMID: 11254718.

23. Davis JK, Davidson MK, Schoeb TR, Lindsey JR. Decreased intrapulmonary killing of Mycoplasma pulmonis after short-term exposure to NO2 is associated with damaged alveolar macrophages. The American review of respiratory disease. 1992;145(2 Pt 1):406-11. doi: 10.1164/ajrccm/145.2_Pt_1.406. PubMed PMID: 1736750.

24. Gordon SB, Read RC. Macrophage defences against respiratory tract infections. British medical bulletin. 2002;61:45-61. PubMed PMID: 11997298.

25. Nash TW, Libby DM, Horwitz MA. Interaction between the legionnaires' disease bacterium (Legionella pneumophila) and human alveolar macrophages. Influence of antibody, lymphokines, and hydrocortisone. The Journal of clinical investigation. 1984;74(3):771-82. doi: 10.1172/JCI111493. PubMed PMID: 6470140; PubMed Central PMCID: PMC425231.

26. Guth AM, Janssen WJ, Bosio CM, Crouch EC, Henson PM, Dow SW. Lung environment determines unique phenotype of alveolar macrophages. Am J Physiol Lung Cell Mol Physiol. 2009;296(6):L936-46. doi: 10.1152/ajplung.90625.2008. PubMed PMID: 19304907; PubMed Central PMCID: PMC2692811.

27. Cheung DO, Halsey K, Speert DP. Role of pulmonary alveolar macrophages in defense of the lung against Pseudomonas aeruginosa. Infect Immun. 2000;68(8):4585-92. PubMed PMID: 10899859; PubMed Central PMCID: PMC98382.

28. Hickman-Davis JM, Michalek SM, Gibbs-Erwin J, Lindsey JR. Depletion of alveolar macrophages exacerbates respiratory mycoplasmosis in mycoplasma-resistant C57BL mice but not mycoplasma-susceptible C3H mice. Infect Immun. 1997;65(6):2278-82. PubMed PMID: 9169764; PubMed Central PMCID: PMC175316.

29. Broug-Holub E, Toews GB, van Iwaarden JF, Strieter RM, Kunkel SL, Paine R, 3rd, et al. Alveolar macrophages are required for protective pulmonary defenses in murine Klebsiella pneumonia: elimination of alveolar macrophages increases neutrophil recruitment but decreases bacterial clearance and survival. Infect Immun. 1997;65(4):1139-46. PubMed PMID: 9119443; PubMed Central PMCID: PMC175109.

30. Long GW, Oprandy JJ, Narayanan RB, Fortier AH, Porter KR, Nacy CA. Detection of Francisella tularensis in blood by polymerase chain reaction. J Clin Microbiol. 1993;31(1):152-4. PubMed PMID: 8417022; PubMed Central PMCID: PMC262641.

31. Forestal CA, Malik M, Catlett SV, Savitt AG, Benach JL, Sellati TJ, et al. Francisella tularensis has a significant extracellular phase in infected mice. The Journal of infectious diseases. 2007;196(1):134-7. doi: 10.1086/518611. PubMed PMID: 17538893.

32. Yu JJ, Raulie EK, Murthy AK, Guentzel MN, Klose KE, Arulanandam BP. The presence of infectious extracellular Francisella tularensis subsp. novicida in murine plasma after pulmonary challenge. European journal of clinical microbiology & infectious diseases : official publication of the European Society of Clinical Microbiology. 2008;27(4):323-5. doi: 10.1007/s10096-007-0434-x. PubMed PMID: 18087734.

# CHAPTER 5

## IDENTIFICATION OF *FRANCISELLA NOVICIDA* MUTANTS THAT FAIL TO INDUCE PROSTAGLANDIN E2 SYNTHESIS BY INFECTED MACROPHAGES[1,2]

## OVERVIEW

*Francisella tularensis* is the causative agent of tularemia. We have previously shown that infection with *F. tularensis* Live Vaccine Strain (LVS) induces macrophages to synthesize prostaglandin $E_2$ ($PGE_2$). Synthesis of $PGE_2$ by *F. tularensis* infected macrophages results in decreased T cell proliferation *in vitro* and increased bacterial survival *in vivo.* Although we understand some of the biological consequences of *F. tularensis* induced $PGE_2$ synthesis by macrophages, we do not understand the cellular pathways (neither host nor bacterial) that result in up-regulation of the $PGE_2$ biosynthetic pathway in *F. tularensis* infected macrophages. We took a genetic approach to begin to understand the molecular mechanisms of bacterial induction of $PGE_2$ synthesis from infected macrophages. To identify *F. tularensis* genes necessary for the induction of $PGE_2$ in primary macrophages, we infected cells with individual mutants from the closely related strain *Francisella tularensis* subspecies *novicida* U112 (U112) two allele mutant library. Twenty genes were identified that when disrupted resulted in U112 mutant strains unable to induce the synthesis

---

[1] Contributing authors: Matthew D. Woolard, Lydia M. Barrigan, James R. Fuller, Adam S. Buntzman, Joshua Bryan, Colin Manoil, Thomas H. Kawula, and Jeffrey A. Frelinger

[2] This work was published in Frontiers in Microbiology: Front. Microbio. 4:16. Doi:10.3389/fmicb.2013.00016

of $PGE_2$ by infected macrophages. Fourteen of the genes identified are located within the *Francisella* pathogenicity island (FPI). Genes in the FPI are required for *F. tularensis* to escape from the phagosome and replicate in the cytosol, which might account for the failure of U112 with transposon insertions within the FPI to induce $PGE_2$. This implies that U112 mutant strains that do not grow intracellularly would also not induce $PGE_2$. We found that U112 *clpB*::Tn grows within macrophages yet fails to induce $PGE_2$, while U112 *pdpA*::Tn does not grow yet does induce $PGE_2$. We also found that U112 *iglC*::Tn neither grows nor induces $PGE_2$. These findings indicate that there is dissociation between intracellular growth and the ability of *F. tularensis* to induce $PGE_2$ synthesis. These mutants provide a critical entrée into the pathways used in the host for $PGE_2$ induction.

## INTRODUCTION

*Francisella tularensis* is a facultative intracellular bacterium and the causative agent of tularemia. *F. tularensis* has a low infective dose, high morbidity, and can persist in the environment (1). *F. tularensis* has also been produced as a bioweapon (2), and is classified as a Category A Select Agent. There are four major subspecies of *F. tularensis*: *F. tularensis* subspecies *tularensis, F. tularensis* subspecies *holarctica, F. tularensis* subspecies *mediasiatica,* and *F. tularensis* subspecies *novicida. F. tularensis, F. holarctica* (including the Live Vaccine Strain (LVS)) and *F. novicida* all cause a fulminate disease in mice that is similar to tularemia in humans (3). There are clear differences in virulence between strains in mice. *F. novicida, F. holarctica* and *F. tularensis* can have and $LD_{50}$ of less than 10 organisms in intranasally inoculated mice, while *F. holarctica* LVS $LD_{50}$ in mice is much higher (4). Each strain varies in its capacity to cause disease in humans. *F. novicida* is

highly attenuated in humans, only causing disease in immuno-compromised individuals (5, 6). *F. holarctica* is highly infectious in humans, but causes a milder form of tularemia compared to *F. tularensis. F. holarctica* LVS is highly attenuated for disease in humans but can cause disease in immunocompetent individuals (1, 7, 8). Though each strain has a different level of virulence in humans, they share high nucleotide sequence identity. *F. novicida* shares 95% nucleotide sequence identity with *F. tularensis* and *F. holarctica* (9), suggesting that homologous proteins function via similar mechanisms.

Key to *F. tularensis'* virulence is its ability to escape the phagosome and replicate within the cytosol of host cells. Previous studies have identified over 200 genes that are necessary for intracellular growth of *F. tularensis* (10-14). Some of the genes required for escape from the phagosome and intracellular growth reside within the *Francisella* pathogenicity island (FPI) (15). The FPI is a set of 16 genes that are highly conserved among all subspecies of *F. tularensis* (15). The FPI likely encodes a secretion system that is related to the recently discovered type VI secretion systems (T6SS) (16, 17). The T6SS is involved in the virulence of several bacterial pathogens (18-21). Several regulators of FPI expression have been described. Two of the best studied are MglA and SspA, which positively regulate the transcription of FPI genes (22-24). The mechanisms by which FPI proteins promote *F. tularensis* escape and intra-macrophage growth are unknown. There is evidence that translocated products of T6SS in other bacteria are capable of modulating host immune responses (18, 25-27). Though FPI gene products are clearly involved in phagosome escape and intracellular growth, the ability of these gene products to induce immunomodulatory responses has not been demonstrated to date.

$PGE_2$ synthesis induced by LVS from host cells alters both innate and adaptive immune responses. We demonstrated that *F. tularensis* LVS was capable of inducing macrophages to synthesize $PGE_2$ and that this was independent of intracellular growth of *F. tularensis* (28). *In vitro*, LVS induced $PGE_2$ synthesis inhibits T cell proliferation and skews their phenotypic development from IFN-$\gamma^+$ T cells to IL-$4^+$ T cells (28). Through an indirect mechanism $PGE_2$, induces ubiquitin mediated degradation of MHC II which results in decreased MHC II protein levels on the surface of macrophages (29). Decreased MHC II surface expression would decrease the antigenic stimulatory capacity of these macrophages, likely making them less capable of activating *F. tularensis* specific T cells. T cells are required for both clearance of *F. tularensis* and generation of long-term immune protection (30), thus the biological activity of $PGE_2$ would be beneficial to *F. tularensis* survival *in vivo*. LVS-induced $PGE_2$ synthesis during respiratory tularemia inhibits the generation of beneficial T cell response. The inhibition of $PGE_2$ synthesis *in vivo* by indomethacin leads to increased number of IFN-$\gamma^+$ T cells and decreased bacterial burden (31). It is clear that induction of $PGE_2$ synthesis is an important immune modulation mechanism utilized by *F. holarctica* to persist in the host.

Presently, none of the *F. tularensis* product(s) responsible for the induction of $PGE_2$ synthesis in eukaryotic cells are known. Several bacterial products have been identified that are capable of inducing $PGE_2$ synthesis. Bacterial peptidoglycan, LPS, and CpG DNA can up-regulate prostaglandin synthesis through interactions with TLR2, TLR4, and TLR9 respectively (32-36). It is not known if *F. tularensis* is capable of inducing $PGE_2$ through a similar mechanism. To date, few *F. tularensis* TLR ligands have been identified. *F. tularensis* LpnA and FTT1103 have been reported to be TLR2 ligands and DnaK a TLR4

ligand (37-39). *F. tularensis* LPS fails to or only weakly stimulates a cytokine response by host cells (40, 41). If *F. tularensis* LPS does stimulate host cells, it is likely in a TLR4 independent manner. Both TLR2 and TLR4 deficient macrophages produce $PGE_2$ after infection (Woolard et al. unpublished).

In this study we demonstrate that along with LVS, *F. novicida* U112 (U112), and *F. tularensis tularensis* Schu S4 (Schu S4) induce $PGE_2$ synthesis by macrophages. We tested a *F. novicida* (U112) comprehensive transposon mutant library to identify genes necessary for induction of $PGE_2$ synthesis by infected bone marrow-derived macrophages. This library allowed us to identify 20 genes that when disrupted result in U112 strains that are unable to induce the synthesis of $PGE_2$ by infected macrophages. Identified genes included genes of the FPI and regulators of the FPI. All genes identified are highly conserved among all sequenced strains of *F. tularensis* (17, 23, 42, 43). We also demonstrate that the ability of *F. novicida* to induce $PGE_2$ synthesis is likely not dependent on phagosome escape nor intracellular growth. This work likely suggests that the FPI is involved in immune modulation along with previously established mechanisms of phagosomal escape and intracellular growth.

## MATERIALS AND METHODS

### Bacteria and mouse strains

The *F. tularensis* subspecies *holarctica* LVS was obtained from ATCC (29684; American Type Culture Collection (Manassas, VA) (44), the *F. tularensis* subspecies *novicida* U112 strain was previously published (45), and the *F. tularensis* subspecies *tularensis* Schu S4 strain (catalog no. NR-643) was obtained from the Biodefense Emerging

Infections Research Resources Repository (Manassas, VA). The two allele transposon library was previously described (46). For all studies, except for the original screen, *F. novicida* was propagated on tryptic soy agar supplemented with 0.1% cysteine while the *F. novicida* transposon mutants where propagated on the same agar with the addition of 20 μg/ml of kanamycin. *F. holarctica* LVS and *F. tularensis* Schu S4 where propagated on chocolate agar. Inocula were generated by collecting plate grown bacteria and diluting them in PBS to reach an $OD_{600}$ of 1.00. Inocula where then diluted into appropriate cell culture medium for inoculation.

The *F. novicida* two allele transposon library was previously described (Gallagher et al., 2007). The LVS Δ*mglA*, LVS Δ*sspA*, LVS *ΔmglA pmglA*, and LVS Δ*sspA psspA* were previously published (47). The *dotU* deletion construct was made by splice overlap extension PCR retaining the start and stop codons of *dotU and* fusing the first four and last two codons in frame and retaining 0.8 kb of flanking sequence. The constructs were cloned into the suicide vector pMP590 and sequenced to confirm the integrity of the DNA sequence. The LVS *dotU* mutant was generated by allelic exchange, selection for plasmid co-integrates, and counter selection on sucrose containing media to identify plasmid and *dotU* allele resolution as described (48). The following primers were utilized to generated the SOE fragment; FTL0119 5' ext 5'-GAGTTTTTTCCACCTCTGAGGATGTTTC, FTL0119 5' int 5'-GAAAGACTTTAAAGAGATAGAATAATAAGGGTAAGAGGAGATTTATATGAGTCAGATAATATC, FTL0119 3' int 5'-CTCCTCTTACCCTTATTATTCTATCTCTTTAAAGTCTTTCATTTATAATATCCTTTATATAGAG, FTL0119 3' ext 5'-CATACATATTTAACCAAGTATTAGAAGATAATGGCTCAG. Loss of the wild type and retention of the deletion *dotU* alleles were confirmed by PCR. Since *dotU* is duplicated in the LVS genome, a second

round of mutagenesis was performed on the single *dotU* mutant strain to create an LVS *dotU* double deletion strain. Plasmids for complementation were created by ligating cloned region of *dotU* into the PKK MCS plasmid. *dotU* expression from the PKK MCS plasmid was regulated by the putative PI promoter. The following primers were used: FTL0119 forward 5'-CTTAATTAAATGAAAGACTTTAAAGAGATAGAAATTATTCTAGATATTATAA AAC, FTL0119 reverse 5'-TGTCGACCCAGCTTAATAAAATTAGTAAGCTTAAAAGA AACAGTC.

C57Bl/6J (B6) mice were purchased from the Jackson Laboratory (Bar Harbor, ME). All animals used in this study were maintained under specific pathogen-free conditions in the American Association of Laboratory Animal Care-accredited University of North Carolina Department of Laboratory Animal Medicine Facilities or American Association of Laboratory Animal Care-accredited Louisiana State University Health Science Center at Shreveport Animal Medicine Facilities. All work was approved by each facility's Animal Care and Use Committee (UNC #04-200, LSUHSC P10-010).

**Generation of bone marrow-derived macrophages**

Bone marrow cells from B6 mouse femurs were cultured in 30% L cell conditioned medium as previously described (28). Briefly bone marrow cells were flushed from B6 mouse femurs and incubated for 7 days on nontissue culture-treated 15-$cm^2$ dishes with L cell-conditioned medium as a source of GM-CSF. Following differentiation, nonadherent cells were removed by multiple washes with PBS and bone marrow-derived macrophages were removed from plates by incubation with 10 mM EDTA in PBS. Since L cell condition media and FBS batches can affect the amount of $PGE_2$ induction by infected macrophages

we utilized the same L cell conditioned media and FBS batches for each series of experiments to minimize variability in $PGE_2$ synthesis between experiments.

**Bone marrow-derived macrophage infections**

BMDM were plated in 96 well flat bottom plates ($10^5$/well). Macrophages were allowed to adhere for two hours. Macrophages were mock infected or infected with LVS, Schu S4, U112, or U112 transposon insertion strains at different MOIs as indicated. Bacteria were centrifuged onto the macrophage monolayer at 300 g for 5 min to allow closer contact and more efficient infection. Two hours after inoculation, extracellular bacteria were killed by the addition of 50 μg/ml of gentamicin for 45 minutes. Supernatants were removed and cells were washed with antibiotic free complete medium. Fresh antibiotic free complete medium was added and cells were incubated for 24 hours. Supernatants were then collected and spun at 300 g for 10 minutes to remove eukaryotic cells. Supernatants were sterilized by UV. Representative supernatants were plated onto chocolate agar after UV treatment to ensure complete killing of *F. tularensis*. Supernatant was then stored at -80$^o$ C until needed.

**Identification of transposon insertion strains**

The transposon library has previously been described (46). In brief, the 3,050-member library includes two insertion alleles for 1488 genes the majority of total *Francisella* ORFs. The alleles chosen were primarily insertions positioned between 5% and 70% within the ORF and are thus likely to represent null mutations. After single-colony purification, the mutants were arrayed in 96-well format and sequence-mapped to confirm their identities. See table 2 of (46) for the summary of this information.

The two allele mutant library was screened in a 96 well format. Transposon insertion strains were grown up in 96 well deep well plates containing 1 ml of Tryptic Soy broth

containing 15µg/ml carbenicillin, 20 µg/ml kanamycin, and supplemented with 0.1% l-cysteine-HCl. After over-night growth an aliquot of supernatants from each transposon insertion strain was taken and OD600 was determined. MOI were normalized by average plate $OD_{600}$. B6 BMDM was inoculated at an MOI of 500:1 to guarantee sufficient inocula in each well to induce $PGE_2$ synthesis. In our experience increasing MOI inocula increases the number of macrophages infected. Twenty four hours after inoculation supernatants were collected and then stored at -80$^{o}$C until needed.

**$PGE_2$ assay**

$PGE_2$ in cell culture supernatants was measured using a commercial $PGE_2$ enzyme immunoassay kit (Assay Design, Ann Arbor, MI) as per manufacturer's instructions. Transposon insertion strains were deemed defective in the ability to induce of $PGE_2$ when the levels of $PGE_2$ by any transposon insertion strain were 3 standard deviations below the mean of the entire plate.

**Bacterial growth assay**

Macrophages were mock infected or infected with U112, U112 *clpB*::Tn, U112 *pdpA*::Tn, or U112 *iglC*::Tn strains at an MOI of 100:1. At 4 and 24 hours post-inoculation, supernatants were removed. 100 µl of 0.05% sodium dodecyl sulfate in PBS was used to lyse the BMDM. Samples were transferred to tubes containing 900 µl PBS and vortexed on high setting for one minute. Samples were serially diluted and plated on chocolate agar to determine bacterial numbers.

**Confocal and transmission electron microscopy**

J774.1 macrophages (from ATCC #TIB-67) were seeded on coverslips at a density of $6x10^5$ cells/well. Prior to infection, bacteria were carboxyfluorescein succinimidyl ester

(CFSE) labeled as previously described (49) with the following modifications: CFSE was added to bacteria at a final concentration of 5 μM and incubated for 20 minutes at 37˚C. Macrophages were inoculated with CFSE-labeled U112, U112 *clpB*::Tn, U112 *pdpA*::Tn, or U112 *iglC*::Tn mutants at an MOI of 200:1. Bacteria were centrifuged onto the macrophages at 300 g for 5 min. Two hours after inoculation, extracellular bacteria were killed by the addition of 25 μg/ml of gentamicin for 45 minutes and then media was replaced with antibiotic free media. At four hours post-inoculation, LAMP-1 association with bacteria was determined as previously described (50). Briefly, wells were washed with PBS and fixed for 20 minutes at room temperature with 2% (w/v) formaldehyde and 1% (w/v) sucrose in PBS. Cells were permeabilized using methanol. Coverslips were blocked with 5% bovine serum albumin, incubated overnight at 4$^{o}$C with anti-mouse LAMP-1 (1D4B eBioscience), washed three times with PBS, and stained with donkey anti-rat IgG Alexafluor594 secondary antibody (Invitrogen) for two hours at room temperature. After three PBS washes, the coverslips were mounted in DAPI-containing mounting media (Vector Laboratories, Inc.) to label the DNA. Cells were imaged using a Leica SP2 Laser Scanning Confocal Microscope using a 63x oil immersion lens. A minimum of 20 cells per strain were captured. To remove subjectivity in determining co-localization of bacteria with LAMP-1 images were analyzed using Volocity software (Improvision/Perkin Elmer) to determine bacterial association with LAMP-1. Co-localization was determined by the shared of red and green pixels at the same location. To determine whether a bacterium resided in a LAMP-1 positive vesicle, the voxel spy tool was used closely examine whether the LAMP-1 red pixels surrounded the CFSE green pixels that labeled the bacterium. If the red pixels surrounded greater than 50% of the green pixels, the bacterium was categorized as residing within a LAMP-1+ vesicle.

B6 BMDMs were inoculated with U112, U112 *clpB*::Tn, U112 *iglC*::Tn, or U112 *pdpA*::Tn at an MOI of 500:1 at an MOI of 500:1 to maximize the number of infected BMDMs. 2 hours after inoculation, the media was removed and replaced with media containing 50 μg/mL gentamicin (Sigma-Aldrich, St. Louis, MO). Gentamicin-containing media was removed 1 hour after treatment and replaced with antibiotic-free media. 4 hours post-inoculation, the BMDM monolayer was fixed using gluteraldehyde and post-fixed with osmium tetroxide. Images were obtained using a Phillips CM-12 transmission electron microscope using 25,000x magnification.

**Statistical analysis**

Student's *t* tests were used for statistical analysis between two group experiments. Multi group comparisons were done by ANOVA followed by Dunnett's Multiple Comparison Test. When appropriate, data were logarithmically transformed before statistical analysis and confirmed by a demonstrated increase in power of the test after transformation of the data. Data analysis on the rescreen (figure 2) was accomplished by one-way ANOVA analysis followed by Student's *t* test. A $p$ value $\leq 0.05$ was considered statistically significant.

## RESULTS

### *F. tularensis* subspecies *novicida* and *tularensis* induced the synthesis of $PGE_2$ by infected macrophages

We have previously demonstrated that *F. tularensis* subspecies *holarctica* LVS induces $PGE_2$ synthesis in infected macrophages. To enable the use of the two allele transposon mutant library we needed to determine if the ability to induce $PGE_2$ synthesis by

infected macrophages is shared among *Francisella* subspecies. We tested both *F. novicida* U112 and *F. tularensis* Schu S4 for their ability to induce B6 bone marrow-derived macrophages (BMDM) to synthesize $PGE_2$ upon infection. We inoculated BMDM with LVS, U112, or Schu S4 at an MOI of 100:1. All strains tested were capable of inducing synthesis of $PGE_2$ by infected macrophages (figure 1). This demonstrates that the ability to induce $PGE_2$ synthesis is conserved among *F. tularensis* strains.

**Screening the two allele mutant library identifies several genes necessary for the *Francisella* induction of $PGE_2$ by infected macrophages**

Since we demonstrated that U112 induced macrophage synthesis of $PGE_2$, we used the *F. novicida* two allele transposon mutant library (46) to identify mutants that were unable to induce $PGE_2$ synthesis. During the initial testing of the 3050 *F. novicida* U112 transposon mutants, we defined a *F. novicida* U112 transposon mutant as defective in induction of $PGE_2$ synthesis by infected BMDM when BMDM produced relative $PGE_2$ amounts that were three standard deviations lower than the plate average amount of $PGE_2$. The use of the three standard deviation rule allowed us to minimize the likelihood (0.3%) of identifying false positives. The initial screen identified 33 genes that when disrupted made *F. novicida* unable to induce $PGE_2$ synthesis by infected macrophages. This included 10 genes located in the FPI. We retested all U112 transposon insertion mutants with transposon insertions in the identified 33 genes. Furthermore, since the initial screen identified 10 genes of the FPI, we included all FPI transposon mutants within the two allele transposon mutant library in this rescreen to ensure these genes important in pathogenesis were carefully evaluated. BMDM were inoculated with individual transposon insertion strains (89 mutants representing the original 33 genes identified and 10 genes from the FPI not originally identified) at an MOI of

200:1 and $PGE_2$ levels were measured 24 hours post-inoculation (figure 2). We utilized an MOI of 200:1 since we have previously demonstrated this MOI results in a reproducible significant increase in detectable $PGE_2$ from infected macrophages (28). Each U112 transposon mutant was tested a minimum of four times. No difference was noted between strains with insertions in the same gene; as such the values were combined for representation in figure 2. We were able to confirm 20 genes that when disrupted resulted in *F. novicida* strains that did not induce the synthesis of $PGE_2$ by infected BMDM (figure 2). With the exception of *mglA* and *rpoB*, which were only represented once, each gene identified encodes a product involved in the induction of $PGE_2$ that was represented at least twice in the U112 two allele transposon mutant library. The genes identified in the screen of the two allele mutant library are summarized in Table 1. The identified genes were located in the FPI or were genes that encode some of the previously identified regulators of the FPI (*sspA, mglA*, *mglB*, and *trmE*) with the exception of *rpoB* and *clpB* (17, 22, 23, 42, 51). These genes are highly conserved in all *F. tularensis* subspecies sequenced to date (17, 23, 42, 43). Of note: not all genes encoded within the FPI are necessary for U112 induced $PGE_2$ synthesis as *pdpA::Tn, pdpD::Tn,* and *pdpE::Tn* were able to induce $PGE_2$ synthesis similarly to wild type U112. Thus the screen identified 20 *F. novicida* genes that are necessary for the induction of $PGE_2$.

**_F. tularensis_ LVS mutant strains with deletions of _mglA_, _sspA_ or _dotU_ do not induce $PGE_2$ synthesis from infected macrophages**

To begin to address if the genes identified in U112 also encode products that contribute to LVS to induce $PGE_2$ synthesis by infected macrophages we utilized clean deletion mutants. Two of the genes identified in the screen of the two allele library, U112

*mglA*::Tn and U112 *sspA*::Tn, encode positive transcriptional regulators (22-24). We also identified several genes of the FPI, including *dotU*. DotU is necessary for stabilization of the FPI secretion apparatus, and mutants lacking *dotU* do not have a functional FPI secretion system (52). To examine the possibility that LVS mutants lacking *mglA, sspA* or *dotU* do not to induce $PGE_2$ synthesis, we tested these mutant strains for induction of $PGE_2$ synthesis by BMDMs. BMDM were inoculated with LVS, LVSΔ*mglA*, LVSΔ*mglA* (*pmglA*), LVSΔ*sspA*, LVSΔ*sspA* (*psspA*), LVSΔ*dotU*, or LVSΔ*dotU* (*pdotU*) at an MOI of 200:1. Twenty-four hours after inoculation the levels of $PGE_2$ were determined. Neither LVSΔ*mglA*, LVSΔ*sspA* nor LVSΔ*dotU* mutant strains induce significant $PGE_2$ synthesis from infected macrophages (figure 3). This phenotype was reversed by trans complementation with the appropriate plasmid (figure 3) suggesting that U112 and LVS induce $PGE_2$ synthesis through similar mechanisms.

**Dissociation of intracellular growth and induction of $PGE_2$ by *Francisella***

Escape from the phagosome and replication in the cytosol of host cells are critical for *F. tularensis* survival. All of the genes identified in this screen have been identified in other screens examining disease pathogenesis and intracellular growth (10-12, 14, 53, 54). Thus, it may be that failures to either escape the phagosome or replicate explains why these *F. novicida* mutants did not to induce $PGE_2$ synthesis. Previous studies that examined infection of macrophages by *F. novicida pdpA*::Tn and Δ*pdpA* strains demonstrated that PdpA is required for escape from the phagosome (50, 55). Similarly, IglC has been shown to be required for *F. novicida* and *F. holarctica* phagolysosomal escape (56, 57). In contrast, *F. holarctica* mutants with a transposon insertion in *clpB* escape the phagosome and replicate (43). The characterization of the trafficking phenotypes of *Francisella* strains with mutations

in *clpB, pdpA,* and *iglC* suggested we could use the two allele mutant library *clpB::*Tn*, pdpA::*Tn*,* and *iglC::*Tn mutant strains as tools to investigate the requirement of escape and intracellular growth for $PGE_2$ induction. We understand these experiments do not prove that these genes are necessarily involved in the induction of $PGE_2$, but rather eliminate or confirm if either the act of escaping the phagosome or replicating in the cytosol is what is necessary and sufficient to induce $PGE_2$ synthesis in macrophages.

To determine the intracellular localization of these strains, we inoculated the J774.1 macrophage cell line, as we and others have successfully used this cell line in the past to examine intracellular localization of *F. tularensis* (48, 58), at an MOI of 500:1 with CFSE labeled U112, U112 *clpB*::Tn, U112 *iglC*::Tn, and U112 *pdpA*::Tn and examined their association with LAMP-1 using confocal microscopy (figure 4). A high MOI was used to ensure our ability to identify intracellular bacteria and their respective intracellular localization. We confirmed that U112 infected J774 cells synthesize increased amounts of $PGE_2$ upon both U112 and LVS infection compared to uninfected samples (data not shown). We analyzed the associations of bacteria and LAMP-1 using Volocity image software and showed the percentage of bacteria associated with LAMP-1 by pixel association (figure 4a). We found only 34% of U112 remained associated with LAMP-1 four hours post-inoculation. Similarly, 34% of U112 *clpB*::Tn remained associated with LAMP-1 four hours post-inoculation. In contrast, U112 *iglC*::Tn and U112 *pdpA*::Tn resided mainly in the phagosome four hours post-inoculation displaying 71% and 70% LAMP-1 association, respectively. We confirmed the intracellular localization of U112 *clpB*::Tn, U112 *iglC*::Tn, and U112 *pdpA*::Tn by transmission electron microscopy (figure 4b) These data indicate U112 *clpB*::Tn, U112 *iglC*::Tn, and U112 *pdpA*::Tn have intracellular trafficking patterns

that are similar to those of previously published *clpB*, *iglC*, and *pdpA* transposon insertion strains (43, 50, 55-57). As noted above, these data show that the U112 *pdpA*::Tn mutant is able to induce $PGE_2$ even though it was diminished in its ability to escape the phagosome. If $PGE_2$ synthesis induction required phagosomal escape, we would expect U112 *pdpA*::Tn would not induce $PGE_2$ synthesis, as seen with U112 *iglC*::Tn. However, *pdpA*::Tn does induce $PGE_2$ at similar levels to wild-type U112 (figure 2).Thus our data suggest $PGE_2$ induction is unaffected by intracellular trafficking/localization.

To determine if intracellular growth was required for *F. novicida* induction of $PGE_2$ synthesis we inoculated BMDM at an MOI of 100:1 with U112, U112 *clpB*::Tn, U112 *pdpA*::Tn, and U112 *iglC*::Tn and counted intracellular CFUs over time. We used an MOI 100:1 to maximize differences in intracellular CFUs at 4 and 24 hours post-inoculation. At higher MOIs extensive cell death of BMDMs by 24 hours post-inoculation made it difficult to measure intracellular growth (data not shown). The number of intracellular bacteria was determined at 4 and 24 hours post-inoculation, while the concentration of $PGE_2$ in supernatants was determined at 24 hours post-inoculation. The U112 *clpB*::Tn strain grew within BMDM similarly to wildtype U112, while the U112 *pdpA*::Tn and U112 *iglC*::Tn strains failed to grow in BMDM (figure 5). In fact, there were fewer intra-macrophage U112 *pdpA*::Tn and U112 *iglC*::Tn bacteria at 24 hours post-inoculation than at 4 hours post-inoculation. Wild type U112 and U112 *pdpA*::Tn were able to induce $PGE_2$ synthesis, while U112 *clpB*::Tn and U112 *iglC*::Tn did not. The fact that *pdpA*::Tn induced $PGE_2$ synthesis without intra-macrophage growth and *clpB*::Tn did not induce $PGE_2$ synthesis while still able to grow in the macrophage demonstrates dissociation between intracellular growth and the ability of *F. novicida* to induce infected BMDM to synthesize $PGE_2$.

## DISCUSSION

The induction of $PGE_2$ synthesis by LVS infected macrophages disrupts T cell responses allowing LVS to persist in the host (28, 31). We demonstrate here that induction of $PGE_2$ synthesis by infected bone marrow-derived macrophages is conserved among *F. novicida, F. holarctica,* and *F. tularensis*. Synthesis of $PGE_2$ by U112 infected macrophages allowed us to screen the comprehensive U112 two allele transposon mutant library to identify *Francisella* genes that are potentially involved in the induction of $PGE_2$ synthesis by *Francisella* infected macrophages. Our screen identified 20 genes that when disrupted resulted in strains that failed to induce $PGE_2$ synthesis by *F. novicida* infected BMDM. These 20 genes are highly conserved in all sequenced *Francisella* subspecies (17, 23, 42, 43). Eighteen of the genes identified in this study either mapped to the FPI or represent positive transcriptional regulators of the FPI (17). 17 of the 20 identified genes have been demonstrated to be involved in mouse virulence (14, 54). Most, but not all of these genes, encode proteins that have been implicated in escape from the phagosome and intracellular growth (14, 54). The data presented here suggest these gene products may be responsible for the induction of $PGE_2$ biosynthesis in infected BMDM independent of their role in phagosomal escape and intracellular growth.

The FPI likely encodes a secretion system. The FPI proteins PdpB, VgrG, DotU, IglA, and IglB proteins are homologous to T6SS proteins from other bacterial pathogens (16, 52, 59, 60). The FPI was initially identified in *F. novicida* via mutations in *iglA* and *iglC* that resulted in *F. novicida* strains that no longer replicated within macrophages (61). Recent work has identified the FPI genes that encode proteins required for intracellular growth and

include *pdpA, pdpB, dotU, vgrG, iglABCDEFHJ,* and potentially *iglG* and *iglI* (56, 59, 62-66). The genes *pdpC, pdpD, pdpE,* and *anmK* are not required for intracellular growth (59). Our screen demonstrated that disruptions in FPI genes *dotU, vgrG, pdpBC,* and *iglABCGEDFGHIJ* resulted in U112 strains unable to induce $PGE_2$ synthesis by infected macrophages. At this time we are unsure whether all gene products are necessary, or whether some mutants where identified due to polar effects of transposon insertions. This is possible as the FPI is believed to be organized in two operons (17). Future work will be necessary to define which FPI gene products are truly necessary for induction of $PGE_2$ synthesis from infected macrophages. Disruptions in *pdpADE* and *anmK* did not impair the bacteria's ability to induce synthesis of $PGE_2$. We were not surprised that *pdpD* and *anmK* mutants are not impaired, as we believe the mechanism of induction of $PGE_2$ synthesis is conserved between *Francisella* strains. The *anmK* gene is not present in LVS while the *pdpD* is truncated in LVS and presumably nonfunctional (16). The deletion of *pdpE* from *F. novicida* had no effect on the bacteria's ability to grow in macrophages or cause disease. At this time the role of PdpE in FPI function is unknown (59). PdpA is involved in both intracellular growth and virulence. However PdpA is not believed to be a component of the FPI secretion system (50, 55) which may explain why the *pdpA::Tn* mutant is still capable of inducing $PGE_2$ synthesis. Some of the transposon mutants (*pdpE*::TN, *pdpD*::Tn, and *anmK*::Tn) were capable of inducing enhanced $PGE_2$ secretion from infected macrophages. The mechanism behind this is unknown and future work will be done to examine this phenomenon. Regardless, it is clear that disruption of *F. novicida's* genes in the FPI diminishes its ability to induce $PGE_2$ synthesis from infected macrophages.

There are 6 genes located outside of the FPI that when disrupted resulted in strains unable to induce the synthesis of $PGE_2$ from U112 infected macrophages. Four of those (*trmE, sspA*, *mglA,* and *mglB)* have previously been identified to encode positive transcriptional regulators of genes found both in FPI and outside the FPI (22-24, 42, 50, 55). The work of the Dove laboratory has clearly identified other transcriptional regulators which include CaiC, CphA, PigR, and SpoT in *F. tularenisis* LVS(42). The two allele mutant library lacks transposon insertional mutants in *spoT* and *pigR,* while the *caiC* and the *cphA* transposon mutant strain induced $PGE_2$ synthesis from macrophages. This result suggests differential transciprional regulation of the FPI between U112 and LVS; however future work would be required to corroborate this observation. RpoB is a component of the RNAP catalytic core responsible for the transcription of genes (67). The U112 *rpoB*::Tn was likely identified due to a general disruption of transcription. The fact the *rpoB*::Tn mutant failed to induce $PGE_2$ synthesis would predict finding other components of the RNAP catalytic core. However, the two allele library did not contain mutants with transposon insertions in either *rpoA* or *rpoD,* while *rpoC*::Tn and *rpoZ*::Tn mutants strains induced $PGE_2$ synthesis. ClpB, a stress response protein, has been previously demonstrated to be important in *Francisella* disease pathogenesis. A U112 *clpB* mutant was identified due to a delay in intramacrophage growth, while a disruption of *clpB* in *F. holarctica* LVS resulted in a strain that could grow *in vitro* in macrophages, but failed to effectively multiply in mice (43, 61). We did not observe a intramacrophage growth defect of the the two allele *clpB*::Tn. In *Listeria monocytogenes* and *Porphyromonas gingivalis,* ClpB homologs are necessary for virulence during animal infections (68, 69). ClpB/ClpV homologs have been identified in other T6SS where their AAA+ ATPase activity supply energy for the protein secretion process (19, 21,

70, 71). ClpB regulates the protein levels of DnaK, FTL_0525, FTL_0311, FTL_0588, and FTL_0207 (43). Since none of these genes were identified as necessary for induction of $PGE_2$ synthesis, it would suggest ClpB may have other unidentified functions. It has not been demonstrated to regulate the protein levels of the FPI. Future work will be needed to define the mechanism of ClpB mediated induction of $PGE_2$ synthesis from infected macrophages, and whether this is through regulation of FPI genes, function of FPI gene products, or through a FPI independent mechanism.

Infection of macrophages with U112, LVS, or Schu S4 results in the induction of $PGE_2$. This demonstrates that the ability to induce $PGE_2$ synthesis from infected macrophages is conserved among *F. tularensis* subspecies. In fact, U112 and Schu S4 induce more $PGE_2$ than LVS at similar doses. This difference in $PGE_2$ induction may be partially responsible for difference in virulence in these different subspecies. While we have previously demonstrated differences in innate immune responses to Schu S4, LVS, and U112 in intranasally inoculated mice, it is unknown if these different responses are due to differences in $PGE_2$ induction (72). Further work will address this difference in $PGE_2$ induction and the potential effect of $PGE_2$ on disease pathogenesis. The demonstration that inactivation of FPI genes in *F. novicida* results in the inability to induce $PGE_2$ biosynthesis and the fact that the FPI is highly conserved among all subspecies of *F. tularensis* would suggest that the mechanism of $PGE_2$ induction is conserved among these subspecies. The fact that LVS *mglA, sspA* and *dotU* mutant strains did not induce $PGE_2$ synthesis further suggests the likelyhood that *F. tularensis* subspecies *tularensis, F. tularensis* subspecies *holarctica,* and *F. tularensis* subspecies *novicida* have conserved mechanisms of induction of $PGE_2$ synthesis. However, we cannot discount the possibility that *F. tularensis* subspecies

*tularensis* may possess additional mechanisms for induction of $PGE_2$ synthesis that *F. novicida* or *F. holarctica* do not.

The FPI is necessary for the organism to escape the phagosome and replicate in the cytosol (59, 64-66). The reason the transposon insertion mutants we identified in U112 failed to induce $PGE_2$ synthesis may be due to their failure to escape the phagosome and subsequently replicate. Failure to escape the phagosome may create a physiologic barrier between *F. tularensis* and the eukaryotic molecule that is responsible for sensing and responding to *F. tularensis.* There are many intracellular receptors that can recognize bacterial products (73). ASC, a component of the inflammasome, and AIM2 (which recognizies *F. tularensis* DNA) are crucial for control of *Francisella* intra-macrophage growth *in vitro* and infection *in vivo* (74-76). Inflammasome activation is also capable of inducing eicosanoid production (77). However, we believe that failure to escape into the cytosol is not the reason the transposon insertion mutant strains we identified in this study failed to induce $PGE_2$ synthesis by infected macrophages. In other studies, *pdpA*::Tn and Δ*pdpA F. novicida* mutants fail to fully escape the phagosome (50, 55, 76). The U112 *pdpA*::Tn strain in the U112 two allele mutant library does not escape the phagosome to the same level as wildtype U112. Recently, 92 transposon mutant strains from the two allele mutant library were identified that did not escape the phagosome (10). We showed all of these strains were able to induce $PGE_2$. Thus it is unlikely that the mutants we did identify failed to induce $PGE_2$ solely because they failed to escape from the phagosome. Future work that identifies both the *F. tularensis* effector molecule and the corresponding eukaryotic binding partner will allow us to more definitively dissociate *F. tularensis* trafficking and induction of $PGE_2$ synthesis from *Francisella* infected macrophages.

Previous studies have identified 201 genes outside the FPI that are required for *Francisella* intra-macrophage growth (10, 11, 13, 53). U112 strains with insertions in any one of these 201 genes were all capable of inducing $PGE_2$ synthesis from infected macrophages. We did not identify known *F. tularensis* auxotrophs as being defective in the ability to induce $PGE_2$. Transposon insertions in *purA, purF, carA, carB*, and *pyrB* produce strains that have a defect in intracellular growth yet are able to induce macrophage synthesis of $PGE_2$ (53, 78, 79). Our studies using U112, U112 *clpB*::Tn, U112 *pdpA*::Tn, and U112 *iglC*::Tn strains demonstrate dissociation between intra-macrophage growth, the ability of *F. tularensis* to fully escape the phagosome, and the ability to induce $PGE_2$. These data also confirm our earlier report that UV inactivation of LVS, which inhibits replication, did not impact LVS's ability to induce $PGE_2$ synthesis from infected macrophages (28). Further characterization and understanding of the molecular interactions between *F. tularensis* and eukaryotic cells that lead to the induction of $PGE_2$ will provide new insight into tularemia pathogenesis.

**Figure 1**

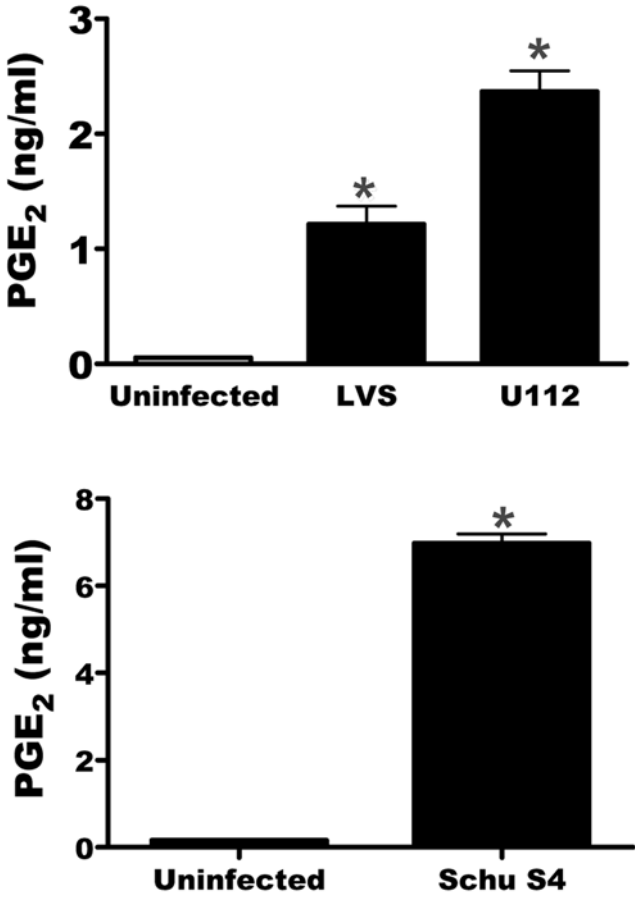


**Figure 1.** ***LVS, U112 and Schu S4 induces the synthesis of $PGE_2$ from bone marrow-derived macrophages.*** Bone marrow-derived macrophages were either mock inoculated or inoculated with LVS, U112, or Schu S4 at an MOI of 200:1. 24 hours after inoculation supernatants were collected and $PGE_2$ concentration was determined. Data represents three independent experiments and expressed as the mean ± standard error. * denotes statistical difference ($p \leq 0.05$) from uninfected BMDM.

**Figure 2**

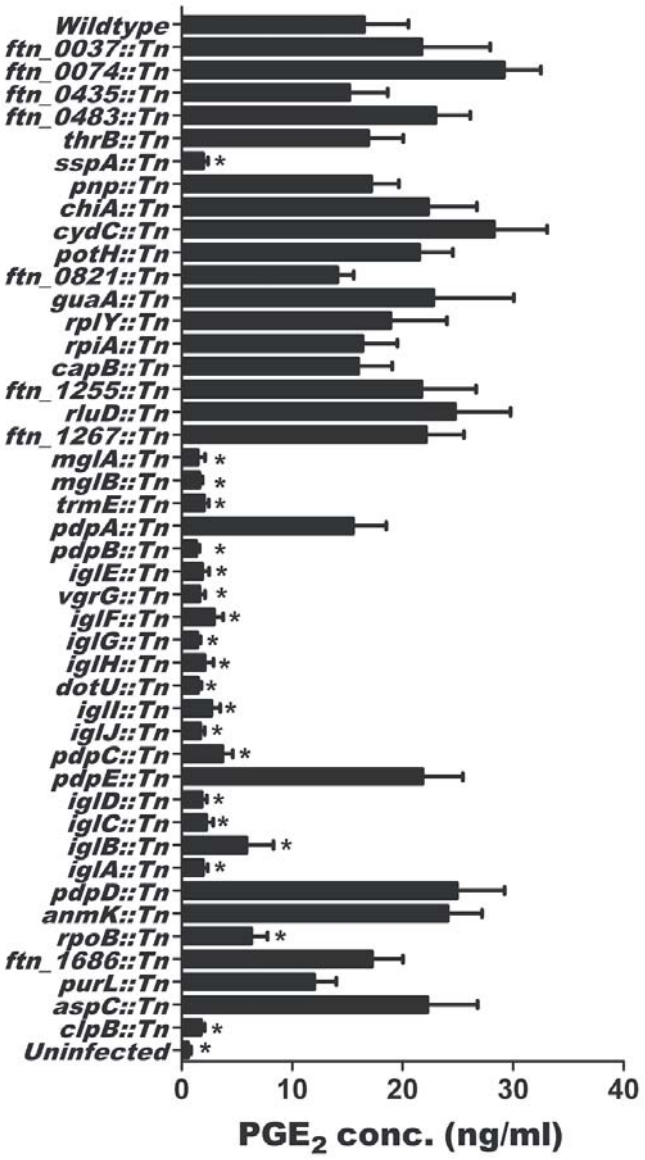


**Figure 2.** ***Identification of U112 genes necessary for the induction of $PGE_2$ from bone marrow-derived macrophages.*** Bone marrow-derived macrophages were inoculated with U112 or individual transposon insertion strains at an MOI of 200:1. 24 hours after inoculation, supernatants were collected and $PGE_2$ concentration was determined. Each transposon insertion mutant strain was tested 4 times. Bars represent the mean of all independent transposon insertions mutants within the same gene ± standard error. * denotes statistical difference ($p \leq 0.05$) from U112 inoculated BMDM.

**Table 1**

**Table 1. Genes required for *Francisella* induction of $PGE_2$ synthesis in *Francisella* infected macrophages.**

| ORF | Gene | Function (postulated) |
|---|---|---|
| FTN_0549 | *sspA* | Regulate virulence genes |
| FTN_1290 | *mglA* | Regulate virulence genes |
| FTN_1291 | *mglB* | Regulate virulence genes |
| FTN_1298 | *trmE* | tRNA modification, GTPase activity |
| FTN_1310 | *pdpB* | Unknown |
| FTN_1311 | *iglE* | Unknown |
| FTN_1312 | *vgrG* | Secreted |
| FTN_1313 | *iglF* | Unknown |
| FTN_1314 | *iglG* | Unknown |
| FTN_1315 | *iglH* | Unknown |
| FTN_1316 | *dotU* | Unknown |
| FTN_1317 | *iglI* | Unknown |
| FTN_1318 | *iglJ* | Unknown |
| FTN_1319 | *pdpC* | Unknown |
| FTN_1321 | *iglD* | Replication in cytosol |
| FTN_1322 | *iglC* | Escape from phagosome |
| FTN_1323 | *iglB* | Unknown |
| FTN_1324 | *iglA* | Unknown |
| FTN_1568 | *rpoB* | DNA directed RNA polymerase subunit beta |
| FTN_1743 | *clpB* | Chaperone, ATPase activity |

**Figure 3**

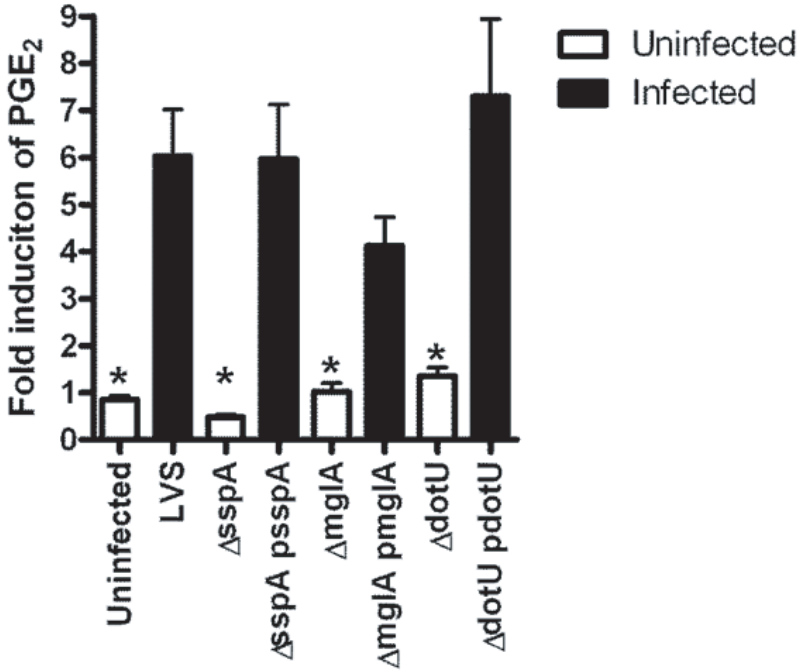


**Figure 3. mglA, sspA, *and* dotU *are necessary for LVS induction of $PGE_2$ synthesis.*** Bone marrow-derived macrophages were inoculated with LVS, LVSΔsspA, LVSΔsspA (psspA), LVSΔmglA, LVSΔmglA (pmglA), LVSΔdotU, or LVSΔdotU (pdotU) at an MOI of 200:1. 24 hours after inoculation the levels of $PGE_2$ were determined. Samples were analyzed in triplicate. Data represents three independent experiments and expressed as the mean ± standard error. * denotes statistical difference ($p \leq 0.05$) from LVS inoculated BMDM.

**Figure 4**

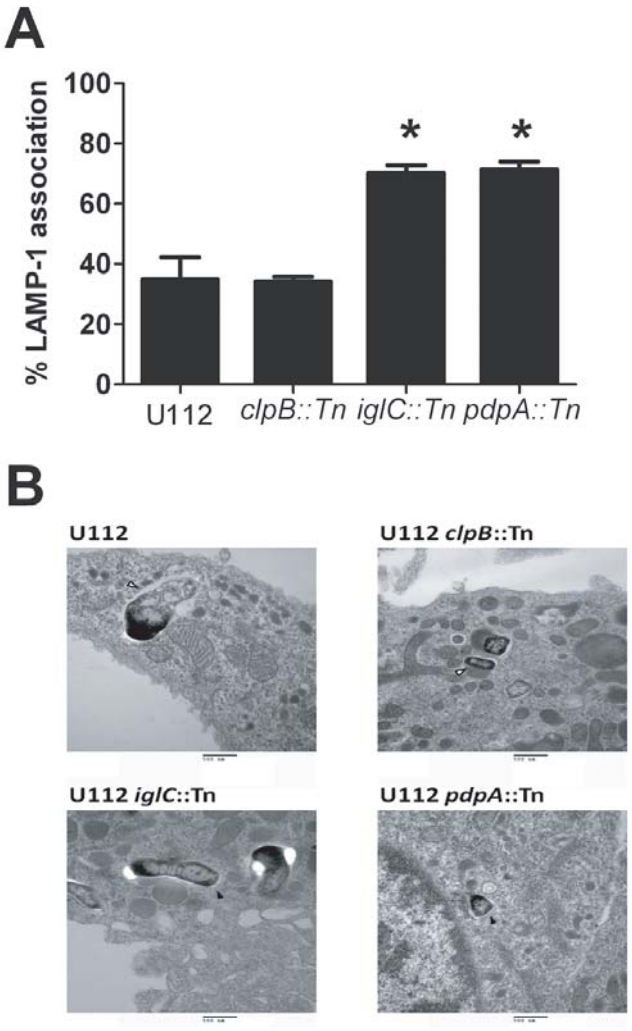


**Figure 4.** ***Induction of $PGE_2$ does not require full escape from the phagosome.*** A) Bacterial association with LAMP-1 was scored using Volocity (n= at least 20 imaged cells per strain with an average of one bacterium per macrophage). Co-localization was determined by the shared of red and green pixels at the same location. Data represents three independent experiments and expressed as the mean ± standard error. *, denotes statistical difference ($p \leq 0.05$) from U112 infected cells. B) BMDMs were inoculated with U112, U112 clpB::Tn, U112 iglC::Tn, or U112 pdpA::Tn at an MOI of 500:1. Association of the bacterium with the phagosomal membrane was determined 4 hours post-inoculation using transmission electron microscopy. Open arrowheads denote bacteria no longer surrounded by an intact phagosomal membrane. Filled arrowheads denote bacteria surrounded by a phagosomal membrane.

**Figure 5**

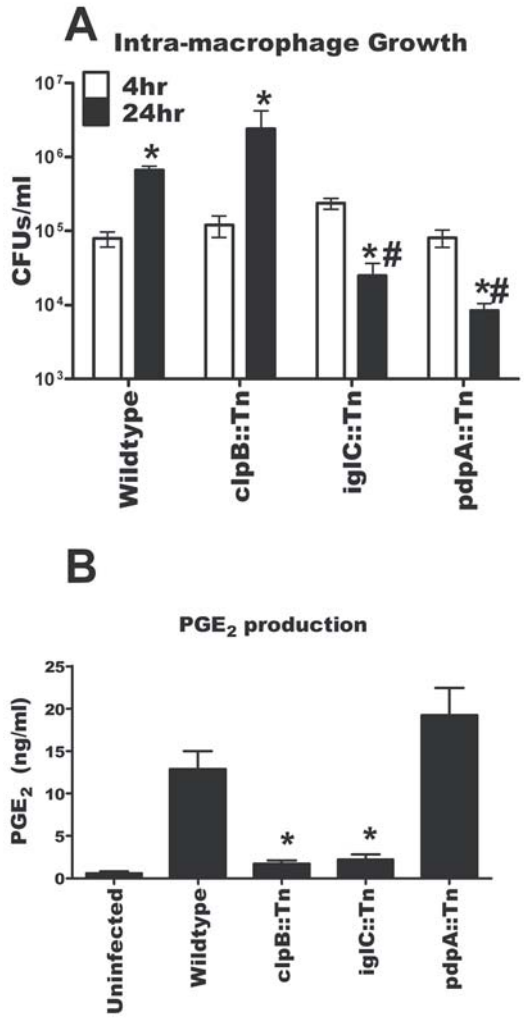


**Figure 5.** ***Dissociation of intracellular growth and the induction of $PGE_2$ from bone marrow-derived macrophages.*** A) Bone marrow-derived macrophages were inoculated with U112 , U112 clpB::Tn, U112 iglC::Tn, or U112 pdpA::Tn at an MOI of 100:1. CFU were determined at 4hr and 24hr post-inoculation. Data represents three independent experiments and expressed as the means ± standard error. * denotes statistical difference ($p \leq 0.05$) from corresponding 4 hour sample. # BMDM denotes statistical difference ($p \leq 0.05$) from 24 hour U112 infected BMDM (n=3). B) Bone marrow-derived macrophages were inoculated with U112 , U112 clpB::Tn, U112 iglC::Tn, or U112 pdpA::Tn at an MOI of 100:1. 24 hours after inoculation supernatants were collected and $PGE_2$ concentration was determined. Data represents three independent experiments and expressed as the mean ± standard error. * denotes statistical difference ($p \leq 0.05$) from U112 infected BMDM.

## REFERENCES


1. Ellis J, Oyston PC, Green M, Titball RW. Tularemia. Clin Microbiol Rev. 2002;15(4):631-46. Epub 2002/10/05. PubMed PMID: 12364373; PubMed Central PMCID: PMC126859.

2. Dennis DT, Inglesby TV, Henderson DA, Bartlett JG, Ascher MS, Eitzen E, et al. Tularemia as a biological weapon: medical and public health management. JAMA. 2001;285(21):2763-73. Epub 2001/06/21. doi: jst10001 [pii]. PubMed PMID: 11386933.

3. Rick Lyons C, Wu TH. Animal models of Francisella tularensis infection. Ann N Y Acad Sci. 2007;1105:238-65. PubMed PMID: 17395735.

4. Pechous RD, McCarthy TR, Zahrt TC. Working toward the future: insights into Francisella tularensis pathogenesis and vaccine development. Microbiol Mol Biol Rev. 2009;73(4):684-711. Epub 2009/12/01. doi: 73/4/684 [pii] 10.1128/MMBR.00028-09. PubMed PMID: 19946137; PubMed Central PMCID: PMC2786580.

5. Hollis DG, Weaver RE, Steigerwalt AG, Wenger JD, Moss CW, Brenner DJ. Francisella philomiragia comb. nov. (formerly Yersinia philomiragia) and Francisella tularensis biogroup novicida (formerly Francisella novicida) associated with human disease. J Clin Microbiol. 1989;27(7):1601-8. Epub 1989/07/01. PubMed PMID: 2671019; PubMed Central PMCID: PMC267622.

6. Hand J, Scott-Waldron C, Balsamo G. Outbreak of *Francisella novicida* Infections Among Occupants at a Long-Term Residential Facility - Louisiana, APril-July, 2011. Louisiana Morbidity Report. 2012;23(1):1 & 6.

7. Hornick RB, Eigelsbach HT. Aerogenic immunization of man with live Tularemia vaccine. Bacteriol Rev. 1966;30(3):532-8. Epub 1966/09/01. PubMed PMID: 5917334; PubMed Central PMCID: PMC378235.

8. Tigertt WD. Soviet viable Pasteurella tularensis vaccines. A review of selected articles. Bacteriol Rev. 1962;26:354-73. Epub 1962/09/01. PubMed PMID: 13985026; PubMed Central PMCID: PMC441156.

9. Rohmer L, Fong C, Abmayr S, Wasnick M, Larson Freeman TJ, Radey M, et al. Comparison of Francisella tularensis genomes reveals evolutionary events associated with the emergence of human pathogenic strains. Genome Biol. 2007;8(6):R102. PubMed PMID: 17550600.

10. Asare R, Abu Kwaik Y. Molecular complexity orchestrates modulation of phagosome biogenesis and escape to the cytosol of macrophages by Francisella tularensis. Environmental microbiology. 2010;12(9):2559-86. doi: 10.1111/j.1462-2920.2010.02229.x. PubMed PMID: 20482590; PubMed Central PMCID: PMC2957515.

11. Asare R, Akimana C, Jones S, Abu Kwaik Y. Molecular bases of proliferation of Francisella tularensis in arthropod vectors. Environ Microbiol. 2010;12(9):2587-612. Epub 2010/05/21. doi: EMI2230 [pii] 10.1111/j.1462-2920.2010.02230.x. PubMed PMID: 20482589; PubMed Central PMCID: PMC2957557.

12. Kraemer PS, Mitchell A, Pelletier MR, Gallagher LA, Wasnick M, Rohmer L, et al. Genome-wide screen in Francisella novicida for genes required for pulmonary and systemic infection in mice. Infect Immun. 2009;77(1):232-44. doi: 10.1128/IAI.00978-08. PubMed PMID: 18955478; PubMed Central PMCID: PMC2612238.

13. Qin A, Mann BJ. Identification of transposon insertion mutants of Francisella tularensis tularensis strain Schu S4 deficient in intracellular replication in the hepatic cell line HepG2. BMC microbiology. 2006;6:69. doi: 10.1186/1471-2180-6-69. PubMed PMID: 16879747; PubMed Central PMCID: PMC1557513.

14. Weiss DS, Brotcke A, Henry T, Margolis JJ, Chan K, Monack DM. In vivo negative selection screen identifies genes required for Francisella virulence. Proc Natl Acad Sci U S A. 2007;104(14):6037-42. Epub 2007/03/29. doi: 0609675104 [pii] 10.1073/pnas.0609675104. PubMed PMID: 17389372; PubMed Central PMCID: PMC1832217.

15. Barker JR, Chong A, Wehrly TD, Yu JJ, Rodriguez SA, Liu J, et al. The Francisella tularensis pathogenicity island encodes a secretion system that is required for phagosome escape and virulence. Mol Microbiol. 2009;74(6):1459-70. PubMed PMID: 20054881; PubMed Central PMCID: PMC2814410.

16. Ludu JS, de Bruin OM, Duplantis BN, Schmerk CL, Chou AY, Elkins KL, et al. The Francisella pathogenicity island protein PdpD is required for full virulence and associates with homologues of the type VI secretion system. J Bacteriol. 2008;190(13):4584-95. doi: 10.1128/JB.00198-08. PubMed PMID: 18469101; PubMed Central PMCID: PMC2446798.

17. Nano FE, Schmerk C. The Francisella pathogenicity island. Ann N Y Acad Sci. 2007;1105:122-37. Epub 2007/03/31. doi: annals.1409.000 [pii] 10.1196/annals.1409.000. PubMed PMID: 17395722.

18. Ma AT, Mekalanos JJ. In vivo actin cross-linking induced by Vibrio cholerae type VI secretion system is associated with intestinal inflammation. Proc Natl Acad Sci U S A. 2010;107(9):4365-70. Epub 2010/02/13. doi: 0915156107 [pii] 10.1073/pnas.0915156107. PubMed PMID: 20150509; PubMed Central PMCID: PMC2840160.

19. Mougous JD, Cuff ME, Raunser S, Shen A, Zhou M, Gifford CA, et al. A virulence locus of Pseudomonas aeruginosa encodes a protein secretion apparatus. Science. 2006;312(5779):1526-30. doi: 10.1126/science.1128393. PubMed PMID: 16763151; PubMed Central PMCID: PMC2800167.

20. Pukatzki S, Ma AT, Sturtevant D, Krastins B, Sarracino D, Nelson WC, et al. Identification of a conserved bacterial protein secretion system in Vibrio cholerae using the Dictyostelium host model system. Proc Natl Acad Sci U S A. 2006;103(5):1528-33. doi: 10.1073/pnas.0510322103. PubMed PMID: 16432199; PubMed Central PMCID: PMC1345711.

21. Shalom G, Shaw JG, Thomas MS. In vivo expression technology identifies a type VI secretion system locus in Burkholderia pseudomallei that is induced upon invasion of macrophages. Microbiology. 2007;153(Pt 8):2689-99. Epub 2007/07/31. doi: 153/8/2689 [pii] 10.1099/mic.0.2007/006585-0. PubMed PMID: 17660433.

22. Baron GS, Nano FE. MglA and MglB are required for the intramacrophage growth of Francisella novicida. Mol Microbiol. 1998;29(1):247-59. Epub 1998/08/14. PubMed PMID: 9701818.

23. Charity JC, Costante-Hamm MM, Balon EL, Boyd DH, Rubin EJ, Dove SL. Twin RNA polymerase-associated proteins control virulence gene expression in Francisella tularensis. PLoS Pathog. 2007;3(6):e84. Epub 2007/06/19. doi: 06-PLPA-RA-0512 [pii] 10.1371/journal.ppat.0030084. PubMed PMID: 17571921; PubMed Central PMCID: PMC1891329.

24. Lauriano CM, Barker JR, Yoon SS, Nano FE, Arulanandam BP, Hassett DJ, et al. MglA regulates transcription of virulence factors necessary for Francisella tularensis intraamoebae and intramacrophage survival. Proc Natl Acad Sci U S A. 2004;101(12):4246-9. Epub 2004/03/11. doi: 10.1073/pnas.0307690101 [doi] 0307690101 [pii]. PubMed PMID: 15010524; PubMed Central PMCID: PMC384726.

25. Pukatzki S, Ma AT, Revel AT, Sturtevant D, Mekalanos JJ. Type VI secretion system translocates a phage tail spike-like protein into target cells where it cross-links actin. Proc Natl Acad Sci U S A. 2007;104(39):15508-13. Epub 2007/09/18. doi: 0706532104 [pii] 10.1073/pnas.0706532104. PubMed PMID: 17873062; PubMed Central PMCID: PMC2000545.

26. Suarez G, Sierra JC, Erova TE, Sha J, Horneman AJ, Chopra AK. A type VI secretion system effector protein, VgrG1, from Aeromonas hydrophila that induces host cell toxicity by ADP ribosylation of actin. J Bacteriol. 2010;192(1):155-68. Epub 2009/11/03. doi: JB.01260-09 [pii] 10.1128/JB.01260-09. PubMed PMID: 19880608; PubMed Central PMCID: PMC2798274.

27. Suarez G, Sierra JC, Kirtley ML, Chopra AK. Role of Hcp, a type 6 secretion system effector, of Aeromonas hydrophila in modulating activation of host immune cells. Microbiology. 2010;156(Pt 12):3678-88. Epub 2010/08/28. doi: mic.0.041277-0 [pii] 10.1099/mic.0.041277-0. PubMed PMID: 20798163; PubMed Central PMCID: PMC3068704.

28. Woolard MD, Wilson JE, Hensley LL, Jania LA, Kawula TH, Drake JR, et al. Francisella tularensis-infected macrophages release prostaglandin E2 that blocks T cell proliferation and promotes a Th2-like response. J Immunol. 2007;178(4):2065-74. Epub 2007/02/06. doi: 178/4/2065 [pii]. PubMed PMID: 17277110.

29. Wilson JE, Katkere B, Drake JR. Francisella tularensis induces ubiquitin-dependent major histocompatibility complex class II degradation in activated macrophages. Infect Immun. 2009;77(11):4953-65. Epub 2009/08/26. doi: IAI.00844-09 [pii] 10.1128/IAI.00844-09. PubMed PMID: 19703975; PubMed Central PMCID: PMC2772548.

30. Yee D, Rhinehart-Jones TR, Elkins KL. Loss of either CD4+ or CD8+ T cells does not affect the magnitude of protective immunity to an intracellular pathogen, Francisella tularensis strain LVS. J Immunol. 1996;157(11):5042-8. Epub 1996/12/01. PubMed PMID: 8943413.

31. Woolard MD, Hensley LL, Kawula TH, Frelinger JA. Respiratory Francisella tularensis live vaccine strain infection induces Th17 cells and prostaglandin E2, which inhibits generation of gamma interferon-positive T cells. Infect Immun. 2008;76(6):2651-9. Epub 2008/04/09. doi: IAI.01412-07 [pii] 10.1128/IAI.01412-07. PubMed PMID: 18391003; PubMed Central PMCID: PMC2423094.

32. Chen BC, Chang YS, Kang JC, Hsu MJ, Sheu JR, Chen TL, et al. Peptidoglycan induces nuclear factor-kappaB activation and cyclooxygenase-2 expression via Ras, Raf-1, and ERK in RAW 264.7 macrophages. J Biol Chem. 2004;279(20):20889-97. PubMed PMID: 15007072.

33. Chen Y, Zhang J, Moore SA, Ballas ZK, Portanova JP, Krieg AM, et al. CpG DNA induces cyclooxygenase-2 expression and prostaglandin production. Int Immunol. 2001;13(8):1013-20. PubMed PMID: 11470771.

34. Smith RS, Kelly R, Iglewski BH, Phipps RP. The Pseudomonas autoinducer N-(3-oxododecanoyl) homoserine lactone induces cyclooxygenase-2 and prostaglandin E2 production in human lung fibroblasts: implications for inflammation. J Immunol. 2002;169(5):2636-42. PubMed PMID: 12193735.

35. Treffkorn L, Scheibe R, Maruyama T, Dieter P. PGE2 exerts its effect on the LPS-induced release of TNF-alpha, ET-1, IL-1alpha, IL-6 and IL-10 via the EP2 and EP4 receptor in rat liver macrophages. Prostaglandins Other Lipid Mediat. 2004;74(1-4):113-23. PubMed PMID: 15560120.

36. Uematsu S, Matsumoto M, Takeda K, Akira S. Lipopolysaccharide-dependent prostaglandin E(2) production is regulated by the glutathione-dependent prostaglandin E(2) synthase gene induced by the Toll-like receptor 4/MyD88/NF-IL6 pathway. J Immunol. 2002;168(11):5811-6. PubMed PMID: 12023384.

37. Ashtekar AR, Zhang P, Katz J, Deivanayagam CC, Rallabhandi P, Vogel SN, et al. TLR4-mediated activation of dendritic cells by the heat shock protein DnaK from Francisella tularensis. J Leukoc Biol. 2008;84(6):1434-46. PubMed PMID: 18708593.

38. Forestal CA, Gil H, Monfett M, Noah CE, Platz GJ, Thanassi DG, et al. A conserved and immunodominant lipoprotein of Francisella tularensis is proinflammatory but not essential for virulence. Microb Pathog. 2008;44(6):512-23. Epub 2008/02/29. doi: S0882-4010(08)00003-X [pii] 10.1016/j.micpath.2008.01.003. PubMed PMID: 18304778; PubMed Central PMCID: PMC2483246.

39. Thakran S, Li H, Lavine CL, Miller MA, Bina JE, Bina XR, et al. Identification of Francisella tularensis lipoproteins that stimulate the toll-like receptor (TLR) 2/TLR1 heterodimer. J Biol Chem. 2008;283(7):3751-60. PubMed PMID: 18079113.

40. Hajjar AM, Harvey MD, Shaffer SA, Goodlett DR, Sjostedt A, Edebro H, et al. Lack of in vitro and in vivo recognition of Francisella tularensis subspecies lipopolysaccharide by Toll-like receptors. Infect Immun. 2006;74(12):6730-8. Epub 2006/09/20. doi: IAI.00934-06 [pii] 10.1128/IAI.00934-06. PubMed PMID: 16982824; PubMed Central PMCID: PMC1698081.

41. Kieffer TL, Cowley S, Nano FE, Elkins KL. Francisella novicida LPS has greater immunobiological activity in mice than F. tularensis LPS, and contributes to F. novicida murine pathogenesis. Microbes Infect. 2003;5(5):397-403. PubMed PMID: 12737995.

42. Charity JC, Blalock LT, Costante-Hamm MM, Kasper DL, Dove SL. Small molecule control of virulence gene expression in Francisella tularensis. PLoS Pathog. 2009;5(10):e1000641. Epub 2009/10/31. doi: 10.1371/journal.ppat.1000641. PubMed PMID: 19876386; PubMed Central PMCID: PMC2763202.

43. Meibom KL, Dubail I, Dupuis M, Barel M, Lenco J, Stulik J, et al. The heat-shock protein ClpB of Francisella tularensis is involved in stress tolerance and is required for multiplication in target organs of infected mice. Mol Microbiol. 2008;67(6):1384-401. Epub 2008/02/21. doi: MMI6139 [pii] 10.1111/j.1365-2958.2008.06139.x [doi]. PubMed PMID: 18284578.

44. Cowley SC, Elkins KL. Multiple T cell subsets control Francisella tularensis LVS intracellular growth without stimulation through macrophage interferon gamma receptors. J Exp Med. 2003;198(3):379-89. PubMed PMID: 12885873.

45. Larson CL, Wicht W, Jellison WL. A new organism resembling P. tularensis isolated from water. Public Health Rep. 1955;70(3):253-8. PubMed PMID: 14357545.

46. Gallagher LA, Ramage E, Jacobs MA, Kaul R, Brittnacher M, Manoil C. A comprehensive transposon mutant library of Francisella novicida, a bioweapon surrogate. Proc Natl Acad Sci U S A. 2007;104(3):1009-14. PubMed PMID: 17215359.

47. Fuller JR, Kijek TM, Taft-Benz S, Kawula TH. Environmental and intracellular regulation of Francisella tularensis ripA. BMC microbiology. 2009;9:216. Epub 2009/10/14. doi: 1471-2180-9-216 [pii] 10.1186/1471-2180-9-216. PubMed PMID: 19821974; PubMed Central PMCID: PMC2767360.

48. Fuller JR, Craven RR, Hall JD, Kijek TM, Taft-Benz S, Kawula TH. RipA, a cytoplasmic membrane protein conserved among Francisella species, is required for intracellular survival. Infect Immun. 2008;76(11):4934-43. Epub 2008/09/04. doi: IAI.00475-08 [pii] 10.1128/IAI.00475-08. PubMed PMID: 18765722; PubMed Central PMCID: PMC2573376.

49. Bosio CM, Dow SW. Francisella tularensis induces aberrant activation of pulmonary dendritic cells. J Immunol. 2005;175(10):6792-801. Epub 2005/11/08. doi: 175/10/6792 [pii]. PubMed PMID: 16272336.

50. Schmerk CL, Duplantis BN, Howard PL, Nano FE. A Francisella novicida pdpA mutant exhibits limited intracellular replication and remains associated with the lysosomal marker LAMP-1. Microbiology. 2009;155(Pt 5):1498-504. Epub 2009/04/18. doi: mic.0.025445-0 [pii] 10.1099/mic.0.025445-0. PubMed PMID: 19372155.

51. Guina T, Radulovic D, Bahrami AJ, Bolton DL, Rohmer L, Jones-Isaac KA, et al. MglA regulates Francisella tularensis subsp. novicida (Francisella novicida) response to starvation and oxidative stress. J Bacteriol. 2007;189(18):6580-6. Epub 2007/07/24. doi: JB.00809-07 [pii] 10.1128/JB.00809-07. PubMed PMID: 17644593; PubMed Central PMCID: PMC2045168.

52. Broms JE, Meyer L, Lavander M, Larsson P, Sjostedt A. DotU and VgrG, Core Components of Type VI Secretion Systems, Are Essential for Francisella LVS Pathogenicity. PLoS One. 2012;7(4):e34639. Epub 2012/04/20. doi: 10.1371/journal.pone.0034639 PONE-D-12-02842 [pii]. PubMed PMID: 22514651; PubMed Central PMCID: PMC3326028.

53. Maier TM, Casey MS, Becker RH, Dorsey CW, Glass EM, Maltsev N, et al. Identification of Francisella tularensis Himar1-based transposon mutants defective for replication in macrophages. Infect Immun. 2007;75(11):5376-89. PubMed PMID: 17682043.

54. Su J, Yang J, Zhao D, Kawula TH, Banas JA, Zhang JR. Genome-wide identification of Francisella tularensis virulence determinants. Infect Immun. 2007;75(6):3089-101. Epub 2007/04/11. doi: IAI.01865-06 [pii] 10.1128/IAI.01865-06. PubMed PMID: 17420240; PubMed Central PMCID: PMC1932872.

55. Schmerk CL, Duplantis BN, Wang D, Burke RD, Chou AY, Elkins KL, et al. Characterization of the pathogenicity island protein PdpA and its role in the virulence of Francisella novicida. Microbiology. 2009;155(Pt 5):1489-97. Epub 2009/04/18. doi: mic.0.025379-0 [pii] 10.1099/mic.0.025379-0. PubMed PMID: 19372153.

56. Bonquist L, Lindgren H, Golovliov I, Guina T, Sjostedt A. MglA and Igl proteins contribute to the modulation of Francisella tularensis live vaccine strain-containing phagosomes in murine macrophages. Infect Immun. 2008;76(8):3502-10. doi: 10.1128/IAI.00226-08. PubMed PMID: 18474647; PubMed Central PMCID: PMC2493230.

57. Lindgren H, Golovliov I, Baranov V, Ernst RK, Telepnev M, Sjostedt A. Factors affecting the escape of Francisella tularensis from the phagolysosome. Journal of medical microbiology. 2004;53(Pt 10):953-8. Epub 2004/09/11. PubMed PMID: 15358816.

58. Tempel R, Lai XH, Crosa L, Kozlowicz B, Heffron F. Attenuated Francisella novicida transposon mutants protect mice against wild-type challenge. Infect Immun. 2006;74(9):5095-105. Epub 2006/08/24. doi: 74/9/5095 [pii] 10.1128/IAI.00598-06. PubMed PMID: 16926401; PubMed Central PMCID: PMC1594869.

59. de Bruin OM, Duplantis BN, Ludu JS, Hare RF, Nix EB, Schmerk CL, et al. The biochemical properties of the Francisella pathogenicity island (FPI)-encoded proteins IglA, IglB, IglC, PdpB and DotU suggest roles in type VI secretion. Microbiology. 2011;157(Pt 12):3483-91. Epub 2011/10/08. doi: mic.0.052308-0 [pii] 10.1099/mic.0.052308-0. PubMed PMID: 21980115.

60. Robb CS, Nano FE, Boraston AB. The structure of the conserved type six secretion protein TssL (DotU) from Francisella novicida. J Mol Biol. 2012. Epub 2012/04/17. doi: S0022-2836(12)00319-1 [pii] 10.1016/j.jmb.2012.04.003. PubMed PMID: 22504227.

61. Gray CG, Cowley SC, Cheung KK, Nano FE. The identification of five genetic loci of Francisella novicida associated with intracellular growth. FEMS Microbiol Lett. 2002;215(1):53-6. Epub 2002/10/24. doi: S0378109702009114 [pii]. PubMed PMID: 12393200.

62. Broms JE, Lavander M, Meyer L, Sjostedt A. IglG and IglI of the Francisella pathogenicity island are important virulence determinants of Francisella tularensis LVS. Infect Immun. 2011;79(9):3683-96. doi: 10.1128/IAI.01344-10. PubMed PMID: 21690239; PubMed Central PMCID: PMC3165494.

63. de Bruin OM, Ludu JS, Nano FE. The Francisella pathogenicity island protein IglA localizes to the bacterial cytoplasm and is needed for intracellular growth. BMC microbiology. 2007;7:1. doi: 10.1186/1471-2180-7-1. PubMed PMID: 17233889; PubMed Central PMCID: PMC1794414.

64. Nano FE, Zhang N, Cowley SC, Klose KE, Cheung KK, Roberts MJ, et al. A Francisella tularensis pathogenicity island required for intramacrophage growth. J Bacteriol. 2004;186(19):6430-6. Epub 2004/09/18. doi: 10.1128/JB.186.19.6430-6436.2004 186/19/6430 [pii]. PubMed PMID: 15375123; PubMed Central PMCID: PMC516616.

65. Santic M, Molmeret M, Barker JR, Klose KE, Dekanic A, Doric M, et al. A Francisella tularensis pathogenicity island protein essential for bacterial proliferation within the host cell cytosol. Cell Microbiol. 2007;9(10):2391-403. PubMed PMID: 17517064.

66. Santic M, Molmeret M, Klose KE, Jones S, Kwaik YA. The Francisella tularensis pathogenicity island protein IglC and its regulator MglA are essential for modulating phagosome biogenesis and subsequent bacterial escape into the cytoplasm. Cell Microbiol. 2005;7(7):969-79. Epub 2005/06/15. doi: CMI526 [pii] 10.1111/j.1462-5822.2005.00526.x [doi]. PubMed PMID: 15953029.

67. Allison LA, Moyle M, Shales M, Ingles CJ. Extensive homology among the largest subunits of eukaryotic and prokaryotic RNA polymerases. Cell. 1985;42(2):599-610. PubMed PMID: 3896517.

68. Chastanet A, Derre I, Nair S, Msadek T. clpB, a novel member of the Listeria monocytogenes CtsR regulon, is involved in virulence but not in general stress tolerance. J Bacteriol. 2004;186(4):1165-74. Epub 2004/02/06. PubMed PMID: 14762012; PubMed Central PMCID: PMC344206.

69. Yuan L, Rodrigues PH, Belanger M, Dunn W, Jr., Progulske-Fox A. The Porphyromonas gingivalis clpB gene is involved in cellular invasion in vitro and virulence in vivo. FEMS Immunol Med Microbiol. 2007;51(2):388-98. PubMed PMID: 17854400.

70. Bonemann G, Pietrosiuk A, Diemand A, Zentgraf H, Mogk A. Remodelling of VipA/VipB tubules by ClpV-mediated threading is crucial for type VI protein secretion. The EMBO journal. 2009;28(4):315-25. doi: 10.1038/emboj.2008.269. PubMed PMID: 19131969; PubMed Central PMCID: PMC2646146.

71. Shrivastava S, Mande SS. Identification and functional characterization of gene components of Type VI Secretion system in bacterial genomes. PLoS One. 2008;3(8):e2955. Epub 2008/08/14. doi: 10.1371/journal.pone.0002955. PubMed PMID: 18698408; PubMed Central PMCID: PMC2492809.

72. Hall JD, Woolard MD, Gunn BM, Craven RR, Taft-Benz S, Frelinger JA, et al. Infected-host-cell repertoire and cellular response in the lung following inhalation of Francisella tularensis Schu S4, LVS, or U112. Infect Immun. 2008;76(12):5843-52. Epub 2008/10/15. doi: IAI.01176-08 [pii] 10.1128/IAI.01176-08. PubMed PMID: 18852251; PubMed Central PMCID: PMC2583552.

73. Franchi L, Warner N, Viani K, Nunez G. Function of Nod-like receptors in microbial recognition and host defense. Immunol Rev. 2009;227(1):106-28. PubMed PMID: 19120480.

74. Fernandes-Alnemri T, Yu JW, Juliana C, Solorzano L, Kang S, Wu J, et al. The AIM2 inflammasome is critical for innate immunity to Francisella tularensis. Nat Immunol. 2010;11(5):385-93. Epub 2010/03/31. doi: ni.1859 [pii] 10.1038/ni.1859. PubMed PMID: 20351693; PubMed Central PMCID: PMC3111085.

75. Jones JW, Kayagaki N, Broz P, Henry T, Newton K, O'Rourke K, et al. Absent in melanoma 2 is required for innate immune recognition of Francisella tularensis. Proc Natl Acad Sci U S A. 2010;107(21):9771-6. Epub 2010/05/12. doi: 1003738107 [pii] 10.1073/pnas.1003738107. PubMed PMID: 20457908; PubMed Central PMCID: PMC2906881.

76. Mariathasan S, Weiss DS, Dixit VM, Monack DM. Innate immunity against Francisella tularensis is dependent on the ASC/caspase-1 axis. J Exp Med. 2005;202(8):1043-9. PubMed PMID: 16230474.

77. von Moltke J, Trinidad NJ, Moayeri M, Kintzer AF, Wang SB, van Rooijen N, et al. Rapid induction of inflammatory lipid mediators by the inflammasome in vivo. Nature. 2012;490(7418):107-11. Epub 2012/08/21. doi: nature11351 [pii] 10.1038/nature11351. PubMed PMID: 22902502; PubMed Central PMCID: PMC3465483.

78. Quarry JE, Isherwood KE, Michell SL, Diaper H, Titball RW, Oyston PC. A Francisella tularensis subspecies novicida purF mutant, but not a purA mutant, induces protective immunity to tularemia in mice. Vaccine. 2007;25(11):2011-8. doi: 10.1016/j.vaccine.2006.11.054. PubMed PMID: 17241711.

79. Schulert GS, McCaffrey RL, Buchan BW, Lindemann SR, Hollenback C, Jones BD, et al. Francisella tularensis genes required for inhibition of the neutrophil respiratory burst and intramacrophage growth identified by random transposon mutagenesis of strain LVS. Infect Immun. 2009;77(4):1324-36. doi: 10.1128/IAI.01318-08. PubMed PMID: 19204089; PubMed Central PMCID: PMC2663180.

# CHAPTER 6

## CONCLUDING REMARKS

Survival of bacteria, viruses, fungi, and parasites has required these organisms to evolve sophisticated mechanisms to evade and/or subvert host immunity. The host's immune response is not singly focused; therefore, pathogens must evade many potential assaults from the host and have accordingly developed multiple mechanisms to do so. These mechanisms are shared among organisms, allowing the study of one pathogenic organism to provide insight into how similar organisms also evade host immunity. The study of host-pathogen interactions, specifically immune evasion, increases our understanding of pathogenicity as well as identifies critical aspects of host immunity necessary for pathogen clearance and the development of protective immunity. These studies are increasingly important as the human population continues to encounter existing and emerging pathogens to which new therapies and/or vaccines must be developed to successfully combat infection.

*Francisella tularensis* utilizes a variety of immune evasion strategies to suppress or evade both the host's innate and adaptive immune response. Our laboratory is particularly interested in the immune consequences of prostaglandin $E_2$ ($PGE_2$) production following *F. tularensis* subsp. *holartica* live vaccine strain (LVS) infection. We identified 20 genes necessary for the induction of $PGE_2$ synthesis and secretion by *F. novicida* U112 in bone marrow-derived macrophages. We also determined that $PGE_2$ induction does not require the U112 to escape the phagosome. These data are presented in Chapter 5 and were published in *Frontiers in Microbiology* in 2013 (1). One of the genes necessary for inducing $PGE_2$ synthesis and secretion is *clpB*. ClpB is a conserved chaperone protein of the AAA+ family

of ATPases. We hypothesized LVS *clpB* would be attenuated in vivo because a more robust IFN-γ-mediated adaptive immune response would form in the absence of $PGE_2$-mediated suppression. Importantly, LVS *clpB* does not have an intracellular growth defect compared to wild-type LVS. Intranasal inoculation with LVS *clpB* revealed this strain was attenuated. While we did observe decreased $PGE_2$ concentrations in the BALF of LVS *clpB* infected mice compared to LVS infected mice, LVS *clpB* induced altered innate and adaptive immunity as well. LVS *clpB* fails to suppress early pro-inflammatory cytokine production in the lung following intranasal inoculation, in stark contrast to LVS inoculation. The adaptive immune response in LVS and LVS *clpB* mice was similar in terms of the frequency of responding cells, but T cells from LVS *clpB* infected mice produced more IFN-γ and IL-17A as measured by mean fluorescent intensity. Despite its attenuation, LVS *clpB* induces a protective immune response. Because LVS *clpB* does not have an intracellular growth defect, we attribute its attenuation to the failure to suppress host immunity. Our work revealed a new class of bacterial attenuation caused by altered host immunity and identified *clpB* as a gene necessary to suppress early pro-inflammatory cytokine production by the host. These data are presented in Chapter 2 and were published in *Infection and Immunity* in 2013 (2).

The altered adaptive immune response in LVS *clpB* infected mice raised the possibility that the secondary immune response in LVS and LVS *clpB* infected mice could be different. We therefore characterized the T cell response in mice previously infected with LVS or LVS *clpB* during a lethal challenge with LVS. Mice vaccinated with LVS and LVS *clpB* had similar secondary T cell responses that were exclusively IFN-γ-mediated. During primary intranasal infection, Th17 cells significantly expand in the lung but were not

detectable during the secondary response in numbers greater than unvaccinated mice. We therefore used monoclonal antibody treatment to deplete either IFN-γ or IL-17A during the secondary response to determine the importance of these cytokines for survival during a lethal infection. Vaccinated mice treated with anti-IFN-γ had significantly higher bacterial burdens than isotype treated vaccinated mice, indicating IFN-γ was critical for controlling the infection. Anti-IL-17A depletion in vaccinated mice had no impact on bacterial burdens indicating IL-17A is dispensable during a secondary infection. These studies contributed to our knowledge of the secondary immune response during pneumonic tularemia and revealed that while IL-17A is necessary during the primary response to intranasal LVS infection, it is dispensable for protection during re-infection.

Finally, we sought to identify early interactions between *Francisella* and the host following intranasal or intradermal inoculation. Intranasal and intradermal inoculation with LVS induces two different adaptive immune responses despite similar bacterial burdens in the lung and spleen early after inoculation. We hypothesized that the adaptive immune response was shaped by events occurring early after inoculation. We therefore sought to identify the cell types infected with *Francisella* in the lung and skin after intranasal or intradermal inoculation, respectively. Alveolar macrophages are infected in the lung following intranasal inoculation whereas macrophages, dendritic cells, and neutrophils are infected in the skin. Following bacterial dissemination from the skin to the lung, interstitial macrophages and neutrophils are the dominant infected cell types indicating the route of inoculation influences the types of cells that become infected with *Francisella*. The lung milieu is more pro-inflammatory after intradermal inoculation and bacterial dissemination to the lung compared to lungs early after an intranasal inoculation. We also examined how

disease course changed when alveolar macrophages were depleted and found increased bacterial burdens in the lung on day 3 post-inoculation, suggesting alveolar macrophages are necessary to control an intranasal LVS infection. These data are described in Chapter 4.

Overall, our work has identified *clpB* as a gene required for multiple immune evasion strategies used by *Francisella* to persist in the host (inducing $PGE_2$ and suppression of host pro-inflammatory responses). ClpB is a chaperone protein; therefore, it is unlikely that ClpB itself is the effector molecule responsible for immune evasion. Instead, we hypothesize ClpB is involved in insuring proper folding or trafficking of the true effector molecules. Our laboratory is pursuing the targets of ClpB that induce $PGE_2$ and prevent activation of a pro-inflammatory cytokine response as well as the host pathways involved in the pro-inflammatory response. We are taking advantage of the ability of *Francisella* to evade host immunity to learn more about *Francisella* pathogenesis as well as key players in the host's immune response. Additionally, since ClpB is highly conserved among other bacterial species, identifying ClpB's targets and their role in immune evasion could increase our knowledge of pathogenesis in other organisms as well.

## REFERENCES

1. Woolard MD, Barrigan LM, Fuller JR, Buntzman AS, Bryan J, Manoil C, et al. Identification of *Francisella novicida* mutants that fail to induce prostaglandin $E_2$ synthesis by infected macrophages. Front Microbiol. 2013;4. doi: 10.3389/fmicb.2013.00016.

2. Barrigan LM, Tuladhar S, Brunton JC, Woolard MD, Chen C, Saini D, et al. Infection with *Francisella tularensis clpB* leads to an altered yet protective immune response. Infection and Immunity. 2013;in press.